Assessing the Mechanisms of Defective TGF-β1 Response in Chronic Wound Fibroblasts

Nathanael Glyn Morris BSc MSc

Thesis presented for the degree of Philosophiae Doctor

2018

Wales Kidney Research Unit,
Division of Infection and Immunity (I&I),
School of Medicine
Cardiff University
Heath Park
Cardiff
CF14 4XN

DECLARATION

This work has not previously been accepted in substance for any degree and is not concurrently submitted in candidature for any degree.

Signed…… (candidate) Date ……

STATEMENT 1

This thesis is being submitted in partial fulfilment of the requirements for the degree of ……(insert MCh, MD, MPhil, PhD etc., as appropriate)

Signed…… (candidate) Date ……

STATEMENT 2

This thesis is the result of my own independent work/investigation, except where otherwise stated.

Other sources are acknowledged by explicit references.

Signed…… (candidate) Date ……

STATEMENT 3

I hereby give consent for my thesis, if accepted, to be available for photocopying and for inter-library loan, and for the title and summary to be made available to outside organisations.

Signed…… (candidate) Date ……

STATEMENT 4: PREVIOUSLY APPROVED BAR ON ACCESS

I hereby give consent for my thesis, if accepted, to be available for photocopying and for inter-library loans **after expiry of a bar on access previously approved by the Graduate Development Committee.**

Signed…… (candidate) Date ……

Dedication

In memory of my mother Denize Morris – this thesis is dedicated to her endless support, care and love. You made me who I am today.

Acknowledgements

I would like to express my thanks to my two supervisors, Dr Robert (Bob) Steadman and Dr Ryan Moseley, for their support and guidance. A special thanks must be made to Bob who has shown me the utmost support through the toughest times during my PhD, for which I will be forever grateful.

I've technically had a third supervisor in Dr Adam Midgley, who endlessly provided me support and ideas throughout my project. So thank you very much for everything. Many thanks to the invaluable experimental advice on Western blotting from Dr John Martin and Dr Emma Woods. Thanks also to everyone based in the WKRU who has provided advice, ideas, great memories and excellent banter, especially Dr Daniel Smith, who has provided Star Wars trivia, bakes and tequila to help me get through my PhD.

The project itself was possible thanks to funding from Health and Care Research Wales; it was a pleasure to help contribute to the important research portfolio that helps puts Wales on the map.

Most importantly I have to thank my family, Michael, Denize and Sarah, for their endless support, understanding and love that have helped me get through the bad times and help celebrate the good times. Most significantly my soon to be wife, Sophie, who's always been there for me and has been my partner in crime, escaping and planning as many holidays as we could get past Bob.

Thesis Summary

Chronic wounds are regarded as skin wounds that fail to heal. Their chronic nature and requirement for long term treatment put a large financial burden on the healthcare providers. Prevalence of chronic wounds increases with age and is associated with diabetes; both of these are on the increase in western populations. This makes chronic wound research essential in order to understand the basic biological causes and identify potential therapeutic targets.

The aim of this thesis was to characterise the response of chronic wound fibroblasts (CWFs) in response to Transforming Growth Factor β-1 (TGF-β1) stimulation, the cytokine responsible for fibroblast to myofibroblast differentiation. This differentiation is lost in chronic wounds, resulting in the loss of wound closure. TGF-β1 signals through two independent yet collaborating pathways: the classical TGF-βR and the non-classical HA-CD44-EGFR pathway. I aimed to explore the possible dysfunctional signalling in these pathways that may contribute to the loss of myofibroblast formation in CWFs.

HAS1 was shown to have a higher basal expression of in CWFs, with increasing expression in response to TGF-β1. Altered HASs expression indicated a possible defective HA-CD44-EGFR pathway. HA pericellular coat formation, essential for normal dermal fibroblasts (NFs) differentiation, was lost in CWFs. This loss was found to be caused by the loss of CD44-EGFR co-localisation in CWFs. In CWFs, the EGFR was localised in a perinuclear location surrounded by a lipid envelope. Lipid localisation was associated with lysosomal staining indicating a possible role of a defective lipid metabolism or defective intracellular protein degradation pathways in CWFs.

This data suggests that the non-classical pathway is the primary pathway responsible for the loss of myofibroblast formation. However, there are several factors that may contribute to this loss. Future research is required to pin-point the key players leading to aberrant protein, HA and lipid localisation in CWFs.

Presentations

Glyn Morris, Adam Midgley, Ryan Moseley, Robert Steadman. Characterisation of Defective TGF-β1 Driven Fibroblast Differentiation. Wales Kidney Research Unit Annual Meeting, Cardiff, 2016 (Poster)

Glyn Morris, Adam Midgley, Ryan Moseley, Robert Steadman. Role of Hyaluronan in Defective TGF-β1-Driver Fibroblast Differentiation. European Tissue Repair Society, Brussels, 2017 (Talk)

Glyn Morris, Adam Midgley, Ryan Moseley, Robert Steadman. Defective Protein Transport and Localisation in Chonic Wound Fibroblasts. European Tissue Repair Society, Brussels, 2017 (Poster) (Prize Awarded)

Glyn Morris, Adam Midgley, Ryan Moseley, Robert Steadman. Role of Hyaluronan in Defective TGF-β1-Driver Fibroblast Differentiation. Cardiff Institute of Tissue Engineering and Repair, Cardiff, 2017 (Talk) (Prize Awarded)

Glyn Morris, Adam Midgley, Ryan Moseley, Robert Steadman. Defective Protein Transport and Localisation in Chonic Wound Fibroblasts. Annual Infection & Immunity Meeting, Cardiff, 2017 (Poster)

Glyn Morris, Adam Midgley, Ryan Moseley, Robert Steadman. Defective Protein Transport and Localisation in Chonic Wound Fibroblasts. Wales Kidney Research Unit Annual Meeting, Cardiff, 2017 (Poster)

Glossary of Abbreviations

CWFs	Chronic Wound Fibroblast
NFs	Normal Dermal Fibroblast
ER	Endoplasmic Reticulum
ELISA	Enzyme Linked Immunosorbent Assay
HC	Heavy Chain
α-SMA	α-Smooth muscle actin
ADAM	A disintegrin and metalloproteinase
ANOVA	Analysis of variance
BMP-7	Bone morphogenic protein-7
BSA	Bovine serum albumin
CaMKII	Ca^{2+}/calmodulin kinase II
CD44s	CD44 standard isoform
CD44v	CD44 variant isoform
cDNA	Complementary DNA
CSGAGs	Chondroitin sulphate glycosaminoglycans
CTGF	Connective tissue growth factor
CTX-B	Cholera toxin subunit-B
dCT	Difference in cycle threshold
DMEM	Dulbecco's modified eagle medium
DMSO	Dimethyl sulphoxide
DNA	Deoxyribonucleic acid
dNTPs	Deoxyribonucleotide triphosphates
ECL	Enhanced chemiluminescence
ECM	Extracellular matrix
EDA-FN	Extra domain-A-fibronectin
EDTA	Ethylenediamine tetraacetic aci
EEA1	Early endosome antigen 1
EGF	Epidermal growth factor
EGFR	Epidermal growth factor receptor
EMT	Epithelial to mesenchymal transition
ERK1/2	Extracellular signal-regulated kinase (MAPK)
FAK	Focal adhesion kinase
FCS	Foetal calf serum
FGF	Fibroblast growth factor

FITC	Fluorescein isothiocyanate
GAGs	Glycosaminoglycans
GAPDH	Glyceraldehyde 3-phosphate dehydrogenase
HA	Hyaluronan
HAS	Hyaluronan synthase
HGF	Hepatocyte growth factor
HRP	Horseradish peroxidase
HS	Heparan sulphate
HSGAGs	Heparan sulphate glycosaminoglycans
HYAL	Hyaluronoglucosaminidase
IαI	Inter-α-trypsin inhibitor
ICAM-1	Intercellular adhesion molecule-1
IFNγ	Interferon γ
IgG	Immunoglobulin
IL	Interleukin-1
IL-1β	Interleukin-1β
IL-8	Interleukin-8
JAK	Janus kinase
kDa	Kilodalton
KS	Keratan sulphate
mAb	Monoclonal antibody
MAPK	Mitogen activated protein kinase
MCP-1	Monocyte chemotactic protein-1
miR	MicroRNA
miR-16	MicroRNA-16
miR-7	MicroRNA-7
miR-RT	MicroRNA reverse
MMPs	Matrix metalloproteinases
mRNA	Messenger RNA
MSCs	Mesenchymal stem cells
pAb	Polyclonal antibody
PAI-1	Plasminogen activator inhibitor-1
PBS	Phosphate buffered saline
PDGF	Platlet derived growth factor
PDL	Population doubling level
PGs	Proteoglycans

PKC	Protein kinase C
RIPA	Radio-immunoprecipitation assay
RISC	RNA-induced silencing complex
RNA	Ribosomal nucleic acid
RNase	Ribonuclease
ROS	Reactive oxygen species
rRNA	Ribosomal RNA
RT-PCR	Reverse transcription polymerase chain reaction
RT-QPCR	Real time quantitative polymerase chain reaction
S.D.	Standard deviation
SDS-PAGE	Sodium dodecyl sulphate polyacrylamide gel electrophoresis
siHAS1	siRNA targeting HAS1
siHAS2	siRNA targeting HAS2
siHYAL2	siRNA targeting HYAL2
siRNA	Small interfering RNA
SMCs	Smooth muscle cells
STAT	Signal transducer and activator of transcription
TF	Transcription factor
TGF-α	Transforming growth factor-α
TGF-β	Transforming growth factor-β
TGF-β1	Transforming growth factor-β1
TGF-βR	Transforming growth factor-β receptor
TIMPs	Tissue inhibitors of metalloproteinases
TLR4	Toll like receptor 4
TNF-α	Tumour necrosis factor-α
TRITC	Tetramethylrhodamine isothiocyanate
TSG-6	TNF-stimulated gene-6
UTR	Untranslated region
VEGF	Vascular endothelial growth factor
vWF	Von Willebrand Factor

Chapter 1 ..... **1**
General Introduction **1**
1.1 Dermal Wound Healing Overview 2
1.1.1 Haemostasis 2
1.1.2 Inflammation 3
1.1.3 Proliferation 3
1.1.4 Contraction 4
1.1.5 Maturation and Remodelling 4
1.2 The Fibroblast 6
1.2.1 Role of Fibroblasts in Wound Healing 8
1.2.2 Myofibroblastic Differentiation 8
1.3 Chronic (Non-Healing) Wounds 10
1.4 Extracellular Matrix (ECM) 14
1.4.1 ECM Turnover 15
1.4.2 Collagens 16
1.4.3 Glycoproteins 17
1.4.4 Proteoglycans 17
1.4.5 Glycosaminoglycans 18
1.5 Hyaluronan 19
1.5.1 Hyaluronan synthesis 20
1.6 Immune Regulation of Dermal Wound Healing 22
1.7 Genes and Wound Healing 25
1.8 Project Aims and Objectives 26
Chapter 2 ..... **27**
Materials and Methods **27**
2.1. Materials 28
2.2. Cell Culture 28
2.2.1. Sub-culturing 29
2.2.2. Cryostorage and Revival 30
2.2.3. Cell Counting and Population Doubling Level (PDL) Calculations 30
2.3. Cytokine Stimulations 31
2.4. HA ELISA 31
2.5. Red Blood Cell (RBC) Exclusion Assay 32
2.6. Immunocytochemistry (ICC) 32
2.7. RNA Extraction and Reverse Transcription (RT) 34

2.8. Real Time Quantitative Polymerase Chain Reaction (RT-QPCR) 35
2.8.1. TaqMan Gene Expression QPCR 35
2.8.2. Power SYBR Green QPCR 35
2.8.3. QPCR and Relative Quantification (RQ) 36
2.9. Western Blot Analysis 40
2.10. Laser Confocal Microscopy 42
2.11. Plasmid Generation 42
2.11.1. HAS2 and HAS1 Overexpression Vector 42
2.12. Overexpression Vector Transfection 42
2.13. Small interfering RNA (siRNA) Transfection 43
2.14. MicroRNA-7 RT-PCR 44
2.15. MicroRNA RT-QPCR 44
2.16. Statistical Analysis 45
Chapter 3 46
Characterisation of Chronic Wound Fibroblast response to TGF-β1 Stimulation 46
3.1. Introduction 47
3.1.1. Dermal Fibroblasts and TGF-β1 Stimulation 47
3.1.2. TGF-β1 signalling via the classical TGF-βR pathway 47
3.1.3. Non-classical HA-CD44-EGFR pathway 48
3.1.4. Genes Associated with Fibroblast Activation 49
3.2. Results 52
3.2.1. Dermal fibroblast characterisation 52
3.2.2. Characterisation of CWFs response to TGF-β1 stimulation 54
3.2.3. TGF-β1 Induction of the Classical TGF-β1 Pathway 56
..... 56
..... 56
3.2.4. Analysis of the Downstream Signalling of the Classical TGF-β1 Pathway 57
3.2.5. TGF-β1 Induction of the Non-Classical CD44 / EGFR Pathway 58
3.2.6. Analysis of the Downstream Signalling of the Non-Classical CD44 / EGFR Pathway 59
3.2.7. HA Associated Gene Response to TGF-β1 61
3.2.8. Hyaluronidase Isoform Expression in CWFs 62
3.2.9. HAS Isoform Expression in CWFs 63
3.2.10. TSG-6 and Heavy Chains 65
..... 66
..... 66

3.3. Discussion 67
Chapter 4 72
The Role of Hyaluronan in The Loss of the Myofibroblast Response in Chronic Wound Fibroblasts 72
4.1. Introduction 73
4.1.1. Hyaluronan's role in wound healing 73
4.1.2. Hyaluronan's role in myofibroblast differentiation 74
4.1.3. HAS2 regulation and synthesis of HA pericellular coat 74
4.1.4. HAS1 expression in CWFs 75
4.1.5. HAS1 synthesised HA and inflammation 75
4.1.6. The aims of this chapter are: 76
4.2. Results 77
4.2.1. Localisation of Total HA does not change with TGF-β1 Treatment 77
4.2.2. Visualisation of HA Pericellular Coat Using Red Blood Cell (RBC) Exclusion Assay 79
4.2.3. Distribution of HA by ELISA 81
4.2.4. HAS2 Localisation 83
4.2.5. HAS1 clusters in a perinuclear location in TGF-β1 Treated CWFs 85
4.2.6. Intracellular HA clusters in a perinuclear location in CWFs 87
4.2.7. Silencing HAS1 does not recover a myofibroblast phenotype in CWFs 89
4.2.8. Overexpression of HAS1 does not induce a CWFs phenotype in NFs 91
4.2.9. Overexpression of HAS2 does not recover a myofibroblast phenotype in CWFs 93
4.2.10. HAS1 has No Association with Pro-Inflammatory Cytokines 95
4.3. Discussion 97
Chapter 5 101
Trafficking and Localisation of Proteins in Chronic Wound Fibroblasts 101
5.1. Introduction 102
5.1.1. The HA Receptor CD44 102
5.1.2. EGFR Signalling 104
5.1.3. Intracellular Molecular Synthesis and Modification 104
5.1.4. Intracellular Transport 105
5.2. Results 108
5.2.1. Intracellular localisation of EGFR in CWFs and Reduced Co-localisation with CD44 on the Membrane Compared to NFs 108
5.2.2. EGFR and Lipid Intracellular Localisation in CWFs with Reduced Co-localisation on the Membrane Compared to NFs 110
5.2.3. Comparison of EGFR Antisense expression at mRNA level 112

5.2.4. Comparison of CD44 variant expression at mRNA level 114
5.2.5. CD44 variant 7/8 localisation and expression..... 116
5.2.6. HYAL2 perinuclear localisation in CWFs. Silencing HYAL2 doesn't recover a myofibroblast phenotype 118
5.2.7. No difference in lysosome localisation was observed between CWFs and NFs..... 120
5.2.8. No difference in endosome localisation was observed between CWFs and NFs. .. 122
5.2.9. No difference was seen between ER staining between CWFs and NFs..... 124
5.2.10. No differences in Golgi staining was observed between CWFs and NFs..... 126
5.2.11. No difference in microtubule formation between CWFs and NFs..... 128
5.3. Discussion..... 130
Chapter 6..... 133
General Discussion..... 133
References..... 140
Appendix 1: Supplemental Data..... 155

Chapter 1

General Introduction

1.1 **Dermal Wound Healing Overview**

Skin is an intricate structure composed of the epidermis and dermis, including subcutaneous fat. It also has a diverse range of functions including acting as a barrier, protecting from harmful UV, pathogens, water evaporation and underlying organs from the external environment. Wound healing is an essential highly orchestrated cascade which ensures the repair and regeneration of the human body. Dermal wound healing is essential to maintain a protective barrier of skin (Lim and Nusse, 2013). When this protective barrier is damaged the complex cascade of wound healing develops in four overlapping phases, which have distinct biological characteristics: inflammation, proliferation, contraction and remodelling. These phases require the interaction of multiple different local and systemic cell types and regulatory signalling mediators, such as cytokines and growth factors. The outcome and speed of wound healing is dependent on numerous factors, including: moisture, infection, hormones, genetics, and cytokines (Buganza Tepole and Kuhl, 2013). If factors such as these overcome the wound healing process, it can result in a delayed or failed wound healing response.

1.1.1 Haemostasis

The haemostasis phase of wound healing is initiated immediately following an injury to limit blood loss. The phase results in a clot being formed, vasoconstriction of blood vessels and the initial recruitment of immune cells (Buganza Tepole and Kuhl, 2013). When the endothelium is damaged, the Extracellular Matrix (ECM) is exposed to the blood stream. Plasma Von Willebrand factor (vWF) binds collagen, to which activated platelets bind, beginning to form a clot. As the platelets aggregate, they secrete inflammatory factors: Interleukin-1β (IL-1β), interleukin-6 (IL-6) and macrophage inflammatory protein-1α (MIP-1α). The release of blood plasma proteins, such as factor X and V, and thrombin, triggers the cleavage of soluble fibrinogen to form insoluble fibrin, which cross-links with collagen and platelets to form an insoluble clot. This clot stops loss of blood, but also acts as a scaffold for migrating immune cells. Damaged endothelial cells also release thromboxanes causing blood vessels to constrict, which assist the platelets to aggregate. Arriving platelets and monocytes continue to secrete cytokines and growth factors including, vascular endothelial growth factor (VEGF), platelet derived growth factor (PDGF), Epidermal growth factor (EGF), transforming growth factor-β (TGF-β), interleukin (IL-1β), which stimulate surrounding cells to undergo proliferation and differentiation (Hoffman and Monroe, 2005).

1.1.2 Inflammation

The inflammatory phase is initiated within hours of injury. Neutrophils migrate to the site with their numbers peaking around days 1-2, becoming the predominant wound cell. These are the first responders of the immune system and are responsible for killing pathogens, by the release of proteases and Reactive oxygen species (ROS), phagocytosis of the debris and release of soluble mediators that attract other immune cells. Mast cells release histamines and other vasoactivators, which stimulate the blood vessels at the wound site to vasodilate and become leaky. Leaky blood vessels allow monocytes through, which then differentiate into macrophages around day 2 and remain at high levels until day 5. Macrophages are also responsible for removing bacteria and debriding dead tissue, they also remove apoptotic neutrophils. Macrophages secrete cytokines and growth factors that regulate the proliferative phase, stimulating re-epithelialization and the creation of granulation tissue and ECM products (Buganza Tepole and Kuhl, 2013, Gonzalez et al., 2016).

Inflammation is an essential phase of wound healing, but requires strict regulation to ensure successful wound healing. Chronic wounds are thought to be trapped within the inflammatory phase of wound healing, with prolonged inflammation leading to non-healing. The presence of pathogens can extend the inflammatory phase, with most chronic wounds being colonized with bacteria. Targeting the inflammatory phase is the current strategy for chronic wound treatments, either by the reduction of bacteria or inflammatory cells and their pro-inflammatory products (Han and Ceilley, 2017).

1.1.3 Proliferation

The proliferative phase commences approx. 2-3 days following injury, as fibroblasts, keratinocytes and endothelial cells are stimulated to differentiate, proliferate and migrate, leading to the deposition of new ECM, re-epithelialisation and neovascularisation of the wound. A major role of the proliferative phase is to stimulate angiogenesis, which is imperative to supply oxygen and nutrients for the activity of the proliferative cells. Endothelial cells are activated from the inflammatory phase by cytokines and growth factors, such as angiogenin, fibroblast growth factor (FGF) and TGF-β, which are secreted by other cells. The platelet-fibrin clot also releases growth factors, such as VEGF, PDGF and TGF-β, released from de-granulated platelets. These activated endothelial cells initiate vascular sprouting, where they lay down a new capillary network, chemotactically led towards the site of injury by the hypoxic environment. Matrix metalloproteinases (MMPs) digest the basement membrane and ECM, creating a pathway for infiltrating vessels. Once adequate tissue perfusion is reached this process reduces (Velnar et al., 2009).

The second major role of the proliferative phase is the formation of the granulation tissue by the migrating fibroblasts, which become the predominant cell type by day 7. Fibroblasts migrate from the surrounding unaffected tissue and from circulating precursors (fibrocytes). They adhere to the wound fibronectin and deposit granulation tissue, which is a temporary ECM consisting of collagens, glycosaminoglycans (GAGs), elastin, glycoproteins and proteoglycans (PGs). The main components being collagen, fibronectin and hyaluronan (HA). Collagen type III is the predominant collagen laid down in the granulation tissue. It provides tensile strength for the repairing tissue and together with fibronectin, provides a network for the adhesion of cells. Type III collagen is later replaced by type I collagen, as the granulation tissue is remodelled into mature tissue (Gonzalez et al., 2016).

1.1.4 Contraction

Contraction commences at approximately 7 days. It is an essential phase that reduces the size of the wound. Without it, the wound would remain open, while excessive contraction results in loss of function from scar formation and fibrosis. The cell type responsible for contraction is the contractile α-smooth muscle actin (αSMA)-positive myofibroblast, which differentiates from resident fibroblasts. Myofibroblasts are attracted toward the wound edges by growth factors and fibronectin, where they anchor themselves to the ECM. They attach to wound edges and each other via desmosomes, fibronexus, collagen, fibronectin and HA, to create a network of myofibroblasts at the wound edge. Once adhesions are made, the actin within the myofibroblasts can contract, pulling the wound edges together. The contraction phase ends as the granulation tissue begins to be broken down and remodelled. This breakdown means a decrease of HA and increase in chrondroitin sulphate GAGs are observed, resulting in a decrease in myofibroblast migration and proliferation, triggering the apoptosis of the myofibroblasts (Tracy et al., 2016).

1.1.5 Maturation and Remodelling

The onset of the maturation phase differs greatly from person to person. It depends on the type, size and condition of the wound and also the person’s age and health. The aim of the maturation and remodelling phase is the replacement of type III collagen by type I collagen with the alignment of the fibres to increase the tensile strength of the tissue to its normal state, whilst also removing any redundant cells via apoptosis, along with degradation of HA and fibronectin. This phase can last for a year or longer. This phase results in the return of the tensile strength of the skin, however will only ever return to approx. 80% strength of the original tissue (Gonzalez et al., 2016, Velnar et al., 2009).

The presence of granulation tissue allows for epithelial cells to migrate, allowing for re-epithelialisation of the wound. Basal keratinocytes are the main cell type responsible for re-epithelialisation, by migrating to the wound edges (Velnar et al., 2009). This migration is stimulated by nitric oxide and various growth factors, including TGF-α and hepatocyte growth factor (HGF) together with the lack of contact inhibition of the keratinocytes (Werner et al., 2007). For the migration to occur, the keratinocytes become flat and elongate to make motility easier. Also, they break down the desmosomes and hemidesmosomes that usually keep them adhered to the ECM and other cells. They then begin to form pseudopodia containing actin filaments that contract, causing the movement of the cells (Thomason et al., 2012). Keratinocytes also can debride the tissue and phagocytose bacteria in their path, thus removing the scab as they move (Pastar et al., 2014). The mechanism by which they dissolve tissue, is to secrete a plasminogen activator, activating plasminogen converting it to active plasmin, which along with other proteases digests the scab (Kramer et al., 1995). Keratinocytes can only migrate over viable tissue. Therefore, they also secrete collagenases and proteases to digest damaged components of the ECM. Keratinocytes continue to migrate until they meet, where contact inhibition stimulates them to return to their static form and undergo the reverse of the morphological changes they underwent at the beginning (Martin and Nunan, 2015).

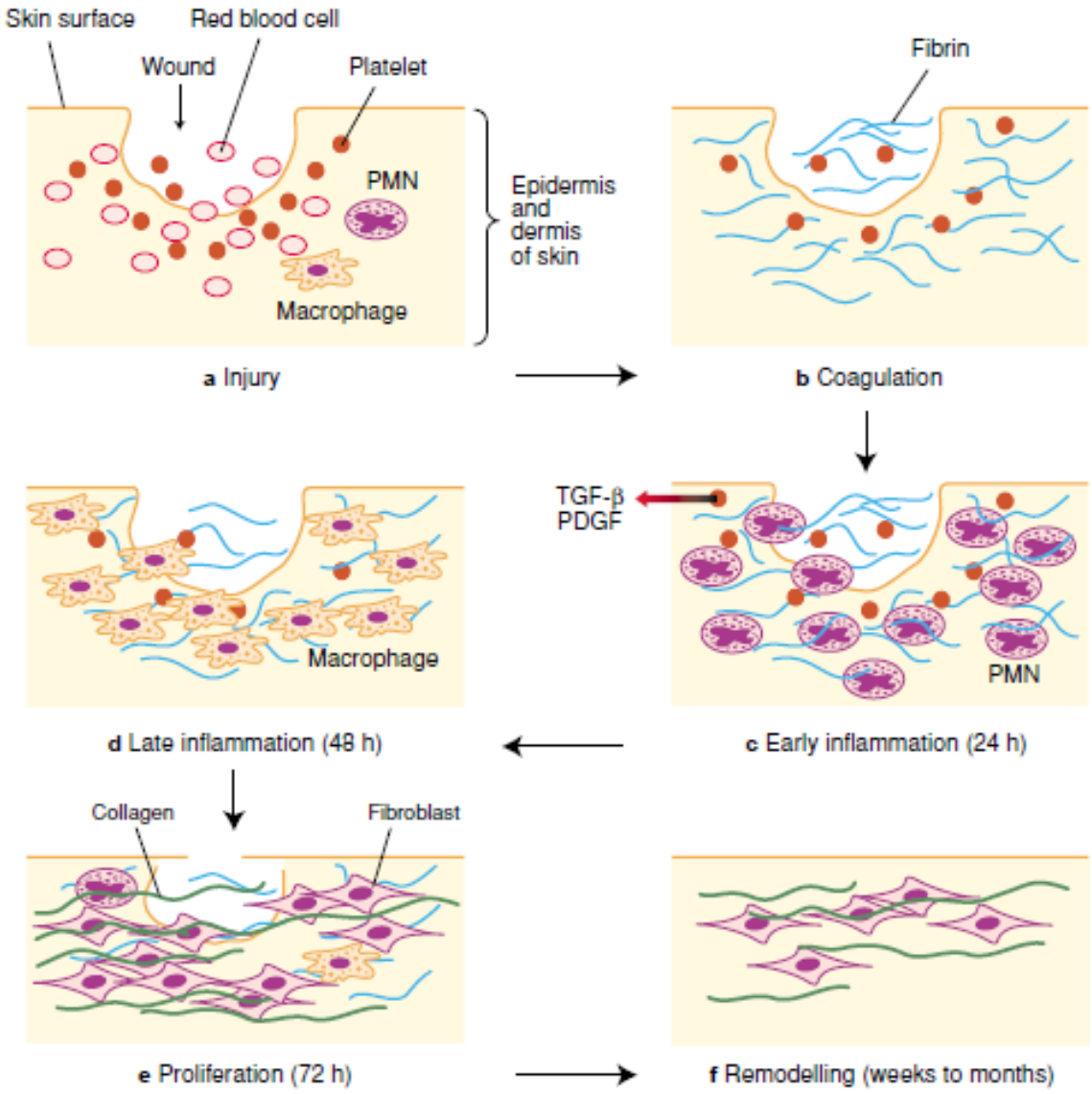

Figure 1.1. Phases of Dermal Wound Healing. (a) Immediately following cutaneous injury, blood elements are released from the damaged endothelium. Vasoconstriction follows, in response to factors released. (b) Haemostasis then occurs with the coagulation cascade. Platelets aggregate within a fibrin glue. (c) Platelets release several factors initiating the inflammatory phase, these factors include PDGF and TGF-β1. (d) After 48 hr macrophages are the predominant immune cell present. Together with other immune cells they remove debris, release growth factors and begin to reorganize the ECM. (e) The proliferation phase begins at 72 hr as recruited fibroblasts synthesis collagen. (f) Collagen crosslinking and reorganisation occurs for months during the remodelling phase. Image was taken from {Beanes, 2003 #308}

1.2 The Fibroblast

Wound healing is a complex process and involves a variety of cell types. The fibroblast is the most prevalent cell in the human dermis and is responsible for the speed and efficiency of wound healing, the extent of scar formation and wound contraction. The fibroblast is the most common cell of connective tissue; it is responsible for tissue metabolism and integrity

by synthesising the ECM precursors such as collagens, GAGs, elastin and glycoproteins and biochemical mediators such as growth factors and proteases. The fibroblast is responsible for the synthesis, degradation and remodelling of the ECM, all important processes in wound healing (Tracy et al., 2016), as the ECM determines the physical properties of the connective tissue.

Fibroblasts are derived from primitive mesenchyme; thus they express the intermediate filament vimentin. It is possible, however, for other sources to give rise to fibroblasts, such as epithelial cells, which can give rise to fibroblasts via a process called epithelial-mesenchymal transition. The fact that fibroblasts can be derived from a variety of precursors emphasises their crucial function in maintaining tissue homeostasis.

Phenotypically fibroblasts are flat, elongated, having multiple processes, a nucleus having two or more nucleoli and a large rough endoplasmic reticulum. Fibroblast shape is regulated by actin in their cytoskeleton, which can assemble and disassemble into various sized actin filaments. Actin also plays a large role in the migration of fibroblasts. Confluent fibroblasts in culture align in parallel clusters, but if they are not confluent they spread out to cover as much area as possible. There is no single specific marker for a fibroblast, which complicates its identification and role in diseases. The fibroblast cell is extremely plastic. In dermal skin, for example, different dermal layers host different subpopulations of fibroblasts, with dermis depth having an effect on collagen type I and type III expression and deeper fibroblasts expressing reduced quantities of collagenases than those in superficial layers (Tracy et al., 2016). Fibroblasts are also very malleable cells, with altering function in differing locations throughout the body. It is, therefore, essential that we characterise these cells under differing conditions, to understand their roles.

Fibroblast heterogeneity produces functional sub-populations which differ in size, morphology, proliferation rates and collagen production. For example, there are three identified sub-populations within skin. Two are defined according to their location in the dermis - the papillary and reticular dermis - and the third is associated with hair follicles (Sorrell and Caplan, 2004). It has been suggested that some pathological conditions are caused by a sub-population of fibroblasts that out-compete the others and become the dominant fibroblast. An example of this is chronic wound fibroblasts compared to their healthy dermal population, aberrantly expressing genes that regulate the ECM, cytoskeleton and migration. In the study by Wall et al 2008, chronic wound fibroblasts from different patients demonstrated very different proliferative capacity, suggesting a heterogeneous wound environment of wounds with the same clinical classification.

1.2.1 Role of Fibroblasts in Wound Healing

The primary role of the fibroblast in skin is to maintain tissue homeostasis. Following an injury, however, resident cells and infiltrating inflammatory cells release cytokines that activate fibroblasts. Fibroblasts migrate from the wound edge into the provisional matrix formed by the fibrin clot. Here, they proliferate and act to restore the ECM. Fibroblasts replace the fibrin matrix with granulation tissue made from new ECM components, for example fibronectin, HA, collagens and PGs. This granulation tissue allows the infiltration of new blood vessels, fibroblasts, inflammatory cells, endothelial cells and myofibroblasts. Granulation tissue allows for the re-epithelialization and construction of a primary dermis. Once the fibroblasts are situated within this new matrix they are further stimulated to differentiate into myofibroblasts, the primary cells involved in the deposition and remodelling of the new ECM. Myofibroblasts also initiate the contraction of the wound, decreasing the size of the wound by contracting the wound edges into closer proximity (Darby et al., 2014).

Under normal resting conditions, fibroblasts have no actin associated cell-cell and cell-matrix associations and produce only ECM components required for resting turnover of the tissue. In this normal state, fibroblasts are under continuing resting tension which allows the connective tissue to maintain its shape and integrity. Following injury, however, the ECM is continuously being remodelled and the protective structure is lost. Mechanotransduction signals are passed through integrins to intracellular focal adhesion complexes and the actin cytoskeleton. A stress stimulus signals fibroblast proliferation, increasing their numbers and ECM synthesis, which increases the matrix tension and applies more force to the granulation tissue (Wang et al., 2001). In response to this mechanical challenge, fibroblasts activate and differentiate into proto-myofibroblasts which have a migratory phenotype, expressing only β- and γ-cytoplasmic actins (Darby et al., 2014).

1.2.2 Myofibroblastic Differentiation

It is possible for myofibroblasts to be formed from numerous different cell types (see Figure 1.1), however the differentiation process follows a well-documented cascade of events. Tissue injury initiates this cascade, which activates fibroblasts initiating the production of contractile stress fibres composed of cytoplasmic actins and increase in focal adhesion proteins. This intermediate stable phenotype is known as the proto-myofibroblast (Santiago et al., 2010, Hinz et al., 2007). Expression of α-smooth muscle actin (αSMA) in stress fibres is the hallmark for full differentiation into a contractile myofibroblast (Rohr, 2009).

Myofibroblasts are specialised cells responsible for wound closure, via exerting contractile forces on their microenvironment, remodelling the tissue ECM and the tissue. Aberrant myofibroblast activation can result in the development of pathological conditions, such as fibrosis, disease progression, cancer invasiveness and non-healing wounds. Myofibroblasts are the primary cells responsible for scar tissue formation and wound closure. But, excessive activation can lead to impaired organ function by excessive scarring. Examples of such conditions include: hypertophic scars, scleroderma and Dupuytren's disease and heart and kidney fibrosis. Contrasting this failed-activation of myofibroblasts leads to non-healing chronic wounds, such as venous, arterial, diabetic and pressure ulcers (Darby et al., 2014).

Morphologically characteristics of myofibroblasts include a flattened, irregular shape with clear cell-matrix interactions and intracellular gap junctions. Myofibroblasts have structural properties between those of a fibroblasts and a smooth muscle cell. They express smooth muscle cell associated proteins, such as desmin, calponin and smooth muscle myosin (Tomasek et al., 2002). The most reliable and used markers for myofibroblasts include increased expression of specialized ECM proteins, like the EDA splice variant of fibronectin, and αSMA. α-SMA positive myofibroblasts have been shown to have 2-fold stronger contractile activity, compared to resting fibroblasts (Hinz et al., 2001). The mechanism responsible for this differentiation has been shown to be TGF-β dependent. Use of a TGF-β neutralizing monoclonal antibody has shown to decrease scarring induction in the dermis (Shah et al., 1994). The action of TGF-β is dependent on local presence of cellular fibronectin splice variant EDA. EDA-fibronectin is produced by fibroblasts in the initial stages of wound healing with collagen type I. It has been shown that absence of either TGF-β or EDA-fibronectin, allows fibroblasts to differentiate to proto-myofibroblasts only (Muro et al., 2008).

Myofibroblasts are responsible for the remodelling and deposition of new ECM, the contraction of the granulation tissue and ultimately wound closure. They are also responsible for the subsequent wound contracture and collagen rich scar formation. They produce fibronectin, and later collagen type I, III, elastin, GAGs and PGs. Myofibroblasts can also secrete enzymes, such as MMPs and tissue inhibitors of metalloproteinase (TIMPs) of the ECM, which can alter ECM composition. Myofibroblasts can also function as immune cells, releasing chemokines, growth factors and cytokines such as monocyte chemotactic protein-1 (MCP-1), IL -1, -6, -8, HGF, TGF-β and EGF (Darby et al., 2014).

Both fibroblasts and myofibroblasts contribute to wound repair. Myofibroblasts however are only present within the wound for a finite period whilst contraction is occurring. Myofibroblast

differentiation is stopped once the wound is fully contracted and re-epithelialized. Following this few α-SMA positive myofibroblasts are found present in the wound. It is unclear how myofibroblasts numbers are reduced in the wound, whether they undergo apoptosis and therefore are terminally differentiated, or whether they revert back to fibroblasts and therefore are only an alternative phenotype. The signal for this remains unclear, however, the reconstruction of the ECM and the subsequent reduction in mechanical stress has been shown to be a promoter of apoptosis and myofibroblast removal (Darby et al., 2014).

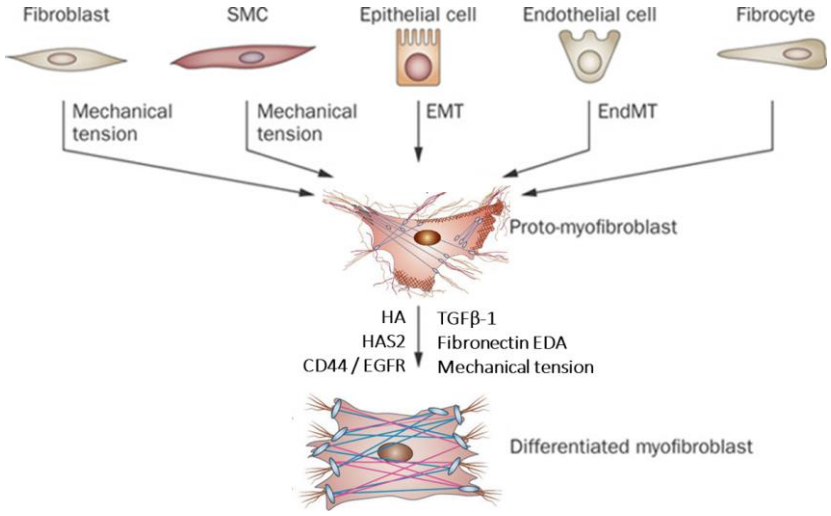

Figure 1.2. Myofibroblasts can be derived from a number of different cell types including fibroblasts, smooth muscle cells (SMC), epithelial cells, via epithelial to mesenchymal transition (EMT), endothelial cells, via endothelial to mesenchymal transition (EndMT) and fibrocytes. With stimuli of mechanical tension or TGF-β1, fibroblasts differentiate into protomyofibroblasts, with the production of cytoplasmic actins. Furthermore, mechanical tension, TGF-β1, fibronectin EDA, Hyaluronan Synthase 2 (HAS2), CD44 / EGFR stimuli drives protomyofibroblasts towards terminal differentiated myofibroblasts, expressing α-SMA. Image was adapted from (Falke et al., 2015, van den Borne et al., 2010)

1.3 Chronic (Non-Healing) Wounds

Chronic wounds are clinically described as skin wounds that fail to progress through the healing process in a timely manner, often described as detained in the inflammatory phase of wound healing. These wounds may never heal and therefore place high emotional and physical stress on the patients. Their chronic nature and the necessary duration of treatment places a huge financial burden on healthcare providers; this burden is expected to increase with the aging population and the prevalence of this wound type (Frykberg and Banks, 2015).

Chronic wounds can be classified into 3 subgroups, vascular ulcer (e.g. venous and arterial ulcers), diabetic ulcer and pressure ulcers. All three share common features, including prolonged inflammation, recurring bacterial infections and the imbalance of ECM homeostasis, leaning towards ECM degradation rather than synthesis. However, all three ulcer types have different underlying pathophysiology.

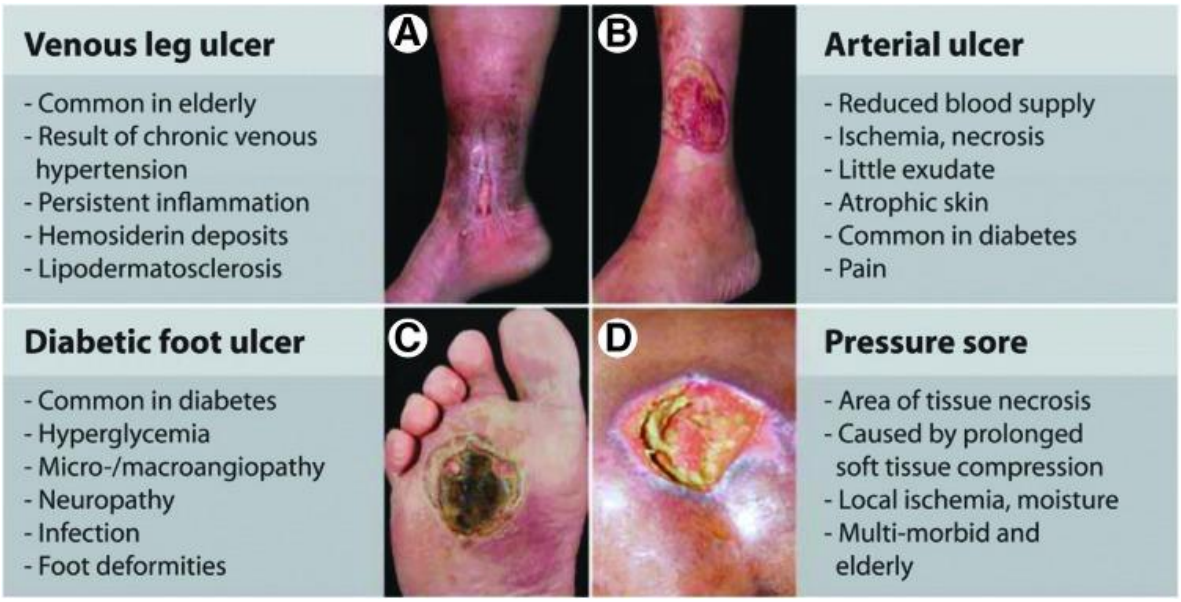

Figure 1.3. Images are representative of the 3 subgroups of non-healing chronic wounds. Venous Ulcer (A) and (B) Arterial ulcer, both can be described as vascular ulcers. Diabetic ulcer (C) and Pressure Ulcer (D) (Larouche et al., 2018).

Venous ulceration is caused by sustained venous hypertension, resulting from venous insufficiency. 10% of the western population have vascular incompetence, with 0.2% developing ulceration, with 70% recurrence in those with contributing risk factors such as obesity or suffering deep vein thrombosis (Grey et al., 2006). Arterial ulceration is caused by reduced blood supply to the lower limbs, the most common cause of which being atherosclerosis (Grey et al., 2006). Diabetic ulcers are a complication of diabetes mellitus, characterised by excessive inflammatory response. These ulcers have multiple contributory factors to their pathology including, cutaneous microcirculation deficiencies, oxidative stress and altered inflammatory response, which lead to dysregulated immune response and decrease in ECM turnover (Garcia-Honduvilla et al., 2018). Increased fibroblast apoptosis has been reported in this wound type, due to glucose toxicity (Berlanga-Acosta et al., 2013). The primary cause of pressure ulcers has been identified as ischemia reperfusion. This damages endothelial cells, producing an oxidative stress and a pro-inflammatory response, which prevents normal wound healing (Motegi et al., 2017). All types of ulcers last on average 12 to 13 months and also recur in up to 60% to 70% of patients. This recurrence is thought to be due to the co-morbidities of the patients that lead to poor circulation, neuropathy and reduced mobility (Frykberg and Banks, 2015).

The pathophysiology of all types of chronic wounds can be attributed to the failure to progress past the inflammatory phase of wound healing, resulting in a negative loop, caused by increasing levels of pro-inflammatory cytokines, proteases, reactive oxygen species (ROS) and senescent cells, as well as persistent infections and deficiency of stem cells that

are often dysfunctional (Frykberg and Banks, 2015). The constant influx and stimulation of immune cells result in the pro-inflammatory cascade becoming amplified and persistent. In acute wounds proteases such as MMPs are regulated by their inhibitors, such as tissue inhibitor of metalloproteinases (TIMPs). In chronic wounds proteases and MMPs levels exceed that of their inhibitors leading to degradation of the ECM. This proteolytic destruction of the ECM prevents the progression into the proliferative phase of wound healing and also attracts more inflammatory cells, therefore amplifying the inflammation cycle. The influx of inflammatory cells increases the presence of ROS in the wound environment to toxic levels. In acute wound healing ROS are responsible for defence against infiltrating microorganisms. In chronic wounds, the constant influx of inflammatory cells creates a ROS, rich hypoxic environment. The aberrant levels of ROS further stimulate the degradation of the ECM by causing DNA damage, gene dysregulation, cell death and a hostile proteolytic environment (Dhall et al., 2014). The db/db mouse model of type II diabetes with impaired wound healing has been associated with the reduction of glutathione (GSH), resulting in reduced glutathione peroxidase (GPx) activity and thus increase in ROS (Mudge et al., 2002). The use of strong anti-oxidants has been shown in animal models to reduce the ROS to normal levels, thus reducing the chronicity of the wound (Dhall et al., 2014).

It has previously been shown that chronic wound cells are characterized by increased senescence with decreased proliferation and secretory capacities, making them unresponsive to wound healing signals. It has also been reported that human dermal chronic wound fibroblasts have early induction of senescence in a telomerase-independent manner (Wall et al., 2008). Together with fibroblasts, chronic wounds have been shown to include senescent keratinocyte, endothelial and macrophage cell populations. The early senescence of cells in chronic wounds has been attributed to a decreased ability to withstand oxidative stress produced by the ROS (Wall et al., 2008).

Mesenchymal stem cells (MSCs) play an important role in acute wound healing. Recruited from the circulatory system towards the site of injury, they are responsible for the remodelling of the new microvasculature. In diabetic mice, stem cells have been shown to be deficient and defective (Cianfarani et al., 2013). Circulating and/or resident MSC's are also prominent pre-cursors of the wound healing cell type, the myofibroblast, in a variety of organs following a response to injury (Bochaton-Piallat et al., 2016). Patients with chronic wounds, therefore, may require deliver of healthy donor MSC's to overcome this deficiency.

Fibroblasts play a key role in wound healing, being responsible for ECM regulation, such as fibronectin and collagen production, but also wound contraction via their differentiation into

contractile myofibroblasts. In chronic wounds, an increase in degradative proteases results in a reduction in matrix proteins, such as fibronectin (Cha et al., 2008). Phenotypic changes in fibroblasts are also observed, with altered morphological appearance, decreased proliferation and unresponsiveness to certain cytokines and growth factors, such as PDGF and TGF-β1 (Kim et al., 2003). TGF-β1 in acute healing is responsible for the differentiation of fibroblasts into myofibroblasts and thus wound contracture. Wound contraction is absent in chronic wounds and has been considered a major cause of non-healing. The unresponsiveness of the fibroblast to TGF-β1 signalling has been attributed to the toxic hypoxic environment of the chronic wound, which has been shown to markedly reduce α-SMA positive myofibroblasts in *in-vitro* studies (Sen and Roy, 2010, Van De Water et al., 2013). This lack of myofibroblast differentiation is an important and understudied area of chronic wound biology, which I will address in this thesis.

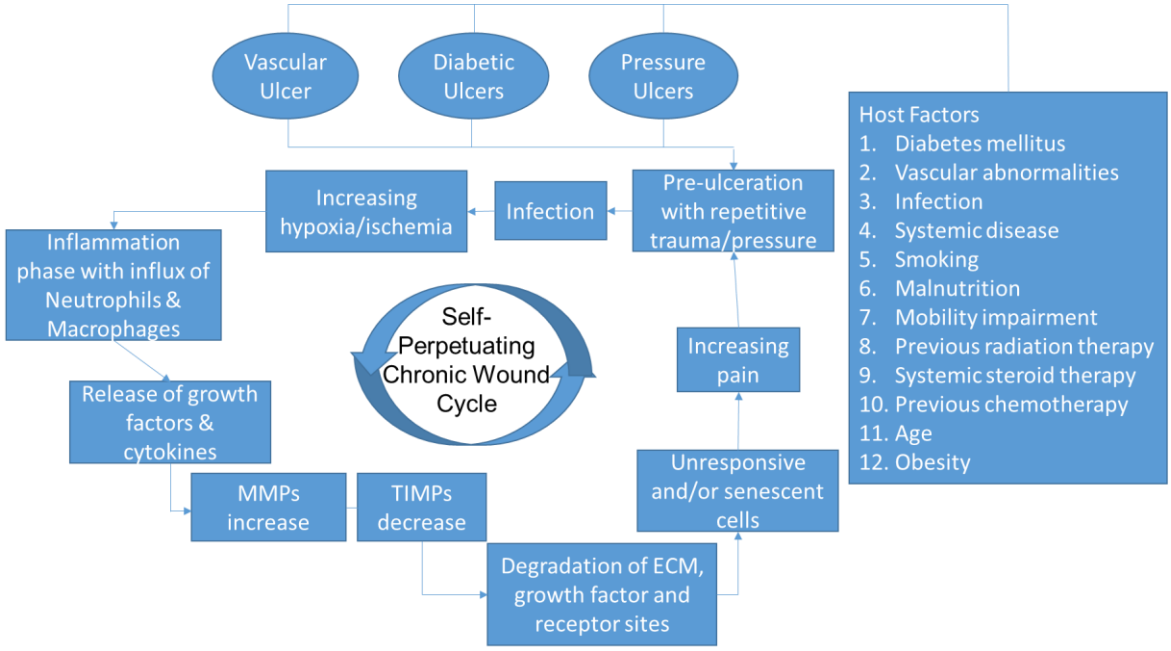

Figure 1.4. Chronic wounds are non-healing wounds trapped in a self-perpetuating cycle. Three types of chronic wounds exist. All types begin with ulceration caused by damage and can become infected. Wound healing cascade causes the induction of an inflammatory response which becomes chronic. This leads to an imbalance between ECM production and degradation. Cells become unresponsive and the wound becomes chronic causing pain. The cycle will continue to develop the ulcer without any medical intervention. There are numerous host risk factors that increase the prevalence of chronic wounds. Image was adapted from (Martin and Nunan, 2015, Shechter and Schwartz, 2013)

1.3.1. Bacterial colonization in Chronic Wounds

Bacterial overload is another major risk factor that determines whether a wound is in danger of becoming non-healing. The wounds microenvironment makes it ideal for bacteria to thrive as complex communities known as biofilms. Mature biofilms can develop as early as within

10 hours and persist indefinitely while the wound remains open. Biofilms are identifiable in up to 60% of chronic wounds but only 6% of acute wounds (Omar et al., 2017).

Biofilms are enclosed in a exopolysaccharide (EPS) and are less metabolically active than their free-living counter parts, making them more resistant to destruction by the hosts immune system and highly resistant to antimicrobial treatment (Clinton and Carter, 2015). Many classes of antibiotics are only effective against actively dividing cells be targeting peptidoglycan produced in the cell wall, protein synthesis or DNA replication (Clinton and Carter, 2015). Biofilms are polymicrobial and may consist of not only bacterial cells but also fungi, viruses, proteins and other biogenic factors, requiring a complex multi treatment approach to eradicate. Staphylococcus aureus, Enterococcus faecalis, Psuedomonas aeruginosa, coagulase-negative staphylococci are the most common cultured species in chronic wounds (Gjodsbol et al., 2006). Bacterial persistence in these wounds has been proposed due to the extreme tolerance of the bacteria to antibiotics, allowing biofilms to develop and the granulation tissue environment in the wound bed, hampering the mechanical clearance of the invading bacteria. Bacteria such as Pseudomonas aeruginosa can also produce rhamnolipids that efficiently shield from the phagocytic activity of polymorphonuclear leukocytes (PMNs). This elimination might contribute to the high levels of proteases and MMP's found in the wound, which are released from PMN by cell lysis (Bjarnsholt et al., 2008). It is also thought that they depend upon the hosts immune response for nutrients and therefore contribute to the isolation of the healing cascade in the inflammatory phase (Costerton et al., 1999). Bacteria express virulence factors that upregulate pro-inflammatory cytokines, ROS and MMP's while down regulating TIMPs. In chronic wounds, biofilms have been shown to disrupt epidermal barrier function by compromising tight junctions resulting in leaky skin measured by water loss (Roy et al., 2014).

A vital step in restoring wound healing in infected chronic wounds is debridement of infected and necrotic tissue. EPS promotes strong attachment of the biofilm to the wound bed and makes full debridement difficult. Even leaving a small amount of cells remaining from the biofilm allows easy regeneration, leading to a high rate of recurrent infections in chronic wounds (Clinton and Carter, 2015).

1.4 Extracellular Matrix (ECM)

The ECM of skin can be divided into fibre-forming structural components, which form a rigid three-dimensional framework of rigid proteins, giving structural strength, and non-fibre

forming components, which are mostly charged molecules (PGs and GAGs) giving a dynamic osmotic space (Tracy et al., 2016). The most prevalent fibre-forming protein is collagen representing 77% of the total fibre-forming proteins. The others include fibronectin, vitronectin, elastin and fibrillin, which all contribute to the structure of the ECM (Frantz et al., 2010). Other structural proteins include glycoproteins such as laminin, which contributes to the structure of the basement membrane and intergrins which are cell membrane receptors for the ECM components. Both contribute to the structure of the cell during adhesion and migration. The most abundant non fibre-forming molecules are HA, decorin, versican and dermatopontin. Their role is to fill space in the ECM; they are negatively charged and hydrophilic. This characteristic allows them to hydrate the tissue, act as a buffer and help disperse molecules throughout the ECM (Frantz et al., 2010).

1.4.1 ECM Turnover

Tissue homeostasis is regulated by tissue remodelling enzymes, MMPs and adamalysins (ADAMs), proteases responsible for the degradation and remodelling of the ECM. They also have a role in regulation of cell signalling pathways in normal and disease states, such as chronic wounds. An imbalance of their production can lead to a progressive ECM degradation and thus non-healing (Bonnans et al., 2014).

MMPs are a large family of enzymes produced by both inflammatory and resident cells, that all have a metal zinc ion at their active site. The differences between MMPs lies in the diversity of the substrates they target such as collagens, gelatin and PGs. Different MMPs may act on different parts of the same protein (Page-McCaw et al., 2007). Together as a family, they all act to breakdown proteins compromising the ECM. They are, therefore, very important in ECM turnover during tissue homeostasis and in disease states, such as chronic wounds. It has been found that an increase in MMP-8 targets the breakdown of collagen type I in chronic wounds (Danielsen et al., 2011). Another, MMP-13, not usually expressed by normal dermal fibroblasts, has been found to be expressed by chronic wound fibroblasts. MMP-13 was found to be play a role in granulation tissue maturation, inflammation, angiogenesis, migration and proliferation (Toriseva et al., 2012). MMP-13 knockout mice also demonstrated delayed organisation of myofibroblasts, indicating its role in regulating myofibroblast formation (Toriseva et al., 2012).

The ADAM family of peptidase proteins also has a key role in the degradation of ECM proteins; they can also process membrane anchored growth factors and cytokines in a process of ‘ectodomain shedding’, thereby acting as post-translational regulators of these signalling factors (Edwards et al., 2008). Included in these are the pro-inflammatory

cytokine, TNF-α and all ligands of the epidermal growth factor receptor (EGFR). The expression of ADAMs has been shown to have a direct role in wound healing. Both ADAM-9 and ADAM-12 knockout mice have accelerated wound repair mediated by increased migration of keratinocytes. ADAM-12 expression has also been reported in chronic wounds, indicating its possible role in preventing wound healing (Mauch et al., 2010, Harsha et al., 2008).

Hyaluronidases (HYALs) are a family of 6 enzymes that degrade HA, an important constituent of the ECM produced by fibroblasts and myofibroblasts. The main 3 family members are HYAL-1, -2 and -3. Hyaluronidase act by hydrolysing the disaccharides at hexosaminic β (1-4) linkages. The size of the HA fragments is dependent on the HYAL (Stern and Jedrzejas, 2006). Additional degradation can also occur by ROS (Buhren et al., 2016). HA fragments have size dependent effects, with high molecular weight HA associated as an anti-inflammatory and low molecular weight HA being pro-inflammatory. Therefore, regulation of these enzymes is key to successful wound healing (Buhren et al., 2016). An example includes the use of bovine testis HYAL to improve wound healing, through increased cell numbers, resulting in increased migration and proliferation of fibroblasts and keratinocytes, leading to improved re-epithelialization and wound closure (Fronza et al., 2014).

1.4.2 Collagens

Collagen is the most abundant protein in the human body, having the vital role of providing tensile strength to the ECM. There are 28 members of the collagens family, the dermis containing of only a few (Kadler et al., 2007). The predominant collagen in skin is type I collagen, followed by type III. Collagen type V is found in the basement membrane of skin, and we also know that collagen types IV, VII and XVII play an important role in the dermis (van der Rest et al., 1991).

The first type of collagens is the fibrillary collagens consisting of types I, III and V in the dermis. Collagen fibrils form a scaffold which allows the adhesion, chemotaxis and migration of cells. The fibrils form in different orientation giving diffuse strength across the tissue. Collagen expression is controlled via feedback from the stress in the tissue and via regulation by other collagens (Gelse et al., 2003). The second type of collagens found in skin is the non-fibrillar collagens, including types IV, VI, VII and XIV. They function by creating interconnecting nets of collagen connecting cells to the basement membrane, and they can aid in organising the formation of the fibrillary collagens (Gelse et al., 2003). Type VI collagen has been shown to promote fibroblast growth and inhibit their apoptosis. It is,

therefore, found to be upregulated for months after a wound (Theocharidis et al., 2015). Type VII assists with fibroblast migration and regulates cytokine expression, with topical application in mice showed a decrease of fibrogenic TGF-β1 and αSMA, whilst increasing anti-fibrogenic TGF-β3 (Wang et al., 2013).

1.4.3 Glycoproteins

Glycoproteins are proteins that have an oligosaccharide chain bound, via the process of glycosylation. Glycoproteins are matrix adhesion molecules, which include laminin, entactin, thrombospondin and fibronectin. Fibronectin is a high molecular weight glycoprotein, which mediates a wide variety of cellular interactions, having a regulatory role in cell adhesion, proliferation and migration (Pankov and Yamada, 2002, Tracy et al., 2016). On the basis of solubility, Fibronectin found in mammalian cells, can be subdivided into two forms: the first is a soluble plasma form found in the blood and produced by hepatocytes in the liver. The second is the less-soluble ECM type, which is secreted primarily by fibroblasts (Pankov and Yamada, 2002). EDA-fibronectin (splice variant of fibronectin) expression has been shown to increase in response to TGF-β1 (Shinde et al., 2015), showing fibronectin has a role in myofibroblast differentiation and therefore can be used as a marker.

1.4.4 Proteoglycans

Proteoglycans (PG) are proteins, heavily glycosylated, via the covalent binding of 1 or more glycosaminoglycan (GAG) chains to the protein core. The type and function of PGs are characterised by their size and GAG chain. The overall function of PGs is to fill space in the ECM by forming large complexes with other PG or other matrix components such as the fibrillar collagens (Kirkpatrick and Selleck, 2007). Proteoglycans have been found to have effects on proliferation, cell signalling and growth factor activity (Kirkpatrick and Selleck, 2007). PGs have a distinct spatial localisation in the skin, having essential roles on tissue's development, structure and wound healing. Versican is a large PG, with widespread distribution throughout the skin. Versican has a predominantly structural role in the ECM, however is capable of influencing cellular behaviour via interactions with growth factors such as epidermal growth factor (EGF) (Du et al., 2010). Decorin, a collagen associated PGs and Biglycan, a cell associated PG, are also important in skin homeostasis and wound healing. These two PGs are part of the small leucine rich PGs (SLRPs), which are expressed predominantly in the skin compared to other tissues throughout the body (Iozzo and Schaefer, 2010). SLRPs are also capable of interacting with TGF-β1, controlling it's bioavailability and therefore skin fibrosis (Smith and Melrose, 2015).

1.4.5 Glycosaminoglycans

GAGs are long unbranched polysaccharides made up or repeating disaccharide units. The repeating unit (with the exception of keratin sulphate (KS)) consists of an amino sugar (N-acetylglucosamie or N-acetylgalactosamine), along with a uronic sugar (glucuronic acid or iduronic acid) or galactose. These long chains make them polar molecules and so hydrophilic; they can therefore fill space and act as a sponge or lubricant (Afratis et al., 2012).

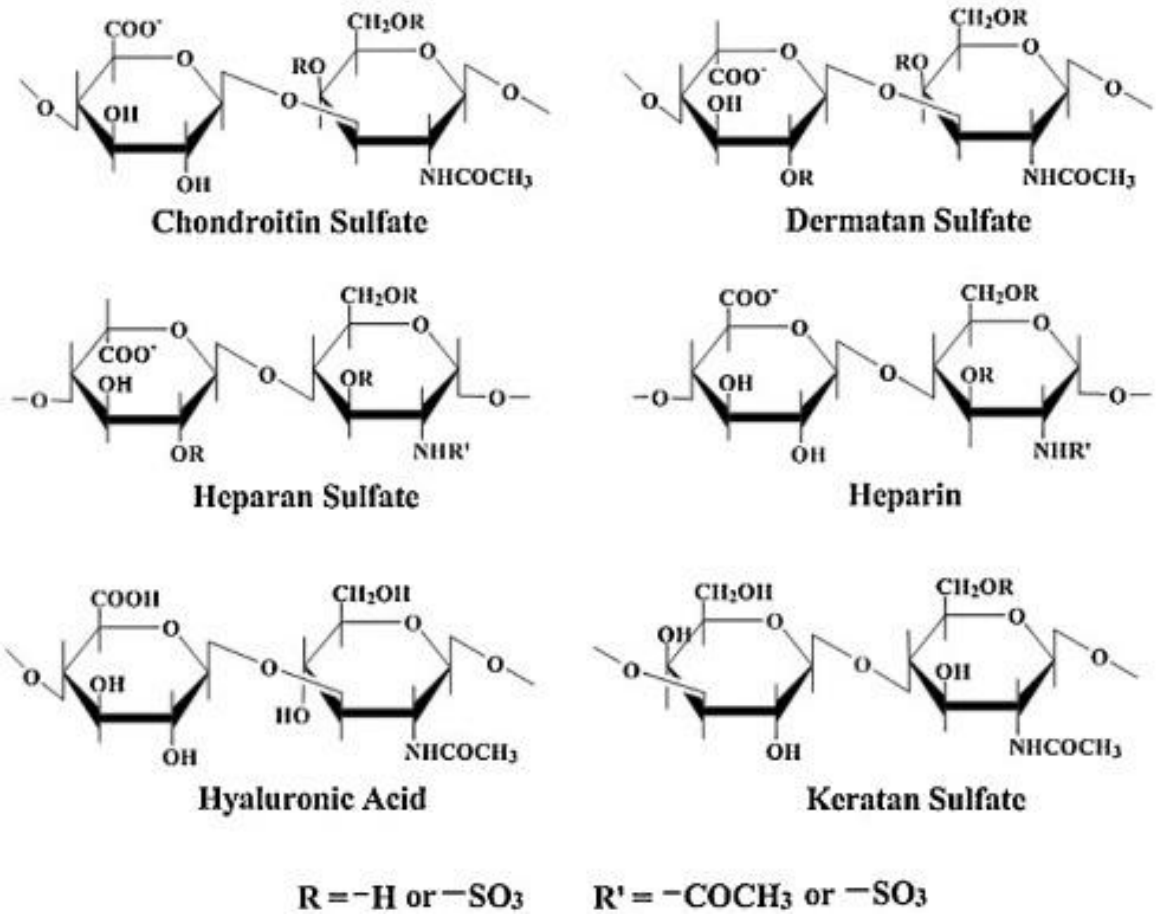

Figure 1.5. The representative structures of disaccharides units of GAGs are shown. Repeating disaccharide units one is an amino sugar (D-glucosamine or D-galactosamine) and the other is typically a uronic acid (D-glucuronic acid or iduronic acid). Each monosaccharide can be N- or O- sulphated (Wang et al., 2017).

There is a high level of heterogeneity in the molecular weight of GAGs, since GAG synthesis is dynamically modified by enzymes. There are four groups of GAGs based on their core disaccharide. The first two: heparin/heparan sulphate (HSGAGs) and chrondroitin/dermatan sulphate (CSGAGs) GAGs, are commonly synthesised in the golgi. The third group is the keratans which differ since they can by modified via O-linked or N-linked glycosylation. The fourth group is HA, which is not synthesised in the golgi, but by integral membrane HA

synthases (HAS). These four groups of GAGs differ in shape, which consequently effects their function (Prydz, 2015).

GAG functions differ greatly. HSGAGs have a role in organizing the ECM through binding other matrix molecules. CSGAGs are located in the extracellular space at the cell membrane and also intracellularly; they are therefore capable of regulating multiple cell processes including proliferation, apoptosis, migration, adhesion and invasion (Afratis et al., 2012). KS GAGs have distinct roles in hydration, and are an anti-adhesive. KS hydration function is specifically important in tissues, such as the cornea, where altered levels of KS are found during macular cornea dystrophy, resulting in loss of hydration and a hazy cornea (Ho et al., 2014).

1.5 Hyaluronan

HA is a high molecular weight anionic, non-sulphated GAG. It is a major component of synovial and soft tissues. 50% of the body's HA is found in the skin tissue. HA content decreases with age, resulting in the loss of moisture and laxity of skin (Buhren et al., 2016).

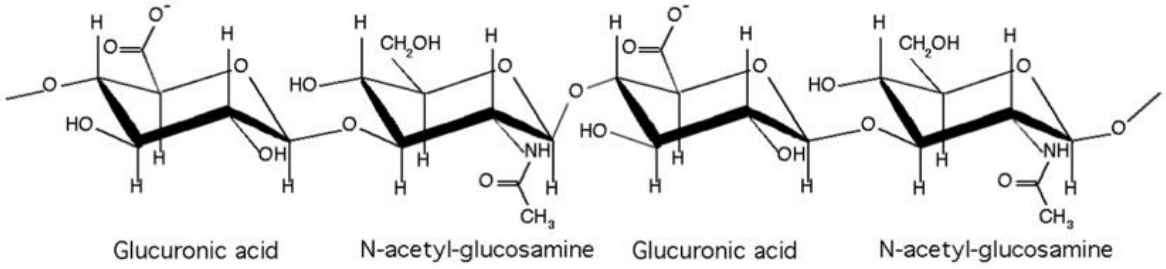

Figure 1.6. The molecular structure of HA, a polymer made of repeated sequences of disaccharides N-acetylglucosamine and D-glucuronic acid, linked together by alternating β-1,2 and β-1,3 glycosidic bonds.

HA also has interactions with matrix and cell surface receptors. Within the matrix HA binds HA binding proteins (HABP) (hyaladherins) e.g. hyaluronectin glial HABP, inter-α-trypsin inhibitor (IαI). Cell surface receptors include CD44, which has been linked to tumour progression and regulation of cell interactions and RHAMM (receptor for hyaluronan-mediated motility) (Day and Prestwich, 2002). Fibroblasts, myofibroblasts, chondrocytes, mesothelial and certain stem cells are known to be surrounded by a pericellular HA coat, which is thought to protect the cells from bacteria and matrix molecules. Stem cells for example are found in their niche rich in HA, which may shield the stem cells from growth factors and thus, differentiation (Qu et al., 2014).

1.5.1 Hyaluronan synthesis

HA has distinct biological functions that are determined, in part, by molecular weight for successful progression through the wound healing stages (Rayahin et al., 2015, Trabucchi et al., 2002). HA is synthesised by three membrane bound enzymes, HAS1, HAS2 and HAS3, of which HAS2 and HAS3 are the primary synthases functional in the dermis. Native HA can have a molecular weight as large as 2×10^4 kDa, but is rapidly cleaved into fragments ranging from 2 to 25,000 disaccharides by several mechanisms including HYAL activity (Reed et al., 2013). HA produced varies by cell type and hyaluronan synthase (HAS) isoenzyme. It is generally thought that high molecular weight HA, approx. 1×10^3 kDa and above inhibits proliferation and migration, and low molecular weight HA, approx. 3-300 kDa, promotes proliferation, migration and is pro-inflammatory. Very low molecular weight HA has also been connected with a reduction in CWFs proliferation (Ferguson et al., 2011).

HAS isoenzymes in mammals are controlled by well-conserved genes with a high degree of homology in their amino acid sequence. But the genes coding for them are located on different chromosomes in humans; HAS1 on Chr 19q13.4, HAS2 Chr 8q24.12 and HAS3 Chr 16q22.1. All three proteins contain seven membrane spanning regions, two at the N-terminal and five at the C-terminal and a large cytoplasmic loop containing the glycosyltransferase catalytic site, with polymerization of HA occurring in the inner side of the plasma membrane (Itano and Kimata, 2002). Each HAS protein alone is capable of HA synthesis. It is thought, however, that each synthase is responsible for the production of different molecular weight HA. Each HAS differs in its ability to synthesis matrix; for example, it has been well-reported that HAS1 produces a smaller pericellular coat than HAS2 and HAS3. This is thought to be due to their differing half-life of activity and binding affinity, with HAS1 having a lower binding affinity and lower half-life. HAS1, therefore has a higher turnover and cannot retain the growing HA chain on the surface. Interestingly, both HAS1 and HAS3 have been associated with the production of low molecular weight HA, while HAS2 produced high molecular weight HA. The idea that each HAS synthase has different enzymatic properties has been attributed to the transcriptional and post-transcriptional regulation of the individual HAS genes, which varies in the context of tissue type and stage of development. Increased transcriptional levels have been linked to increase HA production stimulated by growth factors and cytokines (Itano and Kimata, 2002). This subtly indicates that the regulation of HA biosynthesis by mammalian HAS proteins may be multifaceted, involving enzymatic properties and both transcriptional and posttranscriptional regulation (Itano and Kimata, 2002).

HAS2 has been long established as the primary HAS isoform active in dermal wound healing. Knockout mice of HAS2 also resulted in lethality, demonstrating it is essential for life. Knockout HAS1 or HAS3 mice did not show any phenotypic effects in normal conditions. Double knockout HAS1 and HAS3, however, leads to enhanced inflammation and accelerated wound healing (Siiskonen et al., 2015). These isoenzymes may also form homo- and hetero-meric complexes with each other. It has been shown that HAS2 can form complexes, such as HAS2-HAS1, HAS2-HAS2 and HAS2-HAS3. Heteromeric complexes formed with HAS1 reduced the synthesis of HA, suggesting functional co-operation and regulation of the iso-enzymes (Bart et al., 2015).

HASs are membrane proteins located the cytoplasmic side of the plasma membrane. HA differs from other complex disaccharides, since they are not synthesised in the endoplasmic reticulum and completed in the golgi, but synthesised on the membrane by HAS. It has been recently described that HAS2 and HAS3 travel through the ER golgi, plasma membrane and endocytic vesicles. HAS1 has also been shown to become co-translationally inserted into the ER and travel through the golgi (Rilla et al., 2005).

It has been proposed that HASs secrete extracellular HA, via the creation of an intra-protein lipid-pore, through which a HA-UDP chain is translocated continuously. HAS contains multiple transmembrane domains and its activity is regulated by / dependent on a lipid environment. Cholesterol is a major component in the plasma membrane, playing a role in membrane fluidity and architecture. Cholesterol rich micro domains play a role in optimization of enzyme activity and formation of ordered platforms for assembly of cell signalling molecules (Simons and Ikonen, 1997). This indicates that HAS enzyme activity might be modulated by the same way. However, to date research has only shown that HAS activity can be modulated by the cholesterol environment in a post-translational manner (Ontong et al., 2014). Purified HASs have shown to have low activity without lipids and are activated ~10-fold by exogenous phospholipids. Manipulation of plasma membrane cholesterol content in different cell types causes a decrease in HA production. Modulation of cholesterol might also serve to decrease intracellular synthesis, which could be detrimental to many cellular pathways and functions if in excess (Weigel, 2015). Multiple mechanisms have been suggested as to why cholesterol might affect HAS activity. One suggesting that cholesterol is required for GlcNAc transferase enzymes, producing GlcNAc for HA synthesis, may be structurally stabilized in a cholesterol rich environment (Ontong et al., 2014). The second it that HAS2 activity is regulated by its dimerization and therefore cholesterol might affect its dimerization status. This may be made possible by cholesterol

regulating membrane fluidity, with a richer cholesterol environment resulting in reduced membrane fluidity and therefore increased HAS activity (Ontong et al., 2014). This has previously been shown to have this effect on NA^+ and K^+-ATPase enzymes, with a reduced membrane fluidity leading to a reduction in their activity (Bookstein et al., 1997). HAS1 differs from the other two isoenzymes, since only a small pool of HAS1 protein is located on or near the plasma membrane and it has an intracellular localisation (Siiskonen et al., 2015). This suggests that cholesterol regulation of the HAS enzymes by cholesterol, may be different dependent on their location in the cell.

1.6 Immune Regulation of Dermal Wound Healing

The immune system plays a central role in orchestrating the wound healing process and has therefore been an attractive process to target to promote tissue regeneration. The immune response contributes to wound healing via multiple mechanisms. For example, mobilizing tissue resident progenitor cells, promoting cell differentiation, increasing ECM deposition, stimulating growth factor and cytokine secretion and promoting angiogenesis. Failure of one or many of these processes can cause wound pathologies, such as chronic wounds or scar formation. Chronic wounds are often described having associated persistent infections and microbial films, which result in a prolonged, exacerbated and dysregulated immune and inflammatory response. The result of this are that the wounds are trapped within the inflammatory phase of wound healing. Many of the mechanisms through which immune cells act during wound healing are still unknown. Elucidating these pathways may aid in the development of novel strategies to promote wound healing.

1.6.1. The Role of the Immune System in Acute Wound Healing

Following injury, the wound healing cascade is initiated to restore tissue homeostasis. The wound healing cascade is typically divided into 5 phases: haemostasis, inflammation, proliferation, contraction, and maturation and remodelling. All 5 phases are regulated by various stimuli, of which the immune system plays an integral role.

The innate immune system is considered the first line of defence against infection, involved in the initiation of the inflammatory response. The rapid response of the innate immune system is essential to eliminate the spread of infection and restore tissue homeostasis. This non-specific reaction of this system relies on recognition of highly conserved structures of invading microorganisms, pathogen-associated molecular patterns (PAMPs), or damage-associated molecular patterns (DAMPs). Known PAMPs include: bacterial lipopolysaccharides, lipopeptides, pepdidoglycan, bacterial DNA and double

stranded RNA, and known DAMPs include: heat shock proteins, DNA, inflammation and necrotic cell death (Strbo et al., 2014). These are recognised by a class of receptors called pattern recognition receptors (PRRs), which are expressed on antigen-presenting cells and immune cells. The most well characterised PPR is the Toll-like receptors (TLRs), which upon activation by binding of a PAMP or DAMP, stimulate the release of cytokines, such as IL-1, IL-6, IL-8, IL-12 and TNF-α which promote the migration of inflammatory cells to the site of injury (Strbo et al., 2014). The first of these cells recruited to the site of injury is the neutrophil, facilitated by the expression of TLRs on their surface (Prince et al., 2011). TLR activation on neutrophils leads to the generation of: ROS, antimicrobial peptides and anti-microbial proteases, cytokine and growth factor production, increased cell survival and phagocytosis of invading pathogens with the use of neutrophil extracellular traps (NETs) (Larouche et al., 2018). If this signalling becomes dysregulated it can lead to chronic inflammation and non-healing (Prince et al., 2011). Neutrophil elastase has a direct role in stimulating fibroblast proliferation and differentiation into contractile myofibroblasts, with neutrophil elastase knockout mice displaying reduced myofibroblast formation (Gregory et al., 2015). Secreted cytokines and growth factors are both chemotactic for inflammatory cells, and promote proliferation of fibroblasts, keratinocytes and endothelial cells (Larouche et al., 2018). This secretion also signals neutrophil-mediated monocyte recruitment, the next innate immunity cell type essential for acute wound healing (Larouche et al., 2018).

Monocytes differentiate into mature macrophages, which are regarded as one of the most abundant inflammatory cell types during all stages of wound healing, remaining at the site for several weeks post injury (Willenborg and Eming, 2014). Macrophages primary role during wound healing is to clear cellular debris and necrotic tissue, secondly find and destroy invading pathogens and finally synthesise numerous growth factors which stimulate tissue regeneration (Willenborg and Eming, 2014). It has been reported that following the inflammatory phase of wound healing at the initiation of the prolifaratory phase, macrophages transition from a pro-inflammatory state (M1 state) into an anti-inflammatory state (M2 state). M2 macrophages are capable of secreting anti-inflammatory cytokines such as TGF-β1, promoting ECM synthesis and wound contraction (Larouche et al., 2018). The different roles that macrophages play at different phases of wound healing has been shown, with depletion of early stage macrophages resulting in decreased scar formation, mid stage macrophages resulting in sever haemorrhage, while depletion of late stage macrophage did not have significantly impact the outcome (Lucas et al., 2010). Loss

of macrophages has also been directly linked to impaired wound contracture through the loss of myofibroblast formation (Goren et al., 2009).

The adaptive immune system also plays an integral role in tissue repair and homeostasis, with T lymphocytes (T cells) being critical for tissue remodelling and resolution of inflammation. T cells are recruited to the site of injury via the secretion of IFN-γ from macrophages. There are multiple different types of T cells, each with differential mechanisms that contribute to wound healing. Native γδT cells have been shown to stimulate keratinocyte proliferation via the secretion of various growth factors, such as FGF-7 and FGF-10. γδT cells have been shown to have an attenuated response in chronic wound model, indicating that these cells may also contribute to non-healing in chronic wounds (Xu et al., 2017, Larouche et al., 2018). CD4 and CD69 positive T cells have been shown to contribute to the initial pro-inflammatory wound environment, with αβ T cells capable of regulating this response with an anti-inflammatory response (Rani and Schwacha, 2017). Natural killer T (NKT) cells have also been shown to contribute to early wound repair, with the knockout NKT mice showing significantly accelerated wound closure, by regulating local production of TGF-β1 and collagen deposition (Schneider et al., 2011).

1.6.2. The Immune System and Chronic Wounds

It is well established that the highly coordinated wound healing cascade is halted in the inflammatory phase in chronic wounds, caused by an imbalance between pro- and anti-inflammatory signals. Excess neutrophils at the wound site can lead to an overproduction of ROS. ROS can directly damage the ECM and cell membranes leading to premature cellular senescence. ROS can also activate the proteases and inactivate protease inhibitors (Wlaschek and Scharffetter-Kochanek, 2005, McInnes et al., 2014), which further degrades the ECM and can lead to the degradation of key wound healing factors such as TGF-β1 (Larouche et al., 2018). The excess numbers of neutrophils at the wound site, found in chronic wounds is thought to be caused by the loss of neutrophil apoptosis, a critical event for inflammation resolution. Diabetic chronic wounds in mice have shown to have an increased number of apoptotic cells most being neutrophils (Khanna et al., 2010). Infection has also been shown to effect neutrophil apoptosis, with chronic diabetic wounds in mice infected with *S. aureus* showing reduced neutrophil apoptosis (Hanses et al., 2011).

Macrophages are also an immune cell type affected by the chronic wound environment. The inability of macrophages to changes from an M1 to an M2 phenotype results impairs

healing in humans and mice (Sindrilaru et al., 2011). This switch has also been linked to the suppression of TGF-β1 synthesis, further contributing to non-healing (Okizaki et al., 2015). Wounds with predominant M1 pro-inflammatory macrophage phenotype presence also results in surplus production of proteases and pro-inflammatory cytokine production which further contributes to ECM degradation (Larouche et al., 2018). Similarly, to neutrophils above, macrophages in chronic wound also show reduced apoptosis, prolonging their pro-inflammatory presence in the wounds (Khanna et al., 2010).

The role of the adaptive immune system is less well understood in the context of chronic non-healing wounds, and therefore may be of interest in future studies. It has been found that there are fewer T cells present in chronic wounds and those present have been found to be less responsive (Xu et al., 2017, Loots et al., 1998). The loss of these cells in chronic wound may unveil contributory factors and it is necessary that future work is done to investigate their role in full.

1.7 Genes and Wound Healing

The genetics of wound healing is an understudied area of research. Much is known about the cell and tissue behaviour that lead to repair, but what genes drive these events or in fact which genes are affected in chronic wounds still requires much investigation. Acute wound healing is indicative of initial powerful transcriptional activation of pro-inflammatory genes. These genes include TNF and interferon activation, macrophage markers (CD163, FcγRI and MHC class II α chain), as were markers of T (RAB7L1 and RAB18) and B (immunoglobulin heavy chain) cells. If infection is absent, inflammation subsides and replaced by angiogenic (MMP9 and Progranulin) and remodelling (CTGF and procollagen) genes (Deonarine et al., 2007, Cooper et al., 2005). These genetic markers show us what drives the wound healing cascade. However, it would be of interest to see if genetic risk genes exist that predispose people to developing chronic wounds and thus enable genetic screening of people at risk.

Wound healing is a complex cascade and because of this, investigations into the genetics of chronic wounds have proven to be difficult due to the multifactorial genetic profile that contribute to wound healing in general. However, genetic variations have been identified in patients with chronic wounds, indicating that there may be a genetic element to this multi factorial disease. Gene mutations in the prothrombin and coagulation factor V genes have been identified in patients with venous leg ulcers (VLU), (Peus et al., 1996, Jebeleanu and Procopciuc, 2001). Single nucleotide polymorphisms (SNPs) in the FGF 2 receptor, which

encodes keratinocyte growth factor receptor have been identified in VLU patients, indicating a cause for reduced keratinocyte proliferation and wound healing in these patients (Nagy et al., 2005). SNPs in TNFα gene, encoding a pro-inflammatory cytokine, has also been identified in VLUs linked with the lifestyle factor of obesity (Nagy et al., 2007). A common variant of an estrogen receptor (ESRB), has also been shown to increase risk of VLU development, with estrogen being a well-known accelerator of wound healing by dampening the inflammatory response (Ashworth et al., 2005). Further investigation in this field may provide targets for genetic engineering biotechnologies for enhance chronic wound healing (Sessions et al., 2017).

1.8 Project Aims and Objectives

Chronic wounds are a growing c oncern and have become a significant burden on healthcare providers worldwide. Predominantly age- and diabetes-associated disorders, meaning chronic wounds will become more prevalent, more difficult to treat and have higher associated medical costs. Research into care for these patients has become an industry of its own, with care reported to cost 2-3% of a developed countries healthcare budgets (Frykberg and Banks, 2015). However, long term solutions are yet to be elucidated.

The overall aim of this thesis is to identify which TGF-β1 signalling pathway is responsible for the loss of myofibroblast differentiation in CWFs and identify the key players and mechanisms responsible for this loss. In the longer term, this may reveal potential targets for future therapies.

My specific aims are to:

1. Characterise CWFs response to TGF-β1 stimulation, identifying effects on the two collaborating pathways, classical and non-classical, responsible for myofibroblast differentiation.
2. Determine whether HA has a role in the loss of myofibroblastic differentiation response in CWFs.
3. Elucidate the differences between CWFs and NFs protein synthesis, transport and localisation, and whether changes to protein metabolism may contribute the loss of the myofibroblast phenotype in CWFs.

Chapter 2

Materials and Methods

2.1. Materials

All general and tissue culture reagents were purchased from Sigma-Aldrich (Poole, UK), Thermo-Fisher Scientific (Roskilde, Denmark), BD Biosciences (San Jose, USA), and GIBCO/Life Technologies (Paisley, UK) unless otherwise stated. PCR and QPCR reagents and primers were purchased from Invitrogen and Applied Biosystems (Life Technologies, Paisley, UK). TGF-β1 we purchased from R&D Systems (Abingdon, UK).

2.2. Cell Culture

Primary human non-healing dermal CWFs (AG19642 and AG19285) and apparently healthy dermal NFs (GM23962 and GM23967; NIA Ageing Cell Respiratory Coriell Institute, Camden, USA), were cultured in using a 50:50 ratio of Dulbecco's Modified Eagle's Medium (DMEM: 11966-025; Life Technologies) and F-12 Ham Nutrient mixture (N6658; Sigma-Aldrich) containing 5 mM glucose. This mixture was then supplemented with 2 mM L-glutamine, 100 units/ml penicillin, 100 µg/ml streptomycin and 10 % foetal calf serum (FCS) (Biologic Industries Ltd., Cumbernauld, UK). The cells were maintained at 37°C in a humidified incubator in an atmosphere of 5% CO_2; and fresh growth medium was added to the cells every 3-4 days, until confluent. At confluence, cells were sub-cultured (see below). Prior to experimentation, all cells were growth-arrested in serum-free medium for 48 h to allow cell-cycle synchronisation (arrest at G0) and remove possible effects of serum-borne factors, an established and published technique previously used to study myofibroblast formation (Midgley et al., 2013, Meran et al., 2011, Webber et al., 2009, Simpson et al., 2009, Siani et al., 2015). All experiments were performed in serum-free medium, to avoid any influence of serum factors. Furthermore, all experiments were performed on approximately equivalent cell numbers.

Table 2.1. Coriell Institute Cell Information

Type	Code	Wound Type	Patient age	Race	Infection	Diabetes
NF 1	GM23967	Apparently healthy	52	Caucasian	No	No
NF 2	GM23962	Apparently healthy	27	African American	No	No
CWF 1	AG19285	Venous ulcer	51	Caucasian	Pseudomonas / Staphylococcus	No
CWF 2	AG19642	Pressure ulcer	35	African American	Yes (unkown)	No

2.2.1. Sub-culturing

At confluence, the cell populations were sub-cultured at a ratio of 1:3 and either utilised for experiments, cultured further, or cryopreserved, as described below. Sub-culturing a confluent 75cm^2 culture flask (~2 million cells) (T-75; scale up or down as appropriate), was undertaken by treatment with 5mL 0.05% (w/v) trypsin and 0.53mM EDTA in phosphate buffered saline (PBS). The trypsin was evenly distributed over the base of the flask and incubated at 37°C for 1-5min with slight agitation, or until cells became detached. When examined under a light microscope, detached cells appeared rounded and floating. The resulting cell suspension was treated with an equal volume (5mL) of FCS supplemented medium to neutralise the protease activity. The total volume was then transferred to a centrifuge tube and the suspension centrifuged at 1500×g for 6min at room temperature. Supernatants were carefully aspirated and the cells re-suspended in 50mL medium supplemented with 10% FCS. Cells were seeded into fresh tissue culture flasks for continued growth, or seeded onto tissue culture plates for experimentation. Fibroblasts were cultured, sub-cultured and cryopreserved at various passages until senescence, at which point, senescent cells were no longer used and were discarded. Both normal and chronic wound fibroblasts were determined to retain proliferative capabilities until passage 10, therefore all further experiments were undertaken between passage 8 and 10, this was to generate sufficient cells to undertake all experiments.

2.2.2. Cryostorage and Revival

At sub-culture, low passage fibroblasts were harvested for cryogenic preservation. For one T-75 flask of confluent cells, following trypsin treatment and neutralisation, the cells were re-suspended in a 1.5mL solution containing 10% dimethyl sulphoxide (DMSO), 30% FCS and 60% DMEM/F12 medium. The 1.5mL was then transferred into a cryogenic vial (Thermo-Fisher Scientific). Vials were insulated and initially placed in a -80°C freezer for 24h and then subsequently transferred to liquid nitrogen (-196°C) for long-term storage. Revival of cryopreserved cells was undertaken by rapid thawing at 37°C, using a water bath. Upon complete defrosting of the cryovials contents, the cell solution from each cryogenic vial was transferred directly into 20ml pre-warmed 37°C medium supplemented with 10% FCS. The cell suspension was centrifuged at 1500×g for 6min at room temperature. Supernatant was carefully aspirated and the cells were then re-suspended in 10mL medium supplemented with 10% FCS. Cells were then seeded into a fresh tissue culture T75 flask for continued growth.

2.2.3. Cell Counting and Population Doubling Level (PDL) Calculations

To assess cell numbers, fibroblasts in culture were sub-cultured, as above, using trypsin. Upon cell re-suspension in 10% FCS medium and prior to cell seeding, three 20µL volumes of cell-suspension were taken and each added to 20mL of sterile isotonic water in Coulter Counter compatible sample cups. The average cell counts of three readings were taken for each sample using a Coulter Z2 Series Cell Counter (Beckman Coulter Inc., High Wycombe, UK). The formulae shown below were used to calculate the total number of cells in the re-suspension solution:

Cells/mL = (Average cell number) x 2000

$$Total\ cell\ count = \left(\frac{Cells}{mL}\right) x(Volume\ resuspension\ solution)$$

In order to determine the PDL at the end of each passage number, the following equations were used:

$$Total\ seed\ number[1{:}3\ ratio\ sub-culture] = Total\ cell\ number/3$$

$$PDL = 3.32x(log10(Total\ cell\ count) - log10(Total\ seed\ number)$$

Cumulative population doubling levels were calculated by adding the derived increase to the previous PDL.

2.3. Cytokine Stimulations

Following growth arrest (48 hrs), the medium was removed and the cells washed with PBS. Stimulations were performed by incubation of fibroblasts with the desired stimuli (10 ng/mL TGF-β1, 1 µg/mL IL-1β) in serum-free medium for appropriate times before analysis. Majority of experiments compared cells in either serum-free medium alone or serum-free medium containing 10 ng/mL for 72hrs. This time and duration has been well established in the literature to stimulate full myofibroblast differentiation (Midgley et al., 2013, Meran et al., 2011, Webber et al., 2009, Simpson et al., 2009). The specific details of the cell-stimulations performed for each experiment are covered in the subsequent results chapters.

2.4. HA ELISA

HA ELISA (Corgenix, Inc, Peterborough, UK) was used to quantify HA concentrations. Cells were grown to 90-100% confluence, growth arrested for 48h and then stimulated under serum-free conditions. Supernatant was collected for extracellular HA analysis. Cells were washed with PBS followed with treatment of 500µL trypsin/EDTA and incubated for 5min at room temperature, to detach pericellular HA. Supernatant was collected and heated to 90℃ for 5 min to deactivate trypsin. Remaining cell layer was scraped and re-suspended in 500 µl passive lysis buffer (E194A, Promega, Southampton, UK) to quantify intracellular HA. HA was quantified in the separated cell layers by a commercially available enzyme-linked HA binding protein assay. The assay used micro-wells coated with a highly specific HA binding protein (HABP) from bovine cartilage, to capture HA and an enzyme-conjugated version of HABP to detect and measure HA in the samples. Diluted samples and HA reference solutions were incubated in the micro-wells allowing HA to bind to immobilized HABP. The wells were then washed and HABP conjugated with HRP was added to the wells. Following a second wash, a chromogenic substrate (Tetramethylbenzidine (TMB)/H_20_2) was added to develop a coloured reaction. Stopping solution was added to the wells and the intensity of colour was measured using a spectrometer at 450nm. HA concentrations were analysed by comparing the absorbance of the samples against a reference curve prepared from the blank and five reference solutions (50, 100, 200, 500 and 800 ng/mL) included in the kit. The assay is sensitive to 10ng/mL, with no cross-reactivity with other GAG compounds.

2.5. Red Blood Cell (RBC) Exclusion Assay

RBC exclusion assay was used to confirm the presence or absence of HA pericellular coat. Cells were grown to 70% confluence, growth arrested for 48h and then stimulated under serum-free conditions for 72h. Following stimulation, medium was taken off and the cells were washed with PBS. Formalized horse erythrocytes were washed in PBS and centrifuged at 1,000xg for 6min at 4 ˚C. The pellet was re-suspended in serum-free medium at an approximate density of 1×10^8 erythrocytes/ml. 500 µl of this suspension was added to each 35-mm dish containing sub-confluent cells and swirled gently for even distribution. The dishes were incubated at 37°C for 15min, to allow the erythrocytes to settle around the cells. Control cells were incubated with 200 µg/ml bovine testicular hyaluronidase in serum-free medium for 30min prior to the addition of formalized horse erythrocytes. On settling, the erythrocytes were excluded from zones around those cells with HA pericellular coats. This was viewed under the microscope as an area of erythrocyte exclusion. Zones of exclusion were visualized on a Zeiss Axiovert 100M Inverted Microscope (Zeiss, Cambridge, UK).

2.6. Immunocytochemistry (ICC)

Indirect immuno-fluorescent identification of α-SMA was used as confirmation of myofibroblastic differentiation. All other proteins and markers were visualised to compare localisation in CWFs and NFs. All immunocytochemistry was performed on cells grown on 8-well glass chamber slides (Nunc; Thermo-Fisher Scientific). Cells were grown to 70% confluence, growth arrested for 48h and then stimulated under serum-free conditions. Following stimulation, cells were fixed in cold 4% paraformaldehyde for 15min and then washed thoroughly in PBS. All cells were permeabilised with 0.1% Triton X-100 for 5min and then washed with PBS. Non-specific binding was blocked with 1% (w/v) bovine serum albumin (BSA, Sigma-Aldrich) in PBS (herein referred to as BSA-PBS), for 1h at room temperature and on a STR6 Platform Shaker (Stuart Scientific, Stone, UK). The cells were washed thoroughly in 0.1% (w/v) BSA-PBS. Cells were incubated with the appropriate primary antibody (Table 2.1), diluted in 0.1% (w/v) BSA-PBS overnight at 4°C on a plate Gyro-Rocker. The cells were washed repeatedly in 0.1% (w/v) BSA-PBS, then incubated with the appropriate secondary antibody (Table 2.2), diluted in 0.1% (w/v) BSA-PBS for 1h at room temperature, on a platform shaker under darkness. The cells were washed extensively with 0.1% (w/v) BSA-PBS, before incubation with Hoechst nuclear stain (Sigma-Aldrich; dilution 1:2000 in 0.1% (w/v) BSA-PBS) for 30 minutes at room temperature under darkness. Following further thorough washes with 0.1% (w/v) BSA-PBS, the slides were

mounted with FluorSave mountant (Merck Millipore) and examined under UV-light on a Leica Dialux 20 Fluorescent Microscope (Leica Microsystems UK Ltd, Milton Keynes, UK).

Table 2.2. Primary Antibodies / Markers used for ICC

Antibody	Type	Host	Dilution
Anti-α-SMA (A5228, Life Technologies)	Monoclonal	Mouse	1:25
HAS1 (ab198846, Abcam)	Polyclonal	Rabbit	1:200
HAS2 (sc-34068, Santa Cruz)	Polyclonal	Goat	1:200
CD44 V7/8 (MA5-16964, Thermo Fisher)	Monoclonal	Mouse	1:200
HYAL2 (PA5-24223, Thermo Fisher)	Polyclonal	Rabbit	1:200
Tubulin (ab6160, Abcam)	Monoclonal	Rat	1:1000
LAMP-1 (sc-20011, Santa Cruz)	Monoclonal	Mouse	1:100
EEA-1 (610457, BD Biosciences)	Monoclonal	Mouse	1:500
Endoplasmic Reticulum - Calreticuln (ab92516 Abcam)	Monoclonal	Rabbit	1:200
Golgi - GM130 (ab52649, Abcam)	Monoclonal	Rabbit	1:150
HAPB (Merck, 385911)	-	-	1:100

Table 2.3. Secondary Antibodies / Markers used for ICC

Antibody	Type	Host	Dilution
Anti-Mouse-IgG AlexaFluor 488 (FITC) (A11001)	Polyclonal	Goat	1:1,000
Anti-Rat-IgG AlexaFluor 555 (TRITC) (A21434)	Polyclonal	Goat	1:1,000
Anti-Goat-IgG AlexaFlour 555 (A21432)	Polyclonal	Donkey	1:1,000
Anti-Rabbit-IgG AlexaFlour 488 (A11034)	Polyclonal	Goat	1:1,000
Anti-Rabbit-IgG AlexaFlour 555 (A11037)	Polyclonal	Goat	1:1,000
Avidin (Life Technologies, A21370)	-	-	1:500

2.7. RNA Extraction and Reverse Transcription (RT)

Fibroblasts were grown to confluence in 35mm dishes and washed with PBS, prior to lysis with 500µL TRIzol reagent (Ambion; Life Technologies). RNA was purified from the samples according to the manufacturer's protocol. Briefly, 100µL of chloroform was added to the sample and agitated by inversion for 15sec. The sample was incubated at room temperature for 5 minutes and then centrifuged at 12,000×g for 15min, at 4°C. The transparent aqueous phase was transferred to fresh eppendorfs and mixed with 250µL of isopropanol. The mixture was incubated at room temperature for 10min, briefly vortexed and then centrifuged at 12,000×g for 10min, at 4°C. The supernatant was removed and the pellet washed with 500µL of 75% (v/v) ethanol, briefly vortexed and then centrifuged at 7,500×g for 8min, at 4°C. The supernatant was removed and the pellet air-dried at room temperature for 15min. The pellet was then dissolved in 16µL of RNase-free distilled H_2O (MilliQ; Merck Millipore).

The absorbance was measured at 260nm and 280nm, using a Thermo Fisher Scientific NanoDrop Spectrophotometer. The ratio of 260:280 gave an indication of protein contamination (>1.8 was considered to indicate sufficiently pure RNA for further analysis). The concentration of RNA was calculated from the absorbance at 260nm:

$$\frac{ABS_{260} \text{ x dilution factor (50) x RNA coefficient (40)} = \text{RNA in } \mu g/\mu L}{1000}$$

The RT was performed using the random primer method. The RT was carried out in a final volume of 20µL per reaction, containing 1µg of RNA sample (in 10µL RNase-free distilled H_2O), 2µL of 10x RT random primers, 2µL of 10x RT buffer, 0.8µL of 25x 100mM dNTPs (deoxynucleotide triphosphates; mixed nucleotides: dATP, dCTP, dGTP, and dTTP), 1µL of Multiscribe reverse transcriptase and 1µL of RNase inhibitor. All reagents used were supplied as a high-capacity cDNA reverse transcriptase kit (Applied Biosystems). The RT was performed using a PTC-225 Peltier Thermal Cycler (Bio-Rad Laboratories Inc., Hertfordshire, UK). As a negative control, an RT was performed with RNase-free distilled H_2O replacing the RNA sample. The solution was incubated at 25°C for 5min, to allow the random hexamer primers to anneal to the RNA. The primers were then extended using the reverse transcriptase in the presence of the dNTPs by heating to 37°C for 2h, generating cDNA. The cDNA was then heated to 85°C for 5min, to separate the hybridised complexes consisting of the RNA template and the newly synthesised cDNA, deactivating the reverse transcriptase in the process. The resulting single stranded complementary DNA (cDNA) was stored at -20°C until further use.

2.8. Real Time Quantitative Polymerase Chain Reaction (RT-QPCR)

2.8.1. TaqMan Gene Expression QPCR

Following RT, cDNA samples were made up to 80µL by the addition of 60µL of RNase-free distilled H_2O (MilliQ, Merck-Millipore). QPCR was carried out in a final volume of 20µL per reaction, containing 4µL of cDNA, 10µL of TaqMan Fast Universal PCR Master Mix (20X) (Thermo Fisher), 5µL of H_2O, and 1µL of a TaqMan gene expression assay primer and probe mix (Thermno Fisher) (Table 2.3). A negative control was prepared with RNase-free H_2O substituted for the cDNA. QPCR was simultaneously performed for 18S ribosomal RNA (Thermo Fisher), as a standard reference gene.

2.8.2. Power SYBR Green QPCR

Following RT, cDNA samples were made up to 80µL by the addition of 60µL of RNAse-free distilled H_2O (MilliQ, Merck-Millipore). QPCR was carried out in a final volume of 20µL per reaction, containing 4µL of cDNA, 10µL of Power SYBR Green PCRMaster Mix (Applied Biosystems), 4.8µL of H_2O, 0.6µL of 10µM custom-designed forward primer and 0.6µL of 10µM custom-designed reverse primer (Table 2.4). A negative control was prepared with

H_2O substituted for the cDNA. PCR was simultaneously performed for GAPDH (Table 2.4), as a standard reference gene.

2.8.3. QPCR and Relative Quantification (RQ)

QPCR was performed using the ViiA-7 Real Time PCR System (Applied Biosystems), using either TaqMan Universal or Power SYBR Green PCR Master Mixes (Applied Biosystems) following the manufacturer's instructions. Following completion of the QPCR run, the comparative CT method was used for relative quantification of gene expression. The CT (threshold cycle where amplification is in the linear range of the amplification curve) for the standard reference gene (rRNA or GAPDH) was subtracted from the target gene CT, to obtain the delta CT (dCT). The mean dCT for the experimental control group was then calculated. The expression of the target gene in experimental samples relative to the expression in control samples was then calculated using the formula:

$$2^{-(\,dCT(\text{Experimental Sample}) - dCT(\text{Mean Control Group})}$$

Table 2.4 Taqman Gene Expression Assays

Target	Taqman Gene Expression Assay
18S rRNA	Catalog #: 4319413E
α-SMA (ACTA2)	Hs00426835_g1
EGFR	Hs01076078_m1
CD44	Hs01075861_m1
HAS1	Hs00987418_m1
HAS2	Hs00193435_m1
HAS3	Hs00193436_m1
TSG-6 (TNFAIP6)	Hs01113602_m1
TGF-β1	Hs00998133_m1
TGF-βR1	Hs00610320_m1
SMAD2	Hs00183425_m1
SMAD3	Hs00232222_m1
HYAL1	Hs00537920_g1
HYAL2	Hs011117343_g1
ICAM-1	Hs00164932_m1

Table 2.5 Custom Designed Primers for SYBR Green Assays

Target	Custom Primer Sequence
GAPDH	Forward: 5'-CCTCTGACTTCAACAGCGACAC-3' Reverse: 5'-TGTCATACCAGGAAATGAGCTTGA-3'
EDA-Fibronectin (EDA-FN)	Forward: 5'-GCTCAGAATCCAAGCGGAGA-3' Reverse: 5'-CCAGTCCTTTAGGGCGATCA-3'
FAP	Forward: 5'-AGAACGCCCCCAAAATCTGT-3' Reverse: 5'-GGAAGCTGAAGCCAGGACAA-3'
HYBID (KIA1199)	Forward: 5'-AACCAGCTGGACATGGATGG-3' Reverse: 5'-GTGAGGTAGGAGCCAGGGTA-3'
CD147	Forward: 5'- CAGAGTGAAGGCTGTAAGTCG-3' Reverse: 5'-TCGGAGGAACTCACGAAGAA-3'
HC1	Forward: 5'-TCCATGGAGAACAACGGACG-3' Reverse: 5'-GGGGGTACTGCAAATCCACA-3'
HC2	Forward: 5'-GCCATTTCGATGGTGTTCCG-3' Reverse: 5'--TTCTCTGCTGTGCTACCGTG-3'
HC3	Forward: 5'-CCTTTCGGCTGCTTGGGAAA-3' Reverse: 5'-GACGGCTCTCATGGTGACAA-3'
HC4	Forward: 5'-AGTCACCAAACCCGATGACC-3' Reverse: 5'-GCTCCAGCTGAGTGGACATT-3'
HC5	Forward: 5'-ACTGTCGCTGGAGAACTGTG-3' Reverse: 5'-CGGGGTCCTGATTTCATCGT-3'
IL-1β	Forward: 5'-TCGCCAGTGAAATGATCGCT-3' Reverse: 5'-TGGAAGGAGCACTTCATCTGTT-3'
IFN-γ	Forward:5'-ATGAAATATACAAGTTATATCTTGGCTTT-3' Reverse: 5'-GATGCTCTTCGACCTCGAAACAGCAT-3'
CCL2	Forward: 5'-CCCAAAGAAGCTGTGATCTTCA-3' Reverse: 5'-TCTGGGGAAAGCTAGGGGAA-3'

CCL5	Forward: 5’-CAGTCGTCTTTGTCACCCGA-3’ Reverse: 5’-CGGGTGGGGTAGGATAGTGA-3’
IL-8	Forward: 5’-TTTGGGGTGGAAAGGTTTGG-3’ Reverse: 5’-TCTTGGCAGCCTTCCTGATTT-3’
EGFR-as	Forward: 5’-TCCAGGTGAAGACGCATGAA-3’ Reverse: 5’-GTCTTTTGCAGGCACAGCTT-3’
CD44s	Forward: 5’-GCTACCAGAGACCAAGAC-3’ Reverse: 5’-GCTCCACCTTCTTGACTCCC-‘3
CD44v2	Forward: 5’-CCTGCTACCACTTTGATGAGC-3’ Reverse: 5’-GTGTCTTGGTCTCCAGCCAT-3’
CD44v3	Forward: 5’ -TGCTACCAGTACGTCTTCAAAT-3’ Reverse: 5’-GTGTCTTGGTCTCTGGTGCT-3’
CD44v4	Forward: 5’-CTGCTACCATTTCAACCACACC-3’ Reverse: 5’-TGGTCTCAGTCATCCTTGTGG -3’
CD44v5	Forward: 5’-CAGAATCCCTGCTACCAATGT-3’ Reverse: 5’-TCTTGGTCTCTTGTGCTTGTAGA-3’
CD44v6	Forward: 5’-TGCTACCATCCAGGCAACTC-3’ Reverse: 5’-GGAATGTGTCTTGGTCTCCAGC-3’
CD44v7	Forward: 5’-GAATCCCTGCTACCACAGCCTC-3’ Reverse: 5’-TCTCCCATCCTTCTTCCTGCTT-3’
CD44v8	Forward: 5’-ATGTGTCTTGGTCTGGCGTT-3’ Reverse: 5’-TCCCTGCTACCAATATGGACTC-3’
CD44v9	Forward: 5’-CAGAATCCCTGCTACCAAGC-3’ Reverse: 5’-ACTGGGGTGGAATGTGTCTT-3’
CD44v10	Forward: 5’-TCCCTGCTACCAATAGGAATGA-3’ Reverse: 5’-TAAGGAACGATTGACATTAGAGTTG-3’
CD44v7/8	Forward: 5′AGGAAGAAGGATGGATATGGACT-3′ Reverse: 5′-GTCTTGGTCTCGCGTTGTCA-3′

*Primer efficiency was checked by melt curve analysis, for multiple products.

2.9. Western Blot Analysis

Cells were grown to confluence in 35mm dishes and were scraped and collected in ice-cold PBS. The samples were then centrifuged at 10,000×g for 10 minutes at 4°C and the supernatant discarded, the cell pellet was then re-suspended in RIPA lysis buffer, containing 1% v/v protease cocktail inhibitor, 1% v/v phenylmethylsulfonyl fluoride and 1% v/v sodium orthovanadate (Santa Cruz Biotechnology Inc., Texas, USA). The samples were thoroughly vortexed and kept on ice for 5 minutes, before being centrifuged at 10,000×g for 10min at 4°C. The resulting supernatant was collected and transferred to fresh Eppendorf's. Protein concentrations were determined by Pierce BCA Protein Assay Kit (Thermo Fisher) and the samples were stored at -80°C, until further use. Equal amounts of protein were mixed with equal volumes of 1x reducing buffer and boiled for 5min at 99°C, before being vortexed, briefly centrifuged and allowed to cool on ice for 5min. The samples were then loaded alongside a Westernsure Pre-Stained Chemiluminescent protein ladder onto 7.5% SDS-PAGE gels. Electrophoresis was carried out at 100V for 20min, followed by 150V for 40 minutes; using the Mini-PROTEAN II system (Bio-Rad Laboratories). The separated proteins were then transferred at 100V for 1h to a nitrocellulose membrane (GE Healthcare, Hatfield, UK). The membrane was blocked with PBS containing 0.1% (v/v) Tween-20 (Thermo Fisher) (herein referred to as Tween-PBS) and 1% (w/v) BSA for 1h; and incubated with the appropriate primary antibody (Table 2.5) diluted in Tween-PBS on a plate rocker, at 4°C overnight. The blots were subsequently washed with Tween-PBS, prior to incubation with the appropriate HRP-conjugated secondary antibody (Table 2.6), for 1h at room temperature on a plate shaker. Proteins were visualised using enhanced chemiluminescence (ECL) reagent (GE Healthcare), exposed to Li-cor C-Digit Blot Scanner (Li-cor Biosciences, Cambridge, UK).

Table 2.6 Primary Antibodies and Dilutions used in Western Blot Analysis

Antibody	MW (kDa)	Type	Host	Dilution
P-SMAD2 (3108, Cell Signalling)	60	Monoclonal	Rabbit	1:1000
P-ERK 1/2 (197G2, Cell Signalling)	42, 44	Monoclonal	Rabbit	1:1000
CD44 (217594, Merck Millipore)	~85-95	Monoclonal	Rat	1:1000
Anti-EGFR (GR01, Merck Millipore)	~170	Monoclonal	Mouse	1:200
HAS1 (ab198846, Abcam)	~65	Polyclonal	Rabbit	1:500
GAPDH (sc365062, Santa Cruz)	37	Monoclonal	Mouse	1:2000

Table 2.7 Secondary Antibodies and Dilutions used in Western Blot Analysis

Antibody	Type	Host	Dilution
Anti-Rat-IgG-HRP (ab98391, Abcam)	Polyclonal	Goat	1:5000
Anti-Mouse-IgG-HRP (sc2005, Santa Cruz)	Polyclonal	Goat	1:5000
Anti-Rabbit-IgG-HRP (ab97051, Abcam)	Polyclonal	Goat	1:5000

2.10. Laser Confocal Microscopy

Cells were grown to 70% confluence on sterilised 22mm diameter glass coverslips, in 35mm dishes. Cells were treated and fixed using the same protocol shown in section 2.6. Cells were then incubated with primary and secondary antibodies shown in Table 2.7 and 2.8. Analysis was performed by Zeiss LSM880 Airyscan Laser Confocal Microscopy (Zeiss).

Table 2.8 Primary Antibodies and Markers used in confocal laser microscopy

Antibody	Type	Host	Dilution
Anti-EGFR (GR01, Merck Millipore)	Monoclonal	Mouse	1:200
Anti-EGFR FITC 488 (ab11401, Abcam)	Monoclonal	Rat	1:500
Anti-CD44 (A020, Merck Millipore)	Monoclonal	Rat	1:200
CTX-B AlexaFluor 555 (C22843, Life Technologies)	-	-	1:1000

2.11. Plasmid Generation

2.11.1. HAS2 and HAS1 Overexpression Vector

The pCR3.1 vector containing HAS1 or HAS2 open reading frame was amplified via bacterial transformation into one-shot competent *Escherichia coli* (New England Biolabs); and grown overnight on agar containing ampicillin (100 µg/mL). Single colonies were extracted, cloned and DNA purified, according to the Miniprep Kit protocol (Sigma-Aldrich). Negative RT experiments were performed alongside HAS2 and HAS1 mRNA QPCR, to ensure that pCR-3.1-HAS2 vectors were not conveying false-positive overexpression. All samples were RQ1 DNAse (Promega, Southampton, UK) treated, prior to RT to prevent amplification of open reading frame DNA.

2.12. Overexpression Vector Transfection

Overexpression vectors using the pCR3.1 plasmid were transfected with the Lipofectamine LTX Transfection Kit, according to the manufacturer's protocol (Life Technologies). Briefly, for two 22mm cell culture dishes, 750ng plasmid DNA, 0.75µL PLUS reagent and 4µL Lipofectamine LTX were added to 400µL OPTIMEM transfection medium, mixed well and

incubated at room temperature for 40min. Following incubation, 200µL of transfection solution was then added to each 22mm cell culture dish containing DMEM/F-12 growth medium with 10% FCS. Cells were incubated for 24h, before the medium was replaced with serum-free growth medium for further cell experimentation or analysis. As a negative control, an empty pCR3.1 plasmid (containing no open reading frame sequence) was transfected into cells.

2.13. Small interfering RNA (siRNA) Transfection

Transient transfection of fibroblasts was performed with specific siRNA nucleotides (Table 2.8). Transfection was performed in 35mm dishes using Lipofectamine 2000 transfection reagent (Invitrogen), in accordance with the manufacturer's protocol. Briefly, for transfection of a single 35mm well: two solutions were made, the first consisted of the target siRNA (final transfection concentration of 30nM) in 100µL OPTIMEM transfection medium. The second solution consisted of 4µL Lipofectamine 2000 transfection reagent in 100µL OPTIMEM transfection medium. The solutions were mixed together and incubated for 40min, at room temperature. Following incubation, an additional 800µL of OPTIMEM was added to the transfection solution. The cells were washed with OPTIMEM medium and 1mL transfection solution was added to the cells and incubated 5-7h, after which an additional 1mL of cell culture medium containing 20% FCS was added to the well. Following 24h of incubation, the medium was removed and replaced with serum-free media, in preparation for further cell treatments or analysis. As a negative control, cells were transfected with negative control siRNA (a scrambled sequence that bore no homology to the human genome) (I.D.: AM4611, Thermo Fisher).

Table 2.9 siRNA Nucleotides for siRNA Transfection

Target	siRNA Nucleotides
HAS1	s6454 (Thermo)
HAS2	s5458 (Thermo)
HYAL2	s428 (Thermo)

2.14. MicroRNA-7 RT-PCR

RNA was extracted and purified according to the methods described in conventional RT-PCR (Section 2.7). The RNA sample was diluted to 10ng and RT was performed for miR-7 assay, according to the instructions provided with TaqMan miR Gene Expression Assay Kits (Applied Biosystems). Briefly, a master mix containing 3μL TaqMan looped miR RT primer, 0.15μL 100mM dNTPs, 1μL MultiScribe reverse transcriptase, 1.5μL 10x RT buffer, 0.19μL RNase inhibitor, 4.16μL nuclease-free H_2O was made. Each RT-PCR reaction had a final volume of 15μL, consisting of 10μL Master Mix and 5μL RNA sample. The RT used the following parameters: 30min at 16°C to allow looped RT primer to anneal to the target miR, 30min at 42°C to allow random dNTP and transcriptase extension of the cDNA strand; and 5min at 85°C, to dissociate the looped RT primer from the miR/cDNA strands. The RT was performed on a PTC-225 Peltier Thermal Cycler (Bio-Rad Laboratories Inc.). Samples were cooled to 4°C and then transferred to -20°C, until further use.

2.15. MicroRNA RT-QPCR

MicroRNA RT-QPCR was performed, according to the TaqMan MicroRNA Gene Expression Assay Kit protocol (Applied Biosystems). A Master Mix solution was made consisting of 1μL TaqMan MicroRNA Assay (20X), 10μL TaqMan 2X Universal PCR Master Mix, and 7.67μL nuclease-free H_2O. Analysis was performed in triplicate on a 96-well plate with a final reaction volume of 20μL, consisting of 1.33μL of cDNA and 18.67μL of master mix solution. The plate was briefly centrifuged and the QPCR was performed using the ViiA-7 Real Time PCR System (Applied Biosystems), using TaqMan 2X Universal PCR Master Mix (Applied Biosystems), following the manufacturer's instructions. Following the completion of the QPCR run, the data was calibrated against a house-keeping miR, with no expression change under any experimental conditions performed (miR-16), using the comparative CT method, as described in Section 2.8.3.

Table 2.10 Taqman miR Expression Assay

Target	Taqman miR Expression Assay
miR-16	hsa-miR-16 (UAGCAGCACGUAAAUAUUGGCG
miR-7	hsa-miR-7-5p (UGGAAGACUAGUGAUUUUGUUGU)

2.16. Statistical Analysis

Western blot images were densitometrically analysed by Image Studio (Licor). Graphical data are expressed as averages ± standard deviation (s.d). To test for normal distribution, the Shapiro-Wilk test, followed by the Two-Way ANOVA to test for variances, followed by a Bonferroni post-test to identify statistical significance. Data was analysed using the software Prism 5 (GraphPad) and *$P=<0.05$, **$P=<0.01$ or ***$P=<0.001$ were considered as significant.

Chapter 3

Characterisation of Chronic Wound Fibroblast response to TGF-β1 Stimulation

3.1. Introduction

3.1.1. Dermal Fibroblasts and TGF-β1 Stimulation

Dermal fibroblasts are morphologically characterised by their elongated, flattened and bipolar appearance. They have a branched cytoplasm surrounding a large elliptical, speckled nucleus, containing two nucleoli. Fibroblasts are often described as having a well-defined endoplasmic reticulum and in culture have a differing morphology depending on confluence (Wall et al., 2008). Low confluence fibroblasts in culture have a large surface area and often have multiple protrusions. On the other hand, highly confluent fibroblasts have a smaller surface area, clear bipolar structure and are arranged in parallel to one another (Sutherland et al., 2005).

TGF-β1 stimulates dermal fibroblast to myofibroblast differentiation, which is an essential process for healthy wound healing. Myofibroblasts are characterised by their contractile organized bundles of αSMA positive fibres, which terminate at the fibronexus on the surface of the cell. Functionally, these stress fibres transmit the force to the surrounding ECM. It is important to note that resting fibroblasts lack this contractile, fibrous apparatus (Gabbiani, 2003). The treatment of fibroblasts *in vitro* with exogenous TGF-β1, has previously been described to have marked upregulation of α-SMA gene and protein expression, along with upregulation of the fibronectin variant containing the EDA domain (FN-EDA), which has shown to be essential for fibre formation (Shinde et al., 2015, Evans et al., 2003, Midgley et al., 2013).

Fibroblasts under stress such as aged fibroblasts or CWFs present a ‘stressed morphology’, displaying a larger surface area, stellate appearance and evidence of internal stress fibres (Wall et al., 2008, Simpson et al., 2009). The phenotypic changes observed in these cells are associated with distinct changes in gene and protein expression. These include changes in key genes associated with myofibroblast formation; aged cells have been reported to have a reduced α-SMA gene induction and αSMA fibre formation with TGF-β1 treatment (Simpson et al., 2009). Dermal fibroblasts from chronic ulcers have also been shown to be unresponsive to TGF-β1 treatment, through the loss of gene expression associated with ECM production (Hasan et al., 1997). It is therefore important to understand the mechanisms and pathways that regulate TGF-β1 signalling.

3.1.2. TGF-β1 signalling via the classical TGF-βR pathway

TGF-β1 signalling for fibroblast to myofibroblast differentiation is regulated by two independent but co-operating pathways, the classical TGF-βR pathway and the non-classical HA-CD44-EGFR pathway. TGF-β1 binds a family of transmembrane receptors,

TGF-βRI (ALK5) and TGF-βRII. TGF-βRII binding of TGF-β1 leads to the recruitment of the type-I receptor, forming a heterotetrameric complex which catalyses the phosphorylation of the GS domain of the type I receptor. Both receptors have been shown to be essential for the classical TGF-βR-stimulated pathway (Webber et al., 2009, Zhu et al., 2012). Following activation downstream signalling occurs via SMAD2 and SMAD3 phosphorylation, which together bind a common mediator co-SMAD4 and migrate across the nuclear membrane to activate transcription factors (Gu et al., 2007). Previous research has indicated that SMAD2 is primarily responsible for the TGF-β1 independent alteration in the fibroblast phenotype (Evans et al., 2003).

Research undertaken on CWFs has uncovered defects in the classical pathway that may contribute to the loss of response to stimulating cytokines. This defect in the classical pathway has been determined to be caused by the loss of the TGF-βR2 expression (Kim et al., 2003, Hasan et al., 1997). This loss in receptor expression was also associated with loss of SMAD2 and SMAD3 phosphorylation, which was found to be associated with reduced proliferation in CWFs (Kim et al., 2003).

3.1.3. Non-classical HA-CD44-EGFR pathway

The second pathway regulating the differentiation of fibroblasts into contractile myofibroblasts is the non-classical HA-CD44-EGFR pathway. The HA transmembrane receptor, CD44 can act as a co-receptor for EGFR. Under TGF-β1 stimulation, CD44 is mobile in the membrane and co-localises with EGFR in lipid rafts. Disruption of cholesterol-rich lipid rafts prevents this co-localisation and thus differentiation, showing the essential role of lipid raft formation. Co-localisation also required a HA rich environment for HA-CD44 binding, this interaction is stabilised by TSG-6 and the Inter-Alpha-Inhibitor (IαI) heavy chains, creating a pericellular coat surrounding the cell. TSG-6 interaction with the HC5 of IαI, has been shown to be essential for fibroblast to myofibroblast differentiation and therefore responsible for stabilising the interaction between HA and CD44 (Martin et al., 2016). The synthesis of the HA pericellular coat in fibroblasts is undertaken via HAS2, which is the primary HAS expressed in NFs. Loss of HAS2 in aged fibroblast has been linked to attenuation of myofibroblast formation, with the forced overexpression of HAS2 returning the myofibroblast phenotype (Simpson et al., 2010). CD44-EGFR co-localisation initiates downstream signalling for myofibroblast differentiation via the ERK1/2 and CAMKII pathways. Both ERK1/2 and CAMKII under TGF-β1, signal through a biphasic activation profile, with the early phase of activation being responsible for fibroblast differentiation and the later phase being linked to cellular proliferation (Midgley et al., 2013).

Aged fibroblasts, unresponsive to TGF-β1 signalling, have a compromised HA-CD44-EGFR pathway through the loss of EGFR expression (mRNA and protein) and a reduced motility of CD44 throughout the cellular membrane. This effect was caused by an increased expression of micro-RNA-7 (miR-7), which directly targets EGFR mRNA for breakdown, indirectly causing a downregulation of HAS2 expression. As a result, there is a reduction in HA produced and therefore decrease in HA binding to its receptor CD44. The loss of the HA-CD44 interaction leads to a reduction in CD44 membrane motility which leads to reduced CD44 and EGFR interaction (Midgley et al., 2014). The result of this loss in CD44 and EGFR interaction is seen downstream where a reduction of ERK1/2 signalling is observed in the aged fibroblasts. Similarly, this reduction in ERK1/2 phosphorylation has also been reported in CWFs, which has been hypothesised to be cause by the loss of the TGF-βR pathway. However, it could indicate dysfunction in the HA-CD44-EGFR pathway (Kim et al., 2003, Hasan et al., 1997). To date no one has explored the possibility of a defective non-classical pathway in CWFs, this will be addressed in this chapter.

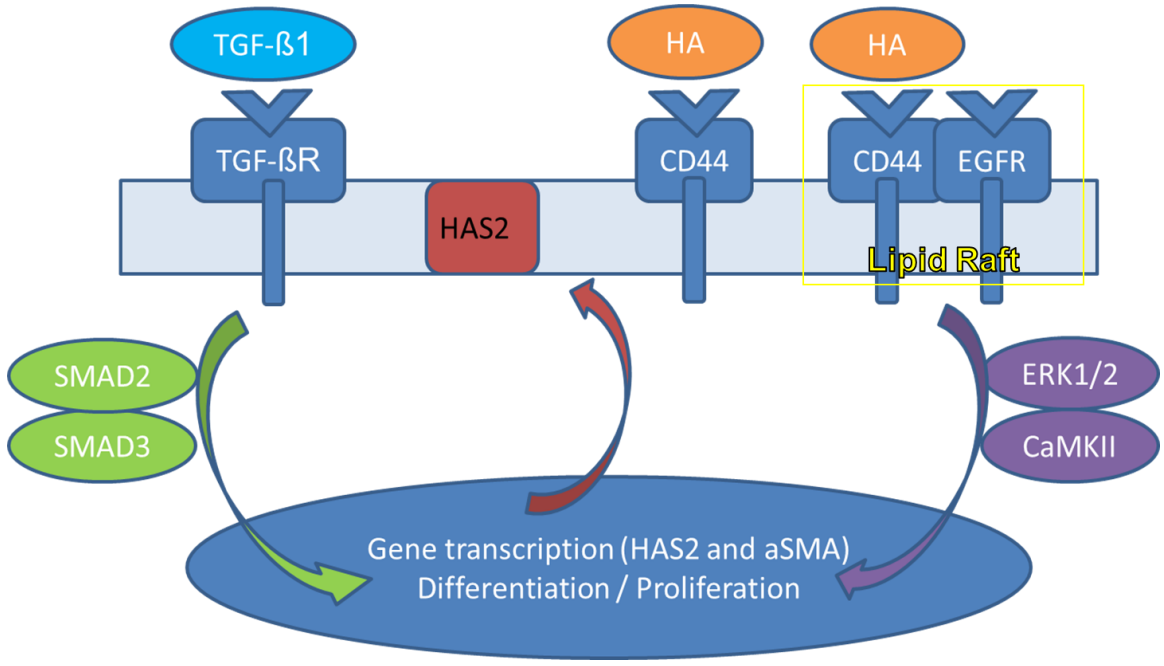

Figure 3.1.1. TGF-β1 stimulated and HA-mediated fibroblast to myofibroblast mechanism. Fibroblasts are stimulated by TGF-β1, TGF-βR is phosphorylated (P), signalling through Smad2/3 and co-Smad4. HA-mediated CD44/EGFR signalling, in membrane bound lipid-rafts, is through ERK1/2 / CaMKII. When both pathways signal in parallel the cell undergoes differentiation into a myofibroblast. Image adapted from (Simpson et al., 2010, Meran and Steadman, 2011)

3.1.4. Genes Associated with Fibroblast Activation

Fibroblast activation protein (FAP) is a homodimeric integral membrane gelatinase belonging to the serine protease family, expressed by stromal fibroblasts in the granulation tissue of healing wounds (Wang et al., 2014). Fibroblasts over-expressing endogenous FAP

have been found to promote fibroblast proliferation and invasion in cancers, and therefore its presence in cancer is unfavourable (Yang et al., 2013). Its activation during wound healing coincides with elevated α-SMA expression, and therefore identifies TGF-β1 activated fibroblasts (Gao et al., 2009, Tillmanns et al., 2015). FAP activation is also associated with increased apoptosis, adhesion and migration, in the fibrotic cell LX-22 hepatic stellate cells. FAP co-localises with collagen and fibronectin, which are essential proteins expressed by myofibroblasts. FAP overexpression is shown to increase expression of the HA receptor CD44, indicating a potential role in the non-classical pathway (Wang et al., 2005). Loss of FAP expression in CWFs may be a novel contribution of this protein has towards non-healing chronic wounds.

Cluster of differentiation (CD)147, also known as basigin (BSG) or extracellular matrix metalloproteinase inducer (EMMPRIN), is another HA-CD44 associated transmembrane glycoprotein, with its expression associated with inflammation, cancer and tissue remodelling (Grass et al., 2014). CD147 is capable of stimulating HA production and co-localises with the HA receptor, CD44, on the membrane, possibly contributing to CD44 membrane motility (Marieb et al., 2004, Slomiany et al., 2009). CD147 also plays a role in intracellular trafficking of proteins from the ER to the plasma membrane (Slomiany et al., 2009). Recently, more evidence demonstrated its involvement in fibroblast to myofibroblast differentiation through an induction of α-SMA in an MMP independent manner (Huet et al., 2008b, Xu et al., 2013). Furthermore, CD147 has been shown to have a regulatory role in Wnt/β-catenin signalling, which controls cell migration, proliferation and the development of fibrosis in the lungs (Hasaneen et al., 2016). Overall, CD147 may be a major contributor to CWFs dysfunction.

HYBID (KIA1199) is a novel HA binding protein, that plays a role in HA degradation independently of hyaluronidase, in dermal fibroblasts (Yoshida et al., 2013b, Yoshida et al., 2013a). HYBID expression increased in disease states, with a subsequent increase in HA degradation (Yoshida et al., 2013a). HYBID expression is supressed by TGF-β1 signalling, correlating with an increase in HAS2 expression (Nagaoka et al., 2015). We know from previous work that HA synthesis via HAS2 is essential for fibroblast differentiation (Simpson et al., 2009).

The aims of this chapter are:

I. Characterise the dermal fibroblasts (normal and chronic) and assess their response to TGF-β1 stimulation.
II. Determine the role of the classical TGF-βR pathway, in the loss of CWFs response to TGF-β1.
III. Analyse the regulation of the non-classical HA-CD44-EGFR pathway, in the loss of the myofibroblast phenotype in CWFs.
IV. Compare HA metabolism in NFs and CWFs and discover whether its dysregulation has a role in CWFs biology.

3.2. Results

3.2.1. Dermal fibroblast characterisation

Initial characterisation of the 4 cell types purchased from Coriel biorepository was undertaken to establish the difference between dermal NFs and CWFs. Phase contrast light microscopy was used to image cells in culture, to define their phenotypic structure. The NFs cells had a typical resting fibroblastic phenotype. The CWFs had a very different structure and morphology, with an enlarged polygonal appearance and prominent stress fibres (Figure 3.1A).

The proliferative lifespans were assessed in all four cell types. CWFs had a decreased replicative life span compared to the NFs, with CWFs reaching their limit at approx. 17 compared to the NFs, which did not reach their limit until approx. 35 PDs. It was also clear that the proliferative capacity of the CWFs was reduced, compared to NFs with reduced population doubling levels observed in CWFs, compared to the NFs following the same period in culture (Figure 3.1B).

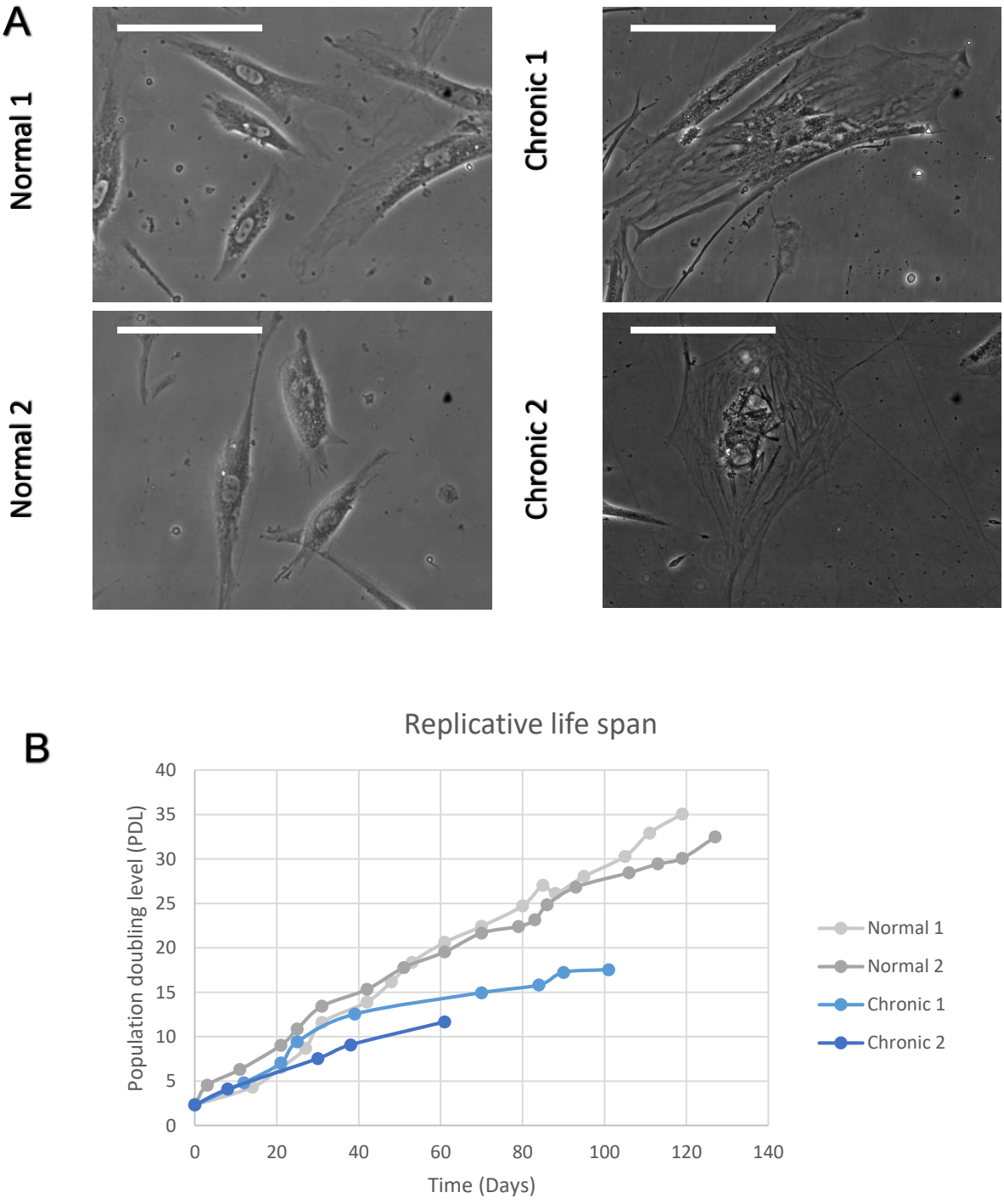

Figure 3.1 Characterisation of dermal fibroblasts. **A**. Representative phase contract micrographs of normal and chronic wound dermal fibroblasts in media containing 10% foetal calf serum (FCS). Original magnification 250x. Scale bar: 100µm. **B**. At each passage (Passage: Confluent T75 flask) cells were counted using a Coulter Particle Count and Size Analyser (Coulter) to calculate PDs. All cells except were still replicating at passage between passage 8-11 and therefore this range was used for all following experiments.

3.2.2. Characterisation of CWFs response to TGF-β1 stimulation

Further to the phenotypic characterisation of the cells, it was important to define their response to the stimulatory cytokine, TGF-β1, which induces myofibroblastic differentiation. The two NFs cells showed clear morphological changes (larger surface area) in response to TGF-β1 stimulation and prominent α-SMA positive fibre formation (Figure 3.2A). TGF-β1 treatment of the CWFs did not induce changes to the same effect. Morphologically, CWFs surface area increased and some α-SMA positive fibres were seen. However, the CWFs response to TGF-β1 was greatly attenuated, compared to that in NFs.

To assess the cellular response to TGF-β1 at a transcriptional level, α-SMA and EDA-FN were measured using qRT-PCR. Both α-SMA and EDA-FN gene expression have been shown to increase in response to TGF-β1 stimulation and are essential for myofibroblast formation. A significant increase in α-SMA and EDA-FN gene expression was observed in the two NFs in response to TGF-β1 treatment (Figure 3.2B/C), thus demonstrating that these cells respond to treatment and underwent myofibroblast differentiation. On the other hand, the CWFs response to TGF-β1 was greatly attenuated. This demonstrates that CWFs are not responsive and are unable to undergo myofibroblast differentiation.

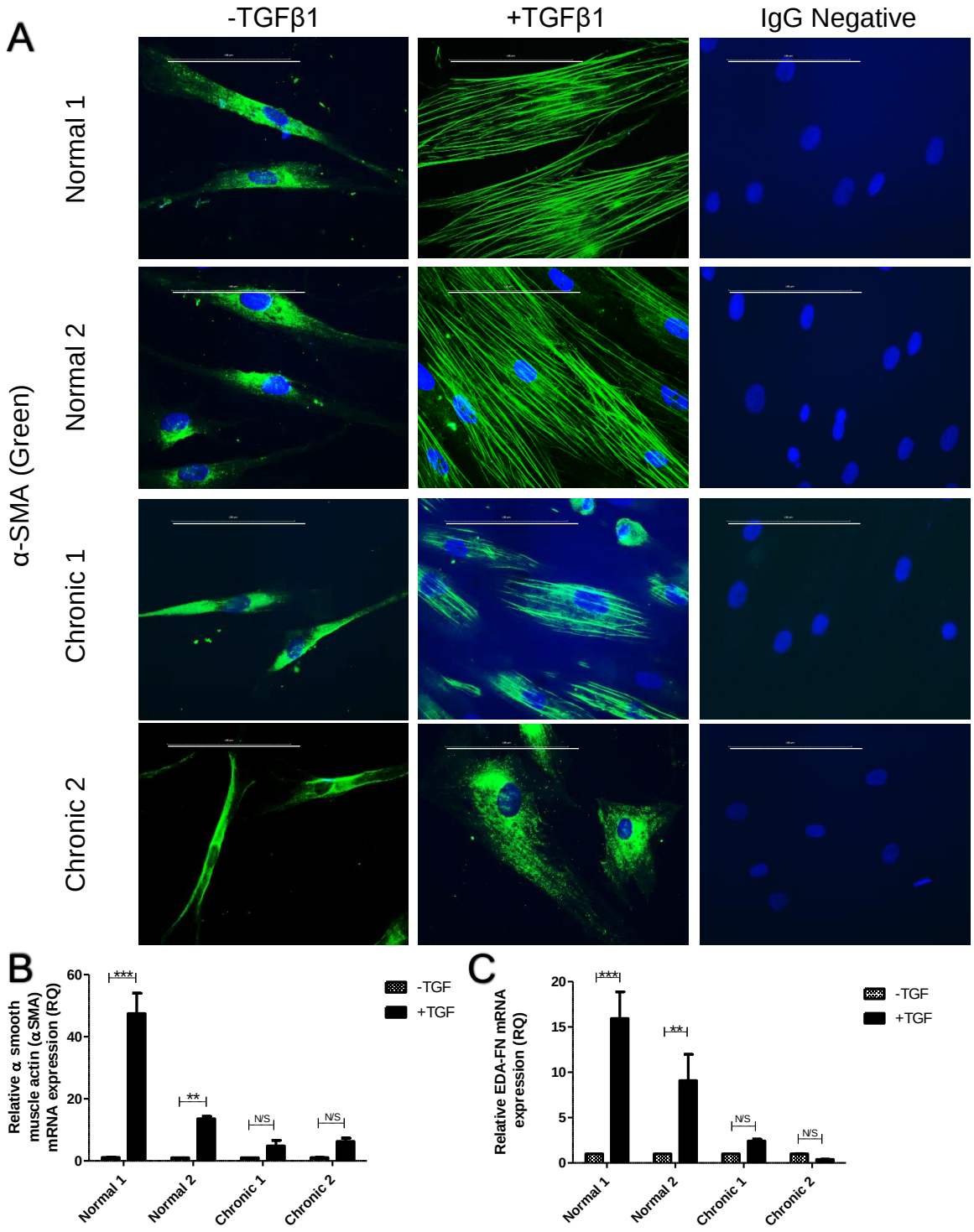

Figure 3.2 Characterisation of CWFs and Normal TGFβ1 induced Myofibroblast Differentiation. A. Cells were grown to 60% confluence and growth arrested for 48hrs. Cells were then incubated in serum-free medium alone (-TGF) or in medium containing 10 ng/mL TGFβ1 (+TGF) for 72hrs. The expression of α-SMA (green) was examined by immunocytochemistry, nuclei were visualised by Hoechst stain. Images shown are a representation of 3 independent experiments. Original Magnification x400. The mRNA expression of **B.** α-SMA **C.** EDA-FN was analysed using QPCR. Results are shown as the mean ± s.d. of 3 individual experiments. Statistical analysis was performed by a 2 way ANOVA with post Bonferroni test: **, p <0.01, **, p<0.001**

3.2.3. TGF-β1 Induction of the Classical TGF-β1 Pathway

Initial results above have indicated that myofibroblast differentiation is lost in CWFs. However, it was still necessary to determine at which point in the pathways (classical or non-classical pathways), this signalling was lost. To determine this, genes associated with the classical TGF-β pathway were measured by qRT-PCR in both the NFs and CWFs, with and without stimulation with TGF-β1. TGF-β1 and its receptor TGF-βR expression were found to significantly increase in response to TGF-β1 stimulation in both the NFs (Figure 3.3 A/B). CWFs also had a significant induction of TGF-β1 gene expression to TGF-β1 treatment. However, TGF-βR gene expression in the CWFs did not respond to TGF-β1 treatment. This may indicate a contributing factor to the loss of differentiation. In order to assess the downstream effects of a loss of TGF-βR induction in the CWFs, the mRNA was measured for the downstream signalling proteins of the TGF-βR (SMAD2 and SMAD3). Overall, no significant change was seen with TGF-β1 treatment in either the NFs or CWFs (Figure 3.3 C/D). This meant that no measurable trend was observed in the NFs, to compare to the dysfunctions in the CWFs.

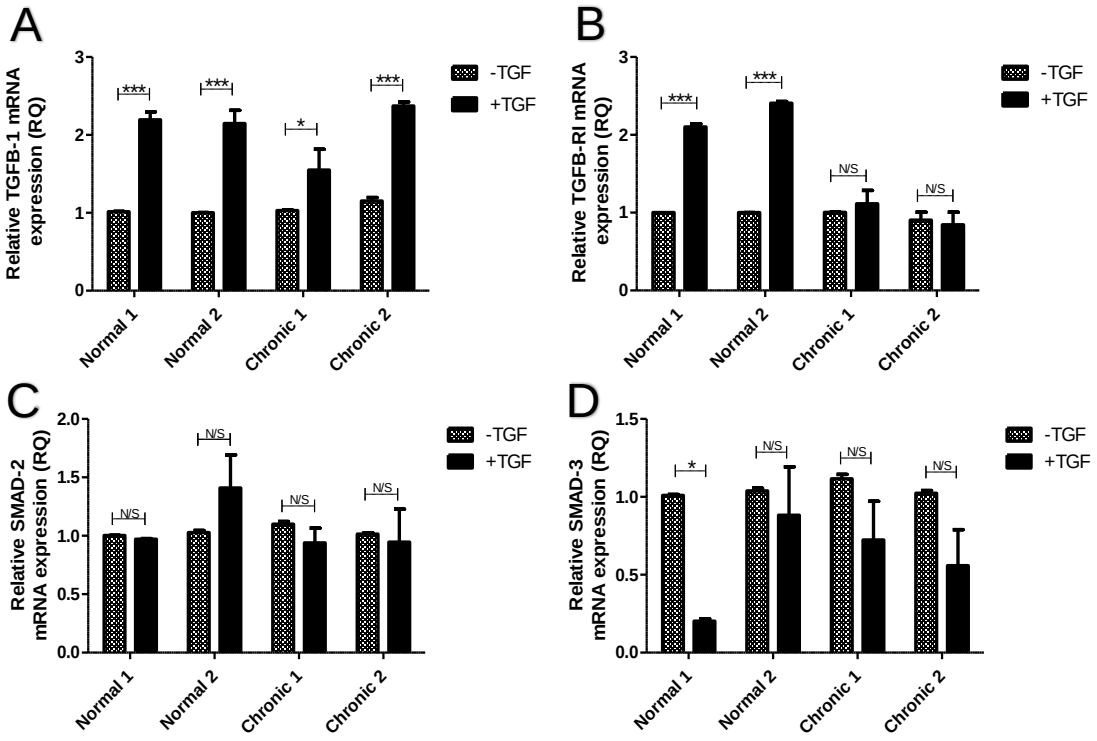

Figure 3.3 Characterisation of the classical TGF-β1 pathway at mRNA level. A/B/C/D. Cells were grown to 100% confluent monolayers and growth arrested for 48hrs. Cells were then incubated in serum-free medium alone (-TGF) or in medium containing 10ng/mL TGF-β1 (+TGF) for 72hrs. The expression of TGF-β1 (A), TGF-βRI (B), SMAD-2 (C) and SMAD-3 (D) were analysed by QPCR. Results are shown as the mean ± s.d. of 3 individual experiments. Statistical analysis was performed by a 2 way ANOVA with post Bonferroni test: *, p <0.01, ***, p<0.001.

3.2.4. Analysis of the Downstream Signalling of the Classical TGF-β1 Pathway

To confirm the previous result, protein analysis was undertaken over a time course to measure SMAD2 phosphorylation and therefore, downstream signalling from the TGF-βR. The NFs saw the greatest increase in SMAD2 phosphorylation at 1h and 3h (Figure 3.4 A/B). Phosphorylation remained increased from 0h up until 72h. This indicates that SMAD downstream signalling was responding to TGF-β1 stimulation and contributing to the differentiation in the NFs. However, the two CWFs had donor specific responses, with Chronic 2 responding more than Chronic 1 to TGF-β1 treatment. Both CWFs showed slightly higher basal levels of phosphorylation at 0hrs compared to NFs. However, increases in SMAD2 phosphorylation were induced at 1hr and 24/72hrs (Depending on donor). This demonstrates that, although apparently different signalling pattern to NFs, CWFs were responding to TGF-β1 signalling via the TGF-βR with downstream signalling via phosphorylation of SMAD2.

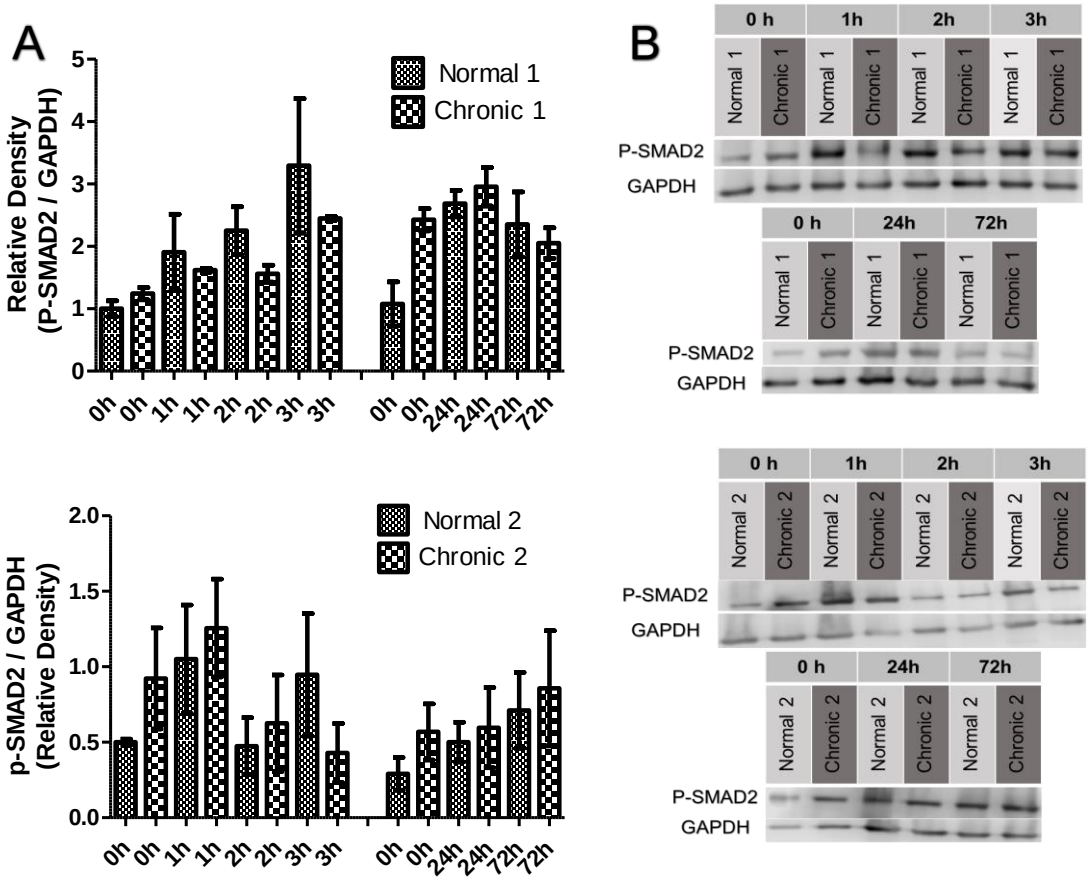

Figure 3.4. SMAD2 phosphorylation, showing downstream signalling of the classical TGF-β1 pathway, is not effected in CWFs. Cells were grown to 100% confluent monolayers and growth arrested for 48h. Cells were then incubated in medium containing 10ng/mL TGF-β1 (+TGF) for either 0, 1, 2, 3, 24 or 72h. Phosphorylation of SMAD2 was analysed by Western blotting. Total GAPDH proteins were used as loading controls. **B.** Images shown are representative of 2 independent experiments. **A.** Densitometric analysis of p-SMAD2, normalised to total GAPDH. Graph shows mean with range of 2 independent experiments.

3.2.5. TGF-β1 Induction of the Non-Classical CD44 / EGFR Pathway

The previous results indicate that the classical TGF-β pathway is largely intact in CWFs and not contributing to the loss of differentiation. The non-classical pathway is an independent yet essential pathway for myofibroblast differentiation. Two main contributors to this pathway are CD44 and EGFR. Both, proteins were measured in the NFs and CWFs, with and without TGF-β1 treatment at mRNA and protein levels. All cells demonstrated a decrease in EGFR expression with TGF-β1 treatment and only Normal 1 exhibited a non-significant decrease (Figure 3.5A). The protein expression followed the same trend, with a decrease in protein quantity measured in all stimulated cell types, compared to their unstimulated controls (Figure 3.5B). CD44 expression also showed a similar trend across all cell types, with decreased expression in response to TGF-β1 treatment (Figure 3.5C). There was no overall trend in CD44 protein expression observed (Figure 3.5D). The similarities between NFs and CWFs demonstrated that production of these proteins were unaffected in CWFs.

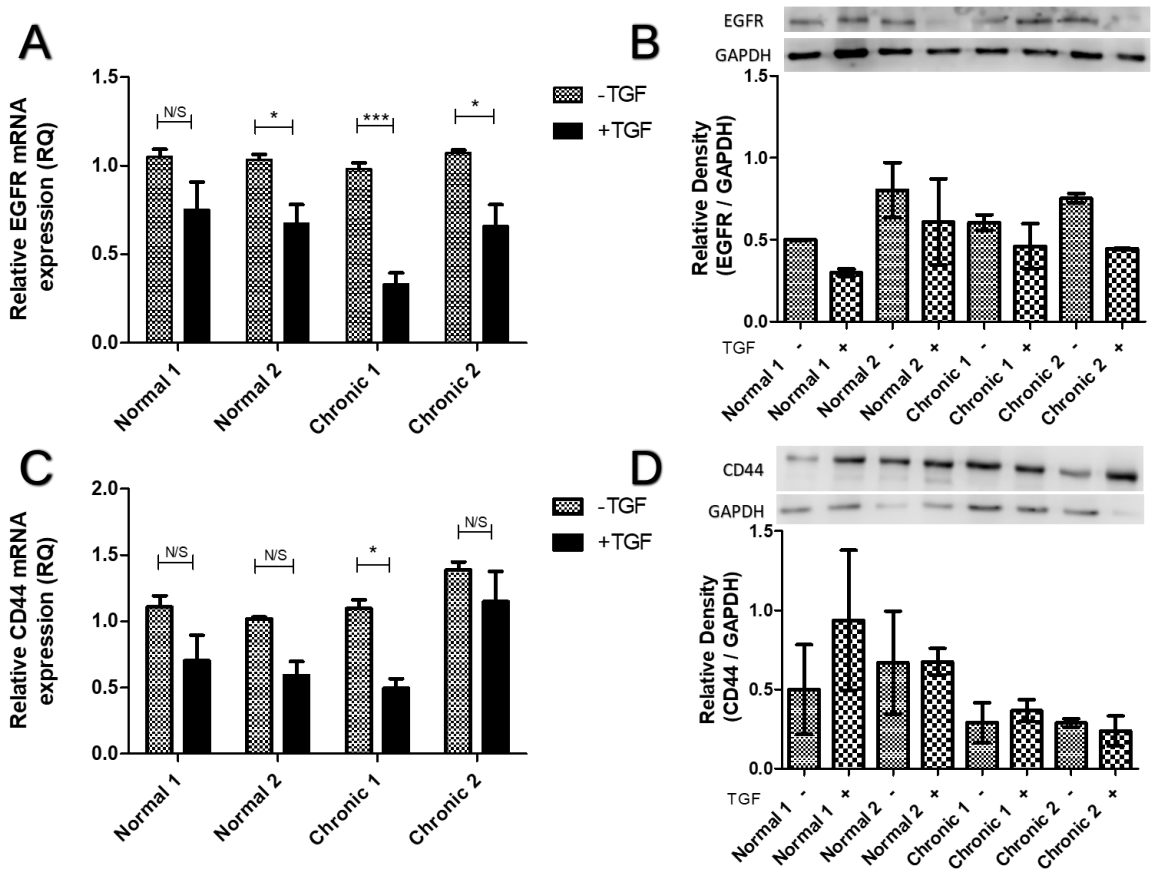

Figure 3.5. Characterisation of CD44 and EGFR expression. Cells were grown to 100% confluent monolayers and growth arrested for 48h. Cells were then incubated in serum-free medium alone (-TGF) or in medium containing 10ng/ml TGF-β1 for 72h (+TGF). The expression of (**A**) EGFR and (**C**) CD44 were analysed by QPCR. Results are shown as the mean ± s.d. of 3 individual experiments. Statistical analysis was performed by a 2-way ANOVA with post Bonferroni test: *, p <0.05, ***, p<0.001. Western blot analysis of total (**B**) EGFR and (**D**) CD44 protein in TGF-β1 treated (+TGF) and control (-TGF) fibroblasts. GAPDH was used as a loading control. Representative blot is shown. Densitometry graph shows mean with range of 2 independent experiments.

3.2.6. Analysis of the Downstream Signalling of the Non-Classical CD44 / EGFR Pathway

The previous result indicated that the production of the two key regulators of the non-classical pathway were unaffected in CWFs. It was, therefore, of interest to quantify the downstream signalling from the non-classical via ERK1/2 phosphorylation (Figure 3.6 A/B). ERK1/2 phosphorylation was quantified across a time-course using Western blotting. Donor specific responses were apparent in all cell types. Normal 1 showed induction at 1h and 3h, whereas, Normal 2 showed induction at 1h and remained at an increased level at 2h and 3h. Chronic 1 phosphorylation followed a similar pattern to Normal 1, with induction at 1h. But, phosphorylation then remained increased at 2h and 3h. On the other hand, Chronic 2 had a high basal level of phosphorylation, which increased slightly at 1h and then slowly decreased over 2h and 3h. Overall, all cell types showed increased ERK1/2 phosphorylation at 1h, demonstrating that the cells were responding to TGF-β1.

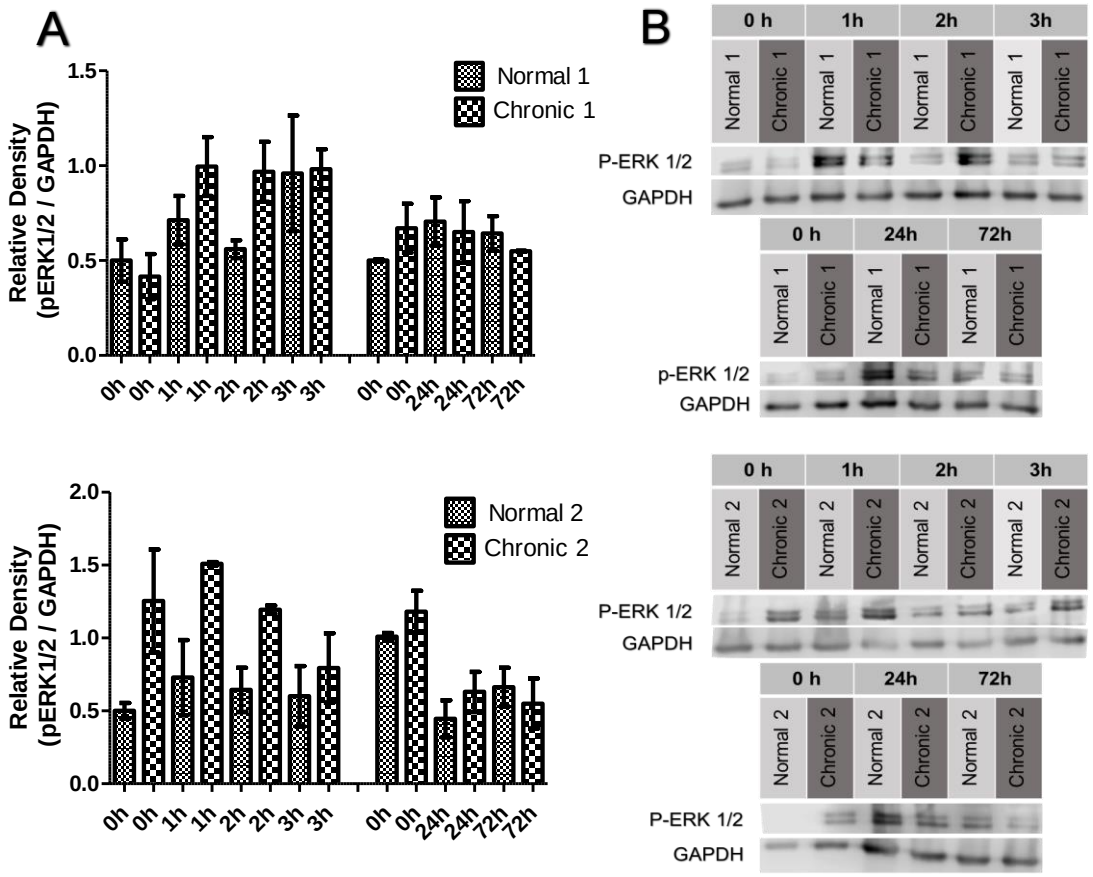

Figure 3.6. ERK phosphorylation showing downstream signalling of the non-classical pathway, is not effected in CWFs. Cells were grown to 100% confluent monolayers and growth arrested for 48h. Cells were then incubated in medium containing 10ng/mL TGF-β1 (+TGF) for either 0, 1, 2, 3, 24 or 72h. Phosphorylation of ERK 1/2 was analysed by Western blotting. Total GAPDH proteins were used as loading controls. **B.** Images shown are representative of 2 independent experiments. **A.** Densitometric analysis of p-ERK 1/2, normalised to total GAPDH. Graph shows mean with range of 2 independent experiments.

3.2.7. HA Associated Gene Response to TGF-β1

HA is another key player in the non-classical pathway responsible for fibroblast differentiation. Four HA associated genes were therefore measured in the two cell types in response to TGF-β1 stimulation. Firstly, there was a significant increase in FAP mRNA expression in the two NFs in response to TGF-β1 treatment, whereas its expression did not change in the CWFs (Figure 3.7A). The loss of this response may contribute to the loss of differentiation in CWFs. Secondly, the overall trend observed in HYBID expression was a significant decrease in its expression with TGF-β1 in all cell types. Since no obvious trend in response was observed between the NFs and CWFs, HYBID can be discounted as having an effect in CWFs (Figure 3.7B).

CD147 and miR-7 expression were more difficult to analyse since, as seen previously, donor specific responses were apparent. Only Normal 2 showed a significant response with treatment, where all other cells had a non-significant response to TGF-β1. Similarly, all cell types showed a non-significant response in miR-7 expression with treatment. The overall trend from these two indicated that they had no role in the loss of CWFs differentiation (Figure 3.7C/D).

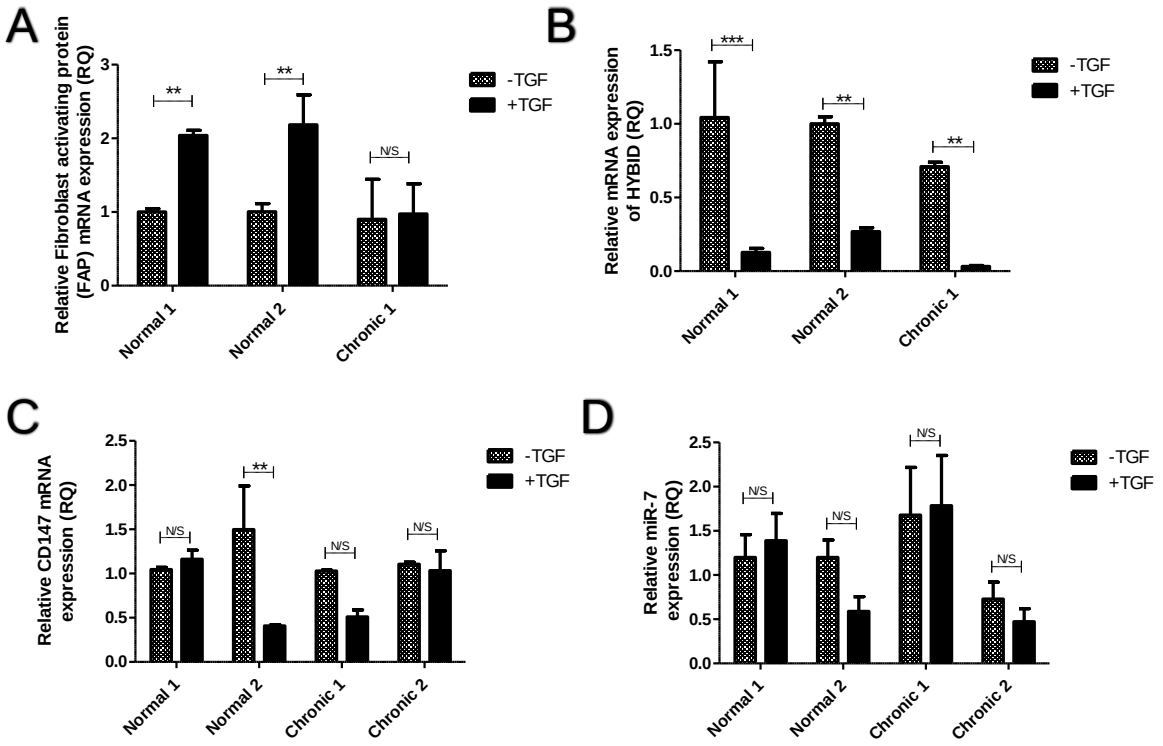

Figure 3.7 Characterisation of HA associated genes in response to TGFβ1 treatment. A/B/C/D. Cells were grown to 100% confluent monolayers and growth arrested for 48hrs. Cells were then incubated in serum-free medium alone (-TGF) or in medium containing 10ng/mL TGF-β1 (+TGF) for 72hrs. The expression of (A) FAP, (B) HYBID, (C) CD147 and (D) miR-7 were analysed by QPCR. Results are shown as the mean ± s.d. of 3 individual experiments. Statistical analysis was performed by a 2 way ANOVA with post Bonferroni test: *, p <0.05, **, p<0.01 ***, p<0.001. Data unavailable for Chronic 2 in A and B, experiments considered pilot experiments.

3.2.8. Hyaluronidase Isoform Expression in CWFs

HA metabolism has been shown to be an essential determinant of fibroblast differentiation. HA breakdown is undertaken via two enzymes, HYAL1 and HYAL2. Aberrant expression of these in CWFs could contribute to dysregulation of the non-classical pathway. mRNA expression of the hyaluronidases was measured using qRT-PCR. No significant difference in expression was found between control and TGF-β1 treated cells in any of the cell types. This indicates that the production of these enzymes was unaffected in CWFs and therefore they did not contribute to CWFs dysfunction (Figure 3.8).

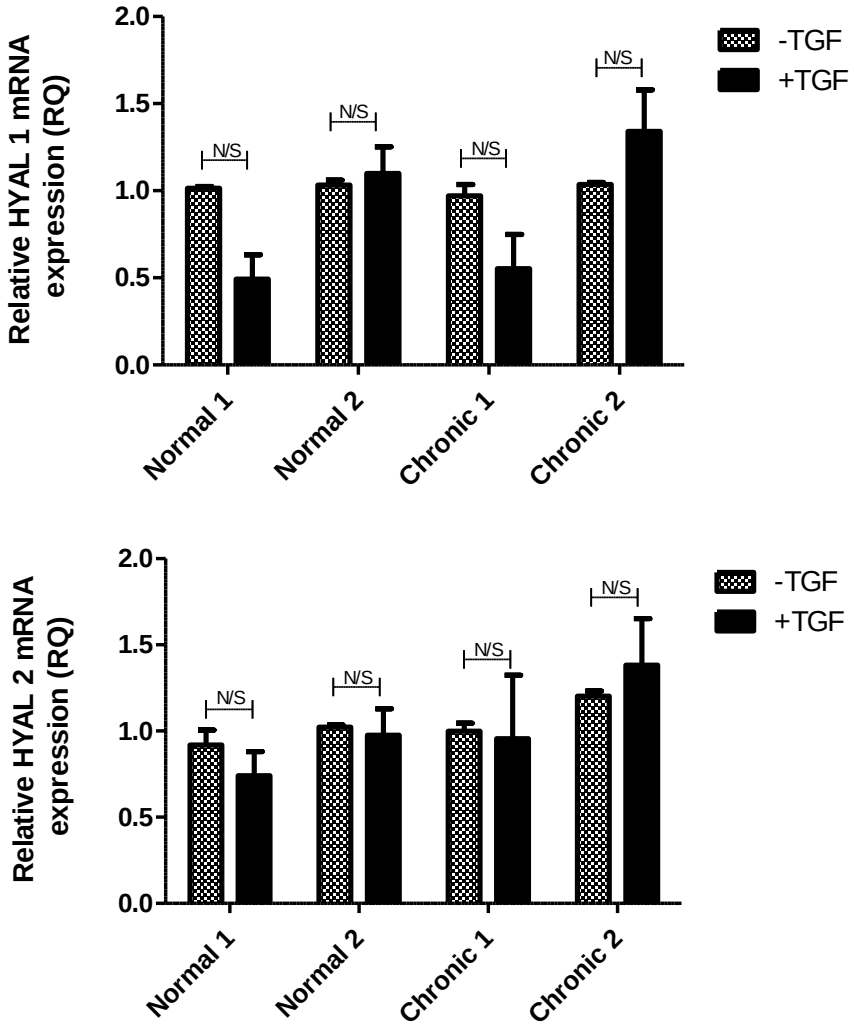

Figure 3.8. Regulation of HA metabolism via Hyaluronidase. Cells were grown to 100% confluent monolayers and growth arrested for 48h. Cells were then incubated in serum-free medium alone (-TGF) or in medium containing 10ng/mL TGF-β1 (+TGF) for 72hrs. The expression of HYAL-1 and HYAL-2 were analysed by QPCR. Results are shown as the mean ± s.d. of 3 individual experiments. Statistical analysis was performed by a 2 way ANOVA with post Bonferroni test: All non-significant (N/S).

3.2.9. HAS Isoform Expression in CWFs

HA is synthesised in mammals via a family of three HAS isoenzymes. The expression of these were measured to obtain any differences between NFs and CWFs. HAS2 has been previously described as the primary HAS isoenzyme involved in the production of the HA coat responsible for myofibroblast formation. Overall, all cell types showed no significant change in HAS2 expression with TGF-β1 treatment (Figure 3.9B). However, a clear trend was seen where HAS2 increased in NFs and decreased in CWFs with TGF-β1 stimulation. This trend maybe contributing to a dysfunctional HA metabolism in CWFs. There was no significant change in HAS3 expression with TGF-β1 in either cell types. The difference with HAS3 compared to HAS2 was that a similar trend was observed in both cell types, with a slight increase in HAS3 expression with TGF-β1 (Figure 3.9C). The most significant finding was from HAS1 expression, where only the CWFs showed a significant increase in expression with TGF-β1 (Figure 3.9A). This was also matched by a higher basal expression observed in the CWFs compared to the NFs. Generally, these results indicate a significant shift in the HAS enzymes, contributing to HA metabolism dysfunction.

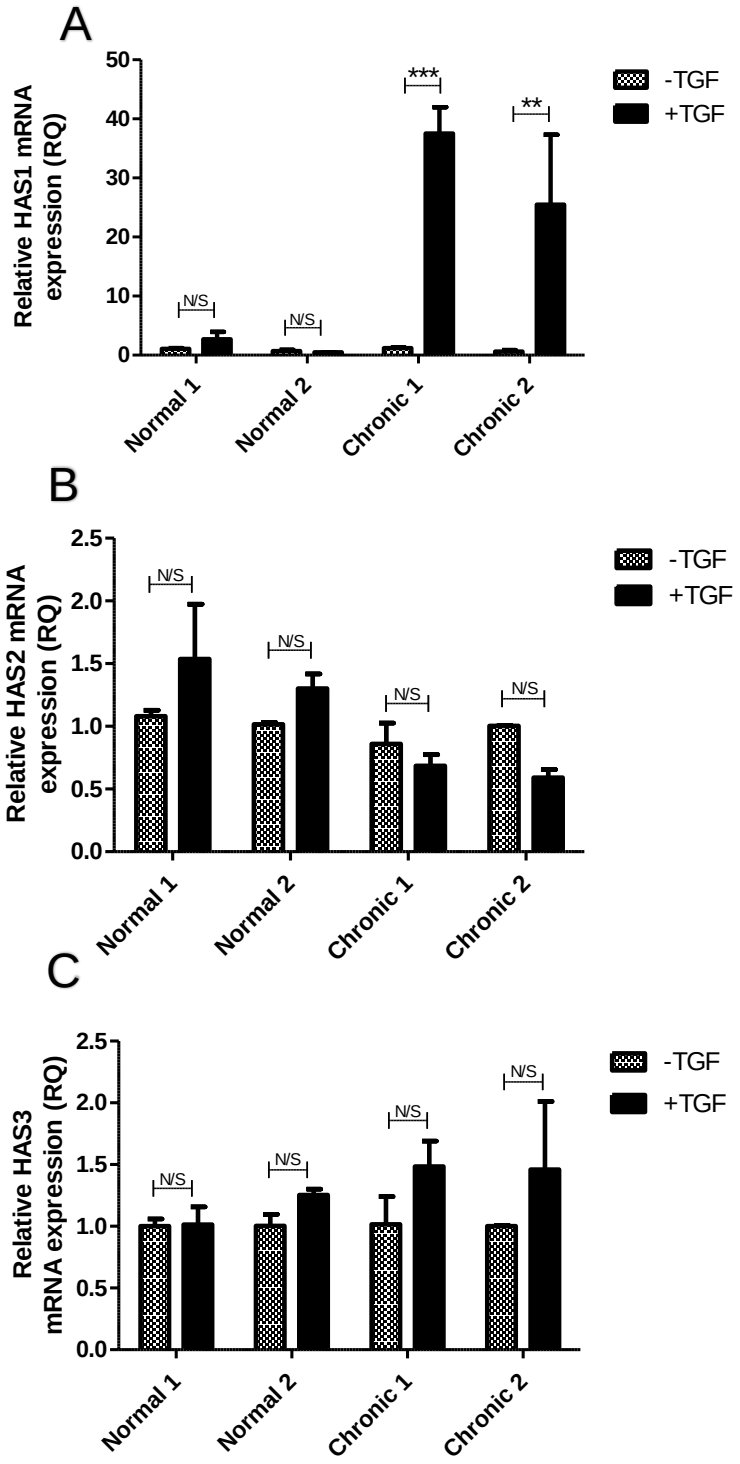

Figure 3.9. HAS isoform expression in normal and chronic fibroblasts. Cells were grown to 100% confluent monolayers and growth arrested for 48h. Cells were then incubated in serum-free medium alone (-TGF) or in medium containing 10ng/Ml TGF-β1 (+TGF) for 72h. The expression of HAS1 (A), HAS2 (B), HAS3 (C) were analysed by QPCR. Results are shown as the mean ± s.d. of 3 individual experiments. Statistical analysis was performed by a 2 way ANOVA with post Bonferroni test: **, $p < 0.01$, ***, $p < 0.001$.

3.2.10. TSG-6 and Heavy Chains

HA binding to its receptor, CD44, is stabilised via TSG-6 and IαI heavy chain interactions. Their expression was therefore measured to understand if they could enlighten further contributions to the dysfunction HA metabolism and non-classical pathway. The overall trend observed with TSG-6 expression was an increase in expression with TGF-β1 treatment, in all cell types. However, it was only a significant increase in Chronic 1 (Figure 3.10A).

The heavy chain expression uncovered some differences between the two cell types. HC1 expression significantly increased with TGF-β1 treatment in the NFs, whereas no changes were observed in the CWFs. The same result was also seen with HC4 and HC5. The opposite result was observed in HC3, with a significant increase in its expression only seen the CWFs. HC2 and HC6 showed no significant change with treatment in either of the cell types (Figure 3.10B. These results might have uncovered further mechanisms that contribute to CWFs dysfunction).

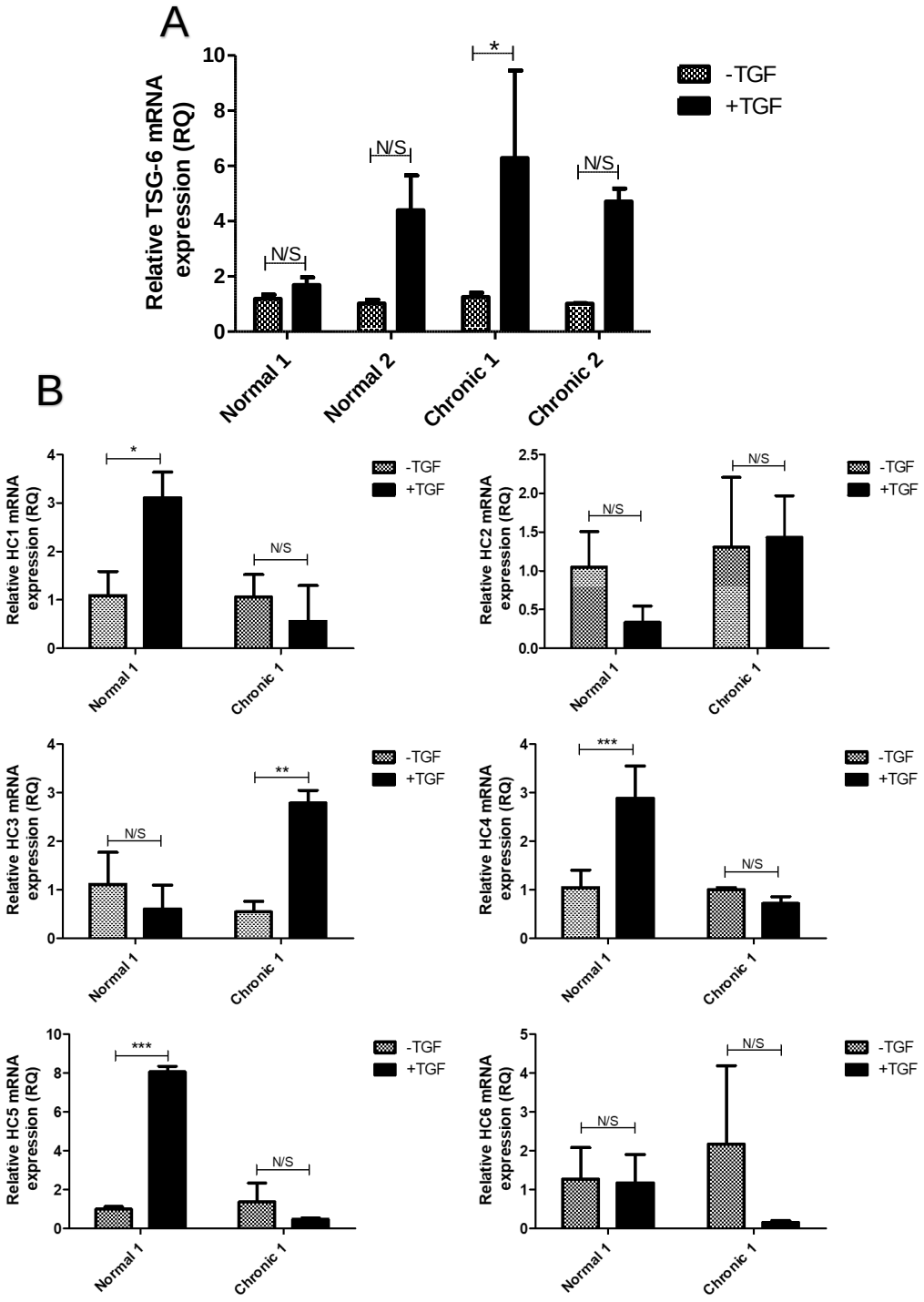

Figure 3.10 Tumour-necrosis-factor-stimulated-gene-6 (TSG-6) and inter-α-inhibitor (Iαl) heavy chains expression in NFs and CWFs. Cells were grown to 100% confluent monolayers and growth arrested for 48hrs. Cells were then incubated in serum-free medium alone (-TGF) or in medium containing 10ng/Ml TGF-β1 (+TGF) for 72hrs. The expression of TSG-6 and heavy chain (HC) 1-6 were analysed by QPCR. Results are shown as the mean ± s.d. of 3 individual experiments. Statistical analysis was performed by a 2 way ANOVA with post Bonferroni test: *, p>0.05, **, p <0.01, ***, p<0.001.

3.3. Discussion

This initial chapter characterises CWFs and their responses to TGF-β1 treatment, in the context of the two contributing pathways that signal myofibroblast differentiation. Insights are provided about possible allied genes to the two pathways and the roles they may play in the loss of CWFs myofibroblast formation. The data reported here build on previous findings on TGF-β1-induced differentiation in NFs, uncovering possible genes that contribute to the loss of the myofibroblast response in CWFs.

CWFs have been previously characterised to have a reduce proliferative lifespan, early onset of senescence with an altered response to TGF-β1 signalling, resulting in the loss of their differentiation capabilities (Kim et al., 2003, Wall et al., 2008). Since the cells used in this thesis had not yet been characterised, specifically in the context of their TGF-β1 response, initial findings from this chapter characterised these cells at a proliferative and differentiation level. The two CWFs showed early onset of senescence and reduced proliferative lifespans, with similar morphologies seen in previous publications such as Wall et al., 2008, confirming their chronic wound phenotype. Further characterisation was undertaken to measure their response to TGF-β1 stimulation and resulting differentiation capacity, as measured via the up-regulation of genes associated with myofibroblasts and the formation α-SMA fibres. Previous studies have shown CWFs to be unresponsive to the stimulatory cytokine TGF-β1 (Hasan et al., 1997, Wu et al., 1999), with other studies demonstrating that the myofibroblast phenotype is absent from the chronic wound environment (Olerud et al., 1995), caused by hypoxia and the loss of granulation tissue from the myofibroblast niche (Alizadeh et al., 2007, Modarressi et al., 2010, Sen and Roy, 2010). To date however, no studies have investigated CWFs α-SMA response *in vitro* and compared to NFs under identical conditions. These results confirmed that CWFs have defective response to TGF-β1 stimulation in the context of differentiation, showing that myofibroblast differentiation is lost in CWFs. This was confirmed with the loss of α-SMA and FN-EDA gene expression, and α-SMA fibre formation in response to TGF-β1 stimulation. Both these genes are known to be essential for the formation of the contractile α-SMA fibres in myofibroblasts (Shinde et al., 2015, Bochaton-Piallat et al., 2016).

The differentiation of fibroblasts to myofibroblasts is regulated by two independent but co-operating pathways, the classical TGF-βR and the non-classical HA-CD44-EGFR pathway. Since differentiation capacity is lost in the CWFs, it was important to establish whether dysregulated signalling in one or both pathways was responsible for this loss. CWFs still significantly responded to TGF-β1 treatment with the upregulation of the TGF-β1 gene.

However, this upregulation was not matched by the upregulation of the receptor TGF-βRI (ALK-5), lost in the CWFs. Previous studies have also shown that TGF-β1 expression does not change between normal and ulcer tissue, but receptor expression is lost in CWFs (Jude et al., 2002, Kim et al., 2003). Since, the loss of receptor expression is apparent in CWFs it was important to measure the downstream signalling from these receptors and therefore gene expression of SMAD2 and SMAD 3 was measured. However, did not show any differences in expression between NFs and CWFs. SMAD2 phosphorylation was subsequently measured over a time-course to compare to previous publications that have indicated that loss of the TGF-β receptor results in the loss of SMAD phosphorylation (Kim et al., 2003). It is apparent from these results that SMAD2 phosphorylation is different compared to NFs, but since the cells used here are not patient matched, they are not directly comparable. Both CWFs show induction of SMAD2 phosphorylation with TGF-β1 at 1h, which is comparable to the 30min induction seen in Kim et al., (2003). These results confirmed previous findings, that SMAD2 phosphorylation is affected in CWFs, but these results also show that SMAD phosphorylation is evident but attenuated, indicating that the TGF-β1 signalling pathway is intact in the CWFs. Aberrant SMAD signalling has also been attributed to a range of other cellular processes, including proliferation, which we know is affected in CWFs (Ten Dijke et al., 2002, Wall et al., 2008). These results clearly indicate that the classical TGF-β1 pathway is affected but intact in CWFs and does not seem to implicate this pathway in the loss of differentiation in CWFs.

The second pathway regulating fibroblast to myofibroblast differentiation is the non-classical pathway, HA-CD44-EGFR. In aged fibroblasts, resistant to myofibroblast differentiation, this pathway has been shown to be impaired, with downregulation of EGFR mRNA and protein expression and reduced CD44 membrane motility (Midgley et al., 2014). Comparatively, the results from this chapter show that neither EGFR or CD44 are affected in CWFs. Combined with the result from Figure 3.7D, showing no difference in miR-7 expression between the CWFs and NFs, confirms that EGFR expression is not affected like the *in vitro* aged fibroblasts shown by Midgley et al, (2014). It has previously been shown that ERK1/2 phosphorylation is lost in the presence of an inhibitor of the EGFR (Midgley et al., 2014). Since EGFR expression is unaffected in the CWFs, it was thought that the downstream signalling via the ERK1/2 pathway would also be unaffected. The results from this chapter, similarly to the SMAD2 phosphorylation results above, show donor specific signalling responses. Overall, ERK1/2 phosphorylation does respond to TGF-β1 treatment in all cell types, with a clear induction seen after 1h. This similarity to the SMAD2 result, conflicts previous evidence that states that ERK1/2 phosphorylation is lost in CWFs (Kim et al., 2003).

This research, however, only examined activation at 30mins, other studies have indicated that TGF-β1 is capable of direct activation of ERK1/2 (Lee et al., 2007). Activation of this pathway may also regulate other cell systems such as proliferation during this time-course (Zhang and Liu, 2002). Simpson et al., (2010) clearly demonstrated that ERK1/2 phosphorylation caused by EGFR signalling was at 10min post TGF-β1 stimulation, which were not assessed. Although these results show discrepancies between ERK1/2 signalling in CWFs and NFs (Kim et al., 2003), they do not conclusively show that the non-classical pathway is inhibited in CWFs and therefore, further associated genes with this pathway were investigated.

FAP is an inflammation and CD44 associated molecule, which has been connected with increased cellular proliferation, adhesion, migration and apoptosis, via TGF-β1 stimulation (Chen et al., 2009, Wang et al., 2005, Bauer et al., 2006). It was therefore interesting to see that FAP induction is lost in CWFs treated with TGF-β1. No current literature directly links FAP activation to myofibroblast formation. However, this loss and the documented co-localisation of FAP and variants of CD44, might indicate its contribution to dysfunction in CWFs (Wang et al., 2005). Another HA-CD44 associated proteins, is the transmembrane glycoprotein, CD147, which is associated with inflammatory diseases, cancer and most importantly tissue remodelling (Grass et al., 2014). Overexpression of CD147 in corneal fibroblasts upregulates αSMA expression and the subsequent contractile potential of these fibroblasts (Huet et al., 2008a). Overall, the results did not indicate any differential expression between NFs and CWFs in response to TGF-β1, thus indicating the lack of a role of CD147 in CWFs biology. The final HA associated gene investigated was HYBID (KIA1199) which has been associated with regulating HA metabolism and synthesis (Nagaoka et al., 2015). In this paper they showed that TGF-β1 stimulation in NFs, decreased HYBID expression which correlated with an increase in HAS2 expression. In Figure 3.7B, NFs also showed a decrease in expression with TGF-β1 treatment. This result is shared with the CWFs, therefore discounting any direct effects HYBID may be having on the loss of the myofibroblast phenotype in CWFs.

CD44 is the receptor for HA, the binding of the two forms a pericellular HA coat that has been shown to be essential for myofibroblast formation. Loss of this coat leads to a non-healing phenotype, such as that shown by *in vitro* aged fibroblasts (Simpson et al., 2009). HA metabolism is therefore a major contributing factor to the successful pro-fibrotic signalling in fibroblasts. HA metabolism is regulated by the enzymes responsible for HA synthesis, HAS1, 2 and 3 and the enzymes responsible for its degradation, the HYALs.

HYALs via their action on HA are modulators of the inflammatory response and are thus generally induced in inflammatory diseases such as chronic ulcers (Fronza et al., 2014, Dechert et al., 2006). HYAL2 has also been specifically linked to TGF-β1 localisation, indicating an interaction (Hsu et al., 2009). The results in Figure 3.8 demonstrated that there were no significant difference in HYAL1 or HYAL2 expressions with TGF-β1 treatment in either NFs or CWFs, indicating it does not have a direct role in the loss of CWFs differentiation. Although, HA degradation does not seem to be affected in CWFs, synthesis of HA was greatly altered. Figure 3.9 demonstrates that HAS1 becomes the predominant HAS isoenzyme expressed in the CWFs compared to HAS2 in NFs. This is evident by a higher resting basal level of HAS1 in CWFs, which has been documented before (Wall et al., 2008), which is also further induced by TGF-β1 stimulation. Corresponding with this was a slight decrease in HAS2 expression in CWFs with TGF-β1, in contrast to the increase seen in the NFs. It has been well documented that HAS2 is the predominant HAS isoenzyme responsible for HA pericellular coat formation in NFs (Simpson et al., 2009). The replacement of this HAS might be significantly detrimental to HA coat formation and thus ability of the CWFs to produce a myofibroblast phenotype.

Changes in HA metabolism are apparent in CWFs but, it is yet to be elucidated whether the HA pericellular coat is lost in this cell type, causing the loss of differentiation. For successful HA coat formation, the interaction between HA and its cell surface receptor, CD44, needs to be stabilised. HA coat stabilisation is undertaken via interaction of TGS-6 and IαI HC5; as knockdown of either inhibits myofibroblast formation (Martin et al., 2016). TSG-6 and HC5 have been shown to respond to TGF-β1 signalling and promote a fibrotic phenotype in fibroblasts (Martin et al., 2016). Although TSG-6 response in CWFs remains similar to that observed in NFs, HC5 response is lost in the CWFs, indicating that the HA coat is lost in these cells. Interestingly, HC1 and HC4 responses are also lost in the CWFs, with HC1 being associated with leukocyte binding to an inflammatory HA matrix (Petrey and de la Motte, 2016) and HC4 being associated with fibrosis in the liver of patients with chronic hepatitis C (Sira et al., 2014). The loss of the response in these two heavy chains may again elucidate contributions to the loss of the pro-fibrotic phenotype in CWFs. HC3 was the only HC that responded to TGF-β1 in CWFs without showing a response in NFs, this may indicate its role in stabilizing the HAS1 produced HA matrix in CWFs.

At this point we cannot exclude that more than one abnormality, possibly several independent ones, exist in CWFs, including aberrant TGF-βR expression and the phosphorylation of key signalling proteins of the SMAD and ERK family. This chapter has

characterised the NFs and CWFs, confirming their chronic wound phenotype and determined that their ability to differentiate into contractile α-SMA positive myofibroblast is lost. This loss however, is not due to the classical TGF-βR pathway that remains intact, responding to TGF-β1 stimulation. Analysis of key regulators of HA metabolism and stabilisation indicate dysregulation of the non-classical HA-CD44-EGFR pathway. The loss of HAS2 congruent with the overexpression of HAS1 indicates a different HA matrix is being synthesised by CWFs, together with the loss of HC5, further adds to the hypothesis that the HA pericellular coat maybe lost in the CWFs, leading to the loss of myofibroblast differentiation signalling.

Chapter 4

The Role of Hyaluronan in The Loss of the Myofibroblast Response in Chronic Wound Fibroblasts

4.1. Introduction

In the previous chapter, it was found that the loss of myofibroblast differentiation in CWFs was not due to defective TGF-β1/TGF-βR pathway or its downstream signalling via SMAD phosphorylation. However, the independent non-classical pathway described previously (Midgley et al., 2013), might be affected in CWFs, as a result of the differential aberrant HAS isoform expression observed in the CWFs treated with TGF-β1. HAS1 had a higher basal expression in the CWFs and its expression was further induced with TGF-β1 treatment, whereas NFs had a very low expression. Previous studies have shown that HA plays a large role in the differentiation mechanism of fibroblasts. HA binds its cell surface receptor, CD44, which causes the formation of a HA pericellular coat surrounding the differentiated myofibroblasts. The loss of this coat prevents differentiation, HA metabolism is therefore essential for differentiation to occur (Meran et al., 2007). HA is synthesised by HAS enzymes, HAS2 has been found to be the primary HAS isoform responsible for producing HA for the formation of the pericellular coat during differentiation in NFs. HAS2 expression is vital for differentiation, with silencing HAS2 resulting in the loss of the myofibroblast phenotype (Simpson et al., 2009).

4.1.1. Hyaluronan's role in wound healing

HA is a ubiquitous GAG component of the ECM, found in almost all connective tissues. 50% of the body's HA is found in the skin, which indicates HA's vital role in wound healing (Buhren et al., 2016). Due to its unique physical qualities, HA creates an excellent wound healing environment. HA synthesis is induced following injury to the skin and has been found to have vital roles in scarless foetal wound healing (Zgheib et al., 2014). In addition, its exogenous application has been found to enhance wound healing in animal models. HA via its receptors can modulate cell inflammation, migration, adhesion, proliferation, differentiation and angiogenesis (Su et al., 2014).

The action of HA is dependent on its molecular weight size. High molecular weight HA has an anti-inflammatory, anti-angiogenic and immunosuppressive function by modulating the immune response. High molecular weight HA also supports cell integrity and is highly expressed in normal tissues. High molecular weight HA can cause cell-cycle arrest, and also protect against apoptosis mediated by nuclear factor kappa-B (NFs-κB) (Wolf et al., 2001). On the other hand, low molecular weight HA is a potent pro-inflammatory, angiogenic and immune stimulatory molecule. The presence of small HA fragments is associated with tissues under stressed conditions. Very small fragments, such as the tertrasaccharides, however, have been found to regulate the intensity of effects caused by the intermediate

low molecular weight HA, by identifying tissue injury through toll-like receptors (Litwiniuk et al., 2016, Aya and Stern, 2014). The increased catabolism of high molecular weight into low molecular weight fragments by the actions of the hyaluronidases, has been linked to inflammatory conditions (Harada and Takahashi, 2007).

HA can exist in a number of forms. HA can be membrane bound to HA-binding proteins known as hyaladherins, such as CD44, or soluble in the ECM or cytoplasm. HA can also be synthesised intracellularly under stressed conditions. The exact role of intracellular HA is still uncertain. Intracellular HA has been linked to: mitosis (by providing a more favourable milieu for nuclear division), endoplasmic reticulum stress and the formation of HA cables (which facilitate monocyte binding and inflammation). The accumulation of perinuclear HA is observed in rat kidney diabetic models, which again was linked to an influx of monocytes and macrophages. Chronic inflammation is proposed to be caused by the lack of breakdown of this uniquely pro-inflammatory HA matrix (Hascall et al., 2004). Multiple cell types have been shown to breakdown and endocytose HA, such as macrophages and keratinocytes, mediated by the cell surface receptor CD44 (Harada and Takahashi, 2007).

4.1.2. Hyaluronan's role in myofibroblast differentiation

HA has functions throughout the wound healing cascade, influencing cellular adhesion, proliferation, migration and a central role in orchestrating myofibroblastic differentiation, via the non-classical HA-CD44/EGFR pathway. This pathway is an independent but collaborating pathway to the classical TGF-β1/TGF-βR pathway, the loss of either pathway results in loss of differentiation. In the non-classical pathway HA binds its cell surface receptor, CD44, creating a HA-rich pericellular coat. CD44 also co-localises with EGFR within lipid rafts on the membrane surface. This co-localisation leads to downstream signalling via the ERK1/2 and CAMKII pathway which signals for differentiation (Midgley et al., 2013). Loss of this HA coat leads to failed differentiation. HA regulates fibroblasts response to TGF-β1 by altering the levels of HA produced, via HAS2 expression (Midgley et al., 2013).

4.1.3. HAS2 regulation and synthesis of HA pericellular coat

HA is synthesised via three identified mammalian HA synthase isoenzymes, of which HAS2 shows the greatest expression in NFs. Each synthase has been shown to produce different quantities and sizes of HA, with HAS2 producing large amounts of high molecular weight HA (Ferguson et al., 2011). Endogenous treatment of TGF-β1 in fibroblasts has shown to induce HAS2 mRNA expression. Loss of HAS2 expression in aged fibroblasts results in the

loss of the cells ability to produce a pericellular coat. Overexpression of HAS2 expression in aged fibroblasts, restored their ability to produce a pericellular coat and thus, differentiation (Simpson et al., 2009). HAS2 ability to create a pericellular coat is due to its membrane association, however this has also been detectable in an ER-golgi area (Bart et al., 2015).

4.1.4. HAS1 expression in CWFs

HAS1 expression during embryogenesis is more limited than HAS2 and HAS3, with knockout HAS1 animals having no apparent phenotype, compared to knockout HAS2 which is lethal during early embryogenesis. Because of its low expression in normal tissue, research into its function has remained elusive. The expression of HAS1 and its splice variants is found to increase under disease states (Siiskonen et al., 2014). It has previously been shown that CWFs have a higher basal expression of HAS1 compared to normal dermal fibroblasts (Wall et al., 2008). HAS1 expression is very low in NFs, however induction has been observed following TGF-β1 and IL-1β stimulation (Siiskonen et al., 2014). The location of HAS1 has been well reported as an intracellular isoenzyme, being present diffusely throughout the cytoplasm, or in patches, with possible co-localisation with the golgi apparatus (Ghosh et al., 2009). This may indicate that HAS1 is responsible for intracellular HA synthesis.

4.1.5. HAS1 synthesised HA and inflammation

HA is generally accepted as a regulator of inflammation, with low molecular weight HA fragments found to be pro-inflammatory (Termeer et al., 2002). HAS1 has been associated with the production of low molecular weight HA (Itano and Kimata, 2002). The previous chapter demonstrated that HAS1 expression can be regulated via the presence of cytokines, such as TGF-β1, with HAS1 expression generally being associated with pro-inflammatory cytokines. IL-1β is a pro inflammatory cytokine implicated in pain, inflammation and autoimmune conditions (Ren and Torres, 2009). HAS1 expression has been shown to be induced by the action of IL-1β, which indicates its role in the inflammatory response (Yamada et al., 2004, Kao, 2006). Numerous other pro-inflammatory cytokines have also been shown to regulate HAS1 expression including, interferon gamma (IFN-γ), tumour necrosis factor alpha (TNF-α) (Campo et al., 2006). Not only does HAS1 respond to cytokines, HA produced by HAS1 may contribute to the regulation of cytokines. These include the pro-inflammatory cytokines, monocyte chemoattractant protein 1 (MCP-1 also known as CCL2), intercellular adhesion molecule 1 (ICAM1) and interleukin 8 (IL-8) that are induced in the presence of low molecular weight HA, that may be produced by HAS1 (Beck-Schimmer et al., 1998, McKee et al., 1996, Oertli et al., 1998). Other pro-inflammatory

mediators such as regulation on activation, normal T-cell expressed and secreted (RANTES also known as CCL5) may contribute to the expression of CD44 molecules expressed on T-cells, allowing them to bind HA present at wound sites (Oertli et al., 1998). Clearly, there is an association of HAS1 derived HA and pro-inflammatory cytokines which may indicate a potential reason for the higher expression of HAS1 in CWFs, observed in the previous chapter. This association between HAS1 and inflammation will be investigated further in this chapter.

4.1.6. The aims of this chapter are:

I. Determine the role of HA in the dysregulation of myofibroblastic differentiation in CWFs.
II. Analyse the location of HAS isoenzymes in relation to endogenously synthesised HA.
III. Attempt to recover the myofibroblast phenotype in CWFs by manipulation of the HA metabolism.
IV. Explore the role of HAS1 expression in CWFs.

4.2. Results

4.2.1. Localisation of Total HA does not change with TGF-β1 Treatment

Total HA (intracellular and pericellular) distribution was analysed using HABP and fluorescence microscopy. Both CWFs and NFs were grown to 60-70% confluence, growth arrested and then either incubated in serum free media or media stimulated with TGF-β1 (10 ng/mL) for 72h. Stimulation of the NFs with TGF-β1 resulted in HA being organised into clear parallel lines (Figure 4.1). Distribution of HA in the CWFs seemed less organised, with possible areas of HA clustering. Overall, the intensity of HA staining between the control and the TGF-β1 stimulated cells did not change in either cell type, which demonstrated only a change in HA distribution in CWFs.

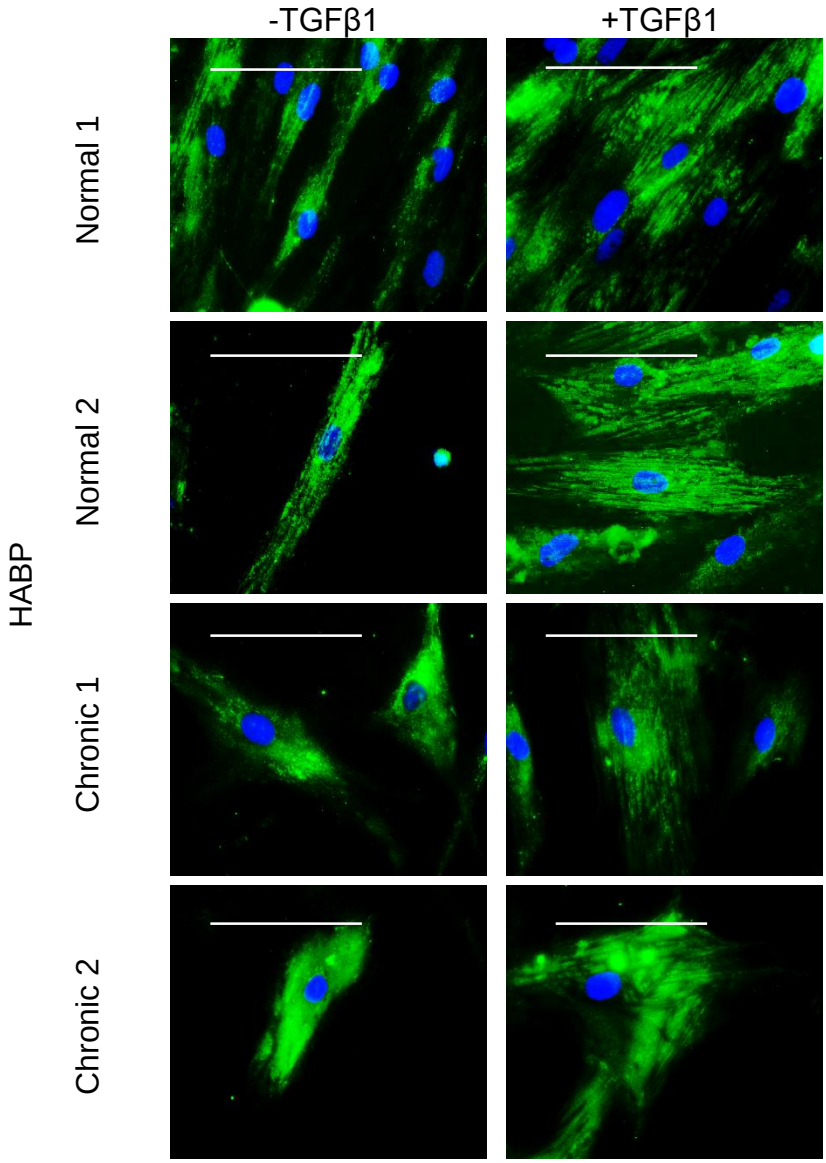

Figure 4.1 Localisation of total Hyaluronan does not change with TGF-β1 treatment. A. Cells were grown to 60-70% confluence and growth arrested for 48h. Cells were then incubated in serum-free medium alone (-TGF) or in medium containing 10 ng/mL TGFβ1 (+TGF) for 72h. The expression of total HA GAG was examined by immunocytochemistry; nuclei were visualised by Hoechst stain. Images shown are a representation of 2 independent experiments. Original Magnification x400. Scale bar 100µm.

4.2.2. Visualisation of HA Pericellular Coat Using Red Blood Cell (RBC) Exclusion Assay

It has previously been described that fibroblasts under the stimulation of TGF-β1 produce a HA pericellular coat. To determine if HA coat formation was lost in CWFs a RBC exclusion assay was used to visualise the pericellular HA coats of both NFs and CWFs, in the absence and presence of exogenous TGF-β1. In the absence of TGF-β1 stimulation both NFs and CWFs showed no HA coat present (Figure 4.2). The NFs responded to TGF-β1 treatment, with the induction of a clearly defined HA pericellular coat surrounding the cells. CWFs showed some RBC exclusion, although to a lesser extent than seen in the NF's. The coat was confirmed to be formed by HA by using a hyaluronidase treated negative control. This eradicated the HA coat and RBC distribution in the TGF-β1 stimulated NFs.

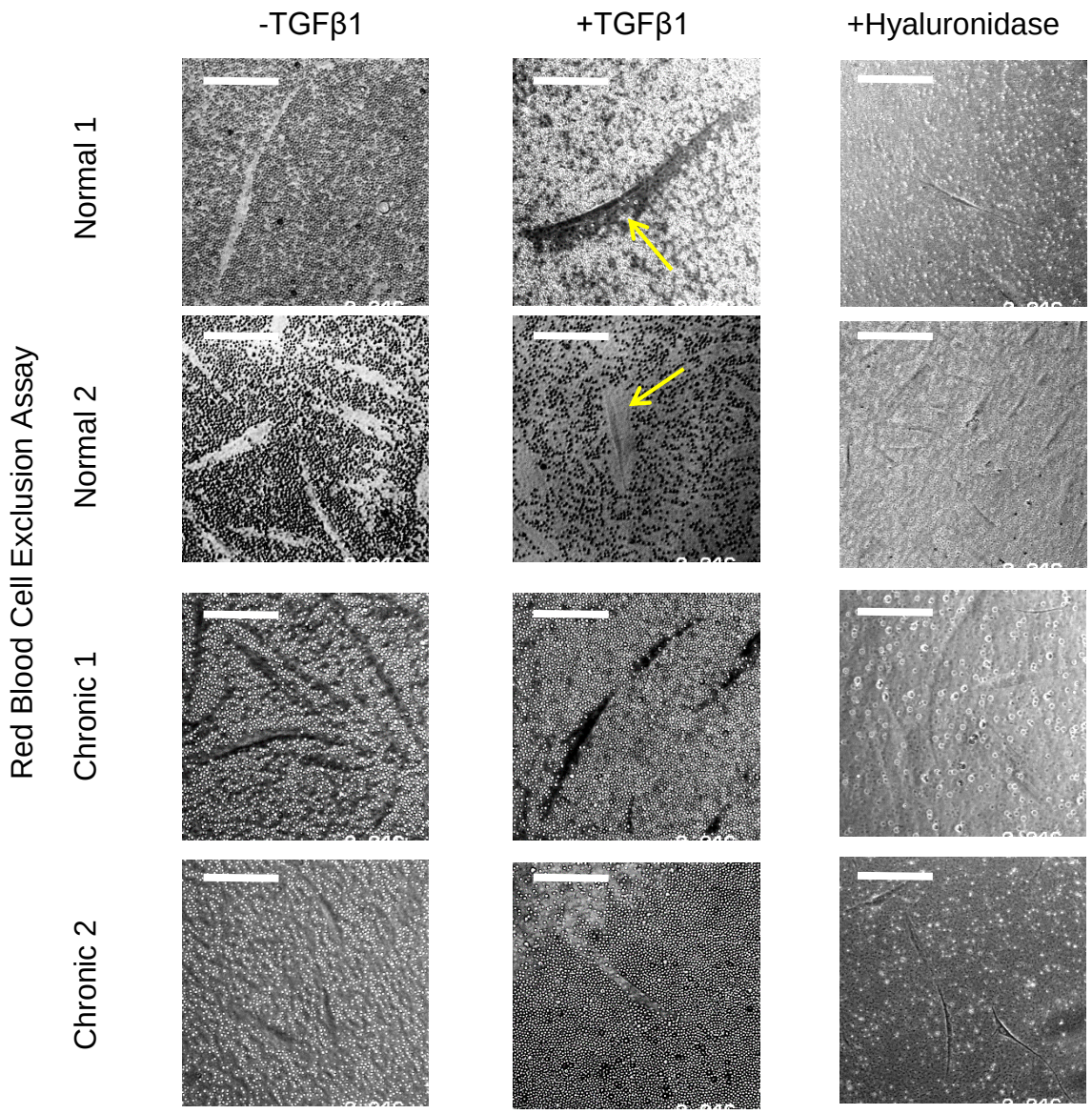

Figure 4.2. Visualisation of HA pericellular coat using Red Blood Cell (RBC) exclusion assay. A. Cells were grown to 60-70% confluence and growth arrested for 48h. Cells were then incubated in serum-free medium alone (-TGF) or in medium containing 10 ng/mL TGFβ1 (+TGF) for 72h. The expression visualisation of HA was examined by RBC exclusion assay. Yellow arrows show HA coat presence. Images shown are a representation of 2 independent experiments. Original Magnification x200. Hyaluronidase treated cells were used as a control, removing pericellular HA. Scale bar: 100µm.

4.2.3. Distribution of HA by ELISA

Given the importance of HA in myofibroblastic differentiation, endogenous HA was quantified using a HA ELISA. HA was quantified from three separate areas: extracellular, pericellular and intracellular. Trypsin was used to isolate pericellular HA, following this treatment the remaining cells were lysed releasing intracellular / cytoplasmic HA. Media was collected prior to the trypsin digestion, which allowed extracellular HA to be quantified. Cells were growth arrested and then incubated for 72hrs in either serum-free conditions or media stimulated with TGF-β1.

Extracellular HA was quantified from the media collected following the 72h incubation. Only Normal 1 and Chronic 2 showed a significant induction of HA with TGF-β1 stimulation (Figure 4.3A). Normal 2 and Chronic 1 were not significant, however these did show a trend of HA induction with TGF-β1 stimulation. No overall difference was observed between the NFs and CWFs, since all cells responded to TGF-β1 treatment with the induction of extracellular HA.

Cytoplasmic HA was quantified by the lysis of cells following trypsin treatment to remove surface HA. Only Normal 1 showed a significant induction of intracellular HA with TGF-β1 treatment (Figure 4.3B). Normal 2 was not significant, but did show an increase of intracellular HA production with TGF-β1. Both the CWFs showed no significant difference in intracellular HA between control and stimulated cells. Overall intracellular HA only increased with TGF-β1 in NFs.

Pericellular HA was isolated using a trypsin digestion, removing surface bound HA. Both NFs's (Normal 1 and 2) demonstrated a significant induction of pericellular HA with the addition of exogenous TGF-β1 to the medium, demonstrating the formation of a pericellular coat (Figure 4.3C). However, the CWFs did respond to TGF-β1 stimulation with an increase of pericellular HA seen. However, this increase was not significant in Chronic 1, and overall was considerably lower induction that that observed in the NFs. Thus, the formation of a HA pericellular coat was attenuated in CWFs.

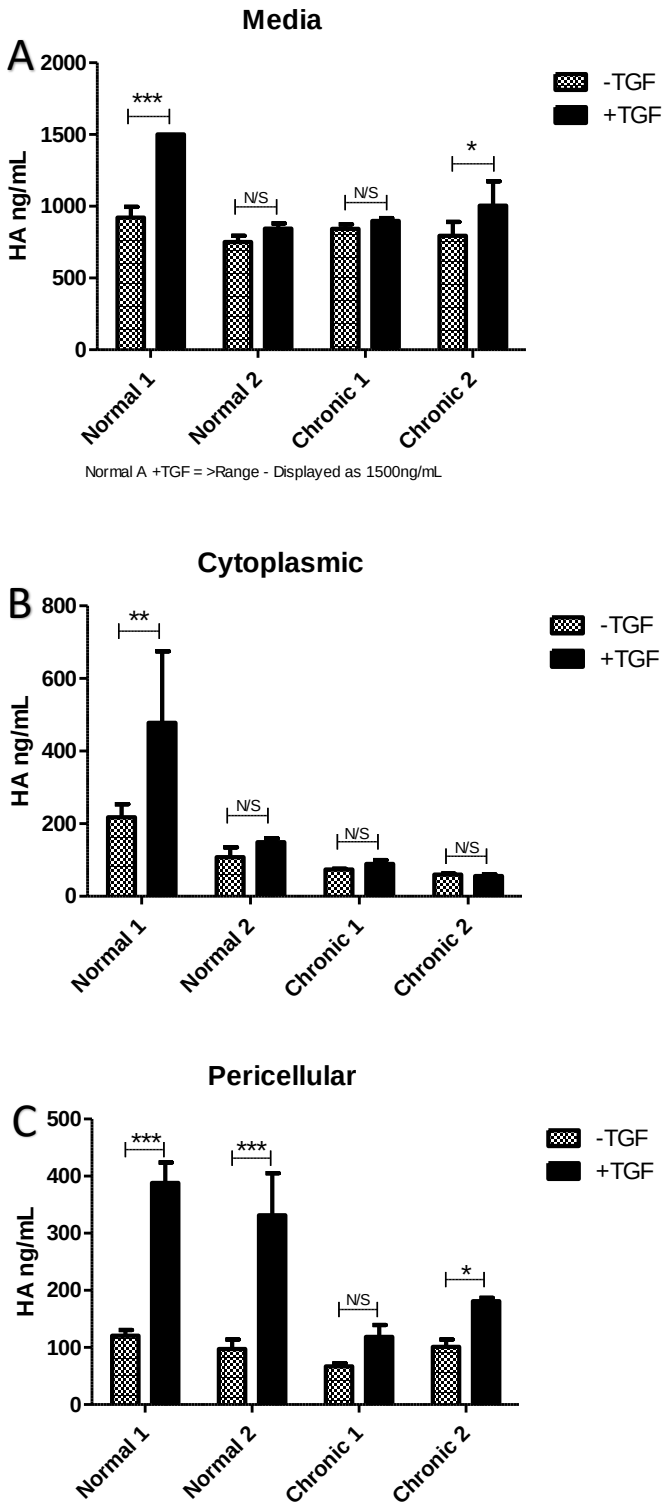

Figure 4.3. Quantification of HA by ELISA. Cells were grown to 90-100% confluence and growth arrested for 48h. Cells were then incubated in serum-free medium alone (-TGF) or in medium containing 10 ng/mL TGFβ1 (+TGF) for 72h. Media was collected before cell lysis to quantify extracellular HA (A). Trypsin was used to isolate the pericellular (C) and cytoplasmic (B) HA. Results are shown as the mean ± s.d. of 3 individual experiments. Statistical analysis was performed by a 2 way ANOVA with post Bonferroni test: **, p <0.05, **, p<0.01, ***, p<0.001**.

4.2.4. HAS2 Localisation

Given the loss of HAS2 mRNA induction with TGF-β1 treatment in CWFs shown in the previous chapter, the location of HAS2 was examined, comparing its location in resting and TGF-β1 stimulated cells. In both NFs HAS2 localisation did not change between resting and stimulated cells. HAS2 had a diffuse staining pattern and was shown to be present within nucleoli (Normal 1, +TGFβ1). HAS2 location in CWFs was similar to that seen in the NFs, however Chronic 1 showed strong staining of HAS2 within the nucleoli and Chronic 2 showed very strong staining in a perinuclear location. This perhaps reveals HAS2 becoming predominantly intracellular in CWFs (Figure 4.4).

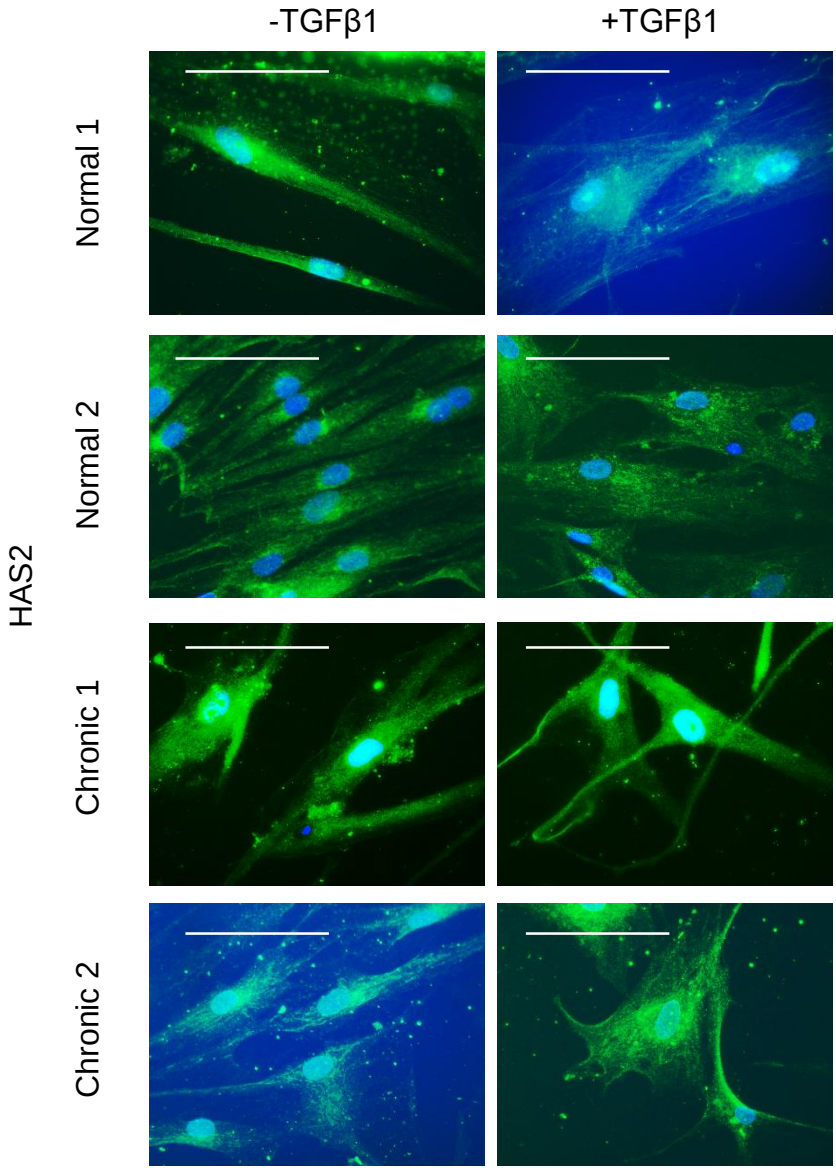

Figure 4.4. HAS2 Localisation. Cells were grown to 60-70% confluence and growth arrested for 48h. Cells were then incubated in serum-free medium alone (-TGF) or in medium containing 10 ng/mL TGFβ1 (+TGF) for 72h. The expression of HAS2 (green) was examined by immunocytochemistry, nuclei were visualised by Hoechst stain. Images shown are a representation of 2 independent experiments. Original Magnification x400. Scale bar: 100μm.

4.2.5. HAS1 clusters in a perinuclear location in TGF-β1 Treated CWFs

The previous chapter demonstrated that CWFs had increased basal expression of HAS1, with HAS1 also responding to TGF-β1 signalling in CWFs alone. It was therefore interesting for me to examine the location of HAS1. In treated CWFs HAS1 showed to cluster into multiple individual bunches, in a perinuclear location. HAS1 therefore not only responds to TGF-β1 at an mRNA level but also at a protein level in CWFs. HAS1 staining in the NFs also showed a predominantly intracellular staining pattern, but, with no significant differences seen between resting and stimulated cells (Figure 4.5). Differences seen are thought to be due to the change in cellular morphology, increasing surface area and thus, the HAS1 stain spreads with it, giving a different staining pattern.

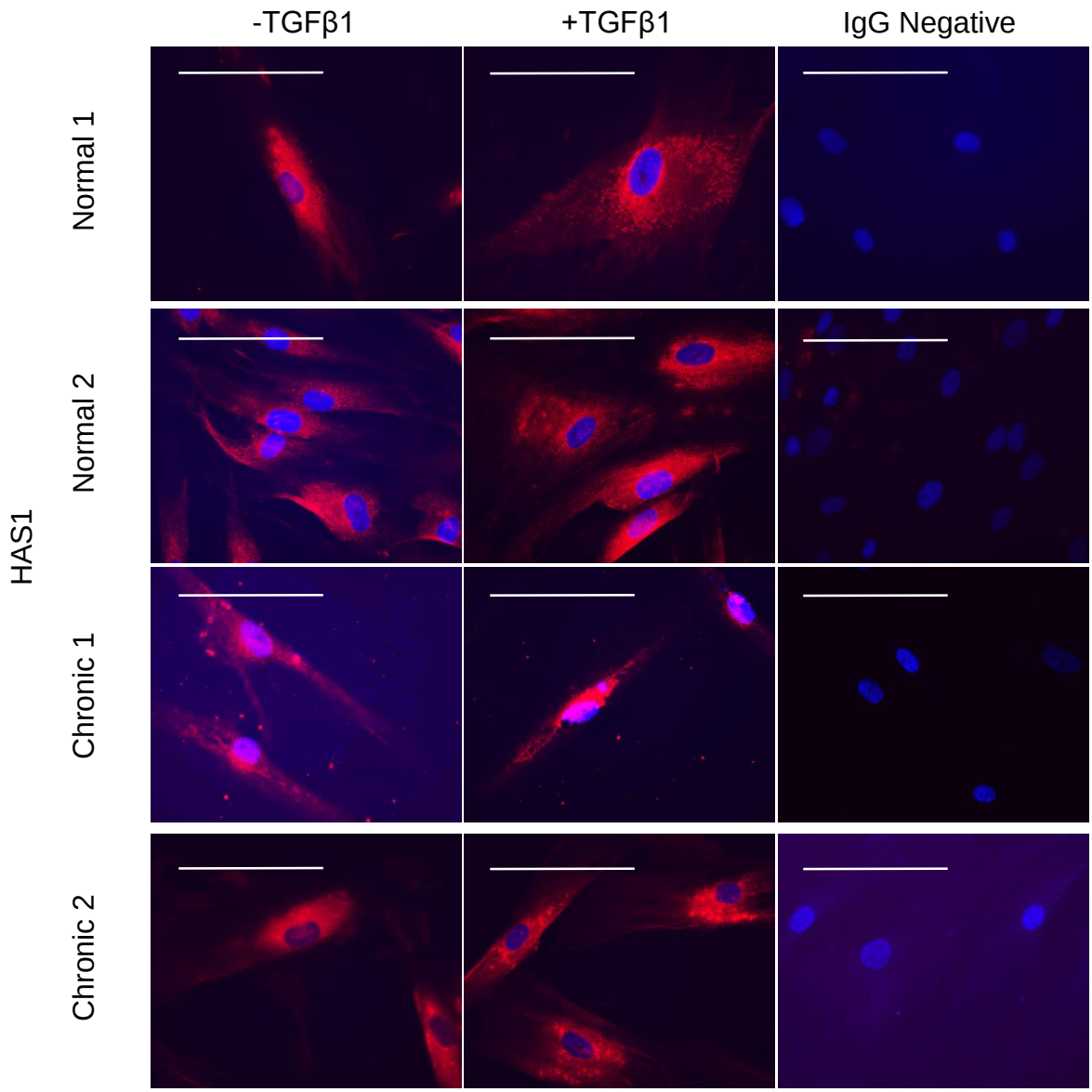

Figure 4.5 HAS1 clusters in a perinuclear location in TGF-β1 Treated CWFs. Cells were grown to 60-70% confluence and growth arrested for 48h. Cells were then incubated in serum-free medium alone (-TGF) or in medium containing 10 ng/mL TGFβ1 (+TGF) for 72h. The expression of HAS1 (red) was examined by immunocytochemistry, nuclei were visualised by Hoechst stain. Images shown are a representation of 3 independent experiments. Original Magnification x400. Scale bar: 100µm.

4.2.6. Intracellular HA clusters in a perinuclear location in CWFs

The results from both Figure 4.3, showed that intracellular HA quantification does not change in CWFs with TGF-β1 treatment. However, Figure 4.1 already demonstrated that differences can be seen in HA localisation without changes in the quantity of HA. This evidence combined with the intracellular location of HAS1, prompted an investigation into the intracellular location of HA in CWFs. Intracellular HA was imaged using HABP and fluorescence microscopy on cells pre-treated with hyaluronidase 30min prior to fixation, to remove surface HA. Intracellular HA in NFs did not differ between resting and TGF-β1 treated cells (Figure 4.6). However, intracellular HA distribution in CWFs was concentrated in a perinuclear location. Some cells (Chronic 1) showed a ring like staining pattern surrounding the nucleus of cells, which could be acting as a barrier. This pericellular location of HA was not observed in any NFs, making this a key finding in CWFs cell biology.

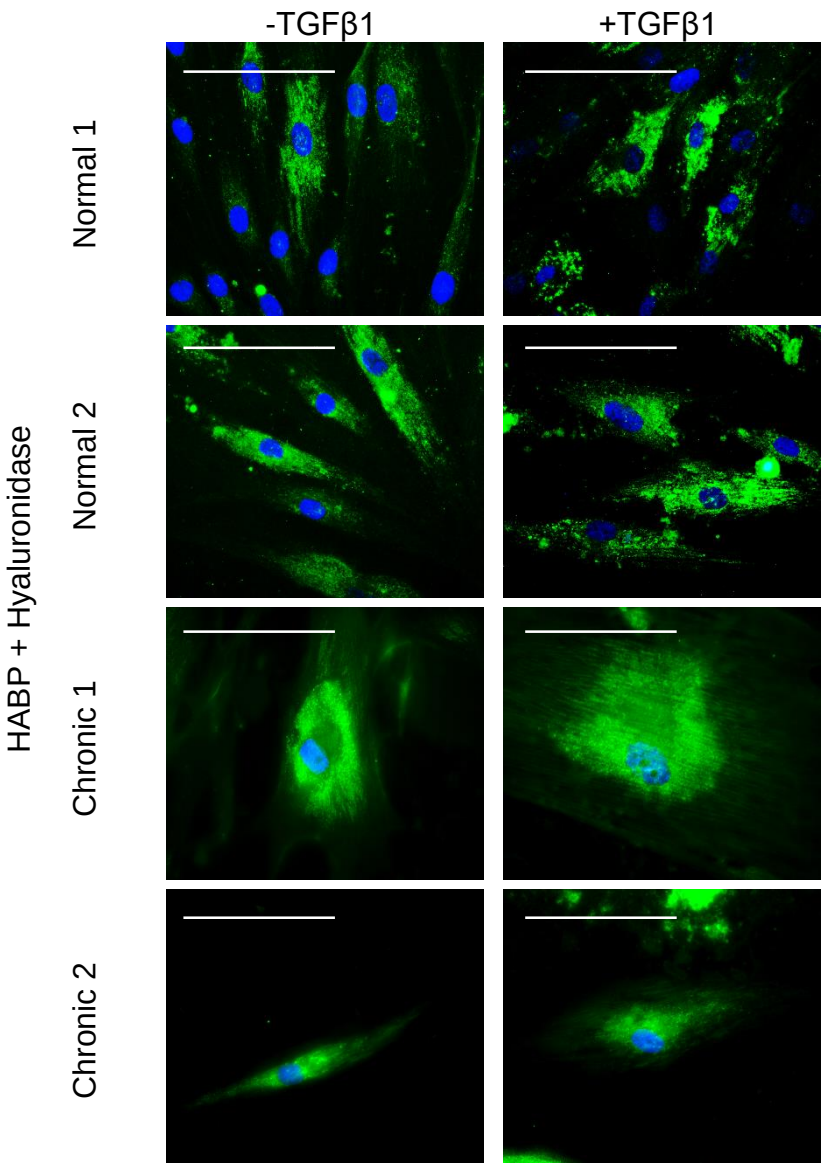

Figure 4.6. Intracellular HA clusters in a perinuclear location in CWFs. Cells were grown to 60-70% confluence and growth arrested for 48h. Cells were then incubated in serum-free medium alone (-TGF) or in medium containing 10 ng/mL TGFβ1 (+TGF) for 72h. The expression of intracellular HA was examined by immunocytochemistry; nuclei were visualised by Hoechst stain. Cells were pre-treated with Streptomyces Hyaluronidase (H1136, Sigma-Aldrich) 30min prior to fixation, to remove pericellular HA. Images shown are a representation of 2 independent experiments. Original magnification x400. Scale bar: 100µm.

4.2.7. Silencing HAS1 does not recover a myofibroblast phenotype in CWFs

The evidence collated throughout this and the previous chapter shows that HA metabolism is altered in CWFs. HAS1 has been implicated to be a key player in the altered and dysregulated HA production in CWFs during attempted TGF-β1 induced myofibroblast differentiation, I therefore sought to silence the expression of HAS1 in CWFs, to a similar level of expression observed in NFs, in order to elucidate whether this would recover a myofibroblast phenotype in CWFs. Initially the optimum concentration of siHAS1 to use was calculated (Figure 4.7B), with 100nmol of siHAS1 showing the greatest decrease in HAS1 expression compared to scramble negative control. Cells were visually checked for viability before lysis. No difference was observed in α-SMA induction at an mRNA level in the cells transfected with siHAS1 compared to scramble control, elucidating that silencing HAS1 did not induce α-SMA mRNA expression and thus a myofibroblast phenotype (Figure 4.7C). To confirm this cells were transfected with 100nmol of siHAS1 and α-SMA was visualised using immunocytochemistry. Although, possible αSMA fibres were visualised in CWFs, induction observed in siHAS1-transfected CWFs was not as great as previously seen in treated NF (figure 3.2), confirming that silencing HAS1 could not recover a myofibroblast phenotype to a comparable level as that observed in the NFs (Figure 4.7A).

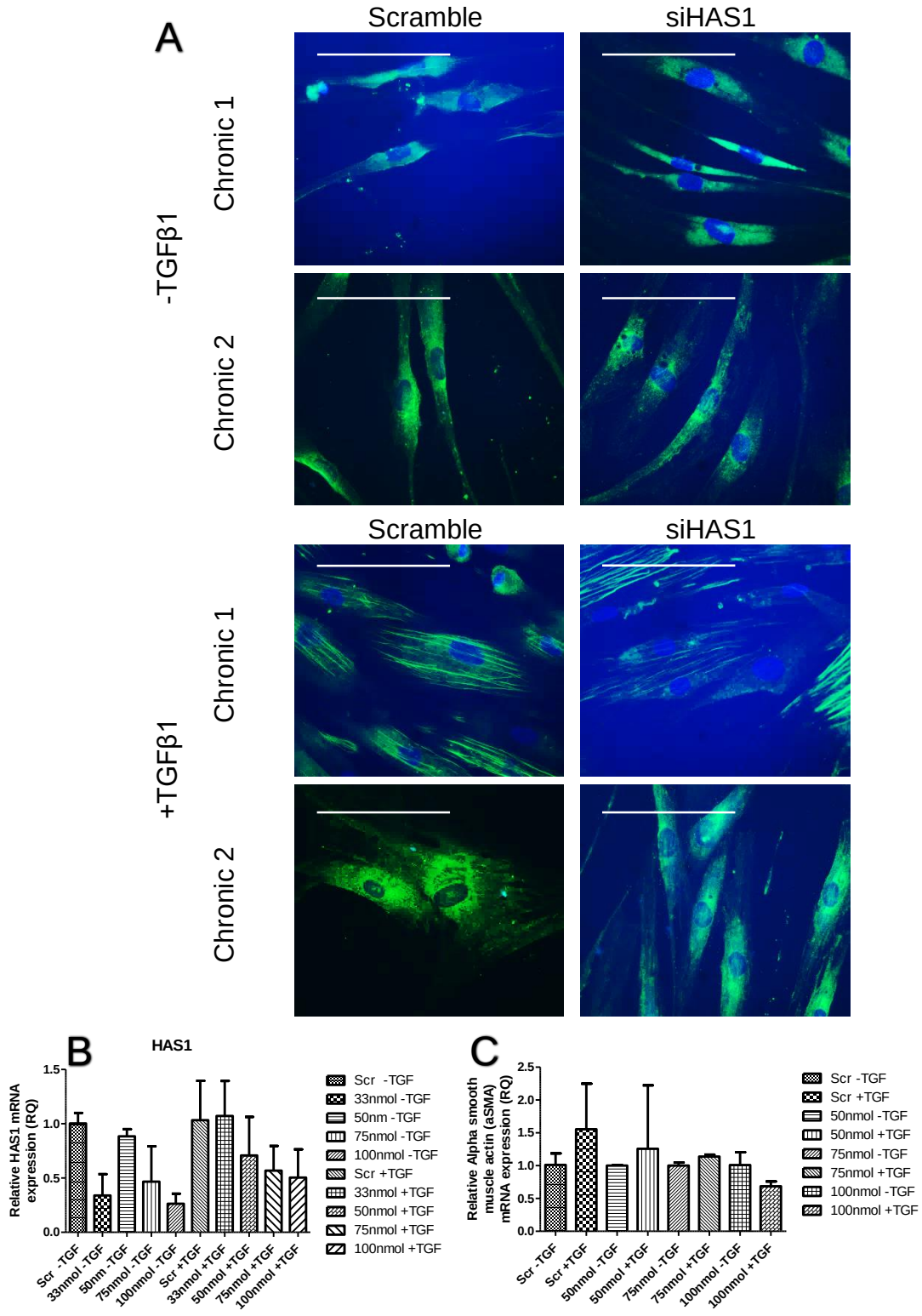

Figure 4.7. Silencing HAS1 does not recover a myofibroblast phenotype in CWFs. A. Cells were grown to 60-70% confluence and growth arrested for 48h. Cells were then incubated in serum-free medium alone (-TGF) or in medium containing 10 ng/mL TGFβ1 (+TGF) for 72h. The localisation of α-SMA was examined by immunocytochemistry; nuclei were visualised by Hoechst stain. Images shown are a representation of 2 independent experiments. Original Magnification x400. Scale bar: 100μm. **B/C.** CWFs 1 and 2 were grown to 90-100% confluent monolayers and growth arrested for 48h. Cells were then incubated in serum-free medium alone (-TGF) or in medium containing 10ng/mL TGF-β1 (+TGF) for 72h. The expression of αSMA and HAS mRNA was analysed by QPCR. Results are shown as the mean with range of 2 individual experiments.

4.2.8. Overexpression of HAS1 does not induce a CWFs phenotype in NFs

To confirm the results obtained in Figure 4.7, HAS1 was overexpressed in NFs to determine whether this would induce a chronic wound phenotype, resistant to TGF-β1 stimulated differentiation. Transfection of the overexpression vector was confirmed by the measurement of HAS1 at mRNA and protein levels. Both showed an increase of HAS1 following transfection of the HAS1 vector (Figure 4.8 B and C). To assess the affect, the overexpression vector had on the myofibroblast phenotype, cells were treated with TGF-β1 (10 ng/mL) and stained using α-SMA antibody. Following transfection and stimulation, no loss of α-SMA fibre formation was observed in either NFs (Figure 4.8A), demonstrating again that HAS1 does not have a direct role in the myofibroblast differentiation machinery.

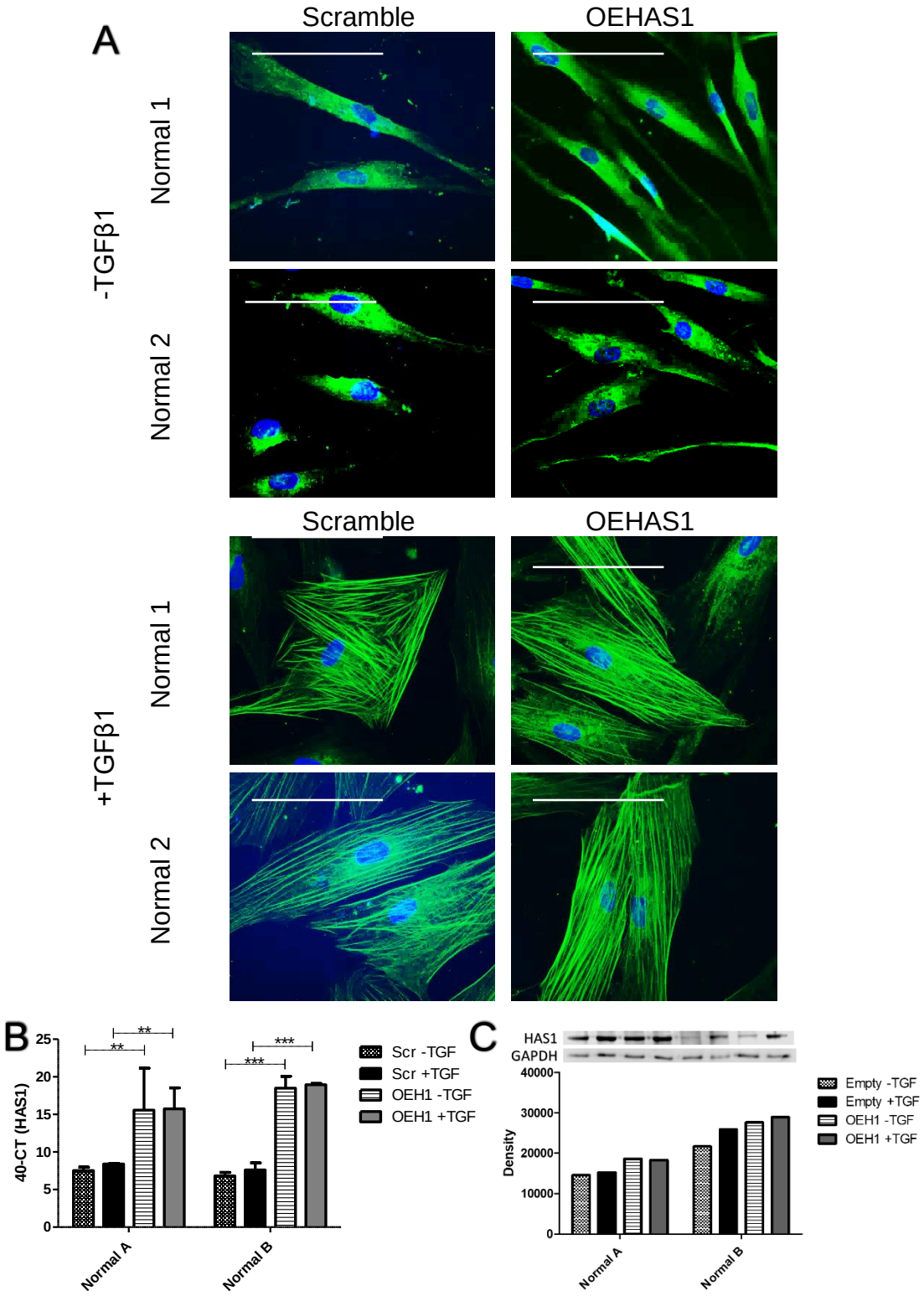

Figure 4.8. Overexpression of HAS1 does not induce a CWFs phenotype in NFs. A. Cells were grown to 60-70% confluence and growth arrested for 48h. Cells were then incubated in serum-free medium alone (-TGF) or in medium containing 10 ng/mL TGFβ1 (+TGF) for 72h. The localisation of αSMA protein was examined by immunocytochemistry; nuclei were visualised by Hoechst stain. Images shown are a representation of 2 independent experiments. Original Magnification x400. Scale bar: 100μm. **B.** Cells were grown to 90-100% confluent monolayers and growth arrested for 48h. Cells were then incubated in serum-free medium alone (-TGF) or in medium containing 10ng/mL TGF-β1 (+TGF) for 72h. The expression of HAS1 mRNA was analysed by QPCR. Results are shown as the mean ± s.d. of 3 individual experiments. **, p<0.01, ***, p<0.001. **B.** Western blot densitometry of HAS1 normalised to GAPDH. Results are one individual experiment.

4.2.9. Overexpression of HAS2 does not recover a myofibroblast phenotype in CWFs

Since it was apparent that HAS1 was not the primary HAS isoform responsible for the loss of myofibroblast differentiation in CWFs, attention turned to HAS2. HAS2 has been previously described as the primary HAS enzyme responsible for HA production during differentiation. The previous chapter also unveiled that CWFs have a decreased response of HAS2 mRNA expression with TGF-β1 treatment. I therefore wished to clarify whether the loss of HAS2 response to stimulation in CWFs, was to blame for the loss of differentiation in CWFs by overexpressing HAS2 in the CWFs. Successful transfection of the overexpression HAS2 vector was confirmed, with an increase in HAS2 mRNA expression in transfected cells, compared to cells transfected with an empty vector control (Figure 4.9A). α-SMA mRNA was measured in the transfected cells, to determine whether HAS2 overexpression induced α-SMA expression and thus differentiated into myofibroblasts. No significant induction of α-SMA was observed between cell transfected with HAS2 and those transfected with an empty vector. Therefore, over expressing HAS2 in CWFs did not return a myofibroblast phenotype.

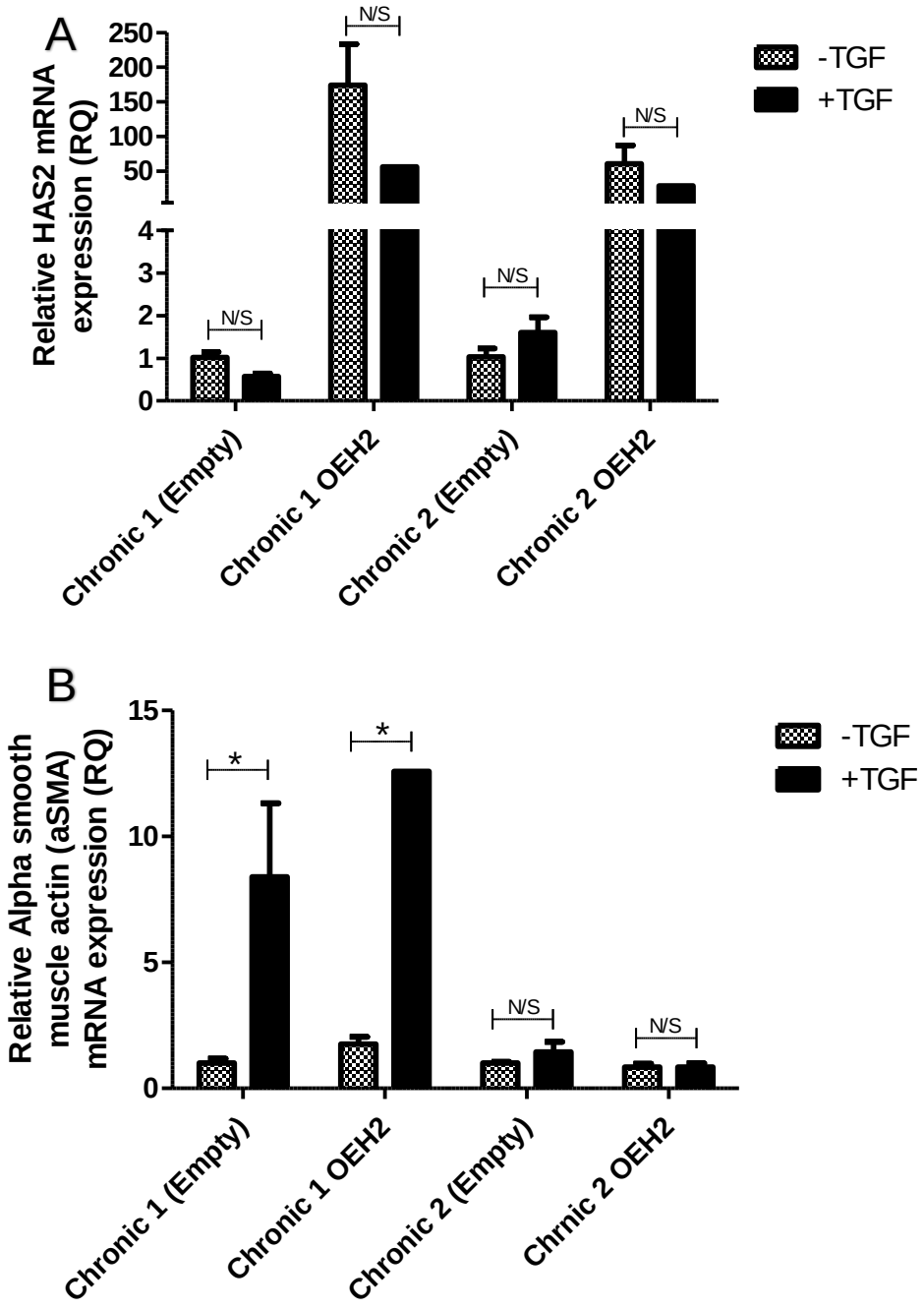

Figure 4.9. Overexpression of HAS2 does not recover a myofibroblast phenotype in CWFs. Cells were grown to 90-100% confluent monolayers and growth arrested for 48h. Cells were then incubated in serum-free medium alone (-TGF) or in medium containing 10ng/Ml TGF-β1 (+TGF) for 72h**.** Fibroblasts were transfected with an overexpression HAS2 vector or empty vector for 24h, prior to TGF-β1 treatment for 72h. The expression of HAS2 and αSMA mRNA were analysed by QPCR. Results are shown as the mean ± s.d. of 3 individual experiments. Statistical analysis was performed by a 2 way ANOVA with post Bonferroni test: *, p <0.05.

4.2.10. HAS1 has No Association with Pro-Inflammatory Cytokines

Previous literature has linked HAS1 expression in cells with activating a pro-inflammatory phenotype, inducing the expression of various pro-inflammatory mediators. To confirm this, the expression of an array of pro-inflammatory gene markers, investigating whether gene expression of these were induced in CWFs compared to NFs and whether they were further induced by TGF-β1 stimulation. mRNA levels were measured for IL-1β, IFN-γ, CCL2, IL-8, CCL5 and ICAM1. Overall, there was no obvious trend to show that HAS1 expression in CWFs induced pro-inflammatory mediator gene expression. IFN-γ showed induction in CWFs with stimulation, while it was not in NFs. CCL5 showed a differing response in CWFs and NFs, in response to stimulation, although this was not significant (Figure 4.10A).

To confirm this, I also treated cells with IL-1β to measure whether HAS1 or HAS2 were induced in CWFs. Interestingly HAS1 was significantly increased in treated CWFs. Although not significant, HAS2 also seemed to increase with treatment in CWFs. In both NFs there was no significant change, however a trend showed a decrease in HAS1 and HAS2 with IL-1β treatment (Figure 4.10B). This did indicate that CWFs were more responsive to pro-inflammatory cytokines, which alter HA metabolism.

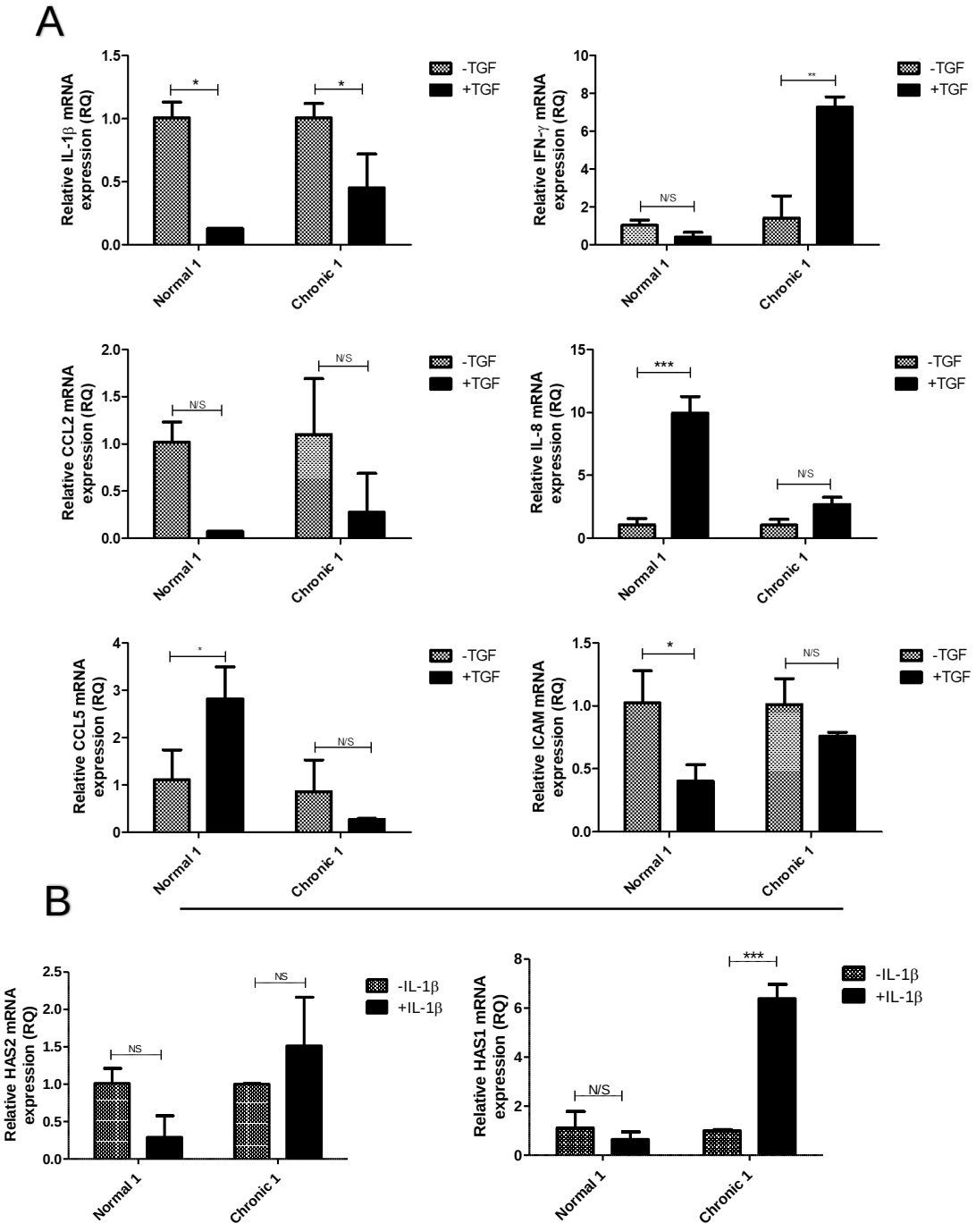

Figure 4.10. HAS1 has No Association with Pro-Inflammatory Cytokines. A. Cells were grown to 90-100% confluent monolayers and growth arrested for 48h. Cells were then incubated in serum-free medium alone (-TGF) or in medium containing 10ng/ml TGF-β1 (+TGF) for 72h. **B.** Cells were then incubated in serum-free medium alone (IL-1β) or in medium containing 10 ng/mL IL-1β (+IL-1β) for 72h The expression of IL-1β, IFN-γ, CCL2, IL-8, CCL5, ICAM, HAS1 and HAS2 mRNA were analysed by QPCR. Results are shown as the mean ± s.d. of 3 individual experiments. Statistical analysis was performed by a 2-way ANOVA with post Bonferroni test: *, $p < 0.05$, ***, $p<0.001$.

4.3. Discussion

The results from this chapter demonstrate for the first time the synthesis and location of HA in response to TGF-β1 stimulation in CWFs, together with investigating HAS1's role in the loss of myofibroblast response in CWFs. findings have novel relevance to the impaired wound healing associated with chronic wounds. Chapter 3 confirmed other studies (Simpson et al., 2009) showing that the primary HAS isoenzyme expressed by NFs is HAS2, and that HAS1 was predominant in CWFs (Wall et al., 2008). It was therefore of interest to investigate the location of these HASs and their production of HA.

Initial findings of this chapter characterised the distribution of HA in CWFs under the influence of TGF-β1. CWFs's showed that total HA staining patterns where that didn't change with TGF-β1 treatment. NFs's showed highly organised HA in clear parallel lines, which indicate association with the NFs cytoskeleton. This supports previous studies showing that HA associates via the ECM protein fibronectin, while its splice variant EDA-fibronectin is essential for myofibroblast differentiation and associated with the myofibroblast marker protein α-SMA *in vitro* (Evanko et al., 2015, Shinde et al., 2015). CWFs did show slightly less organisation of cytoskeletal HA which could be attributed to the loss of fibronectin-EDA expression shown in chapter 3 (Figure 3.2). The remaining organisation observed in the CWFs could be due to focal adhesions and other cytoskeletal proteins, which are not lost in the CWFs (Evanko et al., 2015).

Previous studies have shown the importance of the formation of a HA pericellular coat, formed by the binding of HA to its cell surface receptor CD44, for successful myofibroblast formation (Midgley et al., 2013, Simpson et al., 2009). It was therefore of particular importance to investigate whether the loss of a pericellular coat could be responsible for the loss of differentiation in CWFs. Using the RBC exclusion assay, I found that, in-line with previous findings, NFs responded to TGF-β1 stimulation by forming a clearly defined HA pericellular coat. This result was further supported by the HA ELISA data on the pericellular fraction of the cells, which again showed a significant increase in HA with TGF-β1 stimulation, confirming the presence of the HA pericellular coat. On the other hand, CWFs did not show the formation of a HA coat by RBC exclusion. The HA ELISA did show that CWFs's did respond to TGF-β1 treatment with an attempt of HA pericellular coat formation. This induction was not significant, and only an attenuated smaller HA coat could therefore be formed. It has been established that HA coat loss causes dysfunctional differentiation in fibroblasts, and therefore illuminated a novel finding in the explanation of the CWFs non-healing phenotype. Previous studies have also reported small HA coat formation and

attributed this to differential HAS enzyme expression. HAS1 has been shown to only produce attenuated small HA coats surrounding cells, since HAS1 requires a higher concentration of cellular uridine diphosphate *N*-acetylglucosamine (UDP-GlcNAc) than HAS2 and HAS3 (Rilla et al., 2013). Increasing the concentration of glucose in the media of cells, increases the cell surface HA in breast cancer MCF-7 cells. This could explain the smaller coat produced in these CWFs, since all cells were grown in low glucose (5mM) medium (Siiskonen et al., 2014). This study also highlighted that HAS1 coat formation is dependent on CD44 localisation on the membrane, and also ER-golgi-plasma membrane traffic. Previous work has shown that ER stress is a major contributor to diseases linked to inflammation, such as chronic wounds (Chaudhari et al., 2014).

The attenuation of HAS1 enzymatic activity due to low glucose availability in the media could also help explain the localisation of other fractions of HA shown by the HA ELISA, in the extracellular and intracellular fractions. Firstly, both NFs and CWFs demonstrated that HA synthesis was induced with TGF-β1 treatment, since both cell types demonstrated an increase of HA found in the extracellular space quantified from the collected media. This result was interesting since it is thought that extracellular HA deposition increases after injury and during disease states, such as those found in chronic wounds. Extracellular HA is responsible for immune cell recruitment to the site of injury (Litwiniuk et al., 2016, Petrey and de la Motte, 2014). This result may indicate that the endogenous fibroblasts present in chronic wounds are not the key players in producing pro-inflammatory extracellular HA for the recruitment of immune cells and it is in fact other factors that contribute to the persistent inflammation in chronic wounds. Secondly, intracellular / cytoplasmic HA concentrations in NFs increased with TGF-β1 treatment. CWFs, on the other hand, did not show this response of increased intracellular HA. This was a surprising finding since a number of studies have identified intracellular HA as a marker of inflammation and chronic wounds are well documented to be an inflammatory disease (Hascall et al., 2004). This reduction of HA synthesis could again be due to the physiological levels of glucose in the media and thus HAS1 attenuated enzymatic activity observed. To confirm this result HABP staining following hyaluronidase treatment was used to visualise intracellular HA. The results from this show a different picture, since it may not be quantity of HA synthesised that changes in CWFs, but the intracellular location of HA. HA localisation in the NFs did not change with TGF-β1 and showed diffuse staining throughout the cytoplasm. Contrasting this, intracellular HA in the CWFs was found in a perinuclear location in both unstimulated and stimulated cells. The accumulation of HA, visually resembled an intracellular barrier, which could be contributing to the loss of differentiation in these cells. It was found in a similar location to HAS1

expression in CWFs. HAS1 expression was shown to respond to TGF-β1 stimulation in the previous chapter. Here, we see that it also responds at a protein level, with cytoplasmic clusters forming in response to the treatment. This was not seen in the NFs. Previous studies have shown that HAS1 is found in an intracellular / perinuclear location in cells (Siiskonen et al., 2015). However, the current novel finding shows that HAS1 localisation is changed under cytokine treatment. This change in HAS1 location with the abnormal expression of intracellular HA in the CWFs may be contributing to the loss of an organised pericellular coat, with HA being trapped in a perinuclear location unable to reach the membrane. The loss of the coat is shown to be contributing to the loss of differentiation of these cells. Therefore, modifying the expression of HAS1 was hypothesised to reverse the dysfunction HAS expression and thus, HA distribution.

HAS1 was targeted for silencing, since its actions were thought to be causing the disorganised accumulation of HA and loss of the pericellular coat, contributing to the loss of the myofibroblast phenotype. Figure 4.7B demonstrates that transfecting CWFs proved to be difficult, with only very high concentrations resulting in sufficient knockdown of HAS1 expression. It was thought the difficulty in transfection was due to the decreased proliferation of the CWFs. However, other studies have demonstrated that HA can act as a barrier preventing gene transfer. The intracellular HA found in a barrier formation surrounding the nucleus in CWFs, may explain the poor transfection efficiency of these cells (Ruponen et al., 2003).

To elucidate HAS1 actions on effecting the differentiation of fibroblasts both silencing HAS1 in CWFs, to recover a myofibroblast phenotype and overexpression of HAS1 in NFs, to induce a CWFs phenotype, was attempted. Both silencing HAS1 or overexpressing HAS1 had no effect on the phenotype of the fibroblasts, using α-SMA as a marker of differentiation. These results demonstrated that HAS1's role was not integral to the loss of myofibroblast differentiation in CWFs, since it did not affect α-SMA mRNA expression or protein fibre formation. Previous studies have demonstrated that neither over-expression or down-regulation of HAS1 in NFs, has an effect on their differentiation (Meran et al., 2007). These cells, however, do not have a high basal expression of HAS1, leaving the question what role does HAS1 have in CWFs?

HAS1 has been well-reported to be up-regulated in inflammatory disease states (Siiskonen, et al., 2015). To test this the cells were treated with pro-inflammatory cytokine IL-1β to assess its effect on HAS expression. HAS1 showed a significant increase in expression in responce to IL-1β treatment in the CWFs alone. This may indicate that these cells are more

sensitive to expressing the pro-inflammatory HAS1 isoenzyme. To test whether HAS1 induction in the CWFs correlated with an increase in an increase of pro-inflammatory mediators, IL-1β, IFN-γ, CCL2, IL-8, CCL5, and ICAM-1 were measured. There was no significant induction of the pro-inflammatory cytokines, with only a non-significant trend being observed where IFN-γ being induced with TGF-β1 in the CWFs, and not in the NFs. This result suggests that although an increase in HAS1 is observed in these cells, the HA formed may not be acting endogenously and in fact only affecting surrounding cells.

The question regarding the cause for the loss of pericellular coat and differential intracellular HA localisation in CWFs still remains following investigation into HAS1 as the primary cause. HAS1 has not been attributed as the primary HAS isoenzyme expressed in normal myofibroblasts, since it is HAS2 which is responsible for normal HA pericellular coat formation. HAS2 location was investigated again finding differences between the NFs and CWFs. HAS2 in the NFs showed a diffuse staining pattern found throughout the cell cytoplasm, membrane and nucleus. On the other hand, in the CWFs, HAS2 was found with distinct staining patterns in a perinuclear location and within the nucleoli of the cells. Chapter 1 of this thesis showed that HAS2 expression was not induced with TGF-β1 in the CWFs but was in the NFs, even though this finding was not significant, together with the evidence of aberrant protein localisation strengthened HAS2 as the cause of the loss of the pericellular coat in the CWFs. HAS2 was targeted for overexpression in CWFs in the attempt to recover the myofibroblast phenotype. Although using α-SMA as the marker for differentiation, the over expression of HAS2 did not induce α-SMA expression and thus induce differentiation. Previous studies overexpressing HAS2 in senescent fibroblasts, also resistant to differentiation, only resulted in partial restoration of the myofibroblast phenotype. This was linked to other dysfunctional proteins within the non-classical pathway that contributed to the loss of differentiation. This may also be true of CWFs, with other dysfunctional proteins being the primary cause for the loss of differentiation (Midgley et al., 2014).

Chapter 5

Trafficking and Localisation of Proteins in Chronic Wound Fibroblasts

5.1. Introduction

5.1.1. The HA Receptor CD44

CD44 is a transmembrane glycoprotein that interacts with HA, regulating cell adhesion, migration, proliferation, differentiation and signalling (Prochazka et al., 2014, Midgley et al., 2013, Meran et al., 2011). A combination of alternative splicing and posttranscriptional modification leads to multifunctional isoforms, known as CD44 variants, of the protein, which have different tissue specific effects. The protein has one variable region. Theoretically alternative splicing can produce over 10^3 different isoforms of the variable region of the receptor. Standard CD44 (CD44s) is expressed when all variable exons (V2-v10 and exon 18 in humans) are spliced out, this is the most abundant variant expressed. Molecular weight of the CD44 variants range from 85-250 kDa (Fox et al., 1994, Prochazka et al., 2014, Screaton et al., 1992).

All CD44 variant proteins express three domains; an extracellular, a transmembrane and a cytoplasmic tail domain. The size of the protein is varied because of an insertion of a stem region between the extracellular and transmembrane domain. This, therefore, results in the translation of the exons within the variable region of the gene. The extracellular domain is the HA binding domain, and regulates the receptor interaction with the ECM. The amino domain is also capable of binding ECM proteins such as collagen, laminin and fibronectin (Faassen et al., 1992, Jalkanen and Jalkanen, 1992). A stem region links the amino domain to the transmembrane domain, it is in this that variably spliced exons are incorporated. Modifications in the amino terminal and stem region control the interactions of the receptor with the ECM, which are isoform specific. Posttranslational modifications include N- and O-linked glycosylation, phosphorylation and GAGs attachment, with CD44s being N-glycosylated while variants are mostly O-glycosylated (Hanley et al., 2005). The interaction of the receptors with the ECM, determine their function. This is also true of the cytoplasmic domain, which is capable of binding HA causing differential clustering of the receptor on the surface. This indicates that the receptor can be regulated from outside or inside the cell (Perschl et al., 1995).

The transmembrane domain is composed of 23 hydrophobic amino acids and a single cysteine residue. It's function is not entirely understood, however it is known to play a role in modulation of CD44-HA associations (Liu and Sy, 1997). The transmembrane region has also been associated with lipid raft interaction, indicating CD44 membrane motility and ability to act as a co-receptor with other transmembrane receptors, such as EGFR (Neame et al., 1995, Midgley et al., 2013).

TGF-β1 can affect the expression of CD44 and its variant isoforms, with CD44s expression being essential for HA pericellular coat formation and the regulation of TGF-β1 driven fibroblast to myofibroblast differentiation (Midgley et al., 2013). CD44v6 has been shown to be highly expressed in fibrogenic lung fibroblasts treated with TGF-β1 (Ghatak et al., 2017). The presence of V3 during obstructive nephropathy, increased proliferation in tubular epithelial cells and prevented renal fibrosis development, compared to CD44s which had the opposite effect and increased fibrosis (Rampanelli et al., 2014). CD44 can also interact with downstream signalling molecules of the TGF-βR pathway, with CD44 binding SMAD3, inhibiting recruitment of splicing machinery, thereby promoting expression of CD44s, a tumour promoting factor (Tripathi et al., 2016). CD44v7/8 has been identified as an anti-fibrotic variant, with its expression becoming upregulated following BMP-7 treatment, leading to antagonism of the myofibroblast phenotype. This mechanism involves the translocation of HYAL2 to the nucleus, displacing components of CD44 splicing machinery causing the loss of CD44s and the accumulation of the anti-fibrotic CD44v7/8 at the cell surface (Midgley et al., 2017).

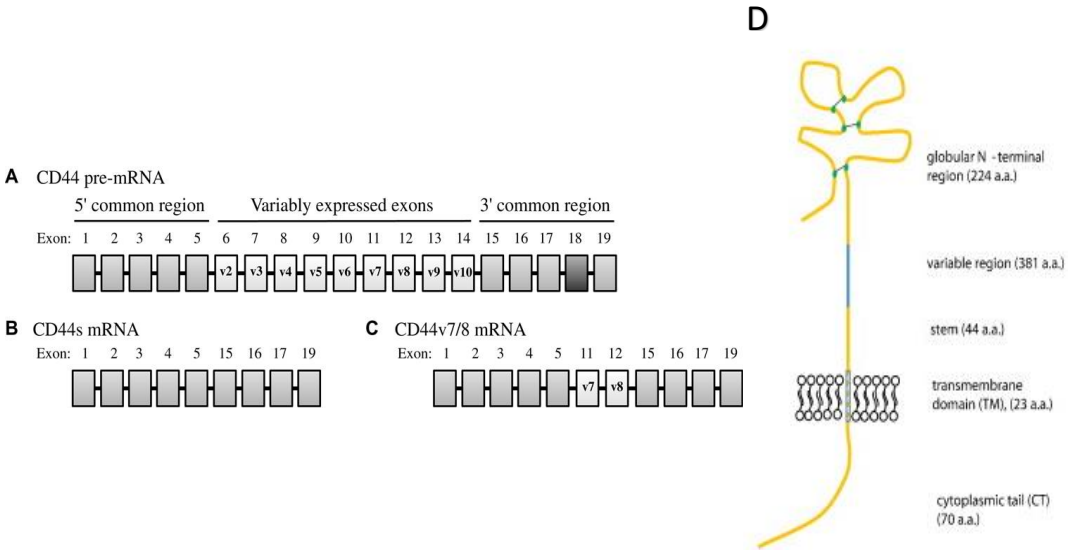

Figure 5.1 Human CD44 structure and alternative splicing. A. Intron-exon structure of CD44 pre-mRNA. The 5′ and 3′ common regions are present in all CD44 splice variants. Exon 18 is removed before translation, and exons 6 to 14 are differentially expressed in different CD44 variant isoforms. **B**. CD44s mRNA contains only 5' and 3' common regions. **C**. The CD44v7/8 mRNA contains the same common region exons as CD44s plus the addition of the variably expressed exons 11 and 12. **D.** CD44 protein structure. The globular N-terminal region contains 3 disulphide bonds and 2 HA binding motifs. The cytoplasmic tail contains intracellular signalling motifs and medicates cytoskeletal interaction. The blue variable region is missing from CD44s. Adapted from (Midgley et al., 2017, Prochazka et al., 2014).

5.1.2. EGFR Signalling

EGFR is a cell surface transmembrane receptor activated by the binding of its ligands; EGF, TGF-α and Heparin binding (HB)-EGF (Leahy, 2004). Upon ligand biding, EGFR undergoes a transition from an inactive monomeric form to an active homodimer (Yu et al., 2002). There is evidence of the existence of inactive dimers, whose activity is regulated by other proteins, receptors or lipids. EGFR co-localisation with CD44 has been previously described to be essential for myofibroblast formation, with this co-localisation occurring within membrane bound lipid rafts (Meran et al., 2011, Midgley et al., 2013). The loss of EGFR expression in cell types resistant to TGF-β1 treatment such as *in vitro* aged fibroblasts, demonstrates its importance as a pro-fibrotic receptor (Midgley et al., 2014). EGFR expression can also be modulated by its anti-sense strand, with over-expression of EGFR anti-sense, reducing the expression of EGFR (Brader et al., 1998). EGFR dimerization stimulates auto phosphorylation of several tyrosine residues in the C-terminal domain of EGFR. This phosphorylation activates downstream signalling cascades through MAPK/ERK, protein kinase B (Akt), c-Jun N-terminal kinases (JNK) and Janus kinase (JAK) pathways. These signals contribute to cellular proliferation, migration, adhesion and differentiation (Andl et al., 2004, Meran et al., 2011, Cordero et al., 2012, Hashimoto et al., 1999).

5.1.3. Intracellular Molecular Synthesis and Modification

The site of protein and lipid synthesis is the ER, which is made up of the nuclear envelope and interconnected flattened membrane sacs called cisternae. There are two compartments called the rough and smooth ER. The Rough ER contains ribosomes, which are the sites of protein synthesis. The smooth ER lacks ribosomes and therefore is responsible for lipid synthesis and acts as the site of vesicle binding and fusion. The rough ER is very prominent in fibroblasts, cells that produce large amounts of the ECM proteins, and the smooth ER is especially abundant in adrenal cells that secrete large amounts of steroids (Shibata et al., 2006, Li and Wang, 2011).

Rough ER manufactures transport vesicles such as lysosomes and is responsible for initial protein N-linked glycosylation. There is no continuous membrane between the ER and golgi, therefore membrane-bound transport vesicles shuttle proteins and lipids between these two organelles (Watson and Stephens, 2005). Only correctly folded proteins are transported from the rough ER to the golgi; unfolded proteins cause a stress response in the ER, leading to accumulation of unfolded proteins and potentially cause damage in hypoxia, insulin resistance and other disorders (Ozcan et al., 2004).

The Golgi is composed of several flattened stacks of membranes devoid of ribosomes. Individual stacks have unique functions, and are thus classically labelled, cis, median, trans, and trans-Golgi network according to their function. The Golgi constantly receives material from the ER, which it must sort and package to their desired destination, such as the, endosomal and lysosomal compartments, the plasma membrane or extracellular space. The Golgi is the main contributor of post-translational modification of lipids and proteins and defective post-translational modification has been associated with multiple different diseases (Potelle et al., 2015). Correct Golgi functioning is essential for stability, activity, trafficking and sub-cellular localization of many proteins.

The previous chapter demonstrated that CWFs had specific intracellular localisation of HA coinciding with the loss of pericellular coat, indicating that dysfunctional transport of key regulators of the differentiation pathway may be effected in CWFs. The previous chapter also reported intracellular accumulation of HAS1 and HAS2 in the CWFs. Previous work has demonstrated that HAS1 accumulates in the Golgi whilst HAS2 accumulates in the ER, indicating that they have a reserve pool of isoenzymes to recruit for rapid HA synthesis (Torronen et al., 2014, Rilla et al., 2005). The dysfunctional synthesis or transport of these proteins may divulge a dysfunction in the loss of CWFs differentiation.

5.1.4. Intracellular Transport

Intracellular transport is the movement of vesicles and substances within the cell along microtubules and actin filaments within the cytoskeleton. Transport vesicles are small structures that have the capacity to hold cargo and transport to specific cellular compartments. To ensure they reach the desired destination, special motor proteins attach to the vesicles and carry them along the cytoskeleton. Failure in this system results in the accumulation or inaccurate transport of molecules leading to disease (Ando et al., 2015).

Endocytosis is the process where material is taken into the cell via inward budding of the plasma membrane into early endosomes. The cargo is then sorted to specific destinations, which include being recycled back into the plasma membrane, the ER, intraluminal vesicles for sorting, lysosomes or to the biosynthetic pathway. These early endosomes, slowly mature into late endosomes which eventually fuse with lysosomes, and the cargo is then degraded by lysosomal hydrolases (Raiborg et al., 2015). A key function of endocytosis is the regulation of cell surface receptor expression at the plasma membrane (Maxfield, 2014). Endosomes are responsible for transporting many key regulators of myofibroblasts formation. These include TGF-βR, whose internalisation regulates TGF-β1 signalling (He et al., 2015, Chen, 2009), HAS transport from the ER / Golgi to the plasma membrane (Deen

et al., 2014) and CD44 transport to the membrane (Maldonado-Baez et al., 2013). The loss of receptor presentation at the surface could cause serious complications in disease states such as chronic wounds.

Lysosomes develop from late endosomes, they are membrane enclosed organelles that contain an array of enzymes capable of breaking down all types of biological polymers- proteins, nucleic acids, carbohydrates and lipids. It therefore, serves to degrade materials taken up externally from the cell and digest obsolete components as an auto-phagosome. Its correct function is essential for intracellular homeostasis (Sridhar et al., 2013, Mauvezin et al., 2015). It has an intracellular pH of approximately 5, which all lysosomal enzymes are active. These enzymes are essential for regulation of molecules associated with myofibroblast formation. Lysosomes have an important role in cholesterol homeostasis, which may indicate its role in lipid raft formation and transport (Lange et al., 2012). An enzymatically active form of HYAL1 has been identified in lysosomes confirming other studies suggesting it contributes to the breakdown of HA (Boonen et al., 2014). Lysosomes have also been shown to contribute to TGF-βR and CD44 degradation, suggesting that lysosomal function is essential for the pro-fibrotic signalling pathways to function and this may be lost in CWFs (Bai et al., 2014, Haakenson et al., 2015).

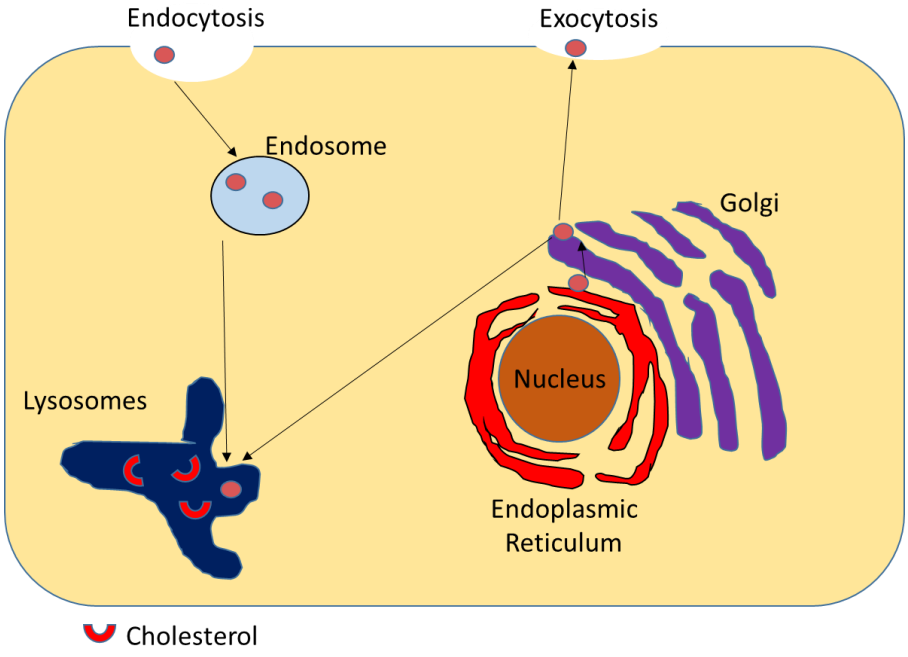

Figure 5.2. Membrane Transport into and out of the Cell. Endocytosis occurs when the membrane engulfs particles outside the cell and forms an endosome. Its contents are digested as it merges with vesicles containing enzymes from the Golgi, transforming the endosome into a lysosome. Cholesterol, produced by hydrolysis of cholesterol esters by lysosomal acid lipase. Exocytosis is the process of membrane transport that releases contents outside the cell. Here, transport vesicles from the Golgi or elsewhere merges with the membrane and releases its contents. Membrane transport also occur between the endoplasmic reticulum and the Golgi. Adapted from: (Maxfield, 2014)

Microtubules are filaments of the cytoskeleton, with fundamental roles in cell division and intracellular transport, acting as rails to facilitate transport. Microtubules form through the polymerisation of αβ-tubulin heterodimers, powered by the hydrolysis of guanosine triphosphate (GTP) bound to β-tubulin. Microtubules have both a plus-end and minus-end of assembly. This enables microtubules to switch between catastrophes, where disassembly via depolymerisation occurs and rescues, where assembly is re-initiated (Akhmanova and Steinmetz, 2015). Motor proteins use the microtubules as tracks to transport; proteins, lipids and other cellular materials. Kinesins and Dyneins are the two types of motor proteins, which move to the plus-end or minus-end respectively (Franker and Hoogenraad, 2013). Microtubule formation has been found to have a role in ER to Golgi transport (Fokin et al., 2014), essential for intracellular trafficking. As part of the cytoskeleton they are also essential for myofibroblast formation, having cross-talk with the actin cytoskeleton (Sandbo et al., 2016, Po'uha et al., 2013). Destabilisation of the microtubule network would affect both intracellular trafficking and the modification of the cytoskeleton to allow myofibroblast formation (Mian et al., 2012).

The aims of this chapter are:

1. Analyse the co-localisation of CD44 and EGFR in membrane bound lipid rafts, to determine whether this mechanism is affected in CWFs differentiation.
2. Understand the role of CD44 variants and EGFR antisense in the context of CWFs differentiation capacity.
3. Examine intracellular protein synthesis and transport system in NFs and CWFs, identifying any discrepancies that may cause CWFs to lose their differentiation ability.

5.2. Results

5.2.1. Intracellular localisation of EGFR in CWFs and Reduced Co-localisation with CD44 on the Membrane Compared to NFs

Previous papers have reported the importance of the TGFβ1 stimulated co-localisation of the HA receptor CD44 with EGFR on the membrane, for myofibroblast differentiation to occur (Midgley et al., 2013). To determine whether the loss of co-localisation of these proteins might be contributing to the loss of differentiation, fluorescence co-staining (CD44 and EGFR) with confocal microscopy was undertaken. Cells were grown to 60-70% confluence and then incubated with either TGF-β1 in serum free media, or media alone. Both NFs showed staining of CD44 and EGFR on the membrane of the TGF-β1 stimulated cells. Merging these images confirmed that the two proteins were co-localised within the membrane of the treated cells, and therefore capable of differentiating (Figure 5.1). However, the two CWFs showed very strong staining of EGFR intracellularly, with reduced staining on the membrane. The CD44 staining in CWFs still remained on the membrane and merging the staining showed attenuation of the co-localisation of CD44 and EGFR on the membrane. The EGFR was not in a specific perinuclear location, however a ring like pattern surrounding the nucleus could be seen. This specific intracellular staining was not observed in any of the NFs, making this a novel finding in CWFs cell biology

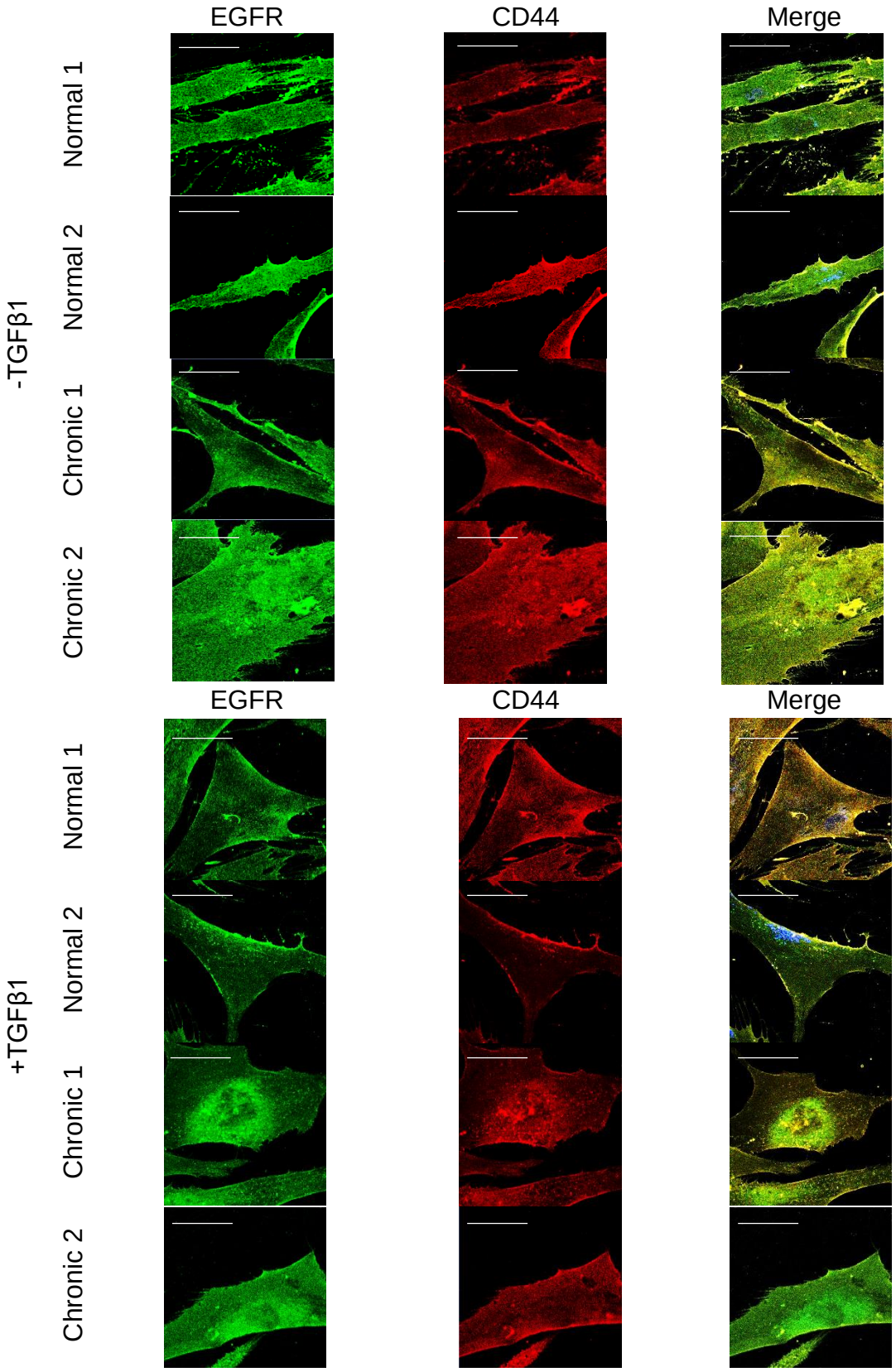

Figure 5.1. Intracellular localisation of EGFR in CWFs and reduced co-localisation with CD44 on the membrane, compared to NFs. Cells were grown to 60-70% confluence and growth arrested for 48h. Cells were then incubated in serum-free medium alone (-TGF) or in medium containing 10 ng/mL TGFβ1 (+TGF) for 72h. The localisation of EGFR (green) and CD44 proteins (Red) were examined by immunocytochemistry and confocal microscopy; nuclei were visualised by Hoechst stain. Images shown are a representation of 3 independent experiments. Original magnification x620. Scale bar: 50μm.

5.2.2. EGFR and Lipid Intracellular Localisation in CWFs with Reduced Co-localisation on the Membrane Compared to NFs

CD44 and EGFR (FITC-EGFR-ab11401) co-localisation has been shown to occur within lipid rafts on the membrane of fibroblasts (Midgley et al., 2013). Since the staining pattern of EGFR was different in CWFs, compared to that observed in NFs, EGFR and lipid localisation was imaged to assess whether the loss of lipid rafts was causing the decrease in CD44-EGFR co-localisation. NFs treated with TGF-β1 showed co-localisation of EGFR and lipids on the membrane with diffuse staining throughout the cell (Figure 5.2). EGFR was imaged intracellularly with a diffuse staining pattern in CWFs. The CTX stain was also observed intracellularly in both the treated and non-treated CWFs. Once the images were merged CWFs showed some co-localisation of intracellular EGFR and lipids. This is an interesting finding, since CD44 was previously thought to be mobile in lipid rafts and EGFR static.

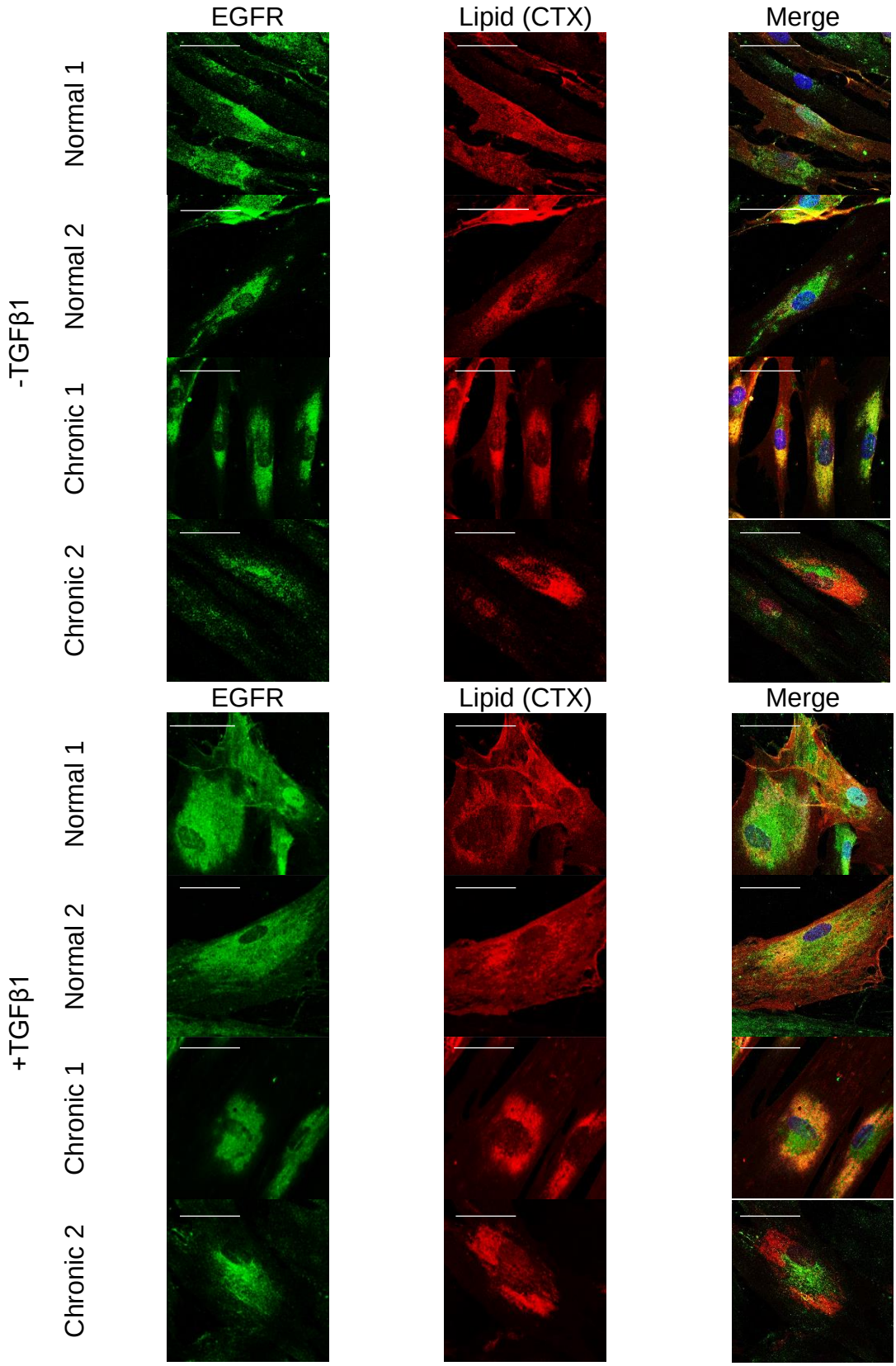

Figure 5.2. EGFR and lipid intracellular localisation in CWFs with reduced co-localisation on the membrane, compared to NFs. Cells were grown to 60-70% confluence and growth arrested for 48h. Cells were then incubated in serum-free medium alone (-TGF) or in medium containing 10 ng/mL TGFβ1 (+TGF) for 72h. The localisation of EGFR protein (green) and lipids (Red) were examined by immunocytochemistry and confocal microscopy; nuclei were visualised by Hoechst stain. Images shown are a representation of 3 independent experiments. Original magnification x620. Scale bar: 50µm.

5.2.3. Comparison of EGFR Antisense expression at mRNA level

A number of studies have demonstrated that antisense therapy is a growing field for diseases, since antisense transcription can act independently to sense transcription to modulate chromatin and therefore, possibly be a method for cellular control (Murray and Mellor, 2016, Alper et al., 2000). Both NFs and CWFs showed a significant decrease in EGFR antisense expression following TGF-β1 treatment (Figure 5.3 A). Comparing this to standard EGFR expression (Figure 5.3 B), this too decreased in both cell types with TGF-β1 treatment, indicating EGFR antisense does not have a direct role in aberrant EGFR protein localisation in CWFs.

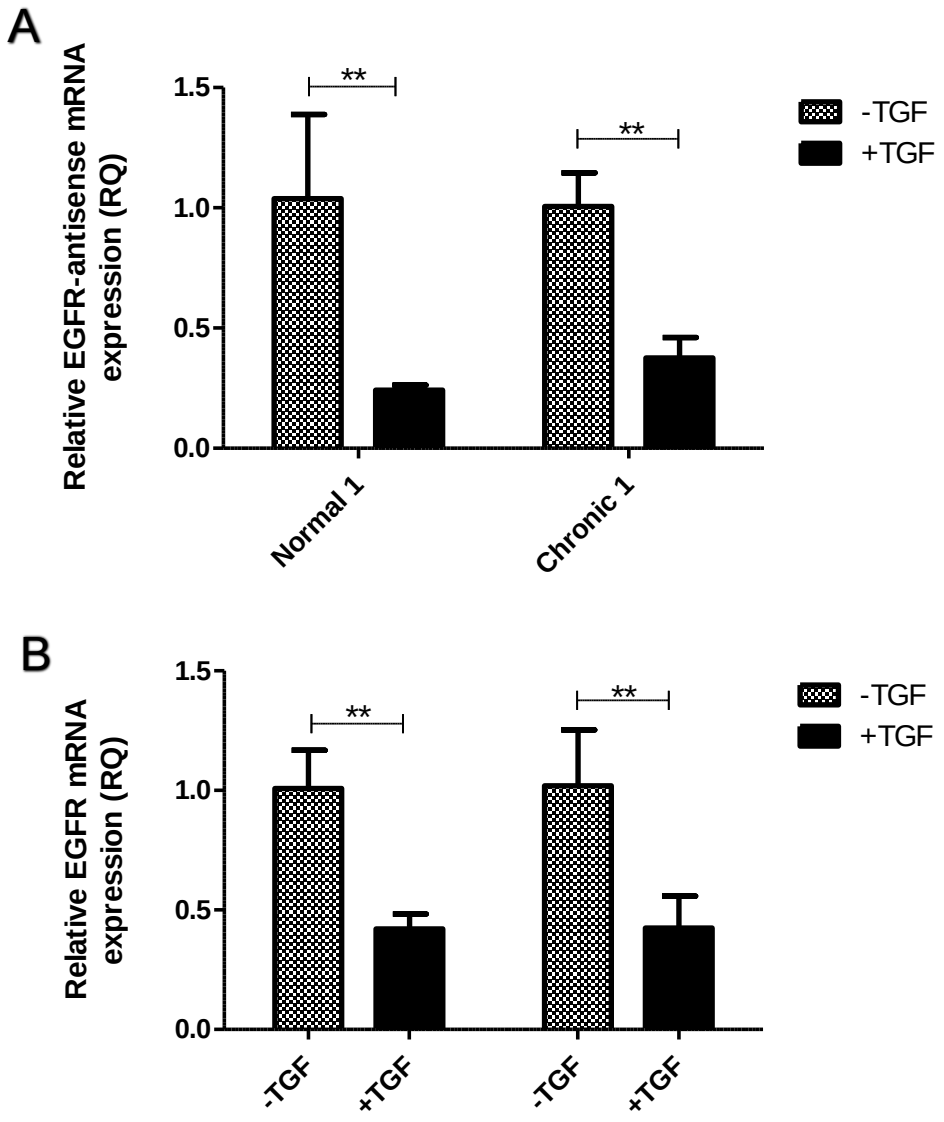

Figure 5.3 No change in EGFR anti-sense expression between CWFs and NFs. Cells were grown to 100% confluent monolayers and growth arrested for 48h. Cells were then incubated in serum-free medium alone (-TGF) or in medium containing 10ng/mL TGF-β1 (+TGF) for 72h. The mRNA expression of (A) EGFR anti-sense and (B) EGFR standard was analysed by QPCR. Results are shown as the mean ± s.d. of 3 individual experiments. Statistical analysis was performed by a 2-way ANOVA with post Bonferroni test: **, $p < 0.01$.

5.2.4. Comparison of CD44 variant expression at mRNA level

Alternative splicing produces distinct isoforms of the protein CD44, which have shown to have significant effects on disease progression, such as cancer and also have differential expression throughout the skin (Prochazka et al., 2014, Hale et al., 1995). It was therefore of interest to investigate the expression of the 10 variant exons of CD44 in CWFs and compare this to their relative expression in NFs, in response to TGF-β1 treatment. CD44s (standard) expression showed significant decreased expression in response to TGF-β1 stimulation in both NFs and CWFs, as shown in chapter 3 (Figure 5.4). Variant 2 and 3 also showed a similar pattern, with decreased expression in both cell types.

Variant 5 was not expressed in either NFs or CWFs. Variant 4, 7, 8, 9 and 10 showed no significant difference between control and TGF-β1 stimulated cells. However, variant 10 showed a trend where its expression increased with treatment in the CWFs, but decreased in NFs. Variant 6 showed the greatest difference, with a significant decrease in response to TGF-β1 only seen in the NFs. Variant 6 did decrease in the CWFs following TGF-β1, but this was not significant. The overall trend therefore showed no significant difference in CD44 variant expression, contributing towards non-healing in CWFs.

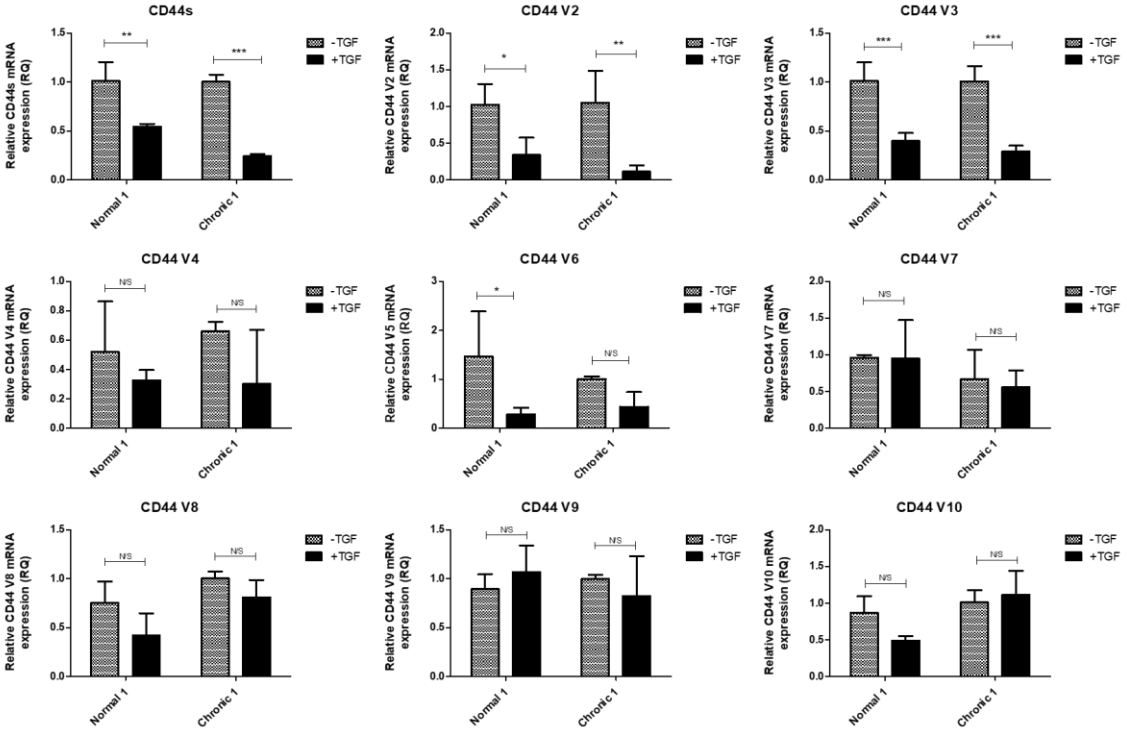

Figure 5.4. Comparison of CD44 variant expression at mRNA level. Cells were grown to 90-100% confluent monolayers and growth arrested for 48h. Cells were then incubated in serum-free medium alone (-TGF) or in medium containing 10ng/mL TGF-β1 (+TGF) for 72h. The CD44 variants mRNA expression were analysed by QPCR. Results are shown as the mean ± s.d. of 3 individual experiments. Statistical analysis was performed by a 2 way ANOVA with post Bonferroni test: *, p <0.05, **, p<0.01, ***, p<0.001.

5.2.5. CD44 variant 7/8 localisation and expression

Previous studies have confirmed that CD44v7/8 is associated with prevention and reversal of the myofibroblast phenotype and thus is anti-fibrotic (Midgley et al., 2017, Midgley et al., 2015). Since CWFs do not differentiate and propagate fibrosis, it was hypothesised that the anti-fibrotic variant, CD44v7/8, might be upregulated in CWFs, contributing to the loss of differentiation. Analysing the variant expression in response to TGF-β1 stimulation (Figure 5.5B) showed that neither the NFs or CWFs had a significant response, although the CWFs showed a trend where the variant expression decreased with treatment, while in the NFs it increased. Comparing the basal expression with the CT values, clearly showed a higher overall expression of the anti-fibrotic variant within the CWFs compared to the NFs (Figure 5.5C). Hence it could be contributing to the non-healing nature of the CWFs.

To assess whether the localisation of the variant protein changed in the CWFs, ICC and fluorescence microscopy were performed (Figure 5.5A). There was diffuse staining throughout the NFs cells, including membrane-bound staining, with no change between the control and TGF-β1 stimulated cells. There was a similar observation in the CWFs, with no change in localisation following treatment, and a diffuse staining pattern throughout the cells.

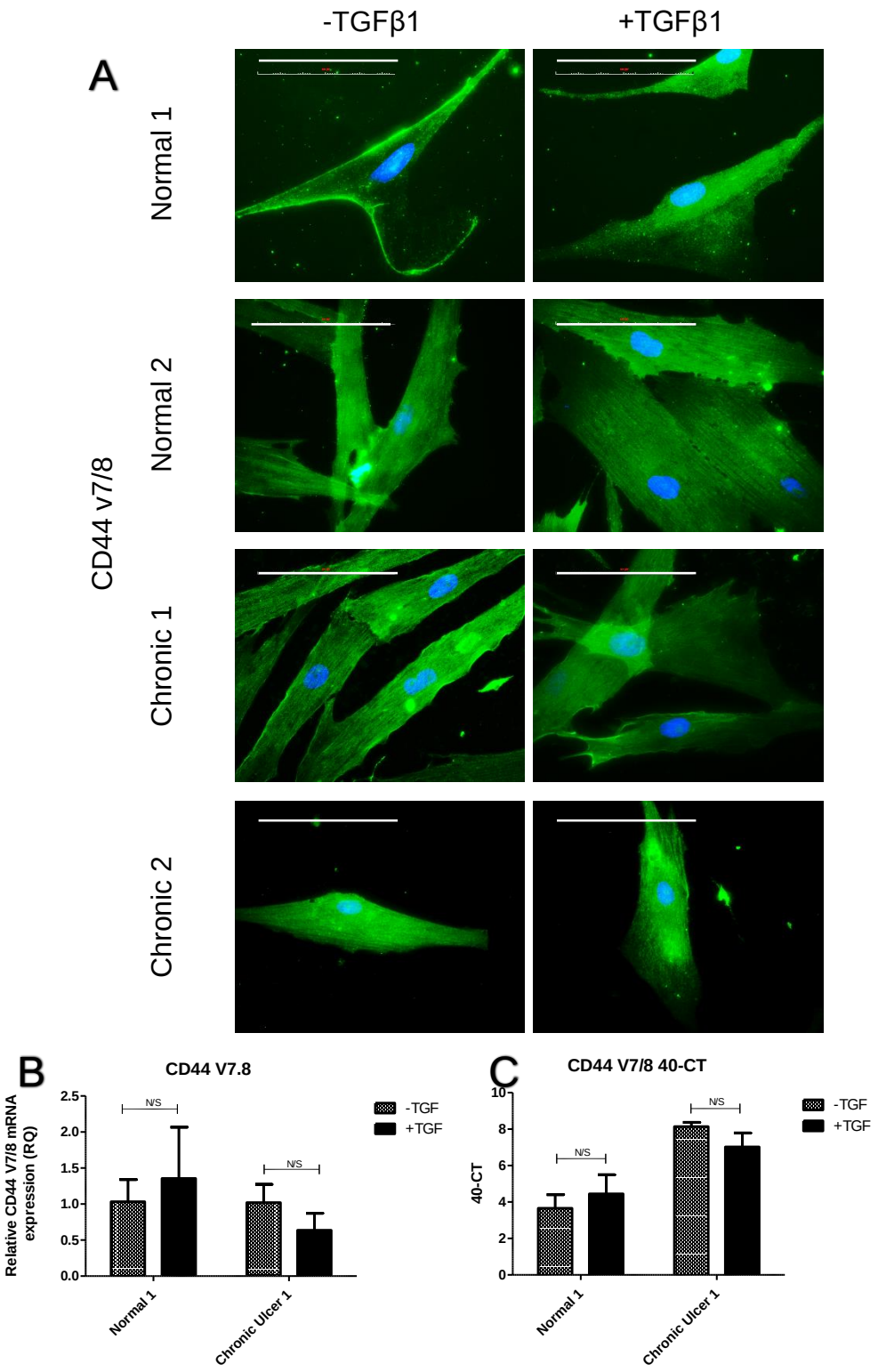

Figure 5.5. CD44 variant 7/8 localisation and expression. A. Cells were grown to 60-70% confluence and growth arrested for 48h. Cells were then incubated in serum-free medium alone (-TGF) or in medium containing 10 ng/mL TGFβ1 (+TGF) for 72h. The localisation of CD44 v7/8 protein was examined by immunocytochemistry; nuclei were visualised by Hoechst stain. Images shown are a representation of 2 independent experiments. Original magnification x400. Scale bar: 100μm. **B/C.** Cells were grown to 90-100% confluent monolayers and growth arrested for 48h. Cells were then incubated in serum-free medium alone (-TGF) or in medium containing 10ng/mL TGF-β1 (+TGF) for 72h. The expression of CD44 v7/8 mRNA was analysed by QPCR. Results are shown as the mean ± s.d. of 3 individual experiments. **B.** Shows relative expression **C.** Shows 40-CT values

5.2.6. HYAL2 perinuclear localisation in CWFs. Silencing HYAL2 doesn't recover a myofibroblast phenotype

The previous research undertaken on CD44v7/8 has shown its actions are facilitated by the translocation of HYAL2 to the nucleus of the cells, it was therefore of interest to visualise the location of HYAL2 in CWFs, confirming the variant was acting through the same mechanism (Midgley et al., 2017). Using fluorescence microscopy, the localisation was imaged in both control and stimulated, NFs and CWFs. Under stimulation, HYAL2 in the NFs became highly organised, aligning with the cytoskeleton (Figure 5.6A). However, CWFs showed internalisation of HYAL2 with TGF-β1 treatment, although some organisation and membrane staining was still present.

To determine a potential role for HYAL2 in the loss of CWFs differentiation, HYAL2 expression was successfully silenced in both NFs and CWFs (Figure 5.6B). α-SMA expression was then quantified in cells with knockdown HYAL2 expression, and compared to scramble controls. Silencing HYAL2 in the NFs did induce a greater response to TGF-β1 stimulation (Figure 5.6C). However, silencing HYAL2 in the CWFs did not recover the α-SMA response.

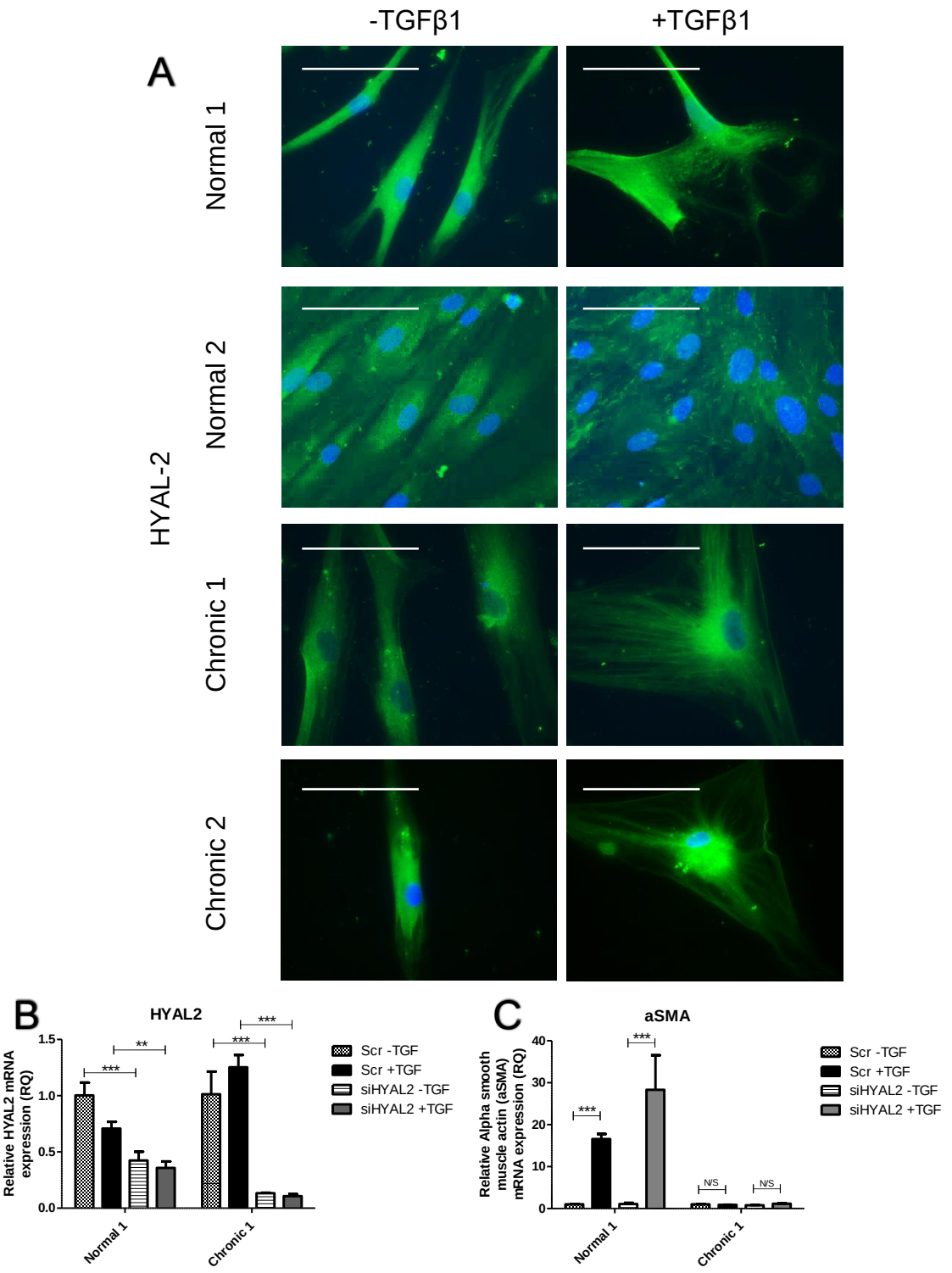

Figure 5.6. HYAL2 perinuclear localisation in CWFs. Silencing HYAL2 doesn't recover a myofibroblast phenotype. A. Cells were grown to 60-70% confluence and growth arrested for 48h. Cells were then incubated in serum-free medium alone (-TGF) or in medium containing 10 ng/mL TGFβ1 (+TGF) for 72h. The localisation of HYAL2 protein was examined by immunocytochemistry; nuclei were visualised by Hoechst stain. Images shown are a representation of 2 independent experiments. Original magnification x400. Scale bar: 100μm **B/C.** Fibroblasts were transfected with a scrambled siRNA sequence or siRNA targeting HYAL2 for 24h, prior to TGF-β1 treatment for 72h. The expression of (B) HYAL2 and (C) αSMA mRNA was analysed by QPCR. Results are shown as the mean ± s.d. of 3 individual experiments. *** P=<0.01, *** P=<0.001*

5.2.7. No difference in lysosome localisation was observed between CWFs and NFs

From the findings throughout this and the previous chapter, it is clear that protein, lipid, and GAG localisation is affected in CWFs. Because of this it was thought that the dysregulation of their localisation was due to dysfunctional transport and therefore important to image key intracellular transport vesicles and their response to TGF-β1 stimulation. Using fluorescence microscopy, the localisation of lysosomes was imaged in both control and stimulated, NFs and CWFs. The localisation of lysosomes in the NFs's did not appear to change following TGF-β1 stimulation. The staining pattern remained in an intracellular location with accumulation towards the surface of the cells and reduced staining surrounding the nucleus (Figure 5.7). This was more clearly seen in the treated cells, since these were larger. There was no change in lysosome number under either of the two serum conditions. Lysosomes in CWFs showed a similar staining pattern as observed in NFs. Furthermore, no significant change in lysosomal concentration is seen between control and stimulated cells. Lysosomal localisation and quantification does not seem to be affected by TGF-β1 treatment, nor abnormally expressed in CWFs compared to NFs.

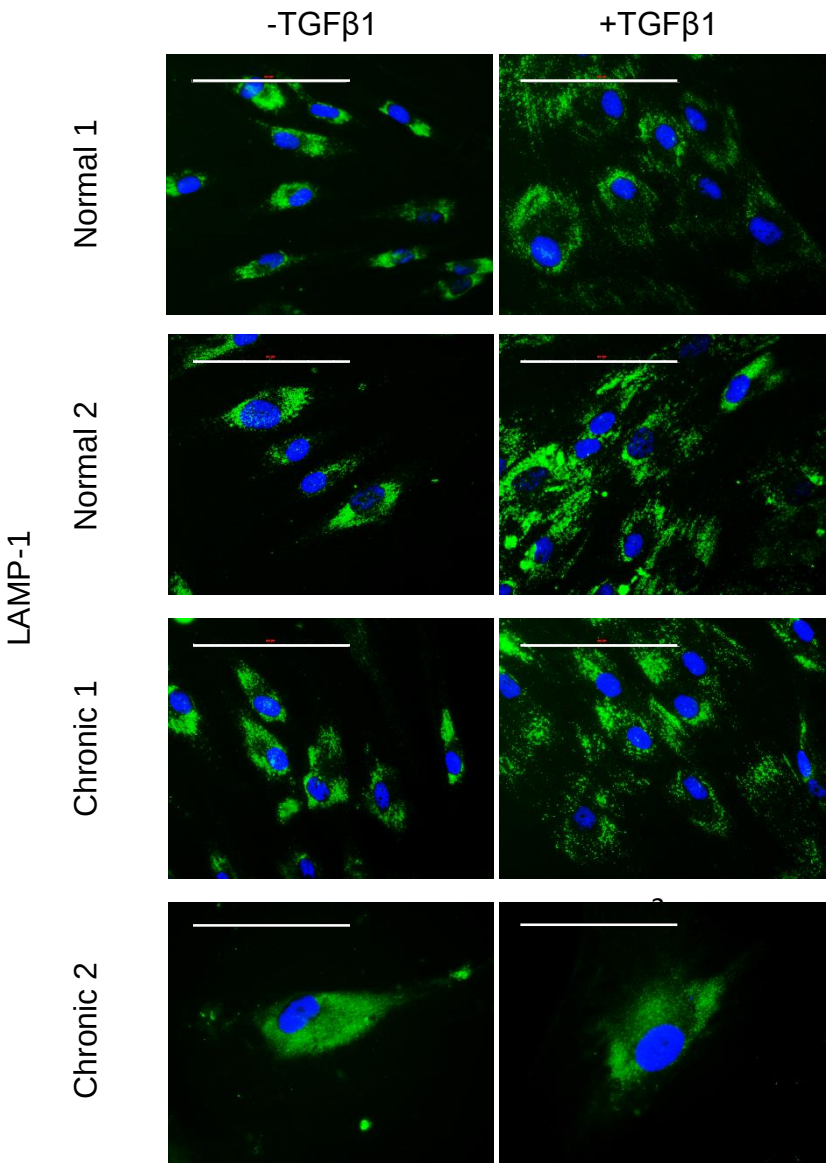

Figure 5.7. No difference in lysosome localisation was observed between CWFs and NFs. A. Cells were grown to 60-70% confluence and growth arrested for 48h. Cells were then incubated in serum-free medium alone (-TGF) or in medium containing 10 ng/mL TGFβ1 (+TGF) for 72h. The localisation of LAMP-1 protein was examined by immunocytochemistry; nuclei were visualised by Hoechst stain. Images shown are a representation of 2 independent experiments. Original magnification x400. Scale bar: 100μm

5.2.8. No difference in endosome localisation was observed between CWFs and NFs.

To confirm that intracellular vesicular trafficking was acting normally in CWFs, as described in the previous lysosomal result, endosomal localisation was imaged in the two cell types, with and without TGF-β1 treatment. Endosomal localisation was very different to that of lysosomes (Figure 5.8). Endosomal staining was specifically localised in a more perinuclear location with reduced staining further from the nucleus. No significant change in localisation or intensity was observed between the unstimulated and stimulated NFs, demonstrating that TGF-β1 does not change localisation of action or quantity of endosomes. The CWFs showed a similar staining pattern, with endosomes again being localised in a perinuclear location. There was no change in fluorescence intensity and thus endosome quantities were similar between NFs and CWFs. Overall intracellular transport did not seem to be responsible for the abnormal staining patterns observed in this and previous chapters regarding protein, HA and lipid localisation.

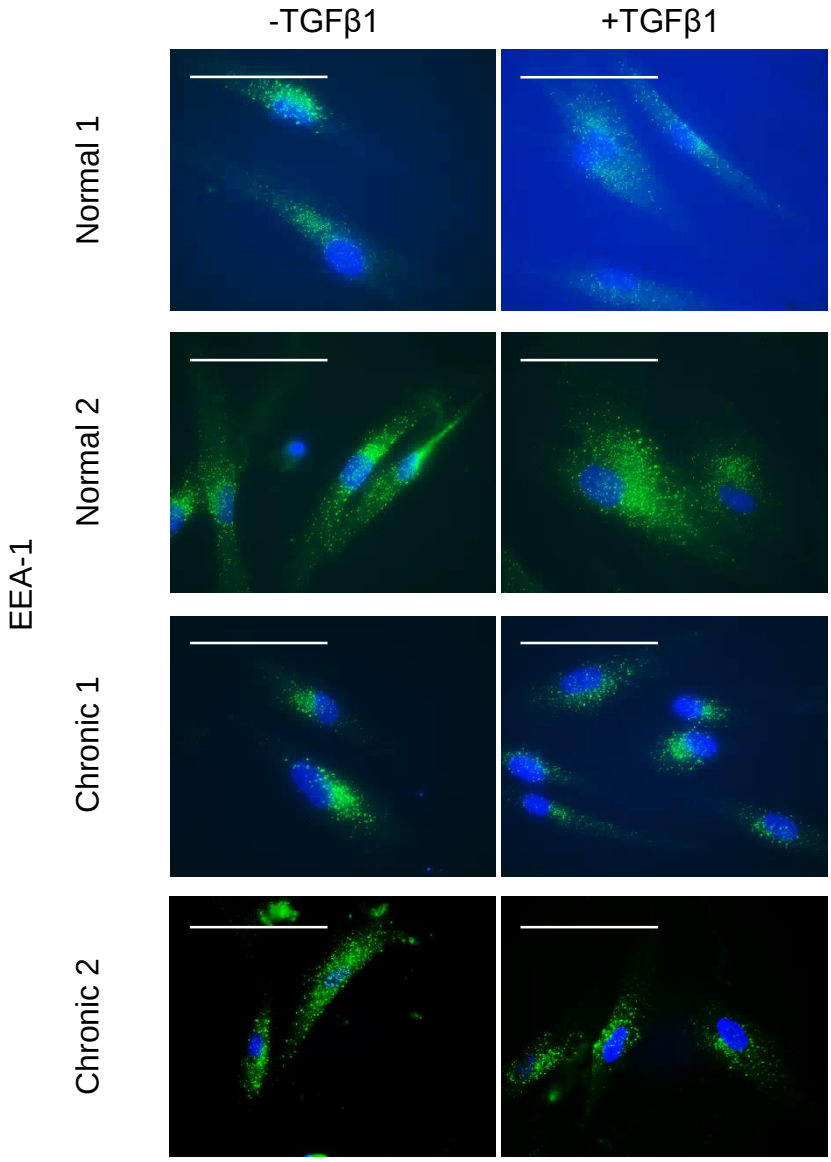

Figure 5.8. No difference in endosome localisation was observed between CWFs and NFs. A. Cells were grown to 60-70% confluence and growth arrested for 48h. Cells were then incubated in serum-free medium alone (-TGF) or in medium containing 10 ng/mL TGFβ1 (+TGF) for 72h. The localisation of EEA-1 protein was examined by immunocytochemistry; nuclei were visualised by Hoechst stain. Images shown are a representation of 2 independent experiments. Original magnification x400. Scale bar: 100μm.

5.2.9. No difference was seen between ER staining between CWFs and NFs

Since it was apparent that intracellular transport was not responsible for the aberrant staining patterns of key molecules involved in the differentiation mechanism, it was hypothesised that dysfunctional organelles responsible for protein synthesis may be causing accumulation of incorrectly synthesised molecules. It has previously been shown that ER stress can contribute to loss of cellular function, with impeded ability to fold or post-translationally modify secretory and transmembrane proteins (Oakes and Papa, 2015). The endoplasmic reticulum was therefore imaged in the two cell types. Staining in both NFs and CWFs showed clear staining in the nucleus, excluding the nucleolus, and diffuse staining throughout the cytoplasm (Figure 5.9). Since, no difference was seen between the NFs and CWFs, the ER was believed to be functioning normally and therefore not responsible for the abnormal staining patterns previously described.

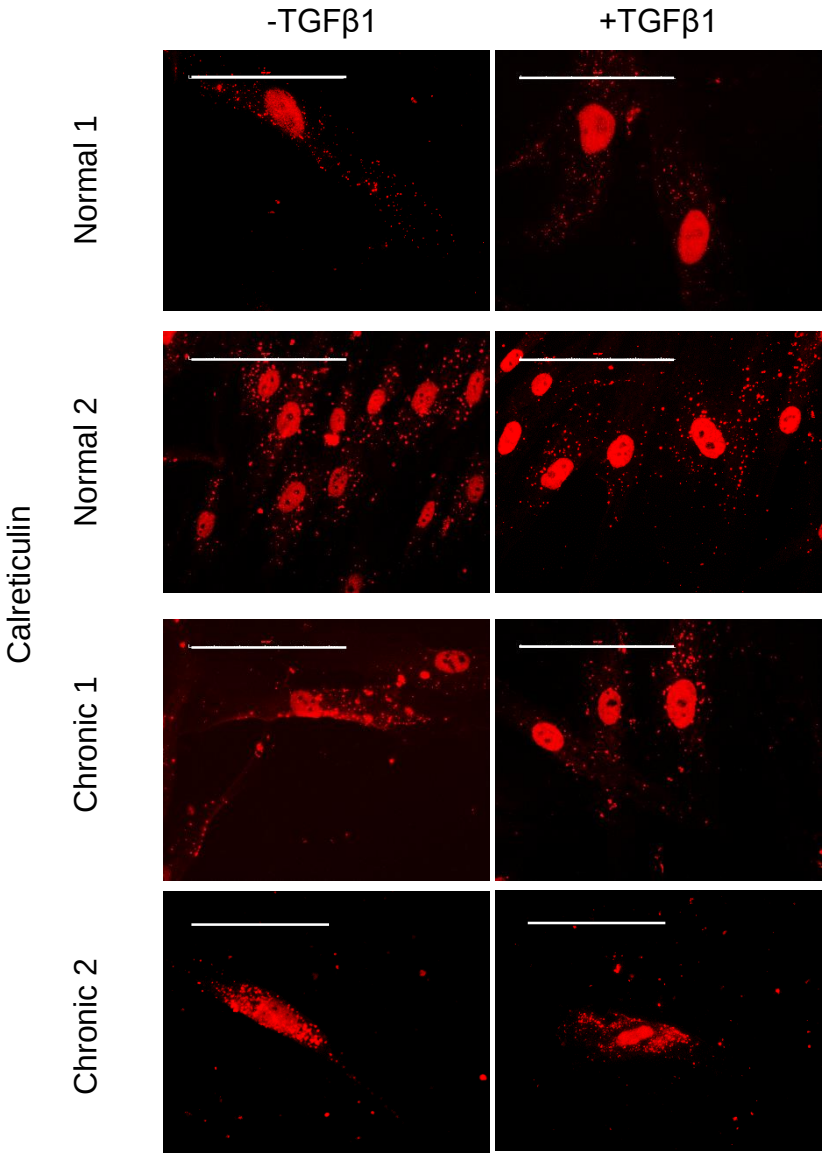

Figure 5.9. No difference was seen between E.R. staining of CWFs and NFs. A. Cells were grown to 60-70% confluence and growth arrested for 48h. Cells were then incubated in serum-free medium alone (-TGF) or in medium containing 10 ng/mL TGFβ1 (+TGF) for 72h. The expression of E.R. protein, calreticulin was examined by immunocytochemistry. No nuclei stain was used to show localisation within the nucleus. Images shown are a representation of 2 independent experiments. Original magnification x400. Scale bar: 100μm.

5.2.10. No differences in Golgi staining was observed between CWFs and NFs

The secondary organelle that may be responsible for trafficking and folding of protein aggregates and thus the abnormal staining patterns observed previously may be due to Golgi abnormalities. It has previously been shown that the Golgi in pathological conditions may cause the loss of cell surface determinants (Morre, 1991). This may be the case, which is in-line with the previous finding of intracellular EGFR in CWFs compared to their membrane location in NFs. The Golgi was therefore imaged using ICC. No change was seen with TGF-β1 treatment in either cell type. Comparing the NFs to the CWFs, also did not uncover any significant differences in the size, structure, or staining intensity of the Golgi, with clear Golgi networks visible in both cells types, indicating that the Golgi was not under stress in the CWFs.

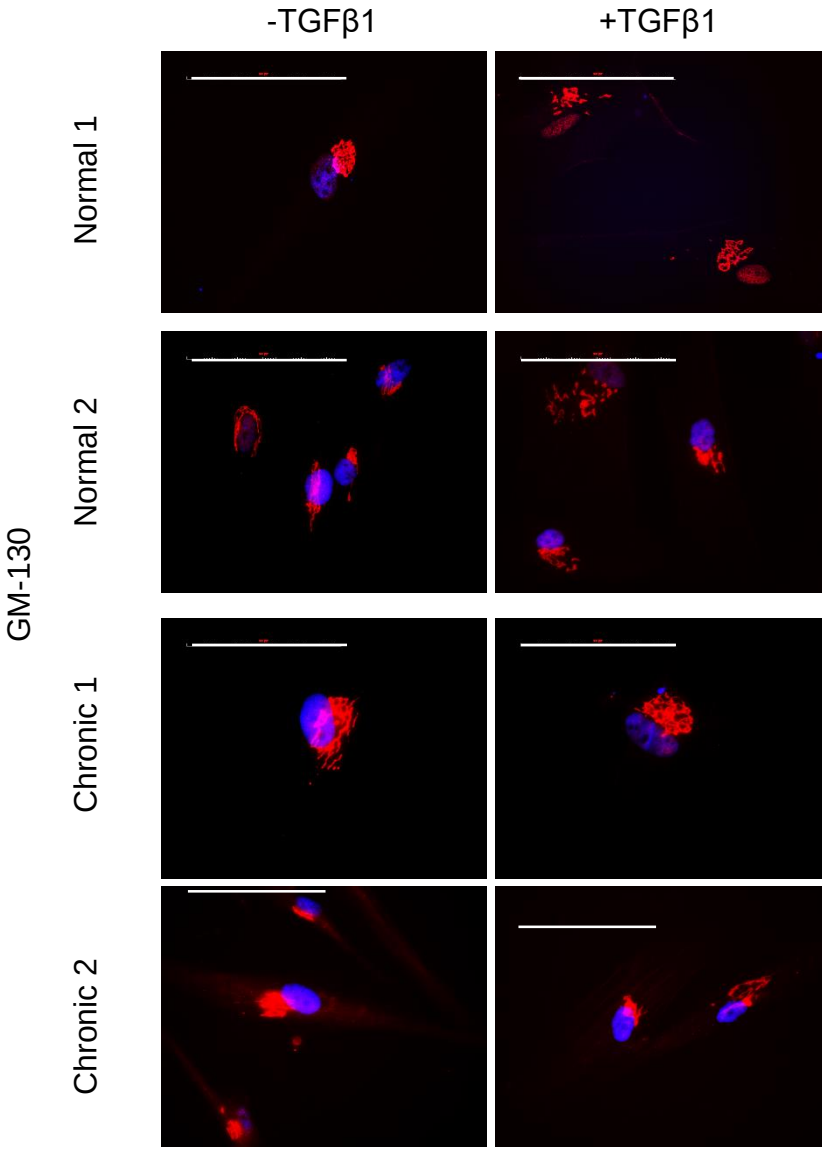

Figure 5.10. No differences in Golgi staining was observed between CWFs and NFs. A. Cells were grown to 60-70% confluence and growth arrested for 48h. Cells were then incubated in serum-free medium alone (-TGF) or in medium containing 10 ng/mL TGFβ1 (+TGF) for 72h. The Golgi protein, GM-130 was examined by immunocytochemistry; nuclei were visualised by Hoechst stain. Images shown are a representation of 2 independent experiments. Original magnification x400. Scale bar: 100μm.

5.2.11. No difference in microtubule formation between CWFs and NFs

Microtubules are essential to cellular microstructure and serve as intracellular transport tracks. Microtubules have been shown to undergo ‘catastrophe’ events, where growth ceases and breakdown increases, these events have been associated with age and pathology (Akhmanova and Steinmetz, 2015). It was therefore important to image the microtubule network in CWFs, to observe whether the network was affected by TGF-β1 stimulation and thus explain the aggregation of intracellular molecules in CWFs.

The NFs demonstrated a clearly defined, dense microtubule network in both the unstimulated and stimulated cells. The CWFs’ microtubule network was also clearly defined in both the unstimulated and stimulated cells.

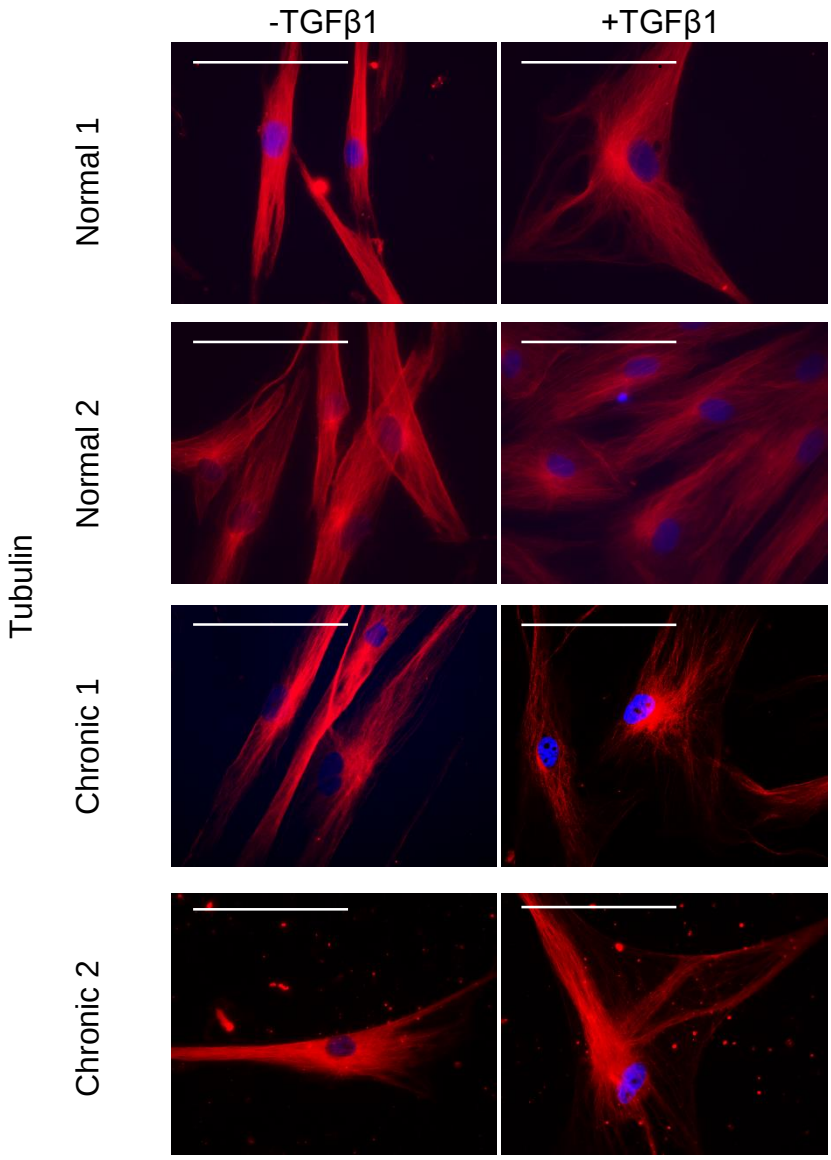

Figure 5.11. No difference in tubulin positive microtubule formation between CWFs and NFs. Cells were grown to 60-70% confluence and growth arrested for 48h. Cells were then incubated in serum-free medium alone (-TGF) or in medium containing 10 ng/mL TGFβ1 (+TGF) for 72h. Tubulin was examined by immunocytochemistry; nuclei were visualised by Hoechst stain. Original magnification x400. Images shown are a representation of 2 independent experiments. Scale bar: 100μm.

5.3. Discussion

The previous chapter highlighted the loss of the HA pericellular coat in CWFs together with an intracellular accumulation of HA. The loss of the coat was not due to aberrant HAS1 isoform expression. Therefore, the aim of this chapter was to investigate other possible causes for the loss of the HA coat. Although both CD44 and EGFR expression remained at comparatively normal levels in the CWFs (Figure 3.5), it has not yet been elucidated where these receptors are located in CWFs and whether they co-localise within lipid rafts on the membrane, a process shown to be essential for normal differentiation (Midgley et al., 2013). The initial aim of this chapter was to investigate the role of CD44 and EGFR in the loss of the HA pericellular coat. The results indicated intracellular localisation of both EGFR and lipids, indicating the discovery of a novel dysfunctional mechanism for the loss of myofibroblast signalling in chronic wounds, leading to their non-healing phenotype. From this result I investigated the role of intracellular trafficking and molecular synthesis, to find the cause of dysfunctional transport of the EGFR to the plasma membrane.

Previous studies have demonstrated that EGFR expression is essential for differentiation to occur (Meran et al., 2011). EGFR co-localises with the HA receptor within lipid rafts on the surface, enabling HA pericellular coat formation and downstream signalling of fibrosis (Midgley et al., 2013). Here, CWFs are shown to lose the expression of EGFR on the surface of CWFs, coinciding with the intracellular accumulation of lipids. The loss of EGFR location on the membrane is caused by a post-translational modification, since both mRNA and protein expression are not effected in the CWFs (Figure 3.5) and any other significant effect of post-transcriptional regulation by EGFR anti-sense was also not discovered (Alper et al., 2000).

As described in chapter 3, we cannot exclude that more than one abnormality, possibly several independent ones, exist in CWFs. The results from this chapter also highlight the increase in expression of the known anti-fibrotic phenotype CD44v7/8 in CWFs. Previously this variant has been shown to complete its action via the translocation of HYAL2 to the nucleus and displacing the spliceosome. This prevented splicing to create the fibrotic CD44s and subsequent accumulation of the anti-fibrotic CD44v7/8 at the cell surface (Midgley et al., 2017). This mechanism was not apparent in the CWFs, with variant 7/8, having diffuse staining through the cytoplasm in the CWFs and not being membrane specific. However, HYAL2, although not translocated to the nucleus as expected if the mechanism described by Midgley et al (2017) was functioning, was located intracellularly in a perinuclear location,

similar to the location imaged for EGFR. However, modification of HYAL2 expression with siHYAL2 did not recover the myofibroblast phenotype, confirming the internalisation of HYAL2 was not contributing to the loss of differentiation in the CWFs. The CD44v7/8 mechanism may be contributing to the loss of differentiation, but the two overlapping results of perinuclear located EGFR and HYAL2 may indicate a greater upstream cause of the loss of the correct localisation of key regulating molecules. The cause may be through the dysregulation of synthesis or trafficking of these proteins.

Intracellular budding occurs at both the ER and Golgi of vesicles responsible for intracellular trafficking. The two primary vesicles responsible for intracellular trafficking are endosomes and lysosomes, which are directed via the microtubule network. These results don't show any significant differences in the presence or locations of endosomes, lysosomes or microtubules in CWFs or NFs. This suggests that their transporting functionality is normal. Although the microtubule network does not seem affected, there are other actin based transport systems located in cells, that may be affected in CWFs (Khaitlina, 2014). One substantial finding is the coincident staining seen in the lysosomal location and lipids. It is well documented that lysosomes have a high lipid density and have a bidirectional relationship with lipids, where they regulate lipid metabolism, and in turn lipids regulate their function (Jaishy and Abel, 2016). The novel documentation of the accumulation of lipids surrounding the nucleus seen in CWFs, indicated that lipid metabolism and transport were dysregulated in this cells type. Lipid-derived signalling, is not well understood in the context of wound healing. However, some have indicated that lipid metabolism does have role in platelet aggregation and inflammation (Dhall et al., 2015). Lipid storage in fact has a link to myofibroblast formation in developing mice (McGowan and McCoy, 2014). Prostaglandin E_2 a ubiquitous bioactive lipid mediator has also been shown to be anti-fibrotic and even capable of reversing the myofibroblast phenotype (Garrison et al., 2013). The dysregulated lipid metabolism in CWFs may have a substantial role in the loss of myofibroblast differentiation.

The ER and Golgi are the two organelles responsible for: proteins and lipids synthesis, post-translational modification and packaging for transport to the appropriate location. Dysfunctional synthesis or packaging at these sites can cause dysfunctional transport. The location of the accumulated EGFR, HYAL2 and lipids in this chapter and HAS2, HAS1 and HA in previous chapters, are concurrent with reported location of the ER and Golgi, meaning that these molecules may be accumulating within these organelles. The staining for the Golgi, looked comparable between the two cell types showing that the Golgi was not affected

in CWFs. The location of the Golgi also confirmed that it had no role in the accumulation of the molecules listed above, since it had a very specific structure and location, compared to the diffuse perinuclear staining observed for the accumulating molecules.

ER stress is defined as the accumulation of unfolded, or mis-folded proteins in the lumen or the ER. ER stress has been associated with glucose or nutrient deprivation, viral infections, lipids, increased synthesis of secretory proteins and expression of mutant or misfolded proteins (Kaufman et al., 2002, Ozcan et al., 2004). We know that such conditions exist in chronic wound biology, and indicate that ER stress maybe contributing to the intracellular accumulation. ICC images of the ER associated protein, Calreticulin, did not show any differences between the ER in CWFs and NFs, suggesting that the ER of CWFs was not stressed. Although Calreticulin is a resident protein of the ER (Chiang et al., 2013), the staining pattern observed in the CWFs is not where the ER was expected as seen in other cells (Sanchez-Alvarez et al., 2014, Jiang et al., 2014). Calreticulin plays two major functions: chaperoning and regulation Ca^{2+} homeostasis (Michalak et al., 1999). It has also been found to have functions elsewhere throughout the cell, with its location in the nucleus associated with regulating steroid-inducible gene expression and the cytosol, where it is involved in the control of cell adhesion by interacting with integrins (Roderick et al., 1997). More staining was observed in the nucleus, associated with glucocorticoid activity, which is known to have a role in wound healing (Grose et al., 2002). Furthermore, calcium homeostasis and signalling has been linked to EGFR signalling, thus dysregulation of the ER may contribute to the loss of EGFR localisation (Leiper et al., 2006). The role of ER in CWFs dysfunction is yet to be elucidated. However, further experiments have the potential to uncover a link for protein localisation and accumulation.

Chapter 6

General Discussion

This thesis characterises the response of CWFs to TGF-β1 stimulation identifying key contributory factors in the two TGF-β1 signalling pathways, classical and non-classical, to the loss of myofibroblast differentiation. At an mRNA level both CWFs and NFs were not found to respond significantly differently to TGF-β1 stimulation, with the exception of TGF-βR and HAS1 expression in the CWFs. Downstream signalling of the TGF-βR pathway was found to respond to TGF-β1 treatment with the phosphorylation of SMAD2. In the non-classical pathway significantly higher basal expression of HAS1 and its significantly increased expression in response to TGF-β1 indicated a potential difference in the non-classical HA-CD44-EGFR pathway. Although manipulating HAS1 expression in both NFs and CWFs did not alter their TGF-β1 induced αSMA response, other results remained to indicate alterations in HA metabolism in the CWFs. This evidence included the loss of the HA pericellular coat, combined with aberrant HA and protein localisation of HAS1, HAS2 and HYAL2 intracellularly in the CWFs. Further investigation unveiled the loss of CD44-EGFR co-localisation in membrane bound lipid rafts on the surface of the CWFs, highlighting a possible cause for the loss of the HA pericellular coat. Under further examination, the accumulation of EGFR and lipids in a perinuclear location, suggesting that the lipids maybe creating a type of barrier surrounding the location of EGFR, preventing EGFR translocating to the membrane of CWFs. This result combined with other visualised aberrant intracellular protein locations in CWFs, prompted the hypothesis that protein synthesis and / or transport could be the cause. Initial investigations did not reveal any significant differences between protein synthesis or transport of the CWFs. Possible causes of the loss of CWFs differentiation will be discussed in this chapter.

The data reported in this thesis build on previous findings on TGFβ1 induced differentiation in dermal fibroblasts and uncover possible affected mechanisms, that contribute to the loss of the myofibroblast response in CWFs. The loss of the CWFs differentiation capacity has long been related to the chronic wound environment, such as increased hypoxia and inflammatory signalling molecules (Alizadeh et al., 2007, Modarressi et al., 2010, Sen and Roy, 2010). This thesis characterises and compares CWFs to NFs, *in vitro* in identical conditions, nullifying *in vivo* wound factors. Characterisation of these cells at an mRNA and protein level confirmed their CWFs phenotype with loss of αSMA expression. Normal fibroblast to myofibroblast differentiation is regulated by two independent but collaborating pathways, the classical TGF-βR and the non-classical HA-CD44-EGFR pathway. Exploring key transcriptional differences in these two pathways, between CWFs and NFs highlighted two abnormal expressional differences; TGF-βRI and HAS1. These two differences indicated potential loss of signalling in both pathways in CWFs.

TGF-βR expression response to TGF-β1 was lost in the CWFs, supporting other studies undertaken on CWFs (Jude et al., 2002, Kim et al., 2003). However, investigation of downstream phosphorylation signalling in the SMAD proteins, indicated no significant loss in signalling downstream from the TGF-β receptor. Although differences were observed between NFs and CWFs, these differences were expected since cells were not patient matched. Aberrant SMAD signalling has also been attributed to other cellular processes, such as proliferation which we know from the growth curve data, was reduced in these senescent-like CWFs populations (Ten Dijke et al., 2002). Defective proliferation also contributes to non-healing in chronic wounds, and is an important area of research (Wall, et al., 2008). A possible future direction may be to investigate the link between the decrease in proliferation in CWFs and alterations in key signalling pathways, assessing these pathways in parallel to viability assays. Since, phosphorylation of SMAD2 and 3 occurred in both CWFs, signalling was taking place and thus the classical TGF-βR pathway was concluded to be intact and not the major player in the loss of CWFs differentiation. The research focus changed to investigate the non-classical pathway as the major contributor to the loss of differentiation.

Previous research has identified the non-classical pathway to be the primary pathway responsible for the loss of differentiation in aged senescent fibroblasts. The loss of differentiation was associated with the aberrant expression of CD44, EGFR and HAS2 which resulted in the loss of their co-localisation on the surface, partially caused by higher expression of miR-7 (Midgley et al., 2014). It was hypothesised that this would be true for senescent CWFs. This thesis shows that this mechanism is not responsible for the loss of differentiation in CWFs, since no significant changes were seen in CD44, EGFR, HAS2 or miR-7 expression between CWFs and NFs responses to TGF-β1. However, evidence of alterations in HA metabolism in CWFs and NFs indicated that the non-classical pathway was still affected. HAS1 was shown to be the primary HAS in CWFs, with a large induction in response to TGF-β1. This was linked to attenuation of HA pericellular coat formation and alteration of intracellular locations of HA in the CWFs. However, transcriptional manipulation of HAS1 did not show direct changes to differentiation capacity in the CWFs or NFs. Previous research has shown that internalisation of HA is linked to the over-expression of a CD44 variant, V7/8, which internalises HA through the action of HYAL2 (Midgley et al., 2017). Examination of V7/8 expression did show it to be elevated with HYAL2 protein internalisation observed in the CWFs. Silencing the expression of HYAL2 in the CWFs did not return the myofibroblast phenotype, and CD44 v7/8 localisation was not membrane specific as described by Midgley *et al*. (2017). This discovery highlights a possible

contributing factor to the loss of myofibroblast formation in CWFs. However, other mechanisms may also be defective. The attenuation of the HA pericellular coat in CWFs, is an important finding since previous research has indicated that this is a primary cause of the loss of differentiation in aged senescent fibroblast populations (Simpson et al., 2009). This previous research has pinpointed the loss of CD44-EGFR co-localisation in lipid rafts on the membrane of fibroblasts, as the cause for pericellular coat loss. This project has found that EGFR-CD44 co-localisation is also lost in CWFs, however the mechanism for this loss is unique for CWFs. Investigation of CD44 and EGFR localisation in CWFs, showed a distinct aggregation in an intracellular, perinuclear location. This location was further surrounded by lipid staining, possibly implying that lipid aggregation creates a barrier preventing EGFR reaching the surface of cells. This intracellular location was confirmed with the use of two antibodies, one targeting the extracellular domain (Merck, GR01) and one targeting an intracellular epitope (Abcam, ab11401). The loss of EGFR location on the membrane is caused by post-translational modification, since neither mRNA or protein are affected in CWFs and any other post-transcriptional regulation by EGFR anti-sense was not discovered. Future work may elucidate this post-translational modification.

Previous studies have discussed the possibility of dysfunctional ER-golgi-plasma membrane trafficking also being essential for HA coat formation and the transfer of molecules to the membrane (Siiskonen et al., 2014). To investigate this staining was performed to assess the location and condition of key organelles. No significant changes were observable in ER, Golgi, microtubule, or endosomal staining. However, ER stress has been previously associated with causing protein mis-folding and hence could explain the aberrant protein localisation in CWFs (Kaufman et al., 2002). Although no changes in ER localisation were found between CWFs and NFs. A possible future direction would be to further investigate staining the ER with other antibodies such as GRP94 to verify the ER location and condition of the ER in CWFs. Protein mis-folding, caused by ER stress, maybe a contributing factor to the accumulation of intracellular proteins. However, it has been well documented that ER stress is a pro-fibrotic response and is capable of driving fibroblast differentiation without a TGF-β1 stimulus (Matsuzaki et al., 2015, Baek et al., 2012). This mechanism is based on the activation of the unfolded protein response (UPR) of the cell. The UPR reduces stress by activating three adaptive pathways: the transcriptional induction of ER chaperone proteins to help protein folding, the translational attenuation of protein synthesis and the promotion of the degradation of misfolded or unfolded proteins. Without successful activation of the UPR, cells eventually enter apoptosis (Baek et al., 2012). It could be said that activation of the UPR in CWFs is unsuccessful leading to the build-up of intracellular

proteins. Assessing the three pathways responsible for UPR activation, we can say that, no evidence of inhibition of protein synthesis was found in the CWFs. Western blots of CD44 and EGFR in CWFs showed comparable quantities to those in NFs, therefore showing that overall protein synthesis was not effected in CWFs. However, a future direction would be to assess pathways involved in the degradation of proteins in CWFs, since aberrant degradative pathways may also contribute to protein build-up within the cells.

The proteasome is a complex protease complex that carries out selective hydrolysis of intracellular proteins. Polymerization of ubiquitin, serves as a degradation signal for numerous target proteins broken down by the proteasome (Tanaka, 2009). The proteasome has been found to be important during wound healing. Inhibitors of the 20S proteasome, responsible for intracellular protein degradation, have been shown to have anti-fibrotic effects. Inhibiting proteasome 20S can downregulate the inflammatory response, block TGF-β1 fibrotic effects and alter MMP and TIMP expressions (Walker et al., 2013). Furthermore, ER stress has been found to compromise the proteasome system, therefore natural inhibition of the proteasome can result from ER stress (Menendez-Benito et al., 2005). Proteasome dysfunction maybe a contributing factor to the loss of intracellular protein clearance in the CWFs. It has been reported that upon proteasome failure, aggregates are transported via microtubule transport to the centrosome, forming an organelle known as an aggresome. A distinct finding by Zaarur (2014) was that upon proteasome failure, lysosomes clustered around the aggresome in a perinuclear location (Zaarur et al., 2014). One coinciding finding of this thesis was the localisation of CWFs lysosomes in a perinuclear location surrounding aggregating proteins. The area of the lysosomes was associated with an area or high lipid density, often associated with lysosomal activity (Hamer et al., 2012). This may be additional evidence showing that in CWFs, the proteasome is dysfunctional leading to the build-up of intracellular proteins. Zaarur (2014) continues to explain an entrapment zone of protein aggregation, surrounding the nucleus, much like that seen in the CWFs. However, the mechanism behind the formation of the entrapment zone, described by Zaarur (2014), is via loss of the microtubule network, which was found to be intact in this area of the CWFs. It would be of interest to measure the activity of the proteasome in CWFs, to assess its functionality. Future research is needed to fully attribute proteasome dysfunction in the CWFs pathobiology.

The localisation of lysosomes in the CWFs, was found to be in the area of high lipid density. Lysosomes have been shown to have a bifunctional relationship with lipids, they are capable of lipid degradation but lipids can also regulate lipid function, which has also been shown to

have a role in regulation myofibroblast formation (Jaishy and Abel, 2016, McGowan and McCoy, 2014). Impaired lipid homeostasis has been associated with senescent characteristics in cells, such as, slow cell proliferation, as seen in CWFs (Tsukamoto et al., 2002). Alteration in the actin cytoskeleton of cells has been found to be a key player in the loss of intracellular lipid transport. Alteration of the cytoskeleton is associated with CWFs, and may indicate a potential mechanism behind the accumulation of intracellular lipids (Raffetto et al., 2001, Tsukamoto et al., 2002). The novel finding of lysosomal and lipid intracellular accumulation in CWFs, may provide unique future directions for this project, in investigating the role of lipid metabolism, an area of research not yet explored in the context of the HA-CD44-EGFR pathway.

The wound environment is a key player on the outcome of wound healing (Raffetto et al., 2001). Pro-inflammatory cytokines, immune cell recruitment, infection, and oxidative stress all contribute to the non-healing outcome of chronic wounds, and can contribute specifically to the loss of fibroblast to myofibroblast differentiation. In this study, CWFs were compared to NFs *in vitro* eliminating the anti-fibrotic effects of the wound-microenvironment. Still, the CWFs fail to differentiate away from external wound stimuli. The question therefore remains what causes CWFs to lose their differentiation abilities. It has been well established that a hallmark of chronic wounds is the immobilisation of wound healing in the inflammatory phase (Zhao et al., 2016). Within this phase extensive damage occurs to the cells via the action of pro-inflammatory cytokines, reactive oxygen species and proteases, which is often exacerbated in chronic wounds by bacterial colonisation (Modarressi et al., 2010, Harsha et al., 2008). It has been reported that chronic inflammation can potentially alter long term gene expression of cells (Chen et al., 2008, Vigl et al., 2011). The up-regulation of HAS1, a pro-inflammatory HAS, in the CWFs suggests that this mechanism may be occurring in CWFs (Siiskonen et al., 2015). The changes to gene expression are thought to be caused by epigenetic modifications in response to environmental influences. These epigenetic modifications can include DNA methylation, methylation and acetylation of Histones and activation of non-coding RNAs, which all have downstream effects on gene expression (Bayarsaihan, 2011). Diabetic chronic wounds have been attributed to epigenetic changes, caused by diabetes, leading to the recruitment of dominant pro-inflammatory M1 macrophages (Sidaway, 2015). Epigenetic DNA methylation has also been attributed in directly affecting genes controlling fibroblast differentiation in idiopathic pulmonary fibrosis (Sanders et al., 2012). Hypoxia, an environmental factor, has been shown to cause epigenetic changes by DNA methylation of Thy-1, a gene associated with the activation of TGF-β1 (Robinson et al., 2012). ROS activity has also been associated with damage to the

proteasome, potentially contributing to the accumulation of intracellular proteins in the CWFs (Aiken et al., 2011). Epigenetic changes can occur as a result of environmental stimuli. Although changes in the primary genes involved in the two TGF-β1 pathways have been analysed in this thesis and found to be at comparable expression levels, there is much need of further investigation to investigate whether epigenetic changes from the chronic wound environment, may be causing intracellular protein aggregation, changes in HA metabolism and ultimately the loss of the myofibroblasts phenotype in CWFs. Future, investigations highlighting these epigenetic changes may allow gene therapy treatments to be developed to modify gene expressions of the fibroblasts back towards a healing phenotype.

6.1 Limitations

This study has identified multiple mechanisms that are defective in CWFs, associated with the loss of myofibroblast differentiation. However, there are several limitations to this study that will need to be addressed in future work to confirm the conclusions. Although the study confirms the variable nature of CWF responses due to the chronic wound environment, this led to the generation of donor specific responses in the results. Therefore, as all experiments were undertaken using 4 unique individual cell lines, this made drawing conclusions difficult from the evidence. Although, this research sets the foundations, it would be beneficial to repeat the experiments increasing the patient population to make the results more statistically significant (e.g. as performed by Wall et al., 2008). There were also limitations evident in the control cells as NFs were not patient matched to CWFs. This made interpretation of data difficult, since responses between cells could not be compared and only differences in response to TGF-β1 stimulation could be analysed. In the future more conclusions could be drawn from this study if patient-matched cells were used.

The majority of findings from this study indicate that it was not gene expression or protein levels that were affected in CWFs, but protein localisation. As this evidence was primarily based on qualitative images, attempts were made to confirm significant findings with repeat experiments, such as the intracellular localisation of EGFR which was confirmed with two separate antibodies, binding an intracellular and extracellular motif. However, this study would benefit from quantitative experiments such as cell fractionation followed by ELISA on separate cellular fractions to simultaneously identify protein location and quantity.

The wound milieu is a complex environment to study *in vitro* and therefore this study looked narrowly at the effect of TGF-β1 signalling and loss of fibroblast differentiation on

wound healing. Understanding these mechanisms is key to identifying the cause of clinical chronic wounds, however it is a contributing mechanisms and we know that other defective mechanisms may also contribute to the loss of healing. To increase our understanding further cell types from other different types of chronic wounds could be investigated, such as diabetic CWFs or CWFs from infected and non-infected chronic wounds. Experiments could also be designed to see the interaction of other cell types on CWFs such as macrophages which we know contribute to TGF-β1 signalling. Another method of investigating these complex interacting mechanisms and ensuring matched samples at high quantities, would be to study in *vivo*, using animal models. Appropriate diabetic wounding mouse models exist, such as the diabetic (db/db) mouse where chronic wounds can be modelled by inducing high oxidative stress following wounding. This can be accomplished using treatment of anti-oxidants immediately post wounding (Kim and Martins-Green, 2016). Pigs can be used for modelling infected and non-infected chronic wounds. Chronic wounds can be induced by surgically cutting blood flow to the site of injury, creating a hypoxic zone. This wound can then have bacteria added, to study the effects of various bacterial strains (Nunan et al., 2014).

The work outlined in this thesis identifies several novel aberrant mechanisms that contribute to the loss of the myofibroblastic response in CWFs. At this point we cannot exclude more than one abnormality, possibly several independent ones, exist in CWFs, causing the loss of myofibroblast formation. However, this thesis has laid the foundations for future research to understand the cause of dysfunctional protein, lipid and HA localisation in CWFs. Identifying these causes may highlight possible therapeutic targets for chronic wounds in the future.

References

AFRATIS, N., GIALELI, C., NIKITOVIC, D., TSEGENIDIS, T., KAROUSOU, E., THEOCHARIS, A. D., PAVAO, M. S., TZANAKAKIS, G. N. & KARAMANOS, N. K. 2012. Glycosaminoglycans: key players in cancer cell biology and treatment. *Febs j,* 279**,** 1177-97.

AIKEN, C. T., KAAKE, R. M., WANG, X. & HUANG, L. 2011. Oxidative Stress-Mediated Regulation of Proteasome Complexes. *Molecular & Cellular Proteomics : MCP,* 10**,** R110.006924.

AKHMANOVA, A. & STEINMETZ, M. O. 2015. Control of microtubule organization and dynamics: two ends in the limelight. *Nat Rev Mol Cell Biol,* 16**,** 711-26.

ALIZADEH, N., PEPPER, M. S., MODARRESSI, A., ALFO, K., SCHLAUDRAFF, K., MONTANDON, D., GABBIANI, G., BOCHATON-PIALLAT, M. L. & PITTET, B. 2007. Persistent ischemia impairs myofibroblast development in wound granulation tissue: a new model of delayed wound healing. *Wound Repair Regen,* 15**,** 809-16.

ALPER, O., DE SANTIS, M. L., STROMBERG, K., HACKER, N. F., CHO-CHUNG, Y. S. & SALOMON, D. S. 2000. Anti-sense suppression of epidermal growth factor receptor expression alters cellular proliferation, cell-adhesion and tumorigenicity in ovarian cancer cells. *Int J Cancer,* 88**,** 566-74.

ANDL, C. D., MIZUSHIMA, T., OYAMA, K., BOWSER, M., NAKAGAWA, H. & RUSTGI, A. K. 2004. EGFR-induced cell migration is mediated predominantly by the JAK-STAT pathway in primary esophageal keratinocytes. *Am J Physiol Gastrointest Liver Physiol,* 287**,** G1227-37.

ANDO, D., KORABEL, N., HUANG, K. C. & GOPINATHAN, A. 2015. Cytoskeletal Network Morphology Regulates Intracellular Transport Dynamics. *Biophys J,* 109**,** 1574-82.

ASHWORTH, J. J., SMYTH, J. V., PENDLETON, N., HORAN, M., PAYTON, A., WORTHINGTON, J., OLLIER, W. E. & ASHCROFT, G. S. 2005. The dinucleotide (CA) repeat polymorphism of estrogen receptor beta but not the dinucleotide (TA) repeat polymorphism of estrogen receptor alpha is associated with venous ulceration. *The Journal of Steroid Biochemistry and Molecular Biology,* 97**,** 266-270.

AYA, K. L. & STERN, R. 2014. Hyaluronan in wound healing: rediscovering a major player. *Wound Repair Regen,* 22**,** 579-93.

BAEK, H. A., KIM, D. S., PARK, H. S., JANG, K. Y., KANG, M. J., LEE, D. G., MOON, W. S., CHAE, H. J. & CHUNG, M. J. 2012. Involvement of endoplasmic reticulum stress in myofibroblastic differentiation of lung fibroblasts. *Am J Respir Cell Mol Biol,* 46**,** 731-9.

BAI, X., JING, L., LI, Y., LI, Y., LUO, S., WANG, S., ZHOU, J., LIU, Z. & DIAO, A. 2014. TMEPAI inhibits TGF-beta signaling by promoting lysosome degradation of TGF-beta receptor and contributes to lung cancer development. *Cell Signal,* 26**,** 2030-9.

BART, G., VICO, N. O., HASSINEN, A., PUJOL, F. M., DEEN, A. J., RUUSALA, A., TAMMI, R. H., SQUIRE, A., HELDIN, P., KELLOKUMPU, S. & TAMMI, M. I. 2015. Fluorescence resonance energy transfer (FRET) and proximity ligation assays reveal functionally relevant homo- and heteromeric complexes among hyaluronan synthases HAS1, HAS2, and HAS3. *J Biol Chem,* 290**,** 11479-90.

BAUER, S., JENDRO, M. C., WADLE, A., KLEBER, S., STENNER, F., DINSER, R., REICH, A., FACCIN, E., GODDE, S., DINGES, H., MULLER-LADNER, U. & RENNER, C. 2006. Fibroblast activation protein is expressed by rheumatoid myofibroblast-like synoviocytes. *Arthritis Res Ther,* 8**,** R171.

BAYARSAIHAN, D. 2011. Epigenetic Mechanisms in Inflammation. *Journal of Dental Research,* 90**,** 9-17.

BECK-SCHIMMER, B., OERTLI, B., PASCH, T. & WUTHRICH, R. P. 1998. Hyaluronan induces monocyte chemoattractant protein-1 expression in renal tubular epithelial cells. *J Am Soc Nephrol,* 9**,** 2283-90.

BERLANGA-ACOSTA, J., SCHULTZ, G. S., LOPEZ-MOLA, E., GUILLEN-NIETO, G., GARCIA-SIVERIO, M. & HERRERA-MARTINEZ, L. 2013. Glucose toxic effects on granulation tissue productive cells: the diabetics' impaired healing. *Biomed Res Int,* 2013**,** 256043.

BJARNSHOLT, T., KIRKETERP-MOLLER, K., JENSEN, P. O., MADSEN, K. G., PHIPPS, R., KROGFELT, K., HOIBY, N. & GIVSKOV, M. 2008. Why chronic wounds will not heal: a novel hypothesis. *Wound Repair Regen,* 16**,** 2-10.

BOCHATON-PIALLAT, M. L., GABBIANI, G. & HINZ, B. 2016. The myofibroblast in wound healing and fibrosis: answered and unanswered questions. *F1000Res,* 5.

BONNANS, C., CHOU, J. & WERB, Z. 2014. Remodelling the extracellular matrix in development and disease. *Nat Rev Mol Cell Biol,* 15**,** 786-801.

BOOKSTEIN, C., MUSCH, M. W., DUDEJA, P. K., MCSWINE, R. L., XIE, Y., BRASITUS, T. A., RAO, M. C. & CHANG, E. B. 1997. Inverse relationship between membrane lipid fluidity and activity of Na+/H+ exchangers, NHE1 and NHE3, in transfected fibroblasts. *J Membr Biol,* 160**,** 183-92.

BOONEN, M., PUISSANT, E., GILIS, F., FLAMION, B. & JADOT, M. 2014. Mouse liver lysosomes contain enzymatically active processed forms of Hyal-1. *Biochem Biophys Res Commun,* 446**,** 1155-60.

BRADER, K. R., WOLF, J. K., CHAKRABARTY, S. & PRICE, J. E. 1998. Epidermal growth factor receptor (EGFR) antisense transfection reduces the expression of EGFR and suppresses the malignant phenotype of a human ovarian cancer cell line. *Oncol Rep,* 5**,** 1269-74.

BUGANZA TEPOLE, A. & KUHL, E. 2013. Systems-based approaches toward wound healing. *Pediatr Res,* 73**,** 553-63.

BUHREN, B. A., SCHRUMPF, H., HOFF, N. P., BOLKE, E., HILTON, S. & GERBER, P. A. 2016. Hyaluronidase: from clinical applications to molecular and cellular mechanisms. *Eur J Med Res,* 21**,** 5.

CAMPO, G. M., AVENOSO, A., CAMPO, S., ANGELA, D., FERLAZZO, A. M. & CALATRONI, A. 2006. TNF-alpha, IFN-gamma, and IL-1beta modulate hyaluronan synthase expression in human skin fibroblasts: synergistic effect by concomital treatment with FeSO4 plus ascorbate. *Mol Cell Biochem,* 292**,** 169-78.

CHA, J., KWAK, T., BUTMARC, J., KIM, T.-A., YUFIT, T., CARSON, P., KIM, S.-J. & FALANGA, V. 2008. Fibroblasts from non-healing human chronic wounds show decreased expression of βig-h3, a TGF-β inducible protein. *Journal of Dermatological Science,* 50**,** 15-23.

CHAUDHARI, N., TALWAR, P., PARIMISETTY, A., LEFEBVRE D'HELLENCOURT, C. & RAVANAN, P. 2014. A molecular web: endoplasmic reticulum stress, inflammation, and oxidative stress. *Front Cell Neurosci,* 8**,** 213.

CHEN, H., YANG, W.-W., WEN, Q.-T., XU, L. & CHEN, M. 2009. TGF-β-induced fibroblast activation protein expression, fibroblast activation protein expression increases the proliferation, adhesion, and migration of HO-8910PM. *Experimental and Molecular Pathology,* 87**,** 189-194.

CHEN, Y.-W., SHI, R., GERACI, N., SHRESTHA, S., GORDISH-DRESSMAN, H. & PACHMAN, L. M. 2008. Duration of chronic inflammation alters gene expression in muscle from untreated girls with juvenile dermatomyositis. *BMC Immunology,* 9**,** 43-43.

CHEN, Y. G. 2009. Endocytic regulation of TGF-beta signaling. *Cell Res,* 19**,** 58-70.

CHIANG, W. F., HWANG, T. Z., HOUR, T. C., WANG, L. H., CHIU, C. C., CHEN, H. R., WU, Y. J., WANG, C. C., WANG, L. F., CHIEN, C. Y., CHEN, J. H., HSU, C. T. & CHEN, J. Y. 2013. Calreticulin, an endoplasmic reticulum-resident protein, is highly expressed and essential for cell proliferation and migration in oral squamous cell carcinoma. *Oral Oncol,* 49**,** 534-41.

CIANFARANI, F., TOIETTA, G., DI ROCCO, G., CESAREO, E., ZAMBRUNO, G. & ODORISIO, T. 2013. Diabetes impairs adipose tissue-derived stem cell function and efficiency in promoting wound healing. *Wound Repair Regen,* 21**,** 545-53.

CLINTON, A. & CARTER, T. 2015. Chronic Wound Biofilms: Pathogenesis and Potential Therapies. *Lab Med,* 46**,** 277-84.

COOPER, L., JOHNSON, C., BURSLEM, F. & MARTIN, P. 2005. Wound healing and inflammation genes revealed by array analysis of 'macrophageless' PU.1 null mice. *Genome Biology,* 6**,** R5-R5.

CORDERO, J. B., STEFANATOS, R. K., MYANT, K., VIDAL, M. & SANSOM, O. J. 2012. Non-autonomous crosstalk between the Jak/Stat and Egfr pathways mediates Apc1-driven intestinal stem cell hyperplasia in the Drosophila adult midgut. *Development,* 139**,** 4524-35.

COSTERTON, J. W., STEWART, P. S. & GREENBERG, E. P. 1999. Bacterial biofilms: a common cause of persistent infections. *Science,* 284**,** 1318-22.

DANIELSEN, P. L., HOLST, A. V., MALTESEN, H. R., BASSI, M. R., HOLST, P. J., HEINEMEIER, K. M., OLSEN, J., DANIELSEN, C. C., POULSEN, S. S., JORGENSEN, L. N. & AGREN, M. S. 2011. Matrix metalloproteinase-8 overexpression prevents proper tissue repair. *Surgery,* 150**,** 897-906.

DARBY, I. A., LAVERDET, B., BONTE, F. & DESMOULIERE, A. 2014. Fibroblasts and myofibroblasts in wound healing. *Clin Cosmet Investig Dermatol,* 7**,** 301-11.

DAY, A. J. & PRESTWICH, G. D. 2002. Hyaluronan-binding proteins: tying up the giant. *J Biol Chem,* 277**,** 4585-8.

DECHERT, T. A., DUCALE, A. E., WARD, S. I. & YAGER, D. R. 2006. Hyaluronan in human acute and chronic dermal wounds. *Wound Repair Regen,* 14**,** 252-8.

DEEN, A. J., RILLA, K., OIKARI, S., KARNA, R., BART, G., HAYRINEN, J., BATHINA, A. R., ROPPONEN, A., MAKKONEN, K., TAMMI, R. H. & TAMMI, M. I. 2014. Rab10-mediated endocytosis of the hyaluronan synthase HAS3 regulates hyaluronan synthesis and cell adhesion to collagen. *J Biol Chem,* 289**,** 8375-89.

DEONARINE, K., PANELLI, M. C., STASHOWER, M. E., JIN, P., SMITH, K., SLADE, H. B., NORWOOD, C., WANG, E., MARINCOLA, F. M. & STRONCEK, D. F. 2007. Gene expression profiling of cutaneous wound healing. *Journal of Translational Medicine,* 5**,** 11-11.

DHALL, S., DO, D. C., GARCIA, M., KIM, J., MIREBRAHIM, S. H., LYUBOVITSKY, J., LONARDI, S., NOTHNAGEL, E. A., SCHILLER, N. & MARTINS-GREEN, M. 2014. Generating and reversing chronic wounds in diabetic mice by manipulating wound redox parameters. *J Diabetes Res,* 2014**,** 562625.

DHALL, S., WIJESINGHE, D. S., KARIM, Z. A., CASTRO, A., VEMANA, H. P., KHASAWNEH, F. T., CHALFANT, C. E. & MARTINS-GREEN, M. 2015. Arachidonic acid-derived signaling lipids and functions in impaired healing. *Wound Repair Regen,* 23**,** 644-56.

DU, W. W., YANG, B. B., SHATSEVA, T. A., YANG, B. L., DENG, Z., SHAN, S. W., LEE, D. Y., SETH, A. & YEE, A. J. 2010. Versican G3 promotes mouse mammary tumor cell growth, migration, and metastasis by influencing EGF receptor signaling. *PLoS One,* 5**,** e13828.

EDWARDS, D. R., HANDSLEY, M. M. & PENNINGTON, C. J. 2008. The ADAM metalloproteinases. *Mol Aspects Med,* 29**,** 258-89.

EVANKO, S. P., POTTER-PERIGO, S., PETTY, L. J., WORKMAN, G. A. & WIGHT, T. N. 2015. Hyaluronan Controls the Deposition of Fibronectin and Collagen and Modulates TGF-beta1 Induction of Lung Myofibroblasts. *Matrix Biol,* 42**,** 74-92.

EVANS, R. A., TIAN, Y. C., STEADMAN, R. & PHILLIPS, A. O. 2003. TGF-beta1-mediated fibroblast-myofibroblast terminal differentiation-the role of Smad proteins. *Exp Cell Res,* 282**,** 90-100.

FAASSEN, A. E., SCHRAGER, J. A., KLEIN, D. J., OEGEMA, T. R., COUCHMAN, J. R. & MCCARTHY, J. B. 1992. A cell surface chondroitin sulfate proteoglycan, immunologically related to CD44, is involved in type I collagen-mediated melanoma cell motility and invasion. *J Cell Biol,* 116**,** 521-31.

FALKE, L. L., GHOLIZADEH, S., GOLDSCHMEDING, R., KOK, R. J. & NGUYEN, T. Q. 2015. Diverse origins of the myofibroblast-implications for kidney fibrosis. *Nat Rev Nephrol,* 11**,** 233-44.

FERGUSON, E. L., ROBERTS, J. L., MOSELEY, R., GRIFFITHS, P. C. & THOMAS, D. W. 2011. Evaluation of the physical and biological properties of hyaluronan and hyaluronan fragments. *Int J Pharm,* 420**,** 84-92.

FOKIN, A. I., BRODSKY, I. B., BURAKOV, A. V. & NADEZHDINA, E. S. 2014. Interaction of early secretory pathway and Golgi membranes with microtubules and microtubule motors. *Biochemistry (Mosc),* 79**,** 879-93.

FOX, S. B., FAWCETT, J., JACKSON, D. G., COLLINS, I., GATTER, K. C., HARRIS, A. L., GEARING, A. & SIMMONS, D. L. 1994. Normal human tissues, in addition to some tumors, express multiple different CD44 isoforms. *Cancer Res,* 54**,** 4539-46.

FRANKER, M. A. & HOOGENRAAD, C. C. 2013. Microtubule-based transport - basic mechanisms, traffic rules and role in neurological pathogenesis. *J Cell Sci,* 126**,** 2319-29.

FRANTZ, C., STEWART, K. M. & WEAVER, V. M. 2010. The extracellular matrix at a glance. *J Cell Sci,* 123**,** 4195-200.

FRONZA, M., CAETANO, G. F., LEITE, M. N., BITENCOURT, C. S., PAULA-SILVA, F. W., ANDRADE, T. A., FRADE, M. A., MERFORT, I. & FACCIOLI, L. H. 2014. Hyaluronidase modulates inflammatory response and accelerates the cutaneous wound healing. *PLoS One,* 9**,** e112297.

FRYKBERG, R. G. & BANKS, J. 2015. Challenges in the Treatment of Chronic Wounds. *Adv Wound Care (New Rochelle),* 4**,** 560-582.

GABBIANI, G. 2003. The myofibroblast in wound healing and fibrocontractive diseases. *J Pathol,* 200**,** 500-3.

GAO, Y., PENG, X., JIN, Z. F. & FU, Z. J. 2009. [Expression of FAP and alpha-SMA during the incised wound healing in mice skin]. *Fa Yi Xue Za Zhi,* 25**,** 405-8.

GARCIA-HONDUVILLA, N., CIFUENTES, A., ORTEGA, M. A., PASTOR, M., GAINZA, G., GAINZA, E., BUJAN, J. & ALVAREZ DE MON, M. 2018. Immuno-modulatory effect of local rhEGF treatment during tissue repair in diabetic ulcers. *Endocr Connect*.

GARRISON, G., HUANG, S. K., OKUNISHI, K., SCOTT, J. P., KUMAR PENKE, L. R., SCRUGGS, A. M. & PETERS-GOLDEN, M. 2013. Reversal of Myofibroblast Differentiation by Prostaglandin E(2). *American Journal of Respiratory Cell and Molecular Biology,* 48**,** 550-558.

GELSE, K., POSCHL, E. & AIGNER, T. 2003. Collagens--structure, function, and biosynthesis. *Adv Drug Deliv Rev,* 55**,** 1531-46.

GHATAK, S., HASCALL, V. C., MARKWALD, R. R., FEGHALI-BOSTWICK, C., ARTLETT, C. M., GOOZ, M., BOGATKEVICH, G. S., ATANELISHVILI, I., SILVER, R. M., WOOD, J., THANNICKAL, V. J. & MISRA, S. 2017. Transforming growth factor beta1 (TGFbeta1)-induced CD44V6-NOX4 signaling in pathogenesis of idiopathic pulmonary fibrosis. *J Biol Chem,* 292**,** 10490-10519.

GHOSH, A., KUPPUSAMY, H. & PILARSKI, L. M. 2009. Aberrant splice variants of HAS1 (Hyaluronan Synthase 1) multimerize with and modulate normally spliced HAS1 protein: a potential mechanism promoting human cancer. *J Biol Chem,* 284**,** 18840-50.

GJODSBOL, K., CHRISTENSEN, J. J., KARLSMARK, T., JORGENSEN, B., KLEIN, B. M. & KROGFELT, K. A. 2006. Multiple bacterial species reside in chronic wounds: a longitudinal study. *Int Wound J,* 3**,** 225-31.

GONZALEZ, A. C., COSTA, T. F., ANDRADE, Z. A. & MEDRADO, A. R. 2016. Wound healing - A literature review. *An Bras Dermatol,* 91**,** 614-620.

GOREN, I., ALLMANN, N., YOGEV, N., SCHURMANN, C., LINKE, A., HOLDENER, M., WAISMAN, A., PFEILSCHIFTER, J. & FRANK, S. 2009. A transgenic mouse model of inducible macrophage depletion: effects of diphtheria toxin-driven lysozyme M-specific cell lineage ablation on wound inflammatory, angiogenic, and contractive processes. *Am J Pathol,* 175**,** 132-47.

GRASS, G. D., DAI, L., QIN, Z., PARSONS, C. & TOOLE, B. P. 2014. CD147: regulator of hyaluronan signaling in invasiveness and chemoresistance. *Adv Cancer Res,* 123**,** 351-73.

GREGORY, A. D., KLIMENT, C. R., METZ, H. E., KIM, K.-H., KARGL, J., AGOSTINI, B. A., CRUM, L. T., OCZYPOK, E. A., OURY, T. A. & HOUGHTON, A. M. 2015. Neutrophil elastase promotes myofibroblast differentiation in lung fibrosis. *Journal of Leukocyte Biology,* 98**,** 143-152.

GREY, J. E., HARDING, K. G. & ENOCH, S. 2006. Venous and arterial leg ulcers. *BMJ : British Medical Journal,* 332**,** 347-350.

GROSE, R., WERNER, S., KESSLER, D., TUCKERMANN, J., HUGGEL, K., DURKA, S., REICHARDT, H. M. & WERNER, S. 2002. A role for endogenous glucocorticoids in wound repair. *EMBO Rep,* 3**,** 575-82.

GU, L., ZHU, Y. J., YANG, X., GUO, Z. J., XU, W. B. & TIAN, X. L. 2007. Effect of TGF-beta/Smad signaling pathway on lung myofibroblast differentiation. *Acta Pharmacol Sin,* 28**,** 382-91.

HAAKENSON, J. K., KHOKHLATCHEV, A. V., CHOI, Y. J., LINTON, S. S., ZHANG, P., ZAKI, P. M., FU, C., COOPER, T. K., MANNI, A., ZHU, J., FOX, T. E., DONG, C. & KESTER, M. 2015. Lysosomal degradation of CD44 mediates ceramide nanoliposome-induced anoikis and diminished extravasation in metastatic carcinoma cells. *J Biol Chem,* 290**,** 8632-43.

HALE, L. P., PATEL, D. D., CLARK, R. E. & HAYNES, B. F. 1995. Distribution of CD44 variant isoforms in human skin: differential expression in components of benign and malignant epithelia. *J Cutan Pathol,* 22**,** 536-45.

HAMER, I., VAN BEERSEL, G., ARNOULD, T. & JADOT, M. 2012. Lipids and lysosomes. *Curr Drug Metab,* 13**,** 1371-87.

HAN, G. & CEILLEY, R. 2017. Chronic Wound Healing: A Review of Current Management and Treatments. *Adv Ther,* 34**,** 599-610.

HANLEY, W. D., BURDICK, M. M., KONSTANTOPOULOS, K. & SACKSTEIN, R. 2005. CD44 on LS174T colon carcinoma cells possesses E-selectin ligand activity. *Cancer Res,* 65**,** 5812-7.

HANSES, F., PARK, S., RICH, J. & LEE, J. C. 2011. Reduced neutrophil apoptosis in diabetic mice during staphylococcal infection leads to prolonged Tnfalpha production and reduced neutrophil clearance. *PLoS One,* 6**,** e23633.

HARADA, H. & TAKAHASHI, M. 2007. CD44-dependent intracellular and extracellular catabolism of hyaluronic acid by hyaluronidase-1 and -2. *J Biol Chem,* 282**,** 5597-607.

HARSHA, A., STOJADINOVIC, O., BREM, H., SEHARA-FUJISAWA, A., WEWER, U., LOOMIS, C. A., BLOBEL, C. P. & TOMIC-CANIC, M. 2008. ADAM12: a potential target for the treatment of chronic wounds. *J Mol Med (Berl),* 86**,** 961-9.

HASAN, A., MURATA, H., FALABELLA, A., OCHOA, S., ZHOU, L., BADIAVAS, E. & FALANGA, V. 1997. Dermal fibroblasts from venous ulcers are unresponsive to the action of transforming growth factor-beta 1. *J Dermatol Sci,* 16**,** 59-66.

HASANEEN, N. A., CAO, J., PULKOSKI-GROSS, A., ZUCKER, S. & FODA, H. D. 2016. Extracellular Matrix Metalloproteinase Inducer (EMMPRIN) promotes lung fibroblast proliferation, survival and differentiation to myofibroblasts. *Respir Res,* 17**,** 17.

HASCALL, V. C., MAJORS, A. K., DE LA MOTTE, C. A., EVANKO, S. P., WANG, A., DRAZBA, J. A., STRONG, S. A. & WIGHT, T. N. 2004. Intracellular hyaluronan: a new frontier for inflammation? *Biochim Biophys Acta,* 1673**,** 3-12.

HASHIMOTO, A., KUROSAKI, M., GOTOH, N., SHIBUYA, M. & KUROSAKI, T. 1999. Shc regulates epidermal growth factor-induced activation of the JNK signaling pathway. *J Biol Chem,* 274**,** 20139-43.

HE, K., YAN, X., LI, N., DANG, S., XU, L., ZHAO, B., LI, Z., LV, Z., FANG, X., ZHANG, Y. & CHEN, Y. G. 2015. Internalization of the TGF-beta type I receptor into caveolin-1 and EEA1 double-positive early endosomes. *Cell Res,* 25**,** 738-52.

HINZ, B., CELETTA, G., TOMASEK, J. J., GABBIANI, G. & CHAPONNIER, C. 2001. Alpha-smooth muscle actin expression upregulates fibroblast contractile activity. *Mol Biol Cell,* 12**,** 2730-41.

HINZ, B., PHAN, S. H., THANNICKAL, V. J., GALLI, A., BOCHATON-PIALLAT, M. L. & GABBIANI, G. 2007. The myofibroblast: one function, multiple origins. *Am J Pathol,* 170**,** 1807-16.

HO, L. T., HARRIS, A. M., TANIOKA, H., YAGI, N., KINOSHITA, S., CATERSON, B., QUANTOCK, A. J., YOUNG, R. D. & MEEK, K. M. 2014. A comparison of glycosaminoglycan distributions, keratan sulphate sulphation patterns and collagen fibril architecture from central to peripheral regions of the bovine cornea. *Matrix Biol,* 38**,** 59-68.

HOFFMAN, M. M. & MONROE, D. M. 2005. Rethinking the coagulation cascade. *Curr Hematol Rep,* 4**,** 391-6.

HSU, L. J., SCHULTZ, L., HONG, Q., VAN MOER, K., HEATH, J., LI, M. Y., LAI, F. J., LIN, S. R., LEE, M. H., LO, C. P., LIN, Y. S., CHEN, S. T. & CHANG, N. S. 2009. Transforming growth factor beta1 signaling via interaction with cell surface Hyal-2 and recruitment of WWOX/WOX1. *J Biol Chem,* 284**,** 16049-59.

HUET, E., GABISON, E. E., MOURAH, S. & MENASHI, S. 2008a. Role of emmprin/CD147 in tissue remodeling. *Connect Tissue Res,* 49**,** 175-9.

HUET, E., VALLEE, B., SZUL, D., VERRECCHIA, F., MOURAH, S., JESTER, J. V., HOANG-XUAN, T., MENASHI, S. & GABISON, E. E. 2008b. Extracellular matrix metalloproteinase inducer/CD147 promotes myofibroblast differentiation by inducing alpha-smooth muscle actin expression and collagen gel contraction: implications in tissue remodeling. *Faseb j,* 22**,** 1144-54.

IOZZO, R. V. & SCHAEFER, L. 2010. Proteoglycans in health and disease: novel regulatory signaling mechanisms evoked by the small leucine-rich proteoglycans. *Febs j,* 277**,** 3864-75.

ITANO, N. & KIMATA, K. 2002. Mammalian hyaluronan synthases. *IUBMB Life,* 54**,** 195-9.

JAISHY, B. & ABEL, E. D. 2016. Lipids, lysosomes, and autophagy. *J Lipid Res,* 57**,** 1619-35.

JALKANEN, S. & JALKANEN, M. 1992. Lymphocyte CD44 binds the COOH-terminal heparin-binding domain of fibronectin. *J Cell Biol,* 116**,** 817-25.

JEBELEANU, G. & PROCOPCIUC, L. 2001. G20210A prothrombin gene mutation identified in patients with venous leg ulcers. *J Cell Mol Med,* 5**,** 397-401.

JIANG, H., XIONG, S. & XIA, X. 2014. Retinitis pigmentosaassociated rhodopsin mutant T17M induces endoplasmic reticulum (ER) stress and sensitizes cells to ER stress-induced cell death. *Mol Med Rep,* 9**,** 1737-42.

JUDE, E. B., BLAKYTNY, R., BULMER, J., BOULTON, A. J. & FERGUSON, M. W. 2002. Transforming growth factor-beta 1, 2, 3 and receptor type I and II in diabetic foot ulcers. *Diabet Med,* 19**,** 440-7.

KADLER, K. E., BALDOCK, C., BELLA, J. & BOOT-HANDFORD, R. P. 2007. Collagens at a glance. *J Cell Sci,* 120**,** 1955-8.

KAO, J. J. 2006. The NF-kappaB inhibitor pyrrolidine dithiocarbamate blocks IL-1beta induced hyaluronan synthase 1 (HAS1) mRNA transcription, pointing at NF-kappaB dependence of the gene HAS1. *Exp Gerontol,* 41**,** 641-7.

KAUFMAN, R. J., SCHEUNER, D., SCHRODER, M., SHEN, X., LEE, K., LIU, C. Y. & ARNOLD, S. M. 2002. The unfolded protein response in nutrient sensing and differentiation. *Nat Rev Mol Cell Biol,* 3**,** 411-21.

KHAITLINA, S. Y. 2014. Intracellular transport based on actin polymerization. *Biochemistry (Mosc),* 79**,** 917-27.

KHANNA, S., BISWAS, S., SHANG, Y., COLLARD, E., AZAD, A., KAUH, C., BHASKER, V., GORDILLO, G. M., SEN, C. K. & ROY, S. 2010. Macrophage dysfunction impairs resolution of inflammation in the wounds of diabetic mice. *PLoS One,* 5**,** e9539.

KIM, B. C., KIM, H. T., PARK, S. H., CHA, J. S., YUFIT, T., KIM, S. J. & FALANGA, V. 2003. Fibroblasts from chronic wounds show altered TGF-beta-signaling and decreased TGF-beta Type II receptor expression. *J Cell Physiol,* 195**,** 331-6.

KIM, J. H. & MARTINS-GREEN, M. 2016. Protocol to Create Chronic Wounds in Diabetic Mice.

KIRKPATRICK, C. A. & SELLECK, S. B. 2007. Heparan sulfate proteoglycans at a glance. *J Cell Sci,* 120**,** 1829-32.

KRAMER, M. D., SCHAEFER, B. & REINARTZ, J. 1995. Plasminogen activation by human keratinocytes: molecular pathways and cell-biological consequences. *Biol Chem Hoppe Seyler,* 376**,** 131-41.

LANGE, Y., YE, J. & STECK, T. L. 2012. Activation mobilizes the cholesterol in the late endosomes-lysosomes of Niemann Pick type C cells. *PLoS One,* 7**,** e30051.

LAROUCHE, J., SHEORAN, S., MARUYAMA, K. & MARTINO, M. M. 2018. Immune Regulation of Skin Wound Healing: Mechanisms and Novel Therapeutic Targets. *Advances in Wound Care,* 7**,** 209-231.

LEAHY, D. J. 2004. Structure and function of the epidermal growth factor (EGF/ErbB) family of receptors. *Adv Protein Chem,* 68**,** 1-27.

LEE, M. K., PARDOUX, C., HALL, M. C., LEE, P. S., WARBURTON, D., QING, J., SMITH, S. M. & DERYNCK, R. 2007. TGF-beta activates Erk MAP kinase signalling through direct phosphorylation of ShcA. *Embo j,* 26**,** 3957-67.

LEIPER, L. J., WALCZYSKO, P., KUCEROVA, R., OU, J., SHANLEY, L. J., LAWSON, D., FORRESTER, J. V., MCCAIG, C. D., ZHAO, M. & COLLINSON, J. M. 2006. The roles of calcium signaling and ERK1/2 phosphorylation in a Pax6+/- mouse model of epithelial wound-healing delay. *BMC Biol,* 4**,** 27.

LI, B. & WANG, J. H. 2011. Fibroblasts and myofibroblasts in wound healing: force generation and measurement. *J Tissue Viability,* 20**,** 108-20.

LIM, X. & NUSSE, R. 2013. Wnt signaling in skin development, homeostasis, and disease. *Cold Spring Harb Perspect Biol,* 5.

LITWINIUK, M., KREJNER, A., SPEYRER, M. S., GAUTO, A. R. & GRZELA, T. 2016. Hyaluronic Acid in Inflammation and Tissue Regeneration. *Wounds,* 28**,** 78-88.

LIU, D. & SY, M. S. 1997. Phorbol myristate acetate stimulates the dimerization of CD44 involving a cysteine in the transmembrane domain. *J Immunol,* 159**,** 2702-11.

LOOTS, M. A., LAMME, E. N., ZEEGELAAR, J., MEKKES, J. R., BOS, J. D. & MIDDELKOOP, E. 1998. Differences in cellular infiltrate and extracellular matrix of chronic diabetic and venous ulcers versus acute wounds. *J Invest Dermatol,* 111**,** 850-7.

LUCAS, T., WAISMAN, A., RANJAN, R., ROES, J., KRIEG, T., MULLER, W., ROERS, A. & EMING, S. A. 2010. Differential roles of macrophages in diverse phases of skin repair. *J Immunol,* 184**,** 3964-77.

MALDONADO-BAEZ, L., COLE, N. B., KRAMER, H. & DONALDSON, J. G. 2013. Microtubule-dependent endosomal sorting of clathrin-independent cargo by Hook1. *J Cell Biol,* 201**,** 233-47.

MARIEB, E. A., ZOLTAN-JONES, A., LI, R., MISRA, S., GHATAK, S., CAO, J., ZUCKER, S. & TOOLE, B. P. 2004. Emmprin promotes anchorage-independent growth in human mammary carcinoma cells by stimulating hyaluronan production. *Cancer Res,* 64**,** 1229-32.

MARTIN, J., MIDGLEY, A., MERAN, S., WOODS, E., BOWEN, T., PHILLIPS, A. O. & STEADMAN, R. 2016. Tumor Necrosis Factor-stimulated Gene 6 (TSG-6)-mediated Interactions with the Inter-alpha-inhibitor Heavy Chain 5 Facilitate Tumor Growth Factor beta1 (TGFbeta1)-dependent Fibroblast to Myofibroblast Differentiation. *J Biol Chem,* 291**,** 13789-801.

MARTIN, P. & NUNAN, R. 2015. Cellular and molecular mechanisms of repair in acute and chronic wound healing. *Br J Dermatol,* 173**,** 370-8.

MATSUZAKI, S., HIRATSUKA, T., TANIGUCHI, M., SHINGAKI, K., KUBO, T., KIYA, K., FUJIWARA, T., KANAZAWA, S., KANEMATSU, R., MAEDA, T., TAKAMURA, H., YAMADA, K., MIYOSHI, K., HOSOKAWA, K., TOHYAMA, M. & KATAYAMA, T. 2015. Physiological ER Stress Mediates the Differentiation of Fibroblasts. *PLoS One,* 10**,** e0123578.

MAUCH, C., ZAMEK, J., ABETY, A. N., GRIMBERG, G., FOX, J. W. & ZIGRINO, P. 2010. Accelerated wound repair in ADAM-9 knockout animals. *J Invest Dermatol,* 130**,** 2120-30.
MAUVEZIN, C., NAGY, P., JUHASZ, G. & NEUFELD, T. P. 2015. Autophagosome-lysosome fusion is independent of V-ATPase-mediated acidification. *Nat Commun,* 6**,** 7007.
MAXFIELD, F. R. 2014. Role of endosomes and lysosomes in human disease. *Cold Spring Harb Perspect Biol,* 6**,** a016931.
MCGOWAN, S. E. & MCCOY, D. M. 2014. Regulation of fibroblast lipid storage and myofibroblast phenotypes during alveolar septation in mice. *American Journal of Physiology - Lung Cellular and Molecular Physiology,* 307**,** L618-L631.
MCINNES, R. L., CULLEN, B. M., HILL, K. E., PRICE, P. E., HARDING, K. G., THOMAS, D. W., STEPHENS, P. & MOSELEY, R. 2014. Contrasting host immuno-inflammatory responses to bacterial challenge within venous and diabetic ulcers. *Wound Repair Regen,* 22**,** 58-69.
MCKEE, C. M., PENNO, M. B., COWMAN, M., BURDICK, M. D., STRIETER, R. M., BAO, C. & NOBLE, P. W. 1996. Hyaluronan (HA) fragments induce chemokine gene expression in alveolar macrophages. The role of HA size and CD44. *J Clin Invest,* 98**,** 2403-13.
MENENDEZ-BENITO, V., VERHOEF, L. G., MASUCCI, M. G. & DANTUMA, N. P. 2005. Endoplasmic reticulum stress compromises the ubiquitin-proteasome system. *Hum Mol Genet,* 14**,** 2787-99.
MERAN, S., LUO, D. D., SIMPSON, R., MARTIN, J., WELLS, A., STEADMAN, R. & PHILLIPS, A. O. 2011. Hyaluronan facilitates transforming growth factor-beta1-dependent proliferation via CD44 and epidermal growth factor receptor interaction. *J Biol Chem,* 286**,** 17618-30.
MERAN, S. & STEADMAN, R. 2011. Fibroblasts and myofibroblasts in renal fibrosis. *Int J Exp Pathol,* 92**,** 158-67.
MERAN, S., THOMAS, D., STEPHENS, P., MARTIN, J., BOWEN, T., PHILLIPS, A. & STEADMAN, R. 2007. Involvement of hyaluronan in regulation of fibroblast phenotype. *J Biol Chem,* 282**,** 25687-97.
MIAN, I., PIERRE-LOUIS, W. S., DOLE, N., GILBERTI, R. M., DODGE-KAFKA, K. & TIRNAUER, J. S. 2012. LKB1 destabilizes microtubules in myoblasts and contributes to myoblast differentiation. *PLoS One,* 7**,** e31583.
MICHALAK, M., CORBETT, E. F., MESAELI, N., NAKAMURA, K. & OPAS, M. 1999. Calreticulin: one protein, one gene, many functions. *Biochem J,* 344 Pt 2**,** 281-92.
MIDGLEY, A. C., BOWEN, T., PHILLIPS, A. O. & STEADMAN, R. 2014. MicroRNA-7 inhibition rescues age-associated loss of epidermal growth factor receptor and hyaluronan-dependent differentiation in fibroblasts. *Aging Cell,* 13**,** 235-44.
MIDGLEY, A. C., DUGGAL, L., JENKINS, R., HASCALL, V., STEADMAN, R., PHILLIPS, A. O. & MERAN, S. 2015. Hyaluronan regulates bone morphogenetic protein-7-dependent prevention and reversal of myofibroblast phenotype. *J Biol Chem,* 290**,** 11218-34.
MIDGLEY, A. C., OLTEAN, S., HASCALL, V., WOODS, E. L., STEADMAN, R., PHILLIPS, A. O. & MERAN, S. 2017. Nuclear hyaluronidase 2 drives alternative splicing of CD44 pre-mRNA to determine profibrotic or antifibrotic cell phenotype. *Sci Signal,* 10.
MIDGLEY, A. C., ROGERS, M., HALLETT, M. B., CLAYTON, A., BOWEN, T., PHILLIPS, A. O. & STEADMAN, R. 2013. Transforming growth factor-beta1 (TGF-beta1)-stimulated fibroblast to myofibroblast differentiation is mediated by hyaluronan (HA)-facilitated epidermal growth factor receptor (EGFR) and CD44 co-localization in lipid rafts. *J Biol Chem,* 288**,** 14824-38.
MODARRESSI, A., PIETRAMAGGIORI, G., GODBOUT, C., VIGATO, E., PITTET, B. & HINZ, B. 2010. Hypoxia impairs skin myofibroblast differentiation and function. *J Invest Dermatol,* 130**,** 2818-27.
MOTEGI, S. I., SEKIGUCHI, A., UCHIYAMA, A., UEHARA, A., FUJIWARA, C., YAMAZAKI, S., PERERA, B., NAKAMURA, H., OGINO, S., YOKOYAMA, Y., AKAI, R., IWAWAKI, T. & ISHIKAWA, O.

2017. Protective effect of mesenchymal stem cells on the pressure ulcer formation by the regulation of oxidative and endoplasmic reticulum stress. *Sci Rep,* 7**,** 17186.

MUDGE, B. P., HARRIS, C., GILMONT, R. R., ADAMSON, B. S. & REES, R. S. 2002. Role of glutathione redox dysfunction in diabetic wounds. *Wound Repair Regen,* 10**,** 52-8.

MURO, A. F., MORETTI, F. A., MOORE, B. B., YAN, M., ATRASZ, R. G., WILKE, C. A., FLAHERTY, K. R., MARTINEZ, F. J., TSUI, J. L., SHEPPARD, D., BARALLE, F. E., TOEWS, G. B. & WHITE, E. S. 2008. An essential role for fibronectin extra type III domain A in pulmonary fibrosis. *Am J Respir Crit Care Med,* 177**,** 638-45.

MURRAY, S. C. & MELLOR, J. 2016. Using both strands: The fundamental nature of antisense transcription. *Bioarchitecture,* 6**,** 12-21.

NAGAOKA, A., YOSHIDA, H., NAKAMURA, S., MORIKAWA, T., KAWABATA, K., KOBAYASHI, M., SAKAI, S., TAKAHASHI, Y., OKADA, Y. & INOUE, S. 2015. Regulation of Hyaluronan (HA) Metabolism Mediated by HYBID (Hyaluronan-binding Protein Involved in HA Depolymerization, KIAA1199) and HA Synthases in Growth Factor-stimulated Fibroblasts. *J Biol Chem,* 290**,** 30910-23.

NAGY, N., SZOLNOKY, G., SZABAD, G., BATA-CSORGO, Z., BALOGH, A., KLAUSZ, G., MANDI, Y., DOBOZY, A., KEMENY, L. & SZELL, M. 2007. Tumor necrosis factor-alpha -308 polymorphism and leg ulceration--possible association with obesity. *J Invest Dermatol,* 127**,** 1768-9; author reply 1770-1.

NAGY, N., SZOLNOKY, G., SZABAD, G., BATA-CSORGO, Z., DOBOZY, A., KEMENY, L. & SZELL, M. 2005. Single nucleotide polymorphisms of the fibroblast growth factor receptor 2 gene in patients with chronic venous insufficiency with leg ulcer. *J Invest Dermatol,* 124**,** 1085-8.

NEAME, S. J., UFF, C. R., SHEIKH, H., WHEATLEY, S. C. & ISACKE, C. M. 1995. CD44 exhibits a cell type dependent interaction with triton X-100 insoluble, lipid rich, plasma membrane domains. *J Cell Sci,* 108 (Pt 9)**,** 3127-35.

NUNAN, R., HARDING, K. G. & MARTIN, P. 2014. Clinical challenges of chronic wounds: searching for an optimal animal model to recapitulate their complexity. *Disease Models & Mechanisms,* 7**,** 1205-1213.

OAKES, S. A. & PAPA, F. R. 2015. The role of endoplasmic reticulum stress in human pathology. *Annu Rev Pathol,* 10**,** 173-94.

OERTLI, B., BECK-SCHIMMER, B., FAN, X. & WUTHRICH, R. P. 1998. Mechanisms of hyaluronan-induced up-regulation of ICAM-1 and VCAM-1 expression by murine kidney tubular epithelial cells: hyaluronan triggers cell adhesion molecule expression through a mechanism involving activation of nuclear factor-kappa B and activating protein-1. *J Immunol,* 161**,** 3431-7.

OKIZAKI, S., ITO, Y., HOSONO, K., OBA, K., OHKUBO, H., AMANO, H., SHICHIRI, M. & MAJIMA, M. 2015. Suppressed recruitment of alternatively activated macrophages reduces TGF-beta1 and impairs wound healing in streptozotocin-induced diabetic mice. *Biomed Pharmacother,* 70**,** 317-25.

OLERUD, J. E., ODLAND, G. F., BURGESS, E. M., WYSS, C. R., FISHER, L. D. & MATSEN, F. A., 3RD 1995. A model for the study of wounds in normal elderly adults and patients with peripheral vascular disease or diabetes mellitus. *J Surg Res,* 59**,** 349-60.

OMAR, A., WRIGHT, J. B., SCHULTZ, G., BURRELL, R. & NADWORNY, P. 2017. Microbial Biofilms and Chronic Wounds. *Microorganisms,* 5**,** 9.

ONTONG, P., HATADA, Y., TANIGUCHI, S. I., KAKIZAKI, I. & ITANO, N. 2014. Effect of a cholesterol-rich lipid environment on the enzymatic activity of reconstituted hyaluronan synthase. *Biochemical and Biophysical Research Communications,* 443**,** 666-671.

OZCAN, U., CAO, Q., YILMAZ, E., LEE, A. H., IWAKOSHI, N. N., OZDELEN, E., TUNCMAN, G., GORGUN, C., GLIMCHER, L. H. & HOTAMISLIGIL, G. S. 2004. Endoplasmic reticulum stress links obesity, insulin action, and type 2 diabetes. *Science,* 306**,** 457-61.

PAGE-MCCAW, A., EWALD, A. J. & WERB, Z. 2007. Matrix metalloproteinases and the regulation of tissue remodelling. *Nat Rev Mol Cell Biol,* 8**,** 221-33.

PANKOV, R. & YAMADA, K. M. 2002. Fibronectin at a glance. *J Cell Sci,* 115**,** 3861-3.

PASTAR, I., STOJADINOVIC, O., YIN, N. C., RAMIREZ, H., NUSBAUM, A. G., SAWAYA, A., PATEL, S. B., KHALID, L., ISSEROFF, R. R. & TOMIC-CANIC, M. 2014. Epithelialization in Wound Healing: A Comprehensive Review. *Adv Wound Care (New Rochelle),* 3**,** 445-464.

PERSCHL, A., LESLEY, J., ENGLISH, N., TROWBRIDGE, I. & HYMAN, R. 1995. Role of CD44 cytoplasmic domain in hyaluronan binding. *Eur J Immunol,* 25**,** 495-501.

PETREY, A. C. & DE LA MOTTE, C. A. 2014. Hyaluronan, a crucial regulator of inflammation. *Front Immunol,* 5**,** 101.

PETREY, A. C. & DE LA MOTTE, C. A. 2016. Thrombin Cleavage of Inter-alpha-inhibitor Heavy Chain 1 Regulates Leukocyte Binding to an Inflammatory Hyaluronan Matrix. *J Biol Chem,* 291**,** 24324-24334.

PEUS, D., SCHMIEDEBERG, S. V., PIER, A., SCHARF, R. E., WEHMEIER, A., RUZICKA, T. & KRUTMANN, J. 1996. Coagulation factor V gene mutation associated with activated protein C resistance leading to recurrent thrombosis, leg ulcers, and lymphedema: successful treatment with intermittent compression. *Journal of the American Academy of Dermatology,* 35**,** 306-309.

PO'UHA, S. T., HONORE, S., BRAGUER, D. & KAVALLARIS, M. 2013. Partial depletion of gamma-actin suppresses microtubule dynamics. *Cytoskeleton (Hoboken),* 70**,** 148-60.

POTELLE, S., KLEIN, A. & FOULQUIER, F. 2015. Golgi post-translational modifications and associated diseases. *J Inherit Metab Dis,* 38**,** 741-51.

PRINCE, L. R., WHYTE, M. K., SABROE, I. & PARKER, L. C. 2011. The role of TLRs in neutrophil activation. *Curr Opin Pharmacol,* 11**,** 397-403.

PROCHAZKA, L., TESARIK, R. & TURANEK, J. 2014. Regulation of alternative splicing of CD44 in cancer. *Cell Signal,* 26**,** 2234-9.

PRYDZ, K. 2015. Determinants of Glycosaminoglycan (GAG) Structure. *Biomolecules,* 5**,** 2003-22.

QU, C., RILLA, K., TAMMI, R., TAMMI, M., KROGER, H. & LAMMI, M. J. 2014. Extensive CD44-dependent hyaluronan coats on human bone marrow-derived mesenchymal stem cells produced by hyaluronan synthases HAS1, HAS2 and HAS3. *Int J Biochem Cell Biol,* 48**,** 45-54.

RAFFETTO, J. D., MENDEZ, M. V., MARIEN, B. J., BYERS, H. R., PHILLIPS, T. J., PARK, H. Y. & MENZOIAN, J. O. 2001. Changes in cellular motility and cytoskeletal actin in fibroblasts from patients with chronic venous insufficiency and in neonatal fibroblasts in the presence of chronic wound fluid. *J Vasc Surg,* 33**,** 1233-41.

RAIBORG, C., WENZEL, E. M. & STENMARK, H. 2015. ER-endosome contact sites: molecular compositions and functions. *Embo j,* 34**,** 1848-58.

RAMPANELLI, E., ROUSCHOP, K. M., CLAESSEN, N., TESKE, G. J., PALS, S. T., LEEMANS, J. C. & FLORQUIN, S. 2014. Opposite role of CD44-standard and CD44-variant-3 in tubular injury and development of renal fibrosis during chronic obstructive nephropathy. *Kidney Int,* 86**,** 558-69.

RANI, M. & SCHWACHA, M. G. 2017. The composition of T-cell subsets are altered in the burn wound early after injury. *PLoS One,* 12**,** e0179015.

RAYAHIN, J. E., BUHRMAN, J. S., ZHANG, Y., KOH, T. J. & GEMEINHART, R. A. 2015. High and low molecular weight hyaluronic acid differentially influence macrophage activation. *ACS Biomater Sci Eng,* 1**,** 481-493.

REED, M. J., DAMODARASAMY, M., CHAN, C. K., JOHNSON, M. N., WIGHT, T. N. & VERNON, R. B. 2013. Cleavage of hyaluronan is impaired in aged dermal wounds. *Matrix Biol,* 32**,** 45-51.

REN, K. & TORRES, R. 2009. Role of interleukin-1beta during pain and inflammation. *Brain Res Rev,* 60**,** 57-64.

RILLA, K., OIKARI, S., JOKELA, T. A., HYTTINEN, J. M., KARNA, R., TAMMI, R. H. & TAMMI, M. I. 2013. Hyaluronan synthase 1 (HAS1) requires higher cellular UDP-GlcNAc concentration than HAS2 and HAS3. *J Biol Chem,* 288**,** 5973-83.

RILLA, K., SIISKONEN, H., SPICER, A. P., HYTTINEN, J. M., TAMMI, M. I. & TAMMI, R. H. 2005. Plasma membrane residence of hyaluronan synthase is coupled to its enzymatic activity. *J Biol Chem,* 280**,** 31890-7.

ROBINSON, C. M., NEARY, R., LEVENDALE, A., WATSON, C. J. & BAUGH, J. A. 2012. Hypoxia-induced DNA hypermethylation in human pulmonary fibroblasts is associated with Thy-1 promoter methylation and the development of a pro-fibrotic phenotype. *Respir Res,* 13**,** 74.

RODERICK, H. L., CAMPBELL, A. K. & LLEWELLYN, D. H. 1997. Nuclear localisation of calreticulin in vivo is enhanced by its interaction with glucocorticoid receptors. *FEBS Letters,* 405**,** 181-185.

ROHR, S. 2009. Myofibroblasts in diseased hearts: new players in cardiac arrhythmias? *Heart Rhythm,* 6**,** 848-56.

ROY, S., ELGHARABLY, H., SINHA, M., GANESH, K., CHANEY, S., MANN, E., MILLER, C., KHANNA, S., BERGDALL, V. K., POWELL, H. M., COOK, C. H., GORDILLO, G. M., WOZNIAK, D. J. & SEN, C. K. 2014. Mixed-species biofilm compromises wound healing by disrupting epidermal barrier function. *J Pathol,* 233**,** 331-343.

RUPONEN, M., HONKAKOSKI, P., RONKKO, S., PELKONEN, J., TAMMI, M. & URTTI, A. 2003. Extracellular and intracellular barriers in non-viral gene delivery. *J Control Release,* 93**,** 213-7.

SANCHEZ-ALVAREZ, M., FINGER, F., ARIAS-GARCIA MDEL, M., BOUSGOUNI, V., PASCUAL-VARGAS, P. & BAKAL, C. 2014. Signaling networks converge on TORC1-SREBP activity to promote endoplasmic reticulum homeostasis. *PLoS One,* 9**,** e101164.

SANDBO, N., SMOLYANINOVA, L. V., ORLOV, S. N. & DULIN, N. O. 2016. Control of Myofibroblast Differentiation and Function by Cytoskeletal Signaling. *Biochemistry (Mosc),* 81**,** 1698-1708.

SANDERS, Y. Y., AMBALAVANAN, N., HALLORAN, B., ZHANG, X., LIU, H., CROSSMAN, D. K., BRAY, M., ZHANG, K., THANNICKAL, V. J. & HAGOOD, J. S. 2012. Altered DNA methylation profile in idiopathic pulmonary fibrosis. *Am J Respir Crit Care Med,* 186**,** 525-35.

SANTIAGO, J. J., DANGERFIELD, A. L., RATTAN, S. G., BATHE, K. L., CUNNINGTON, R. H., RAIZMAN, J. E., BEDOSKY, K. M., FREED, D. H., KARDAMI, E. & DIXON, I. M. 2010. Cardiac fibroblast to myofibroblast differentiation in vivo and in vitro: expression of focal adhesion components in neonatal and adult rat ventricular myofibroblasts. *Dev Dyn,* 239**,** 1573-84.

SCHNEIDER, D. F., PALMER, J. L., TULLEY, J. M., SPEICHER, J. T., KOVACS, E. J., GAMELLI, R. L. & FAUNCE, D. E. 2011. A novel role for NKT cells in cutaneous wound repair. *J Surg Res,* 168**,** 325-33.e1.

SCREATON, G. R., BELL, M. V., JACKSON, D. G., CORNELIS, F. B., GERTH, U. & BELL, J. I. 1992. Genomic structure of DNA encoding the lymphocyte homing receptor CD44 reveals at least 12 alternatively spliced exons. *Proc Natl Acad Sci U S A,* 89**,** 12160-4.

SEN, C. K. & ROY, S. 2010. Oxygenation state as a driver of myofibroblast differentiation and wound contraction: hypoxia impairs wound closure. *J Invest Dermatol,* 130**,** 2701-3.

SESSIONS, J. W., ARMSTRONG, D. G., HOPE, S. & JENSEN, B. D. 2017. A review of genetic engineering biotechnologies for enhanced chronic wound healing. *Exp Dermatol,* 26**,** 179-185.

SHAH, M., FOREMAN, D. M. & FERGUSON, M. W. 1994. Neutralising antibody to TGF-beta 1,2 reduces cutaneous scarring in adult rodents. *J Cell Sci,* 107 (Pt 5)**,** 1137-57.

SHECHTER, R. & SCHWARTZ, M. 2013. CNS sterile injury: just another wound healing? *Trends in Molecular Medicine,* 19**,** 135-143.

SHIBATA, Y., VOELTZ, G. K. & RAPOPORT, T. A. 2006. Rough sheets and smooth tubules. *Cell,* 126**,** 435-9.

SHINDE, A. V., KELSH, R., PETERS, J. H., SEKIGUCHI, K., VAN DE WATER, L. & MCKEOWN-LONGO, P. J. 2015. The alpha4beta1 integrin and the EDA domain of fibronectin regulate a profibrotic phenotype in dermal fibroblasts. *Matrix Biol,* 41**,** 26-35.

SIANI, A., KHAW, R. R., MANLEY, O. W. G., TIRELLA, A., CELLESI, F., DONNO, R. & TIRELLI, N. 2015. Fibronectin localization and fibrillization are affected by the presence of serum in culture media. *Scientific Reports,* 5**,** 9278.

SIDAWAY, P. 2015. Diabetes: Epigenetic changes lead to impaired wound healing in patients with T2DM. *Nat Rev Endocrinol,* 11**,** 65.

SIISKONEN, H., KARNA, R., HYTTINEN, J. M., TAMMI, R. H., TAMMI, M. I. & RILLA, K. 2014. Hyaluronan synthase 1 (HAS1) produces a cytokine-and glucose-inducible, CD44-dependent cell surface coat. *Exp Cell Res,* 320**,** 153-63.

SIISKONEN, H., OIKARI, S., PASONEN-SEPPANEN, S. & RILLA, K. 2015. Hyaluronan synthase 1: a mysterious enzyme with unexpected functions. *Front Immunol,* 6**,** 43.

SIMONS, K. & IKONEN, E. 1997. Functional rafts in cell membranes. *Nature,* 387**,** 569.

SIMPSON, R. M., MERAN, S., THOMAS, D., STEPHENS, P., BOWEN, T., STEADMAN, R. & PHILLIPS, A. 2009. Age-related changes in pericellular hyaluronan organization leads to impaired dermal fibroblast to myofibroblast differentiation. *Am J Pathol,* 175**,** 1915-28.

SIMPSON, R. M., WELLS, A., THOMAS, D., STEPHENS, P., STEADMAN, R. & PHILLIPS, A. 2010. Aging fibroblasts resist phenotypic maturation because of impaired hyaluronan-dependent CD44/epidermal growth factor receptor signaling. *Am J Pathol,* 176**,** 1215-28.

SINDRILARU, A., PETERS, T., WIESCHALKA, S., BAICAN, C., BAICAN, A., PETER, H., HAINZL, A., SCHATZ, S., QI, Y., SCHLECHT, A., WEISS, J. M., WLASCHEK, M., SUNDERKOTTER, C. & SCHARFFETTER-KOCHANEK, K. 2011. An unrestrained proinflammatory M1 macrophage population induced by iron impairs wound healing in humans and mice. *J Clin Invest,* 121**,** 985-97.

SIRA, M. M., BEHAIRY, B. E., ABD-ELAZIZ, A. M., ABD ELNABY, S. A. & ELTAHAN, E. E. 2014. Serum Inter-Alpha-Trypsin Inhibitor Heavy Chain 4 (ITIH4) in Children with Chronic Hepatitis C: Relation to Liver Fibrosis and Viremia. *Hepat Res Treat,* 2014**,** 307942.

SLOMIANY, M. G., GRASS, G. D., ROBERTSON, A. D., YANG, X. Y., MARIA, B. L., BEESON, C. & TOOLE, B. P. 2009. Hyaluronan, CD44, and emmprin regulate lactate efflux and membrane localization of monocarboxylate transporters in human breast carcinoma cells. *Cancer Res,* 69**,** 1293-301.

SMITH, M. M. & MELROSE, J. 2015. Proteoglycans in Normal and Healing Skin. *Adv Wound Care (New Rochelle),* 4**,** 152-173.

SORRELL, J. M. & CAPLAN, A. I. 2004. Fibroblast heterogeneity: more than skin deep. *Journal of Cell Science,* 117**,** 667-675.

SRIDHAR, S., PATEL, B., APHKHAZAVA, D., MACIAN, F., SANTAMBROGIO, L., SHIELDS, D. & CUERVO, A. M. 2013. The lipid kinase PI4KIIIbeta preserves lysosomal identity. *Embo j,* 32**,** 324-39.

STERN, R. & JEDRZEJAS, M. J. 2006. Hyaluronidases: their genomics, structures, and mechanisms of action. *Chem Rev,* 106**,** 818-39.

STRBO, N., YIN, N. & STOJADINOVIC, O. 2014. Innate and Adaptive Immune Responses in Wound Epithelialization. *Advances in Wound Care,* 3**,** 492-501.

SU, Z., MA, H., WU, Z., ZENG, H., LI, Z., WANG, Y., LIU, G., XU, B., LIN, Y., ZHANG, P. & WEI, X. 2014. Enhancement of skin wound healing with decellularized scaffolds loaded with hyaluronic acid and epidermal growth factor. *Mater Sci Eng C Mater Biol Appl,* 44**,** 440-8.

SUTHERLAND, J., DENYER, M. & BRITLAND, S. 2005. Contact guidance in human dermal fibroblasts is modulated by population pressure. *J Anat,* 206**,** 581-7.

TANAKA, K. 2009. The proteasome: Overview of structure and functions. *Proceedings of the Japan Academy. Series B, Physical and Biological Sciences,* 85**,** 12-36.

TEN DIJKE, P., GOUMANS, M. J., ITOH, F. & ITOH, S. 2002. Regulation of cell proliferation by Smad proteins. *J Cell Physiol,* 191**,** 1-16.

TERMEER, C., BENEDIX, F., SLEEMAN, J., FIEBER, C., VOITH, U., AHRENS, T., MIYAKE, K., FREUDENBERG, M., GALANOS, C. & SIMON, J. C. 2002. Oligosaccharides of Hyaluronan activate dendritic cells via toll-like receptor 4. *J Exp Med,* 195**,** 99-111.

THEOCHARIDIS, G., DRYMOUSSI, Z., KAO, A. P., BARBER, A. H., LEE, D. A., BRAUN, K. M. & CONNELLY, J. T. 2015. Type VI Collagen Regulates Dermal Matrix Assembly and Fibroblast Motility. *J Invest Dermatol*.

THOMASON, H. A., COOPER, N. H., ANSELL, D. M., CHIU, M., MERRIT, A. J., HARDMAN, M. J. & GARROD, D. R. 2012. Direct evidence that PKCalpha positively regulates wound re-epithelialization: correlation with changes in desmosomal adhesiveness. *J Pathol,* 227**,** 346-56.

TILLMANNS, J., HOFFMANN, D., HABBABA, Y., SCHMITTO, J. D., SEDDING, D., FRACCAROLLO, D., GALUPPO, P. & BAUERSACHS, J. 2015. Fibroblast activation protein alpha expression identifies activated fibroblasts after myocardial infarction. *J Mol Cell Cardiol,* 87**,** 194-203.

TOMASEK, J. J., GABBIANI, G., HINZ, B., CHAPONNIER, C. & BROWN, R. A. 2002. Myofibroblasts and mechano-regulation of connective tissue remodelling. *Nature Reviews Molecular Cell Biology,* 3**,** 349.

TORISEVA, M., LAATO, M., CARPEN, O., RUOHONEN, S. T., SAVONTAUS, E., INADA, M., KRANE, S. M. & KAHARI, V. M. 2012. MMP-13 regulates growth of wound granulation tissue and modulates gene expression signatures involved in inflammation, proteolysis, and cell viability. *PLoS One,* 7**,** e42596.

TORRONEN, K., NIKUNEN, K., KARNA, R., TAMMI, M., TAMMI, R. & RILLA, K. 2014. Tissue distribution and subcellular localization of hyaluronan synthase isoenzymes. *Histochem Cell Biol,* 141**,** 17-31.

TRABUCCHI, E., PALLOTTA, S., MORINI, M., CORSI, F., FRANCESCHINI, R., CASIRAGHI, A., PRAVETTONI, A., FOSCHI, D. & MINGHETTI, P. 2002. Low molecular weight hyaluronic acid prevents oxygen free radical damage to granulation tissue during wound healing. *Int J Tissue React,* 24**,** 65-71.

TRACY, L. E., MINASIAN, R. A. & CATERSON, E. J. 2016. Extracellular Matrix and Dermal Fibroblast Function in the Healing Wound. *Adv Wound Care (New Rochelle),* 5**,** 119-136.

TRIPATHI, V., SIXT, K. M., GAO, S., XU, X., HUANG, J., WEIGERT, R., ZHOU, M. & ZHANG, Y. E. 2016. Direct Regulation of Alternative Splicing by SMAD3 through PCBP1 Is Essential to the Tumor-Promoting Role of TGF-beta. *Mol Cell,* 64**,** 549-564.

TSUKAMOTO, K., HIRANO, K., YAMASHITA, S., SAKAI, N., IKEGAMI, C., ZHANG, Z., MATSUURA, F., HIRAOKA, H., MATSUYAMA, A., ISHIGAMI, M. & MATSUZAWA, Y. 2002. Retarded intracellular lipid transport associated with reduced expression of Cdc42, a member of Rho-GTPases, in human aged skin fibroblasts: a possible function of Cdc42 in mediating intracellular lipid transport. *Arterioscler Thromb Vasc Biol,* 22**,** 1899-904.

VAN DE WATER, L., VARNEY, S. & TOMASEK, J. J. 2013. Mechanoregulation of the Myofibroblast in Wound Contraction, Scarring, and Fibrosis: Opportunities for New Therapeutic Intervention. *Adv Wound Care (New Rochelle),* 2**,** 122-141.

VAN DEN BORNE, S. W., DIEZ, J., BLANKESTEIJN, W. M., VERJANS, J., HOFSTRA, L. & NARULA, J. 2010. Myocardial remodeling after infarction: the role of myofibroblasts. *Nat Rev Cardiol,* 7**,** 30-7.

VAN DER REST, M., AUBERT-FOUCHER, E., DUBLET, B., EICHENBERGER, D., FONT, B. & GOLDSCHMIDT, D. 1991. Structure and function of the fibril-associated collagens. *Biochem Soc Trans,* 19**,** 820-4.

VELNAR, T., BAILEY, T. & SMRKOLJ, V. 2009. The wound healing process: an overview of the cellular and molecular mechanisms. *J Int Med Res,* 37**,** 1528-42.

VIGL, B., AEBISCHER, D., NITSCHKE, M., IOLYEVA, M., ROTHLIN, T., ANTSIFEROVA, O. & HALIN, C. 2011. Tissue inflammation modulates gene expression of lymphatic endothelial cells and dendritic cell migration in a stimulus-dependent manner. *Blood,* 118**,** 205-15.

WALKER, J. A., ROSSINI, G., THOMPSON, M. W., WENKE, J. C. & BAER, D. 2013. Effect of proteasome inhibitor 1 on wound healing: a potential scar prevention therapy. *Wounds,* 25**,** 28-33.

WALL, I. B., MOSELEY, R., BAIRD, D. M., KIPLING, D., GILES, P., LAFFAFIAN, I., PRICE, P. E., THOMAS, D. W. & STEPHENS, P. 2008. Fibroblast Dysfunction Is a Key Factor in the Non-Healing of Chronic Venous Leg Ulcers. *Journal of Investigative Dermatology,* 128**,** 2526-2540.

WANG, H., WU, Q., LIU, Z., LUO, X., FAN, Y., LIU, Y., ZHANG, Y., HUA, S., FU, Q., ZHAO, M., CHEN, Y., FANG, W. & LV, X. 2014. Downregulation of FAP suppresses cell proliferation and metastasis through PTEN/PI3K/AKT and Ras-ERK signaling in oral squamous cell carcinoma. *Cell Death Dis,* 5**,** e1155.

WANG, H. B., DEMBO, M., HANKS, S. K. & WANG, Y. 2001. Focal adhesion kinase is involved in mechanosensing during fibroblast migration. *Proc Natl Acad Sci U S A,* 98**,** 11295-300.

WANG, M., LIU, X., LYU, Z., GU, H., LI, D. & CHEN, H. 2017. Glycosaminoglycans (GAGs) and GAG mimetics regulate the behavior of stem cell differentiation. *Colloids and Surfaces B: Biointerfaces,* 150**,** 175-182.

WANG, X., GHASRI, P., AMIR, M., HWANG, B., HOU, Y., KHALILI, M., LIN, A., KEENE, D., UITTO, J., WOODLEY, D. T. & CHEN, M. 2013. Topical application of recombinant type VII collagen incorporates into the dermal-epidermal junction and promotes wound closure. *Mol Ther,* 21**,** 1335-44.

WANG, X. M., YU, D. M., MCCAUGHAN, G. W. & GORRELL, M. D. 2005. Fibroblast activation protein increases apoptosis, cell adhesion, and migration by the LX-2 human stellate cell line. *Hepatology,* 42**,** 935-45.

WATSON, P. & STEPHENS, D. J. 2005. ER-to-Golgi transport: form and formation of vesicular and tubular carriers. *Biochim Biophys Acta,* 1744**,** 304-15.

WEBBER, J., JENKINS, R. H., MERAN, S., PHILLIPS, A. & STEADMAN, R. 2009. Modulation of TGFbeta1-dependent myofibroblast differentiation by hyaluronan. *Am J Pathol,* 175**,** 148-60.

WEIGEL, P. H. 2015. Hyaluronan Synthase: The Mechanism of Initiation at the Reducing End and a Pendulum Model for Polysaccharide Translocation to the Cell Exterior. *Int J Cell Biol,* 2015**,** 367579.

WERNER, S., KRIEG, T. & SMOLA, H. 2007. Keratinocyte-fibroblast interactions in wound healing. *J Invest Dermatol,* 127**,** 998-1008.

WILLENBORG, S. & EMING, S. A. 2014. Macrophages - sensors and effectors coordinating skin damage and repair. *J Dtsch Dermatol Ges,* 12**,** 214-21, 214-23.

WLASCHEK, M. & SCHARFFETTER-KOCHANEK, K. 2005. Oxidative stress in chronic venous leg ulcers. *Wound Repair Regen,* 13**,** 452-61.

WOLF, D., SCHUMANN, J., KOERBER, K., KIEMER, A. K., VOLLMAR, A. M., SASS, G., PAPADOPOULOS, T., BANG, R., KLEIN, S. D., BRUNE, B. & TIEGS, G. 2001. Low-molecular-weight hyaluronic acid induces nuclear factor-kappaB-dependent resistance against tumor necrosis factor alpha-mediated liver injury in mice. *Hepatology,* 34**,** 535-47.

WU, L., XIA, Y. P., ROTH, S. I., GRUSKIN, E. & MUSTOE, T. A. 1999. Transforming growth factor-beta1 fails to stimulate wound healing and impairs its signal transduction in an aged ischemic ulcer model: importance of oxygen and age. *Am J Pathol,* 154**,** 301-9.

XU, J., LU, Y., QIU, S., CHEN, Z. N. & FAN, Z. 2013. A novel role of EMMPRIN/CD147 in transformation of quiescent fibroblasts to cancer-associated fibroblasts by breast cancer cells. *Cancer Lett,* 335**,** 380-6.

XU, P., FU, X., XIAO, N., GUO, Y., PEI, Q., PENG, Y., ZHANG, Y. & YAO, M. 2017. Involvements of gammadeltaT Lymphocytes in Acute and Chronic Skin Wound Repair. *Inflammation,* 40**,** 1416-1427.

YAMADA, Y., ITANO, N., HATA, K.-I., UEDA, M. & KIMATA, K. 2004. Differential Regulation by IL-1β and EGF of Expression of Three Different Hyaluronan Synthases in Oral Mucosal Epithelial Cells and Fibroblasts and Dermal Fibroblasts: Quantitative Analysis Using Real-Time RT-PCR. *Journal of Investigative Dermatology,* 122**,** 631-639.

YANG, W., HAN, W., YE, S., LIU, D., WU, J., LIU, H., LI, C. & CHEN, H. 2013. Fibroblast activation protein-alpha promotes ovarian cancer cell proliferation and invasion via extracellular and intracellular signaling mechanisms. *Exp Mol Pathol,* 95**,** 105-10.

YOSHIDA, H., NAGAOKA, A., KUSAKA-KIKUSHIMA, A., TOBIISHI, M., KAWABATA, K., SAYO, T., SAKAI, S., SUGIYAMA, Y., ENOMOTO, H., OKADA, Y. & INOUE, S. 2013a. KIAA1199, a deafness gene of unknown function, is a new hyaluronan binding protein involved in hyaluronan depolymerization. *Proc Natl Acad Sci U S A,* 110**,** 5612-7.

YOSHIDA, H., NAGAOKA, A., NAKAMURA, S., SUGIYAMA, Y., OKADA, Y. & INOUE, S. 2013b. Murine homologue of the human KIAA1199 is implicated in hyaluronan binding and depolymerization. *FEBS Open Bio,* 3**,** 352-6.

YU, X., SHARMA, K. D., TAKAHASHI, T., IWAMOTO, R. & MEKADA, E. 2002. Ligand-independent dimer formation of epidermal growth factor receptor (EGFR) is a step separable from ligand-induced EGFR signaling. *Mol Biol Cell,* 13**,** 2547-57.

ZAARUR, N., MERIIN, A. B., BEJARANO, E., XU, X., GABAI, V. L., CUERVO, A. M. & SHERMAN, M. Y. 2014. Proteasome Failure Promotes Positioning of Lysosomes around the Aggresome via Local Block of Microtubule-Dependent Transport. *Molecular and Cellular Biology,* 34**,** 1336-1348.

ZHANG, W. & LIU, H. T. 2002. MAPK signal pathways in the regulation of cell proliferation in mammalian cells. *Cell Res,* 12**,** 9-18.

ZHAO, R., LIANG, H., CLARKE, E., JACKSON, C. & XUE, M. 2016. Inflammation in Chronic Wounds. *International Journal of Molecular Sciences,* 17**,** 2085.

ZHU, X., LI, L., ZOU, L., ZHU, X., XIAN, G., LI, H., TAN, Y. & XIE, L. 2012. A novel aptamer targeting TGF-beta receptor II inhibits transdifferentiation of human tenon's fibroblasts into myofibroblast. *Invest Ophthalmol Vis Sci,* 53**,** 6897-903.

Appendix 1: Supplemental Data

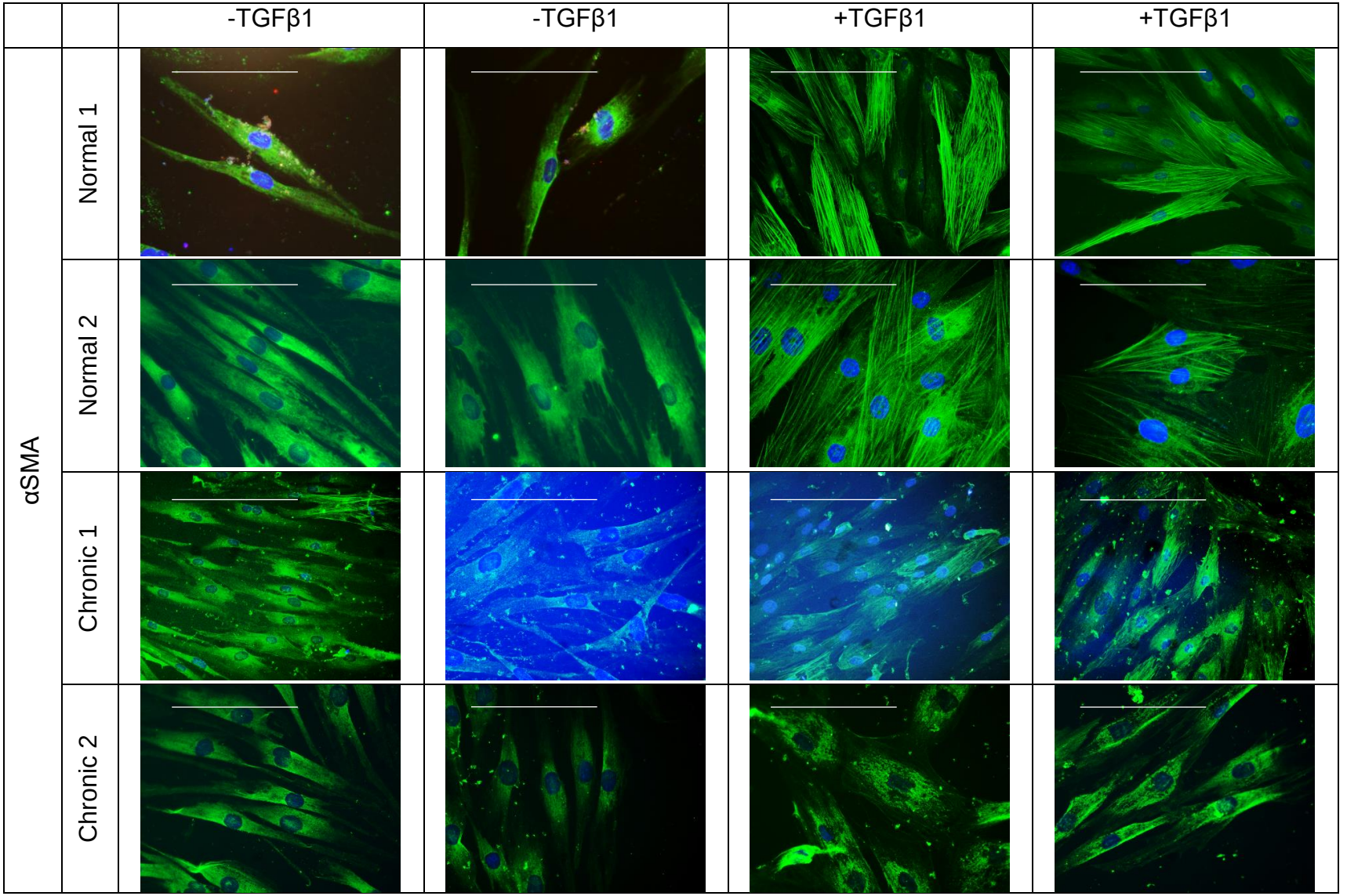

Supplementary Figure 1. αSMA Repeat 1 and 2. Cells were grown to 60-70% confluence and growth arrested for 48h. Cells were then incubated in serum-free medium alone (-TGF) or in medium containing 10 ng/mL TGFβ1 (+TGF) for 72h. The localisation of αSMA protein was examined by immunocytochemistry; nuclei were visualised by Hoechst stain. Images shown are a representation of 2 independent experiments. Original magnification x400. Scale bar: 100μm.

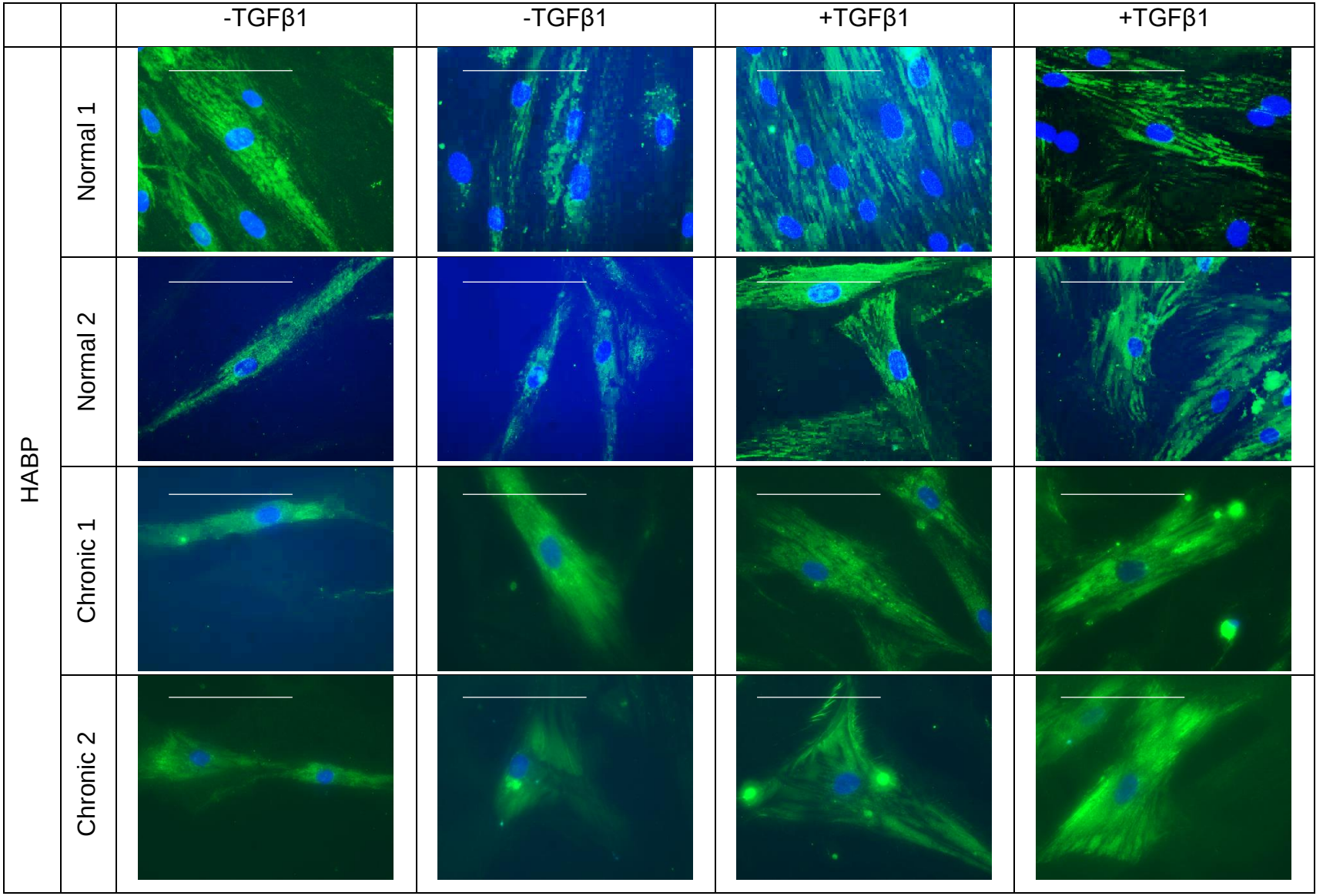

Supplementary Figure 2. Localisation of total Hyaluronan does not change with TGF-β1 treatment. Cells were grown to 60-70% confluence and growth arrested for 48h. Cells were then incubated in serum-free medium alone (-TGF) or in medium containing 10 ng/mL TGFβ1 (+TGF) for 72h. The expression of total HA GAG was examined by immunocytochemistry; nuclei were visualised by Hoechst stain. Images shown are a representation of 2 independent experiments. Original Magnification x400. Scale bar 100µm.

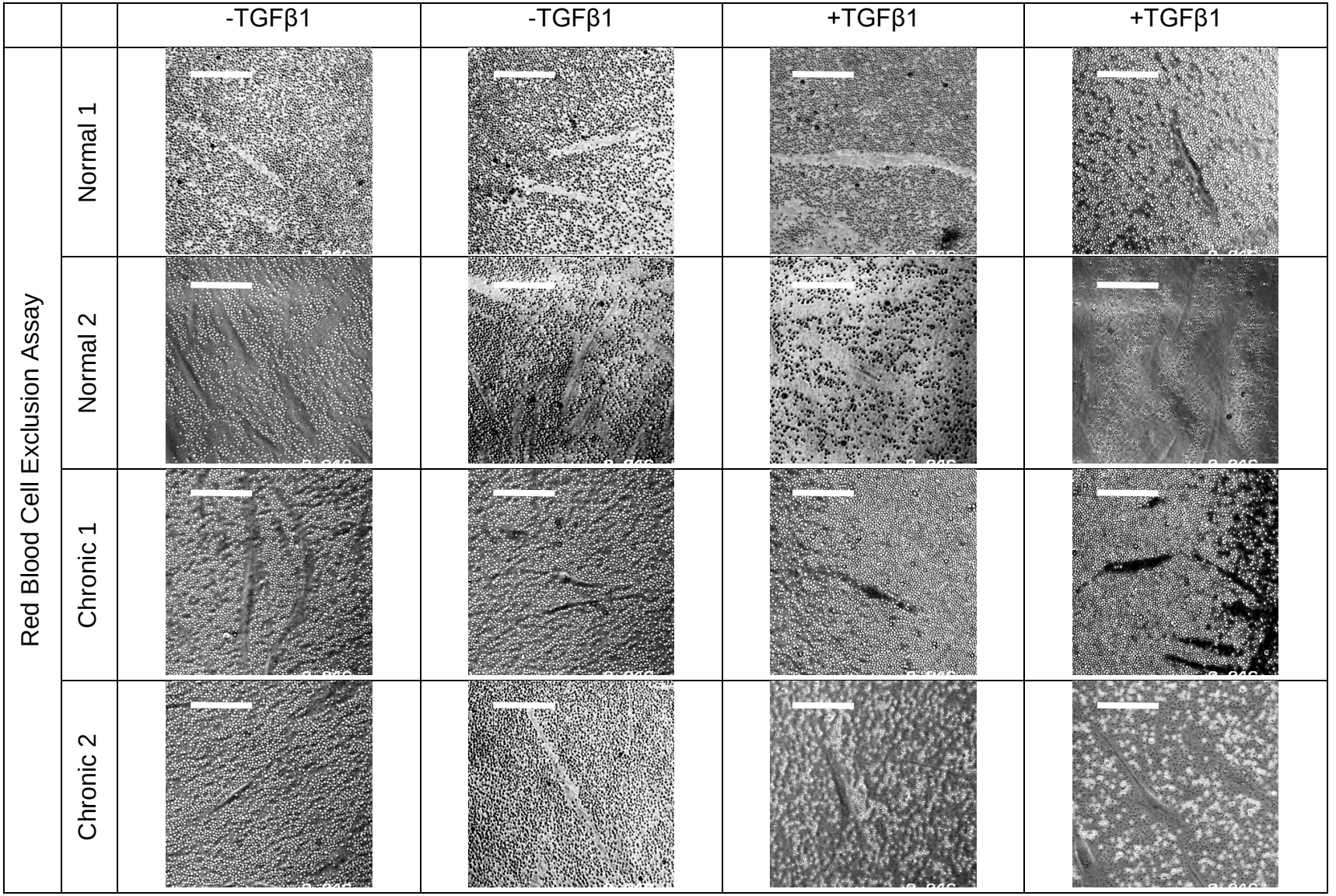

Supplementary Figure 3. Visualisation of HA pericellular coat using Red Blood Cell (RBC) exclusion assay. Cells were grown to 60-70% confluence and growth arrested for 48h. Cells were then incubated in serum-free medium alone (-TGF) or in medium containing 10 ng/mL TGFβ1 (+TGF) for 72h. The expression visualisation of HA was examined by RBC exclusion assay. Yellow arrows show HA coat presence. Images shown are a representation of 2 independent experiments. Original Magnification x200. Hyaluronidase treated cells were used as a control, removing pericellular HA. Scale bar: 100µm.

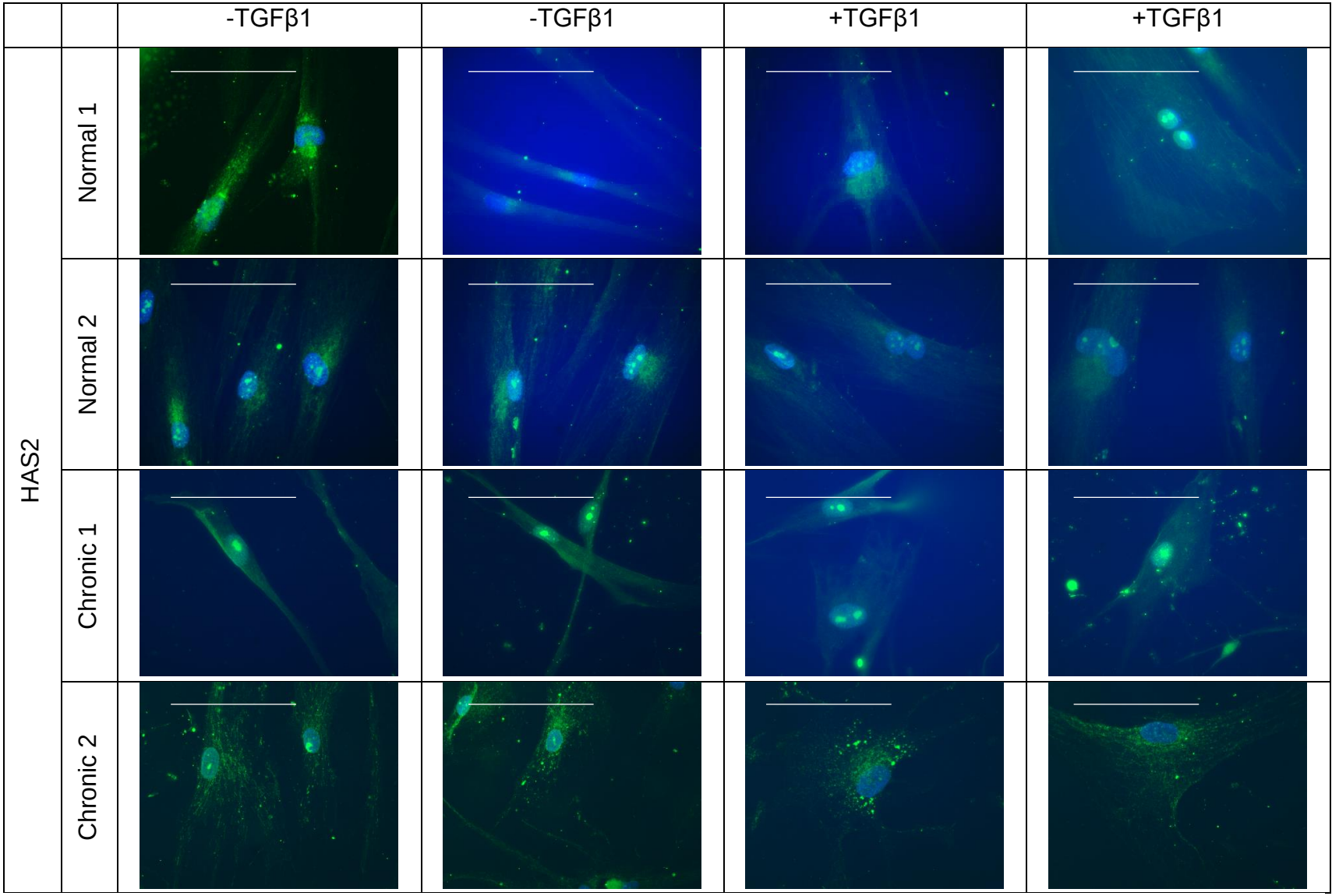

Supplementary Figure 4. HAS2 Localisation. Cells were grown to 60-70% confluence and growth arrested for 48h. Cells were then incubated in serum-free medium alone (-TGF) or in medium containing 10 ng/mL TGFβ1 (+TGF) for 72h. The expression of HAS2 (green) was examined by immunocytochemistry, nuclei were visualised by Hoechst stain. Images shown are a representation of 2 independent experiments. Original Magnification x400. Scale bar: 100μm.

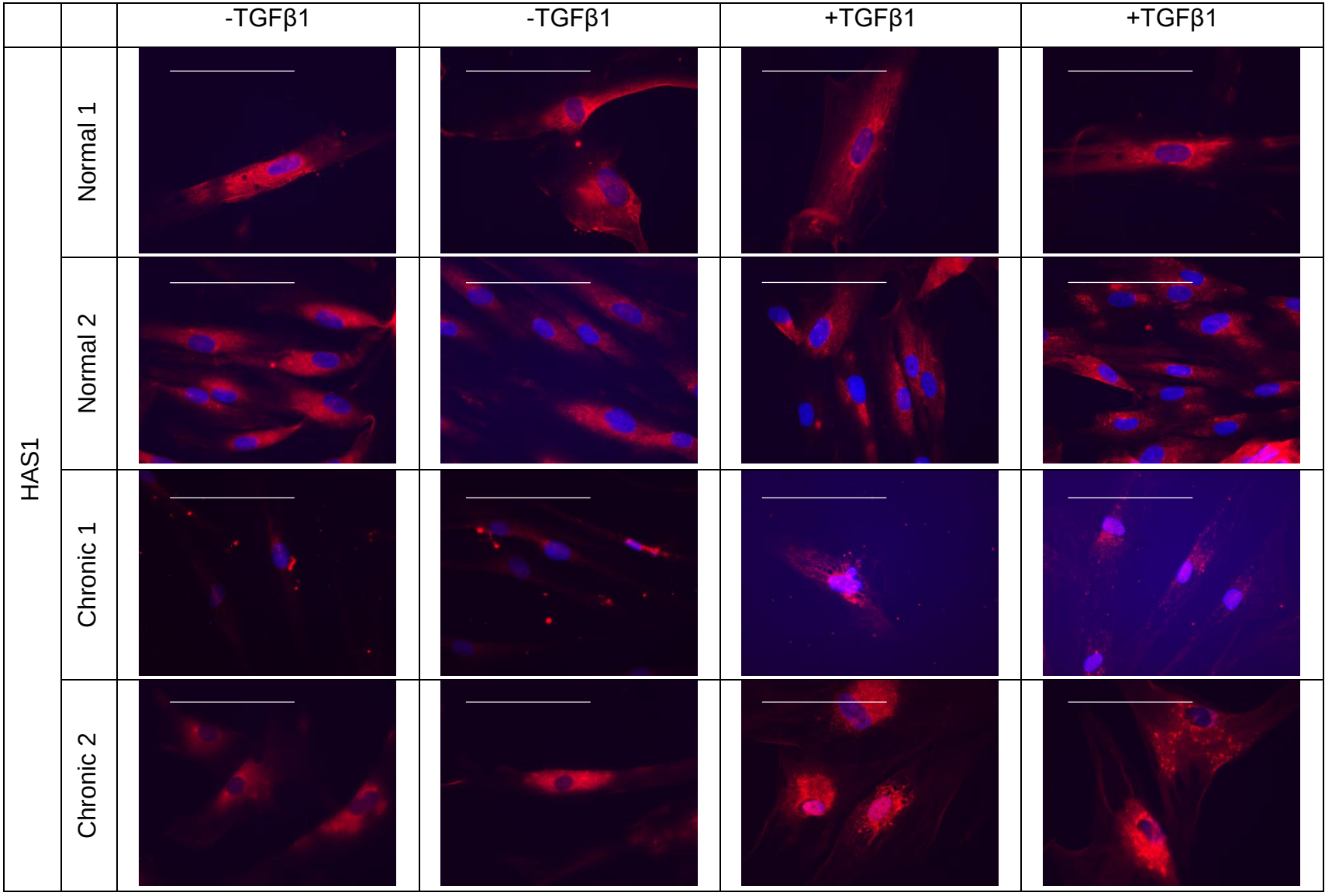

Supplementary Figure 5. HAS1 clusters in a perinuclear location in TGF-β1 Treated CWFs. Cells were grown to 60-70% confluence and growth arrested for 48h. Cells were then incubated in serum-free medium alone (-TGF) or in medium containing 10 ng/mL TGFβ1 (+TGF) for 72h. The expression of HAS1 (red) was examined by immunocytochemistry, nuclei were visualised by Hoechst stain. Images shown are a representation of 3 independent experiments. Original Magnification x400. Scale bar: 100μm.

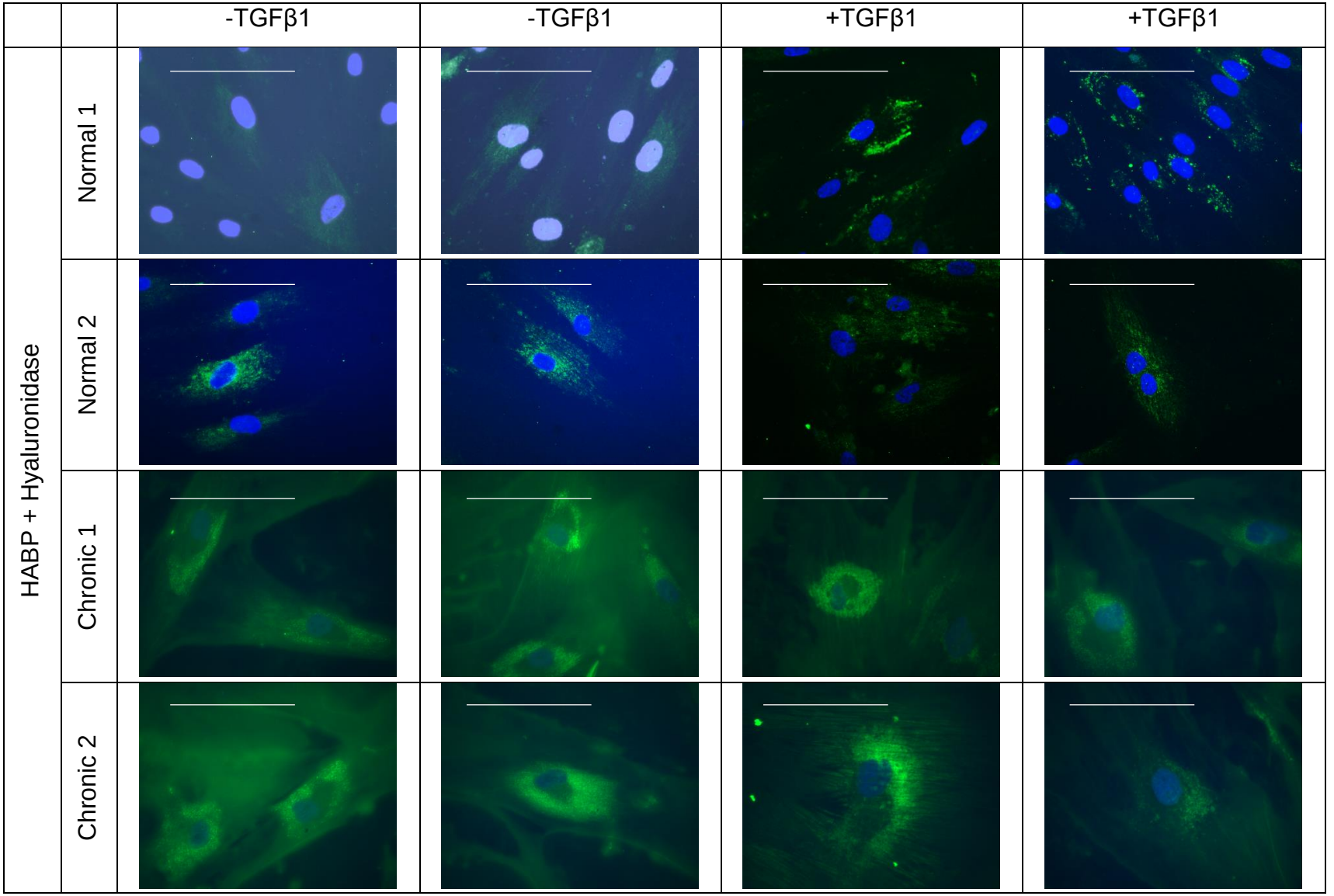

Supplementary Figure 6. Intracellular HA clusters in a perinuclear location in CWFs. Cells were grown to 60-70% confluence and growth arrested for 48h. Cells were then incubated in serum-free medium alone (-TGF) or in medium containing 10 ng/mL TGFβ1 (+TGF) for 72h. The expression of intracellular HA was examined by immunocytochemistry; nuclei were visualised by Hoechst stain. Cells were pre-treated with Streptomyces Hyaluronidase (H1136, Sigma-Aldrich) 30min prior to fixation, to remove pericellular HA. Images shown are a representation of 2 independent experiments. Original magnification x400. Scale bar: 100μm.

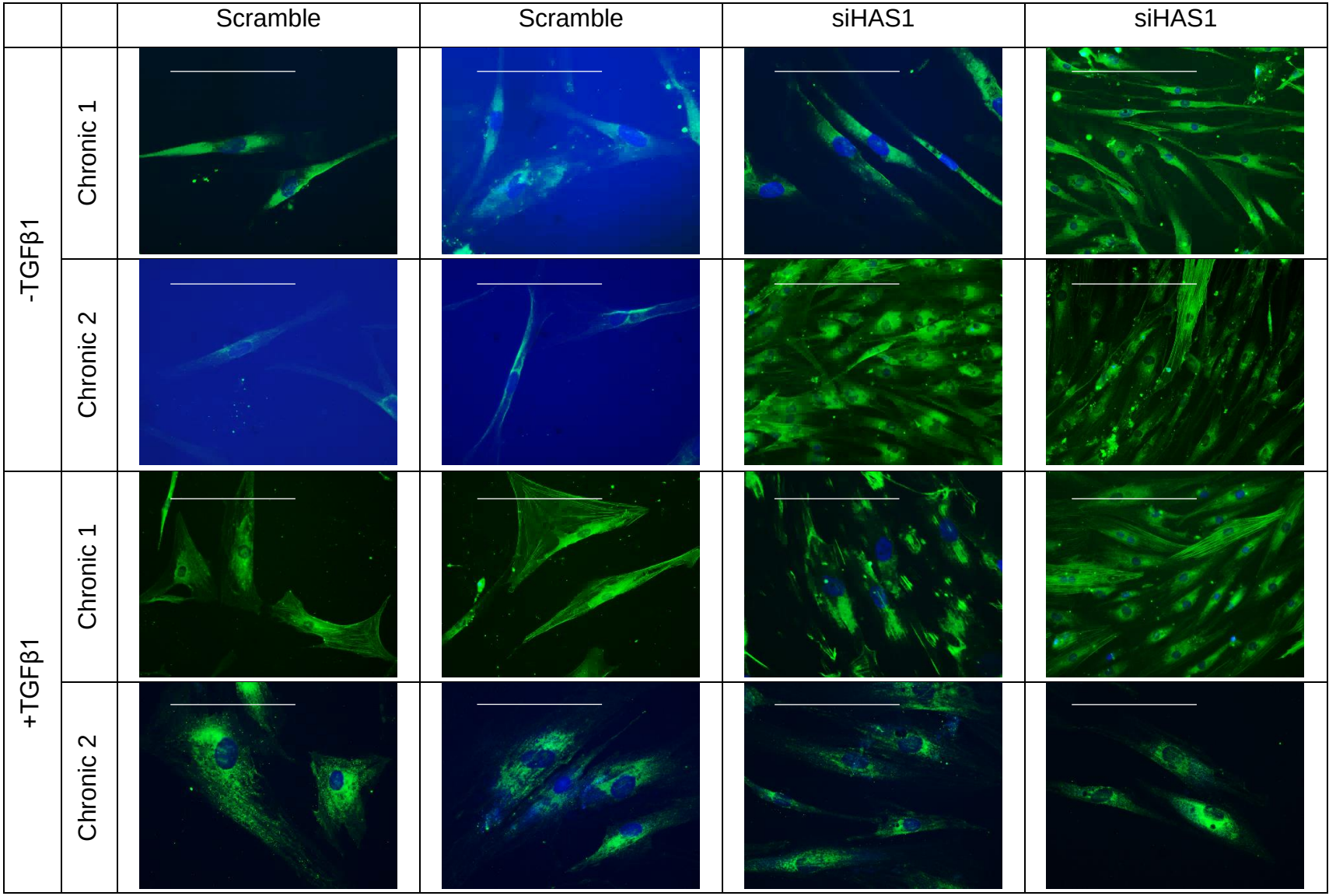

Supplementary Figure 7. Silencing HAS1 does not recover a myofibroblast phenotype in CWFs. Cells were grown to 60-70% confluence and growth arrested for 48h. Cells were then incubated in serum-free medium alone (-TGF) or in medium containing 10 ng/mL TGFβ1 (+TGF) for 72h. The localisation of α-SMA was examined by immunocytochemistry; nuclei were visualised by Hoechst stain. Images shown are a representation of 2 independent experiments. Original Magnification x200 (if available) or x400. Scale bar: 100µm.

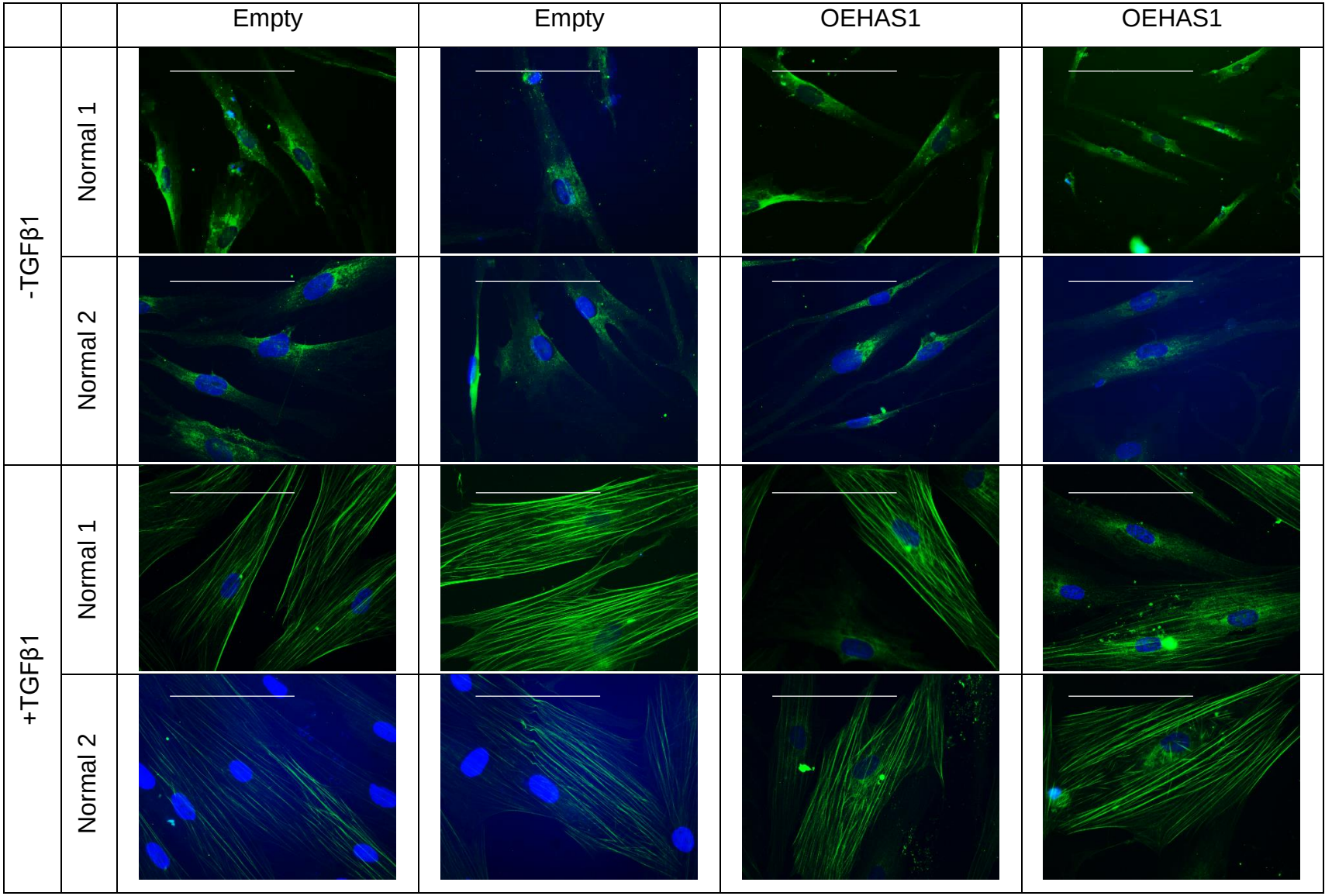

Supplementary Figure 8. Overexpression of HAS1 does not induce a CWFs phenotype in NFs. Cells were grown to 60-70% confluence and growth arrested for 48h. Cells were then incubated in serum-free medium alone (-TGF) or in medium containing 10 ng/mL TGFβ1 (+TGF) for 72h. The localisation of αSMA protein was examined by immunocytochemistry; nuclei were visualised by Hoechst stain. Images shown are a representation of 2 independent experiments. Original Magnification x400. Scale bar: 100μm.

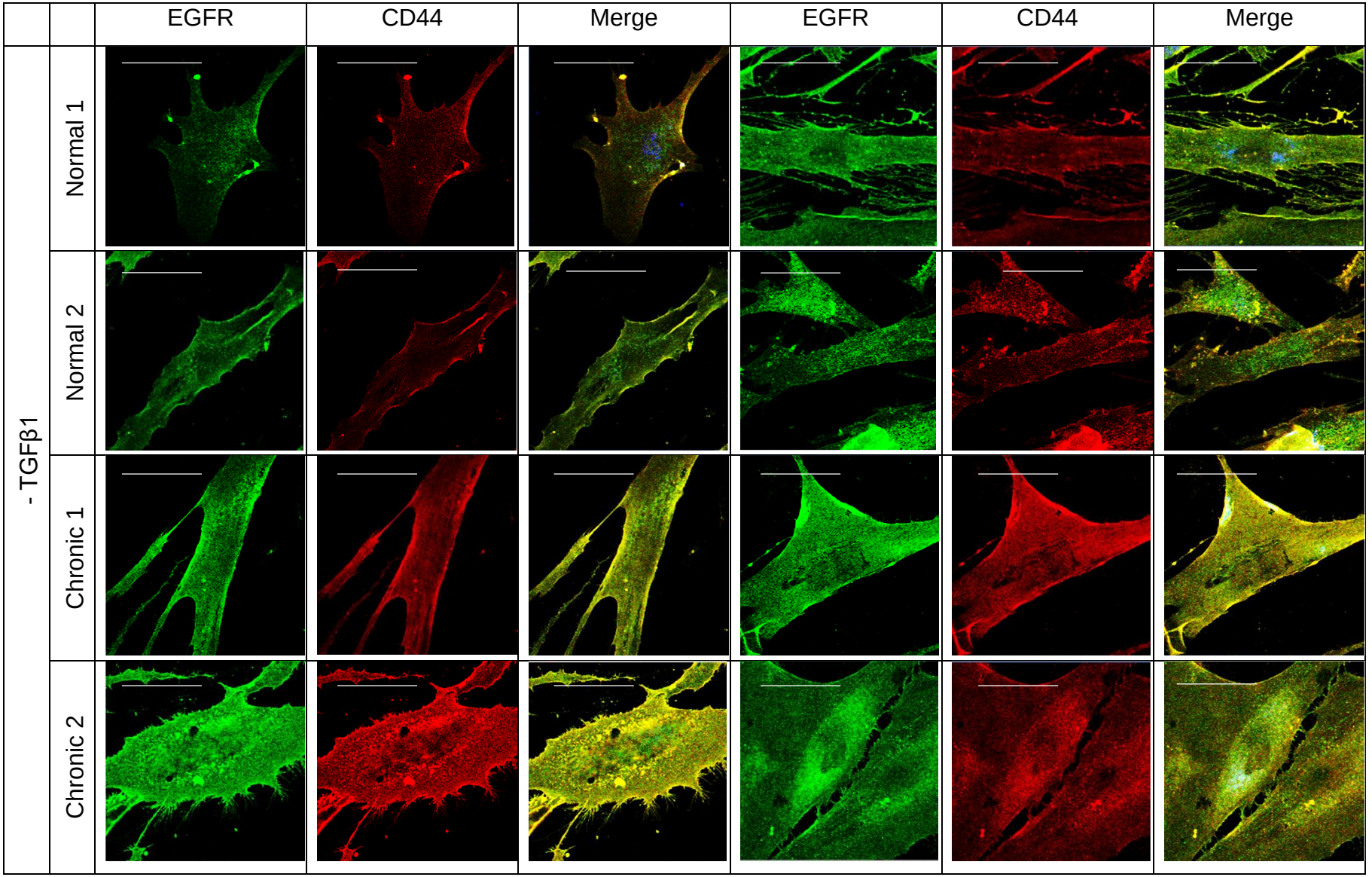

Supplementary Figure 9. Intracellular localisation of EGFR in CWFs and reduced co-localisation with CD44 on the membrane, compared to NFs. Cells were grown to 60-70% confluence and growth arrested for 48h. Cells were then incubated in serum-free medium alone (-TGF) for 72h. The localisation of EGFR (green) and CD44 proteins (Red) were examined by immunocytochemistry and confocal microscopy; nuclei were visualised by Hoechst stain. Images shown are a representation of 3 independent experiments. Original magnification x620. Scale bar: 50µm.

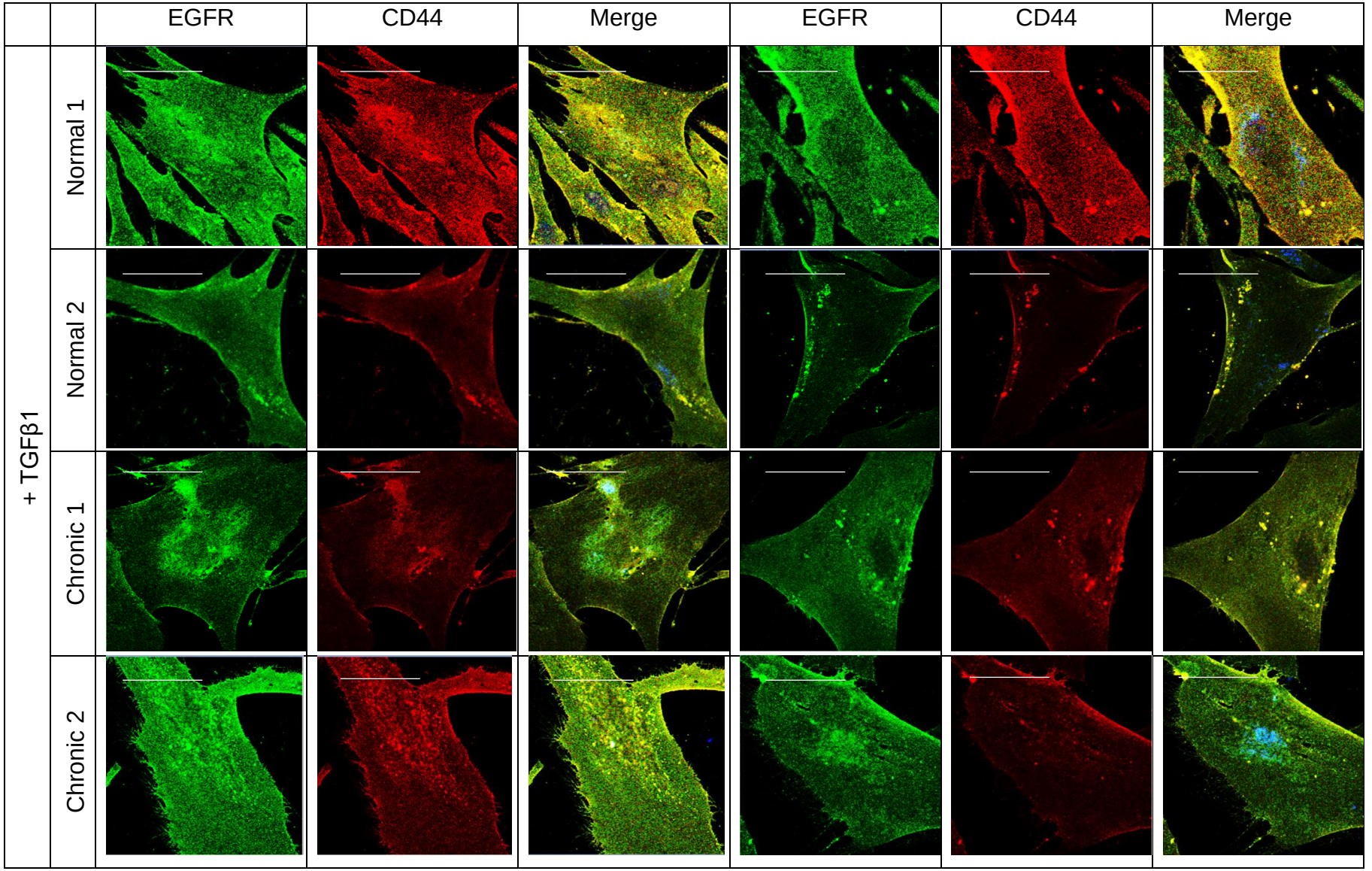

Supplementary Figure 10. Intracellular localisation of EGFR in CWFs and reduced co-localisation with CD44 on the membrane, compared to NFs. Cells were grown to 60-70% confluence and growth arrested for 48h. Cells were then incubated in medium containing 10 ng/mL TGFβ1 (+TGF) for 72h. The localisation of EGFR (green) and CD44 proteins (Red) were examined by immunocytochemistry and confocal microscopy; nuclei were visualised by Hoechst stain. Images shown are a representation of 3 independent experiments. Original magnification x620. Scale bar: 50μm.

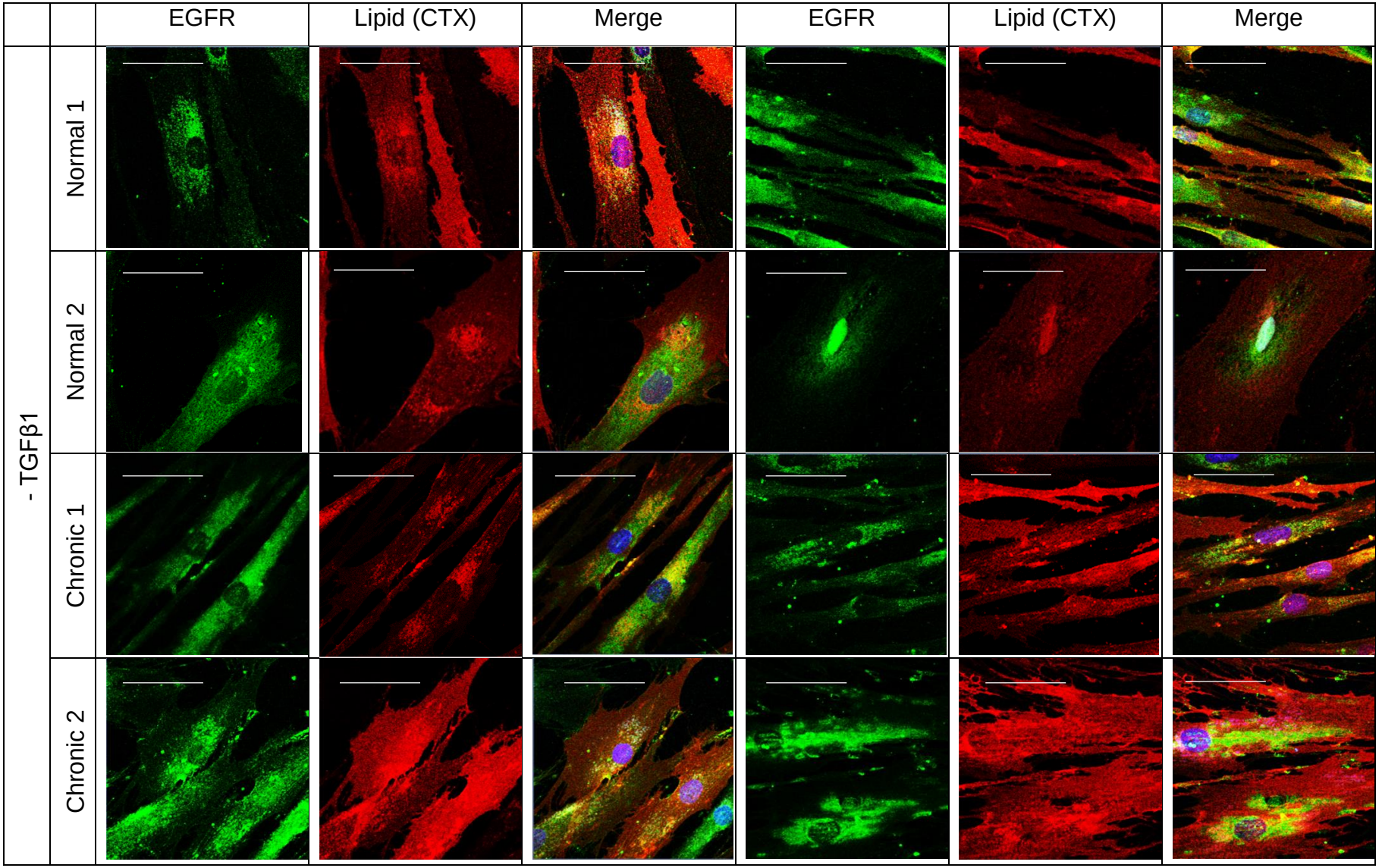

Supplementary Figure 11. EGFR and lipid intracellular localisation in CWFs with reduced co-localisation on the membrane, compared to NFs. Cells were grown to 60-70% confluence and growth arrested for 48h. Cells were then incubated in serum-free medium alone (-TGF) for 72h. The localisation of EGFR protein (green) and lipids (Red) were examined by immunocytochemistry and confocal microscopy; nuclei were visualised by Hoechst stain. Images shown are a representation of 3 independent experiments. Original magnification x620. Scale bar: 50μm.

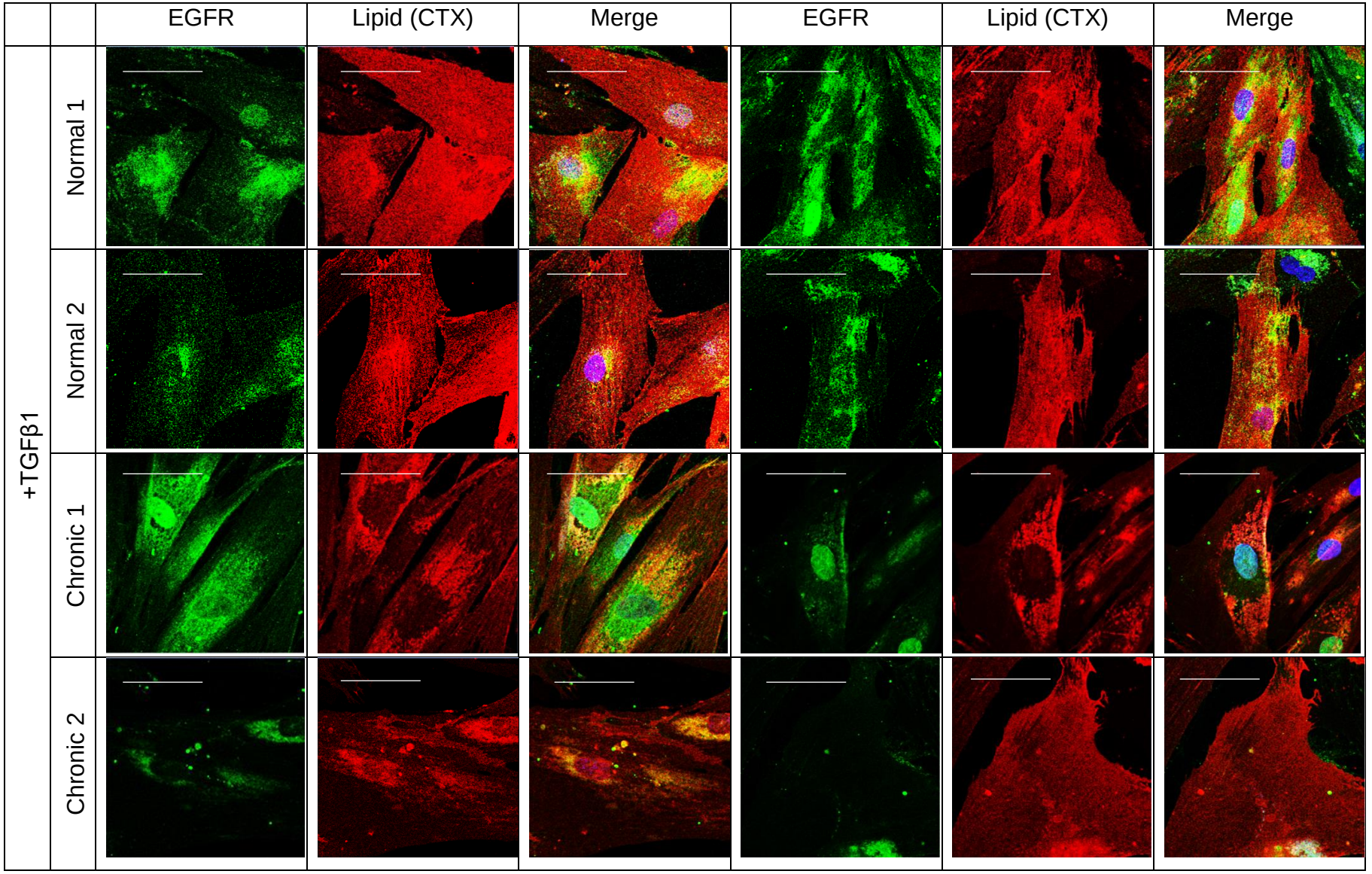

Supplementary Figure 12. EGFR and lipid intracellular localisation in CWFs with reduced co-localisation on the membrane, compared to NFs. Cells were grown to 60-70% confluence and growth arrested for 48h. Cells were then incubated in medium containing 10 ng/mL TGFβ1 (+TGF) for 72h. The localisation of EGFR protein (green) and lipids (Red) were examined by immunocytochemistry and confocal microscopy; nuclei were visualised by Hoechst stain. Images shown are a representation of 3 independent experiments. Original magnification x620. Scale bar: 50μm.

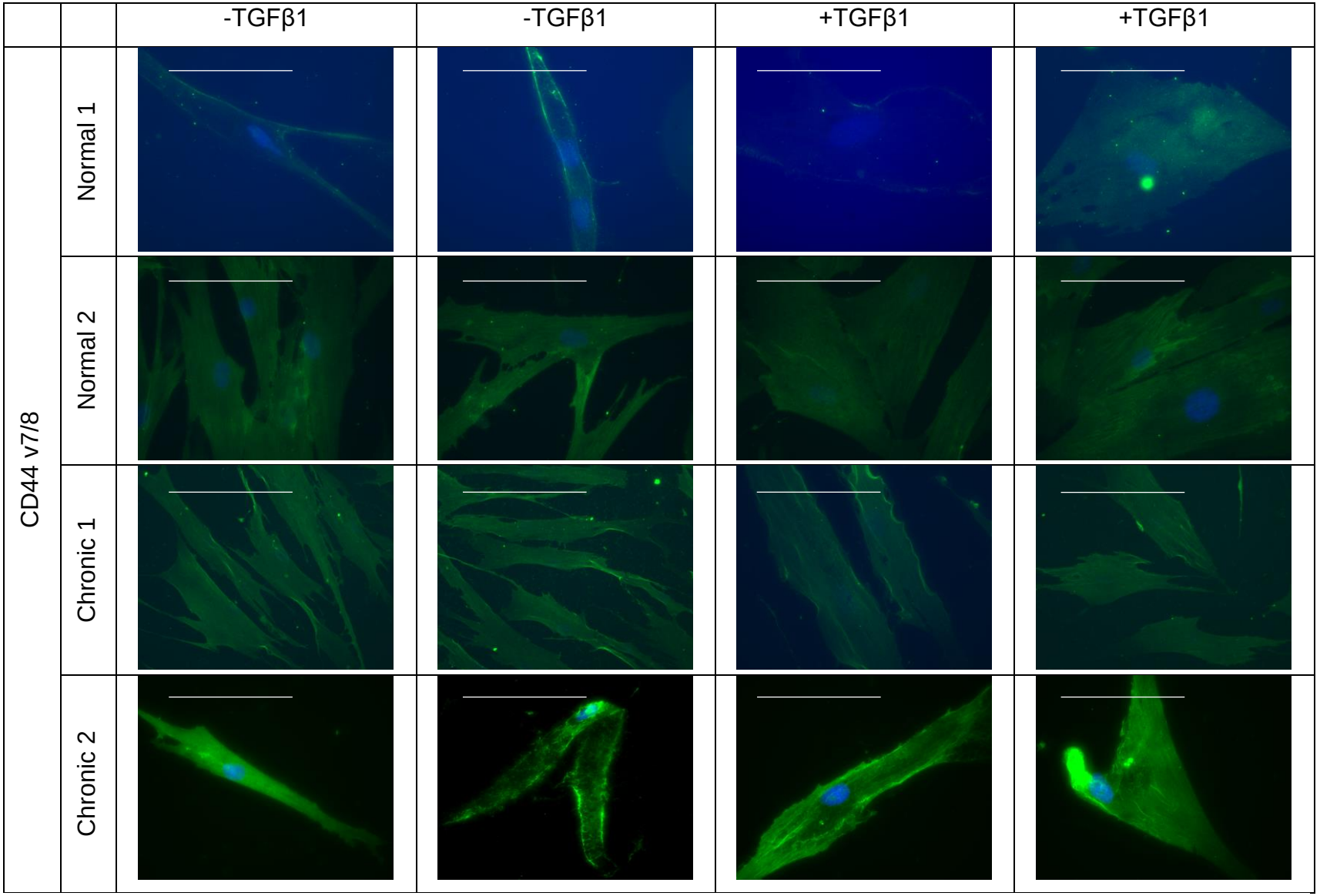

Supplementary Figure 13. CD44 variant 7/8 localisation and expression. Cells were grown to 60-70% confluence and growth arrested for 48h. Cells were then incubated in serum-free medium alone (-TGF) or in medium containing 10 ng/mL TGFβ1 (+TGF) for 72h. The localisation of CD44 v7/8 protein was examined by immunocytochemistry; nuclei were visualised by Hoechst stain. Images shown are a representation of 2 independent experiments. Original magnification x400. Scale bar: 100μm.

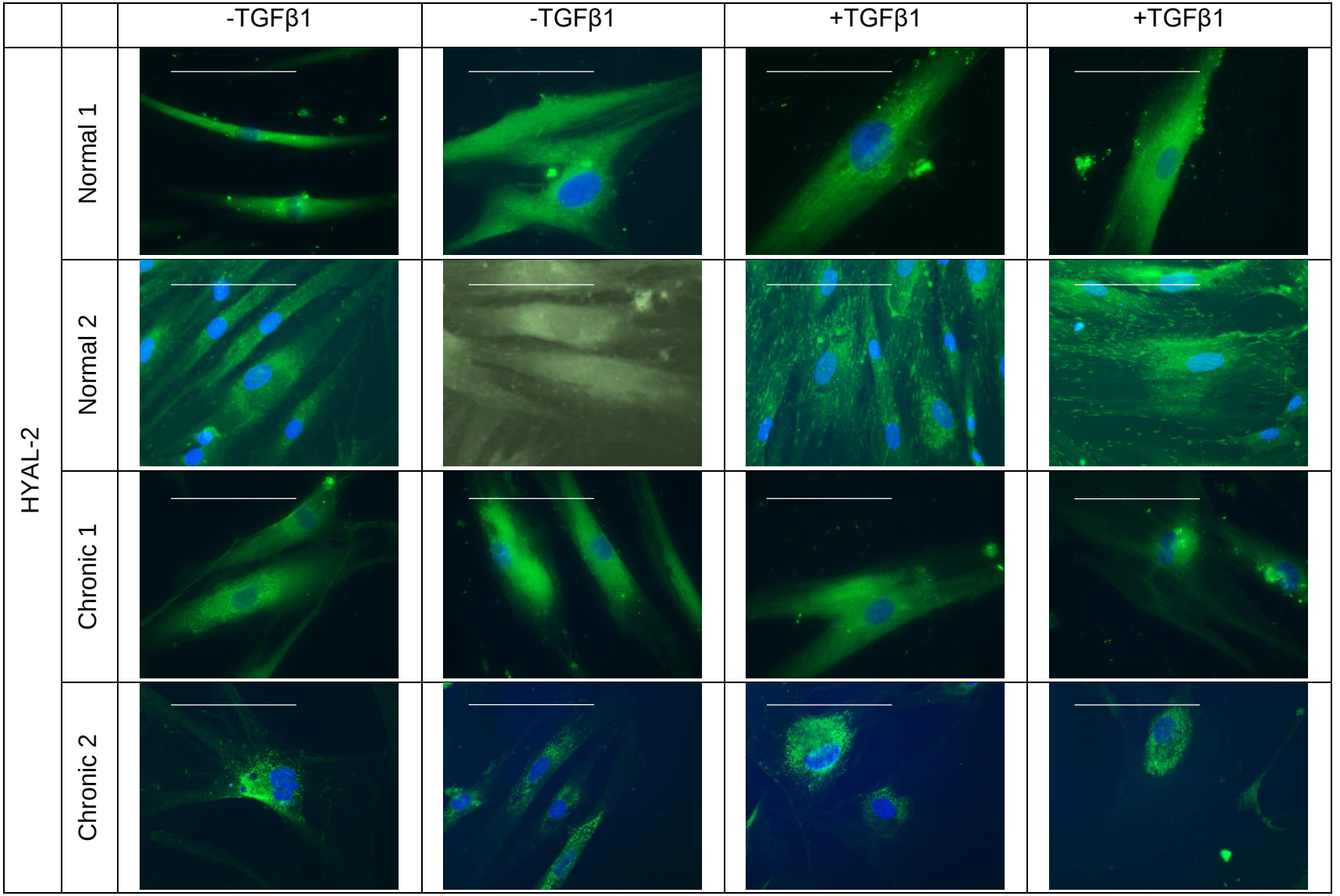

Supplementary Figure 14. HYAL2 perinuclear localisation in CWFs. Silencing HYAL2 doesn't recover a myofibroblast phenotype. Cells were grown to 60-70% confluence and growth arrested for 48h. Cells were then incubated in serum-free medium alone (-TGF) or in medium containing 10 ng/mL TGFβ1 (+TGF) for 72h. The localisation of CD44 v7/8 protein was examined by immunocytochemistry; nuclei were visualised by Hoechst stain. Images shown are a representation of 2 independent experiments. Original magnification x400. Scale bar: 100μm

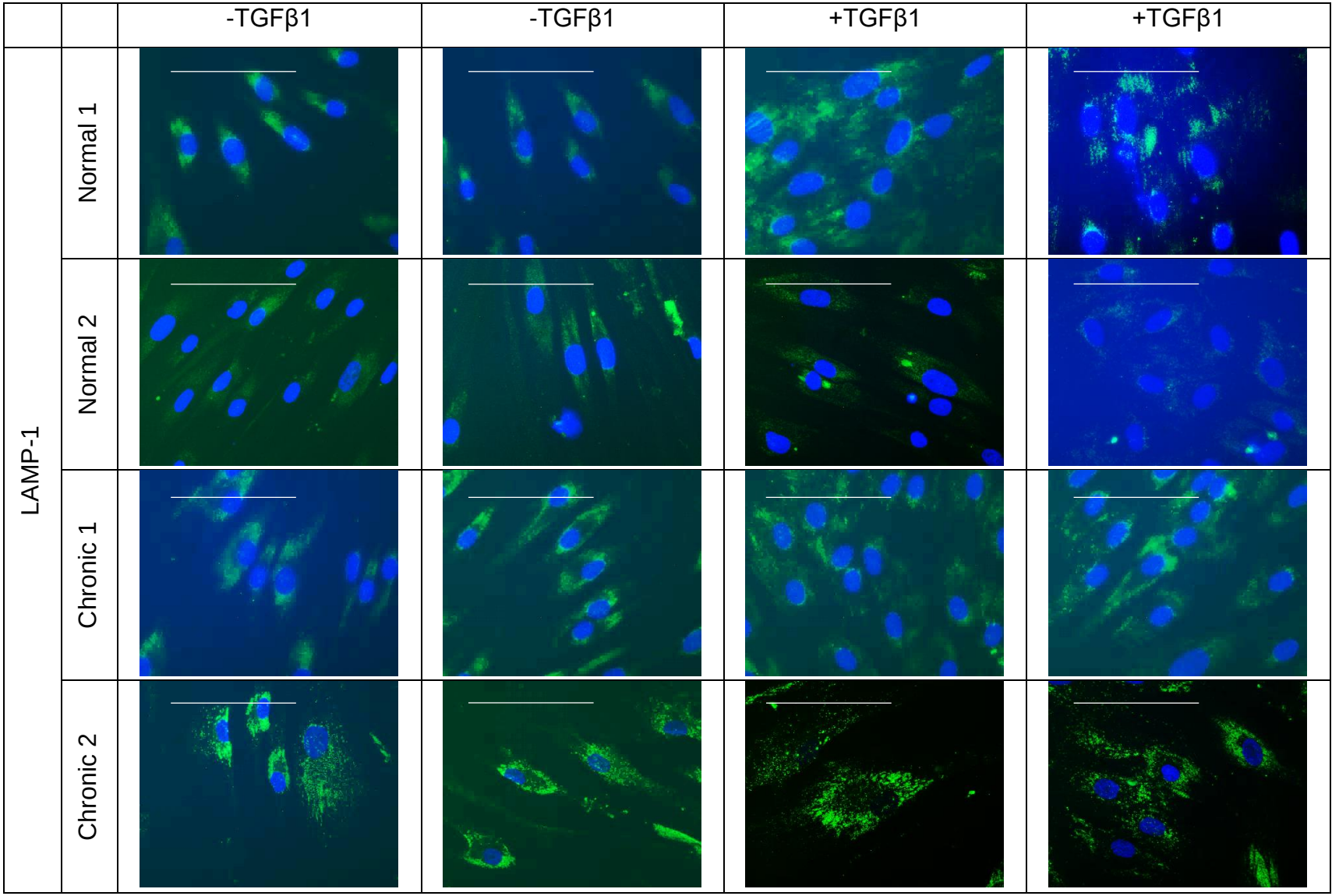

Supplementary Figure 15. No difference in lysosome localisation was observed between CWFs and NFs. Cells were grown to 60-70% confluence and growth arrested for 48h. Cells were then incubated in serum-free medium alone (-TGF) or in medium containing 10 ng/mL TGFβ1 (+TGF) for 72h. The localisation of LAMP-1 protein was examined by immunocytochemistry; nuclei were visualised by Hoechst stain. Images shown are a representation of 2 independent experiments. Original magnification x400. Scale bar: 100μm

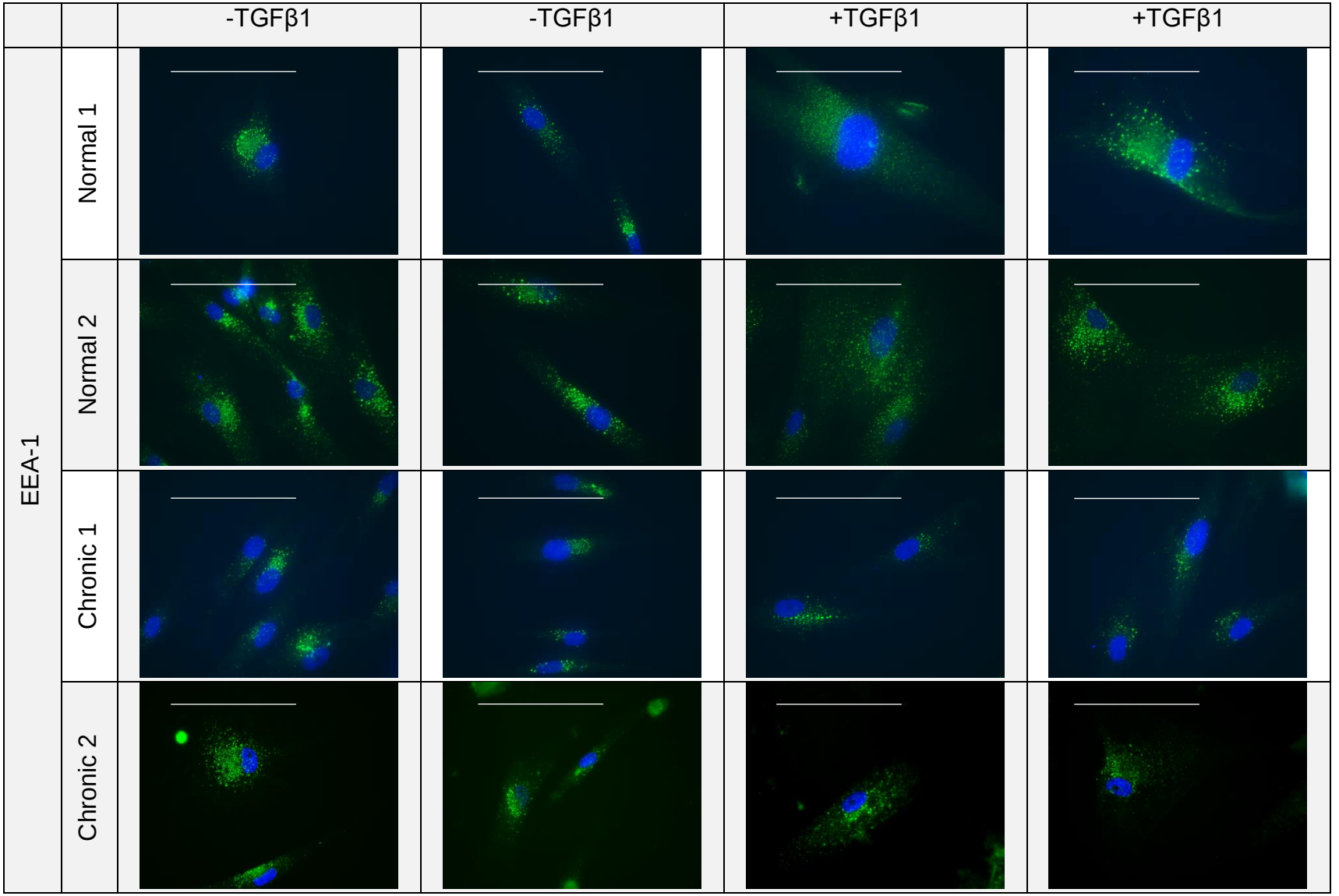

Supplementary Figure 16. No difference in endosome localisation was observed between CWFs and NFs. Cells were grown to 60-70% confluence and growth arrested for 48h. Cells were then incubated in serum-free medium alone (-TGF) or in medium containing 10 ng/mL TGFβ1 (+TGF) for 72h. The localisation of EEA-1 protein was examined by immunocytochemistry; nuclei were visualised by Hoechst stain. Images shown are a representation of 2 independent experiments. Original magnification x400. Scale bar: 100µm.

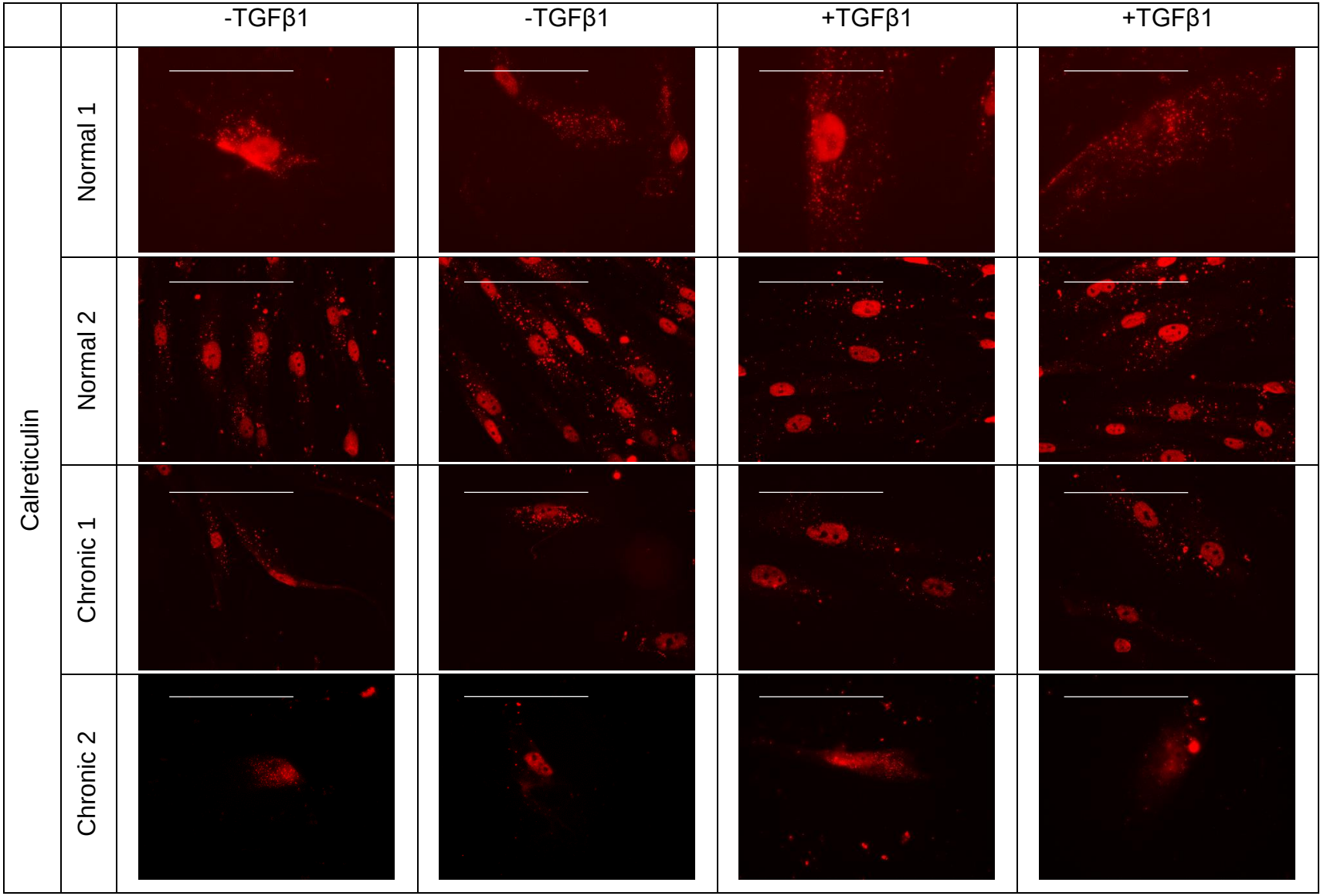

Supplementary Figure 17. No difference was seen between E.R. staining of CWFs and NFs. Cells were grown to 60-70% confluence and growth arrested for 48h. Cells were then incubated in serum-free medium alone (-TGF) or in medium containing 10 ng/mL TGFβ1 (+TGF) for 72h. The expression of E.R. protein, calreticulin was examined by immunocytochemistry. No nuclei stain was used to show localisation within the nucleus. Images shown are a representation of 2 independent experiments. Original magnification x400. Scale bar: 100μm.

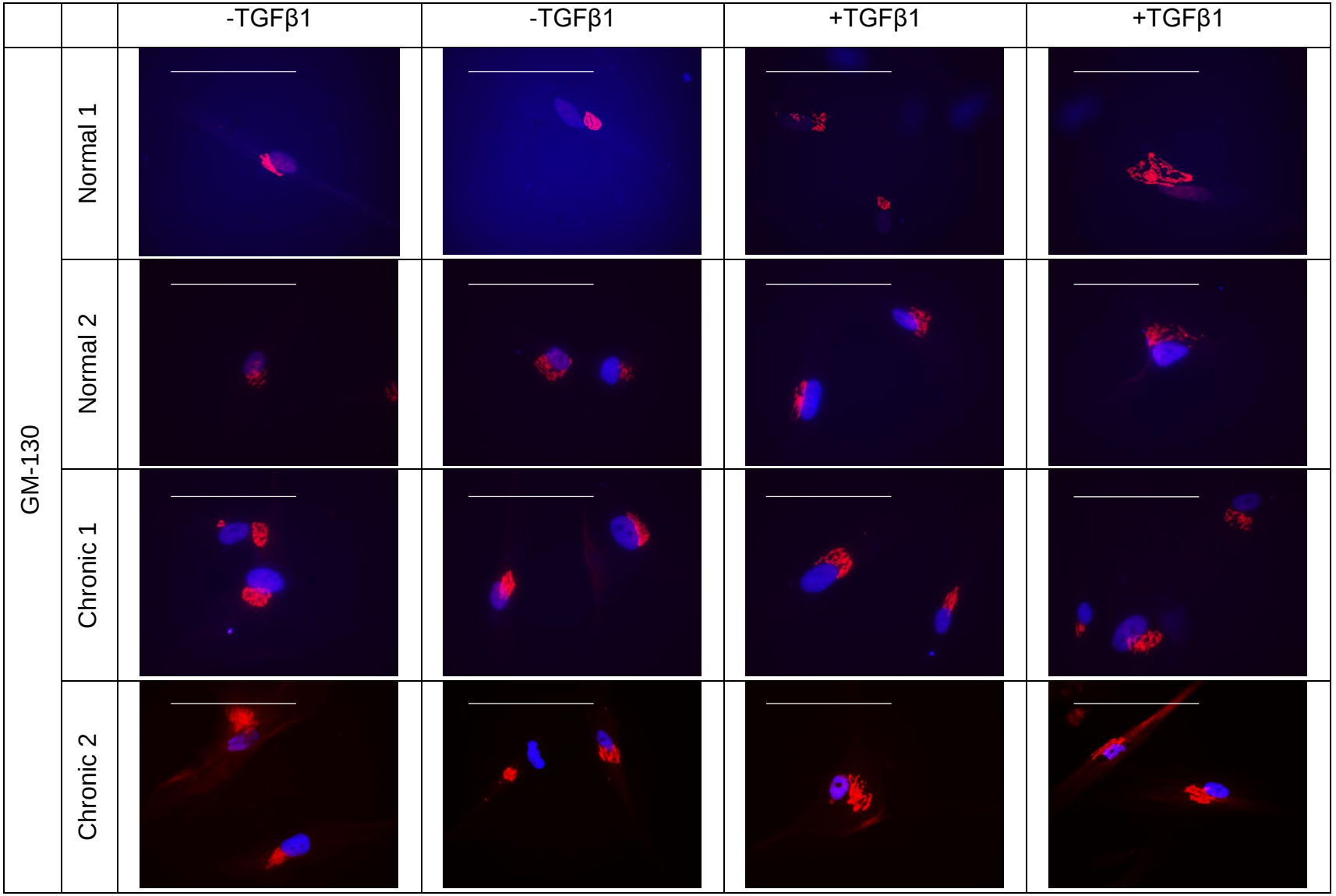

Supplementary Figure 18. No differences in Golgi staining was observed between CWFs and NFs. Cells were grown to 60-70% confluence and growth arrested for 48h. Cells were then incubated in serum-free medium alone (-TGF) or in medium containing 10 ng/mL TGFβ1 (+TGF) for 72h. The Golgi protein, GM-130 was examined by immunocytochemistry; nuclei were visualised by Hoechst stain. Images shown are a representation of 2 independent experiments. Original magnification x400. Scale bar: 100µm.

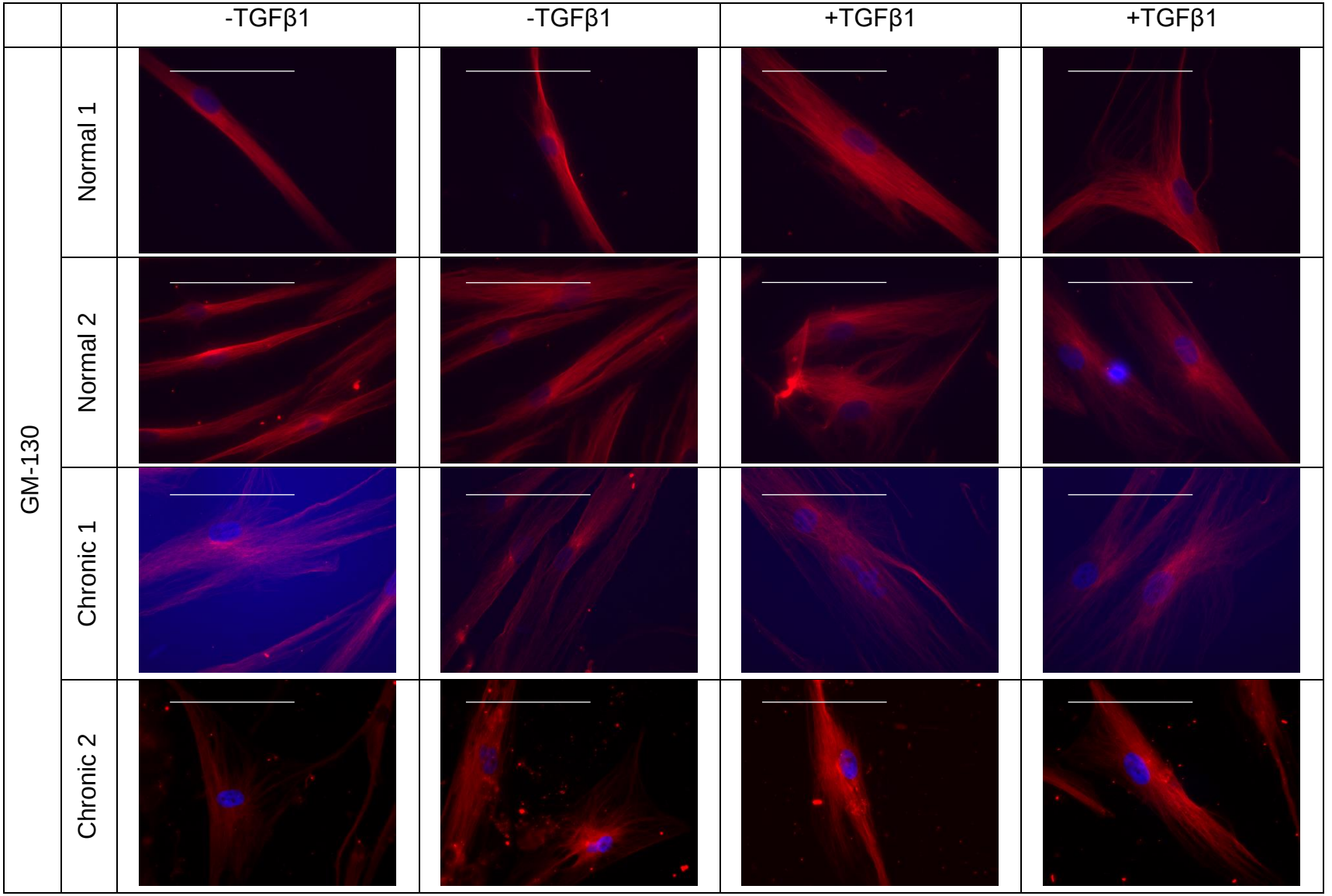

Supplementary Figure 19. No difference in tubulin positive microtubule formation between CWFs and NFs. Cells were grown to 60-70% confluence and growth arrested for 48h. Cells were then incubated in serum-free medium alone (-TGF) or in medium containing 10 ng/mL TGFβ1 (+TGF) for 72h. Tubulin was examined by immunocytochemistry; nuclei were visualised by Hoechst stain. Original magnification x400. Images shown are a representation of 2 independent experiments. Scale bar: 100µm.